NONDESTRUCTIVE TEST METHODS FOR RAPID ASSESSMENT OF FLEXIBLE BASE PERFORMANCE IN TRANSPORTATION INFRASTRUCTURES

A Dissertation

by

HAKAN SAHIN

Submitted to the Office of Graduate and Professional Studies of
Texas A&M University
in partial fulfillment of the requirements for the degree of

DOCTOR OF PHILOSOPHY

Chair of Committee,	Robert L. Lytton
Committee Members,	Jon A. Epps
	Giovanna Biscontin
	Niall C. Slowey
Head of Department,	Robin Autenrieth

August 2014

Major Subject: Civil Engineering

ABSTRACT

Well-built roads with longer service life and lesser life cycle cost are the key to meet the desired target of satisfying the public without compromising the quality of roads. Roads that are constructed and built with poor quality materials and inadequate design considerations frequently require costly maintenance and rehabilitation often resulting in detours and lane closures, which not just reduce the comfort of the public but also interrupt the efficient flow of transporting goods, and hence the associated businesses. Therefore, it is imperative that alternative quality control and quality assurance methods along with effective test methods and smart transportation planning must be considered and implemented to help communities increase the economic prosperity while retaining and ensuring a high quality of life to the people.

The appropriate application of reliability to pavement design is essential to achieve the main objectives of designing quality pavements to serve the traveling public with comfort and safety while being durable in service at a minimum life cycle cost.

The quality of the base layer of the pavement, which is located directly beneath the surface, is one of the most critical components in designing a pavement with increased service life and durability. The base layer is primarily composed of aggregates and contributes to the structural stability of the pavement system by providing load transfer and support. A base course with adequate thickness and built with high quality aggregates is essential to meet the necessary performance criteria and in doing so will cut down on reconstruction cycles and cost of maintenance.

This research attempts to contribute in this regard by evaluating the significance of using the fundamental material properties to develop models which characterize the base layer in a pavement system. These new models will have significant contributions to soil mechanics and highway design procedures. This research and the developed models depend upon fundamental soil properties. This work capitalizes upon the fundamental properties to make extensive use of these models for quality control (QC) and quality assurance (QA), in the pre-design procedure and construction phase. The most significant impact of the work is to replace and improve current methods, increase work efficiency, minimize time spent in the laboratory, find more convenient relationships, reduce costs, and improve sustainability. In addition, the quickly and accurately measured aggregate characteristics of base courses will be used to determine the in-place and as-compacted design properties for QC and QA.

DEDICATION

To my adviser Dr. Lytton,

who believed in and supported me in everything that I have ever wanted to do, and for his love and patience as well.

ACKNOWLEDGEMENTS

I would like to thank my academic advisor and mentor, Dr. Robert Lytton for providing me the opportunity to work with him and for his constant support and guidance throughout my study. I also take this opportunity to express my sincere thanks to my committee members, Dr. Jon Epps, Dr. Niall Slowey, Dr. Giovanna Biscontin from the University Cambridge in England, and Dr. Charles Aubeny for their advice throughout the course of this research. I consider myself fortunate to have had the opportunity to work with them and will cherish these memories for the rest of my life.

Texas A&M University, Texas A&M Transportation Institute, and Southwest Region University Transportation Center have provided me with excellent facilities and opportunities to interact and learn from distinguished professors and eminent scholars, and I am proud to be a part of this magnificent family.

I also want to extend my gratitude to all of my colleagues and friends for their friendship, understanding and making me feel as at home as possible during my time in Bryan/College Station.

Last but definitely not the least; I would like to express my deepest gratitude to my mother, father, older sister, and younger brother for their infinite support and encouragement throughout my education oversea.

TABLE OF CONTENTS

Page

LIST OF FIGURES

Page

Page

Page

Page

Page

Page

LIST OF TABLES

Page

Page

NOMENCLATURE

AASHTO	American Association of State Highway and Transportation Officials
AIMS	Aggregate Image Measurement System
ASTM	American Society for Testing Materials
CCM	Compaction Curve Model
CEC	Cation Exchange Capacity
FWD	Falling Weight Deflectometer
GPR	Ground Penetrating Radar
MEPDG	Mechanistic Empirical Pavement Design Guide
MBT	Methylene Blue Test
MBV	Methylene Blue Value
NCHRP	National Cooperative Highway Research program
NDG	Nuclear Density-moisture Gage
PD	Permanent Deformation
PSDA	Particle Size Distribution Analyzer
QA	Quality Assurance
QC	Quality Control
RLT	Repeated Load Triaxial
SCA	Soil Compactor Analyzer
SDCC	Soil Dielectric Characteristics Curve
SSA	Specific Surface Area
SWCC	Soil Water Characteristics Curve

TTI	Texas A&M Transportation Institute
TxDOT	Texas Department of Transportation
a_d	A parameter in the compaction (CCM) model
af	A function of air entry value of the soil in the SWCC model
a_m	A distinct fitting parameters in the pfc model
b_d	A parameter in the compaction (CCM) model
bf	A function of the rate of water extraction from soil in the SWCC model
b_m	A distinct fitting parameters in the *pfc* model
c_f	A function of the residual water content in the SWCC model
D	Diffusivity
E_y	Resilient modulus of unbound aggregate
Gs	Specific gravity of solids
h_m	Matric suction in the aggregate matrix
h_r	A function of the suction at the residual water content in the SWCC model
I_1	First invariant of the stress tensor
k_1, k_2, k_3	Material parameters in resilient modulus model
LL	Liquid limit
n_d	A parameter in the compaction (CCM) model
n_m	A distinct fitting parameters in the *pfc* model
P_{200}	Mass percentage passing through no.200 sieve

P_a	Atmospheric pressure
pfc	Percent fines content
PI	Plasticity index
S	Degree of saturation
w_{opt}	Optimum gravimetric moisture content
α	A fitting parameter in the SDCC model
γ	A fitting parameter in the SDCC model
γ_d	Dry unit weight of unbound base course aggregate
γ_w	Unit weight of water
$\varepsilon_{\min}$	Dielectric value of unbound aggregate media
ε_r	Dielectric value of unbound aggregate media
ε_{sat}	Saturated dielectric value of unbound aggregate media
θ_s	Saturated water content
θ_w	Volumetric water content
τ_{oct}	Octahedral shear stress

1. INTRODUCTION

1.1 General

Pavement performance and life cycle costs depend very strongly upon the proper functioning of the base course, the most important supporting layer in a pavement system. The likelihood of the base course layer performing well is greatly increased if the properties it was assumed to have when the pavement was designed are the properties it has when it is built. However, the properties of the base course layer that are measured during construction are not the layer properties used in the design. The dry unit weight and water content are the most commonly measured properties of the base course. These as-compacted properties are compared with laboratory compaction curves to assure that an adequate level of compaction has been achieved. For decades, it has been recognized that there is a need to assure that the properties of base courses used in design are what have actually been placed. The design properties of layer modulus and permanent deformation properties are directly related to the subsequent performance of the pavement and ultimately to the cost to the taxpaying public of providing a cost-effective in-service pavement.

A major obstacle to achieving this desired result is the difficulty of measuring the modulus, and even more difficult is the permanent deformation characteristics of the base course properties. Quality assurance (QA) of the compacted base course must be conducted in a timely and efficient manner so as not to impede the pace of construction,

but it must also be done with accuracy and precision that can reasonably assure that the pavement will perform as it was designed.

What is needed is a quick, accurate, and simple process for determining reliable values of the in-place as compacted base course modulus and permanent deformation properties. In addition, the measurements that are made should also contribute to the quality assurance of the process that includes taking the base course from its quarry, transferring it to a job site, and compacting it in-place.

The objective of the measurements is to determine the same unbound aggregate properties, which are related to quality control (QC) and quality assurance (QA) regardless of whether they are measured in the field or in laboratory experiments. The series of tests that are proposed here to do this include the methylene blue test (MBT) developed by the W. R. Grace corporation, particle size analysis by the Horiba analyzer to determine the percent fines content of the base course, the filter paper test to determine the suction of the base course, the percometer test to measure the dielectric constant of the base course, dry sieve analysis to assess the gradation of the particle sizes, and the moisture diffusivity of the compacted base course test at high levels of relative humidity.

The engineering properties of the aggregate base course in place are strongly influenced by the fines in the aggregate materials. Therefore, it is significantly important to determine fines for the base course material. The soil-water characteristic curve (SWCC) is used to accomplish this goal because the SWCC gives matric suction, which is one of the most important unsaturated soil mechanics properties. The magnitude of the

matric suction controls the fundamental engineering properties related to stiffness, shear strength, and diffusion. Therefore, generating the SWCC curve and determining the matric suction is extremely important in determining such engineering properties. However, the usual way of measuring the SWCC requires a special set of laboratory equipment, experienced labor and a long testing program process. The desired approach is that the SWCC and the matric suction must be determined based on more easily determined soil properties such as those mentioned above.

Recently developed models of modulus and permanent deformation properties have shown that they can be predicted accurately if the following soil properties are known: matric suction, water content, percent fines content, MBV, and dry unit weight.

Methylene blue is a test method to assess the amount of the fines fraction of a sample. This test method is capable of determining the fines percentage rather than using the other test methods that require a longer laboratory experiment program.

It is proposed to develop a new method to build up the SWCC using the methylene blue value. Thus, in order to eliminate the difficulties of the laboratory experiment programs, the methylene blue test method is a very efficient alternative. The methylene blue value is utilized to determine the four fitting parameters that govern the shape of the SWCC equation.

The percometer is an instrument that measures dielectric constant, electrical conductivity and temperature at the surface of a material. The percometer is used to measure soil dielectric permittivity and conductivity in soil studies. The percometer is capable of determining the in-place water content of placed aggregate mixtures. There is

a need to combine the dielectric value with soil properties to achieve this goal. Hence, it will allow researchers to use outcomes of the percometer test more frequently to determine base course modulus and permanent deformation properties.

In general, the higher degree of compaction, the higher the shear strength; therefore, achieving a maximum dry density will increase the soil strength significantly. The degree of compaction is measured in terms of dry unit weight. Therefore, the dry unit weight vs. water content curve is a desired quality assurance attribute to be used in controlling the quality of placed aggregate materials. It is also a sensitive factor in predicting the base course modulus in place.

1.2 Research Problem Statement

As previously stated, the pavement performance and life cycle costs depend very strongly on the proper functioning of the base course, which is the most important supporting layer in a pavement. The likelihood of the base course performing well is greatly increased if the properties it was assumed to have when the pavement was designed match the properties it has when it is actually built in-place. However, it turns out that the properties of the base course layer that are measured during construction are never the same as the layer properties used in the design. For decades, it has been recognized that there is a need to assure that the properties of base courses used in design are what have actually been placed. The layer modulus and permanent deformation properties are the primary design properties that can be directly related to

the subsequent performance of the pavement and ultimately to the costs, which are passed on to the taxpaying public for using a cost-effective in-service pavement.

A major obstacle to controlling these design parameters is the difficulty of measuring the modulus, and more so the permanent deformation characteristics of the base course. Quality assurance of the compacted base course must be conducted in a timely and efficient manner so as to not retard the pace of construction, and also with a high degree of accuracy and precision that can reasonably assure that the pavement will perform as it was meant to while being designed. This study attempts to address this challenge by establishing some simple and quick laboratory test protocols to measure essential attributes of the base course that can be extended for use in field investigations.

1.3 Scope of Research

The focus of this research is to develop a quick, accurate, and simple process for determining reliable values of the in-place as compacted base course modulus and permanent deformation properties. In addition, the measurements that are made should also contribute to the assurance of quality during the cycle of operations in the process of taking the base course from its quarry, transferring it to a job site, and compacting it in-place.

The unbound aggregate properties, which are related to quality control (QC) and quality assurance (QA), are sought to be determined accurately regardless of whether they are measured in the field or through laboratory experiments.

Hence, the primary objective of this work is to determine an improved performance protocol regarding base course properties and subsequently develop mathematical relationships, which can be used in engineering design and construction using the proposed protocol. This work will develop new and innovative methods to determine QC and QA for base course materials in-place.

1.4 Organization of the Study

The work plan in the study is organized into the following tasks to meet the objective of this research.

1.4.1 Review of the Literature and Collecting of Information

The objective of this task is to conduct an extensive literature review to gather information on available QC and QA approaches for base course materials, properties, and corresponding evaluation methods. The literature review provides a summary of the search, which has been conducted on soil water characteristics curve, dielectric, and conductivity; on laboratory tests of Atterberg limits, diffusivity test on the base materials; and on field tests with the Falling Weight Deflectometer (FWD) and Ground Penetration Radar (GPR). Based on the literature search the available information has been used to incorporate further theoretical and experimental developments in this study.

1.4.2 Develop Experiment Programs

The objective of this task is to develop a comprehensive laboratory experiment program to characterize the material properties of base course materials for each pit. This study consists of several intense experimental programs, each of which are describing method

and methodology along with the theoretical background work. Therefore, the experiment plan will consider following the test methods, each of which are given a task in this study.

- Permanent Deformation and Resilient Modulus test to determine permanent strain and resilient strain of unbound aggregate material by using the repeated load triaxial test machine
- Methylene Blue test developed by the W.R. Grace corporation to assess the fines clay fraction
- Horiba particle size analyzer to determine the distribution of fines in the base material
- Filter paper test to determine the suction value for base materials and Soil Water Characteristics Curve (SWCC)
- The Percometer test to determine the dielectric constant of base materials and Soil Dielectric Characteristics Curve (SDCC)
- Compaction Optimum Moisture Content (OMC) test to determine dry unit weight at optimum moisture content
- Diffusivity test to determine the moisture diffusion rate of the base materials
- Falling Weight Deflectometer test (FWD) to determine stiffness of the pavement
- Ground Penetration Radar (GPR) to measure layer thickness the pavement system

1.4.3 Permanent Deformation and Resilient Characteristics of the Base Course Materials

This part aims at developing an accurate method to estimate the resilient and permanent strain by using the unbound base course aggregate material properties. To this end, the laboratory repeated load triaxial (RLT) test was performed on the collected samples to determine permanent and resilient strains of the base course aggregates. Both permanent strain and resilient strain are determined based on the cylindrically compacted sample. The VESYS and Lytton-Tseng are the two widely used PD models are used to determine permanent deformation behavior and permanent strain-load repetition curve. Multiple regression analyses were performed to predict models between permanent deformation and unbound aggregate material properties. A similar process has been done to determine the recoverable resilient strain of the sample under a dynamic load repeated by RLT test. The resilient model has three coefficients k_1, k_2, and k_3, which are material parameters that are dependent on material properties of the base course. A series of performance-related base course properties are measured and employed to develop the prediction models. These performance properties are related to the MBV, *pfc*, gradation, and Weibull distribution index form AIMS test.

1.4.4 Determine Percent Fines Content (pfc) Using the Methylene Blue Test

The Horiba particle size distribution analyzer was utilized to determine the percent fines content in base course mixtures. A viscous solution, composed of soil and water, flows through a beam of light to detect the particle sizes. The light scattering device analyzes various particle dimensions in the viscous solution passing through the light beam. The

data analysis runs through the Horiba software and produces a distribution of size fractions from the smallest to largest particle dimension. The particle size distribution analyzer was used to obtain percent fines content for each pit. The amount of the soil passing through the No. 200 sieve and the 2 microns size particles was determined. This device provides a particle size distribution in the shape of a cumulative percent passing gradation curve. In this curve, the percent passing the 2 microns size is the most significant portion because it represents the amount of percent clay particles.

The Horiba analysis outcomes were used to determine the percent fines content (*pfc*) for each of the pits. The percent fines contents (*pfc*) represents the particle size fraction passing the No. 200 (0.075 mm which equals 75 microns) sieve size. The percentage of the 2 micron size of the material is determined through the cumulative distribution curve. The percent fines content fraction (*pfc*) is the percent of the material passing the 2 micron size divided by the percent of the material passing the No. 200 sieve (75 micron size). The *pfc* was determined for base course samples for all of the nine-(9) aggregate quarries by using the same test process.

W.R. Grace has proposed a methylene blue test to determine the Methylene Blue Value (MBV) in aggregate mixes. The MBV is an indicator that represents the solution concentration of percent fines content in the mix. This is a relatively rapid test. However, this test method was not set up to measure directly the amount of active clays in an aggregate base course mixture. Therefore, the W.R. Grace test method is calibrated to enable its use for different types of aggregate to determine the percent fines fraction in the mix. In addition, this test method is further modified to represent a direct relation

between the methylene blue value and percent fines content in any type of aggregate mixture.

1.4.5 Develop a Model between pfc and Methylene Blue Value

The methylene blue test and particle size distribution analysis results were evaluated in this task. Based on the results, a model was developed between methylene blue value and percent fines content (*pfc*). This model was used to identify active and non-active soils. This model also represents change in soil mineralogical characteristics with respect to the methylene blue value.

1.4.6 Develop Soil Dielectric Characteristic Curve (SDCC) Model

The relationship between the base course material suction and the dielectric value was investigated by using a percometer and filter paper measurements of suction. A large number of these measurements were performed on various materials that were compiled from nine-(9) different quarries. All of these measurements were used to develop a unique suction-dielectric constant relationship, which gives the whole range of suction change with the material dielectric constant. This model is denoted as Soil Dielectric Characteristic Curve (SDCC).

1.4.7 Develop Soil Water Characteristic Curve (SWCC) Model for Base Course Materials

The soil-water characteristic curve is a relationship between soil suction and moisture content. The SWCC curve depends on the type of soil and aggregates. All of the

measured test data have been used to generate a SWCC for each of the various aggregate sources.

The experimental study found that the methylene blue test and percent fines content (*pfc*) value have relationships that fit well with several important aggregate characteristics. The *pfc* is an input parameter to generate the suction water characteristic curve (SWCC). This SWCC curve is generated by using four parameters, all of which are functions of the pfc. Consequently, the *pfc* is a vital parameter to be determined in order to generate the entire curve of the SWCC.

The four SWCC curve parameters depend upon two experimental parameters that come from the gradation curve and the methylene blue test. These parameters are the percent of soil weight smaller than 75 μm (#200 sieve) and 2 μm. The second parameter is the percent of fines content, which is the amount of the sample that is smaller than 2 microns (2 μm).

The relationship between the soil moisture content and suction is the soil water characteristic curve. The form of the SWCC, which is based on the volumetric water content and suction, is by Fredlund and Xing (1994).

1.4.8 Develop a Dry Unit Weight Model

There is a need to have a model to determine the unit weight of an aggregate mixture. Thus, the dry unit weight can be estimated very accurately once the water content is known using the compaction curve model that has also been developed. This new model is a relationship between the dry unit weight and the water content of the measured compaction curve using the material properties.

This dry unit weight model consists of three curve shape parameters a_d, b_d, n_d, all of which depend on the percent fines content, methylene blue value and specific gravity. These three parameters show variation based on aggregate sources (pit) and the geological characteristics of the source.

1.4.9 Developing a Diffusivity Model

The soil diffusion rate for the base course from each quarry was determined based on the water weight loss test data. The test results have shown that there is a relationship between percent fines content and diffusion rate. Also, the results illustrated the trends between the diffusion values and the percent fines content, and these relationships are formulated as power equations. The results have demonstrated that the diffusion relationships changed with the soil methylene blue value.

1.4.10 Atterberg Limit Models

Atterberg limits consisting of liquid limit, plastic limit, and plasticity index are among the most extensively used soil index properties to determine engineering properties of soils. There are standard laboratory test procedures to determine the Atterberg limits. These standard test procedures require a certain amount of laboratory work and waiting time. The traditional Atterberg limit method required the determination of the moisture content and is very labor-intensive. According to the standard test manual, drying takes at least 12 hours by using a standard oven to measure water content. On the other hand, the new methylene blue test is a test method capable of determining Atterberg limits in a shorter time, approximately 15 minutes.

1.4.11 FWD and GPR Field Verification

The Falling Weight Deflectometer (FWD) is a nondestructive test device to determine the modulus of both base and subgrade. The structure of a typical FWD mainly consists of a mass load and attached sensors that are 12 inches apart. The FWD applies a dynamic load to the surface to give impulse on the surface, and then the surface deflection is measured through a series of geophone sensors. The deflection profile of each of the geophones is determined and analyzed by using different mathematical models, and the modulus of each layer is calculated based on the analysis. In this analysis process a modulus for each layer is initially assumed, and then the deflection of the surface is determined by using the backcalculation. When the calculated deflections are matched with the measured deflections, the determined layer moduli are recorded as the final values.

These field measurements will be made in a base course that have been taken from a quarry with known aggregate properties that had been measured by TxDOT before the construction began.

They will be used to validate the modulus model, which was developed in TxDOT 0-6621. This model determines the base course moduli using only the suction water content curve (SWCC), dielectric constant, *pfc* and dry unit weight. Base course moduli, which are determined by using the two methods, will be compared. The correlation of the base course model with the modulus measured in the field will demonstrate its degree of validation.

1.4.12 Model of Permanent Deformation and Field Verification

Ground Penetrating Radar (GPR) is a nondestructive testing device used to determine the dielectric constant and layer thickness of pavements. The knowledge of the layer dielectric and structural information is used to identify the presence of the layers' wetter areas, which are more susceptible to permanent deformation. GPR presents the collected data in a colored map analysis system. The percometer is also a nondestructive test device to measure material dielectric value in a precise, accurate fashion. The SDCC model is generated by using the percometer device readings of dielectric constant values. There is considerable synergy in integrating the two analysis methods under the same roof. The integration will carry out a model that is capable of showing the base course layer stiffness map along with showing the water content and suction. This integrated model will present the base course properties and as-built properties. This improvement will be used in the QA phase of construction.

1.4.13 Developing a New Software

Reviewing the properties that are necessary to measure in the field shows that the water content, suction, and percent fines content can be determined by using the MBV relationship with them. A field method was developed to measure all of these rapidly and accurately. The method requires the development of suction vs. water content (SWCC) and suction vs. dielectric constant (SDCC) curves for each source of base course in the laboratory prior to construction. The labor involved in doing this is less than what is required for compaction curves.

In the field, these measurements can be made and evaluated by using a software program. At the end of the work plan a software program was written and programmed to be used as a base course quality management tool. This software program increases the speed of the test process and reduces analysis time of the outcomes in the field and laboratory as well. This software is also a useful tool to calculate base course modulus and determine the performance of the base course materials as built. Since field measurements are simple and quick enough to provide outcomes immediately, this new software is also very prompt to calculate the performance at the location of the base materials where all of the field measurements were taken.

1.4.14 Summary

A summary will conclude all the findings regarding the base course models and the methods that have been developed during this study. The major key findings and improvements determined in each task will be given in a summary.

2. BASE COURSE MODELS: AN OVERVIEW

2.1 Introduction

In flexible pavement system unbound granular materials are the most commonly used substance in the base course and subbase layers to distribute the wheel load. The aggregate base layer provides significant support to the load bearing capacity in a flexible pavement system. The failure of the unbound aggregate material and subgrade layer are proportional to the magnitude of the permanent deformation (rutting) or resilient strain. The mathematical characterization of unbound granular materials in flexible pavement system has been a research challenge for pavement engineers. In order to overcome these challenges the mechanical characteristics of resilient properties and rutting characteristics of unbound aggregates require development of proper plastic deformation and resilient modulus models in the pavement foundations. Existing pavement analysis methods based on the nonlinear behavior of subgrade soil and unbound aggregate with assigned cross-anisotropic properties are well documented (Barksdale et al., 1989; Adu-Osei, 2000; Seyhan, 2005; Oh et al., 2006; Asthiani, 2009).

The resilient behavior of a pavement system plays a very important role in the fatigue cracking analysis. The rutting characteristic of a pavement system requires the permanent deformation properties of unbound aggregate materials. The repeated load triaxial (RLT) test is capable of predicting the resilient and permanent deformation behavior of granular material in the laboratory.

The mechanical properties of unbound aggregate affected by the layer factors like density, stress history, void ratio, temperature, time, and pore water pressure. It is a significant challenge in developing a proper simple model that integrates all of these factors to mimic realistically the unbound aggregate response within the framework of continuum mechanics.

Previous research, for instance, has investigated the aggregate geometric characteristics of angularity, shape, and surface texture, and it was found that aggregate characteristics have an impact on the resilient and permanent deformation responses (Barksdale, 1991).

The repeated load triaxial (RLT) test is performed under a representative stress path to determine deformation behavior of unbound aggregate layer in the laboratory environment. The RLT is the most conventional standard test method and is used in measuring directly the principal stress and strains from a cylindrical sample. The strain measured in RLT includes a resilient (elastic) part, which is used to predict resilient modulus, and a plastic (non-recoverable) part, which is used to characterize the plastic deformation in a pavement system (Lekarp et al., 2000).

This part of the study has investigated previous scholarship related to developing experimental and analytical approaches used in characterization of granular base and subbase layers. The following section briefly examines the resilient modulus models and later discusses briefly the test protocols to determine the permanent deformation model for unbound granular materials in flexible pavement systems.

2.2 Resilient Behavior Models of Unbound Aggregates

The resilient response properties of unbound granular materials is typically characterized by the resilient modulus and Poisson ratio in pavement engineering. The resilient responses of the layers in the pavement system play an important role in calculating the layer thickness and identifying the crucial layer responses with a repeated the traffic load.

Previous researchers have used laboratory test data to model the unbound aggregate materials in the pavement foundation. The following section provides a discussion of the selected models proposed by pavement engineers to describe the resilient behavior of unbound aggregate materials.

2.2.1 Confining Pressure Model

This model originally proposed by Seed shows that resilient modulus is a function of confining pressure. The repeated load triaxial tests were performed on sand and gravel both in saturated and dry moisture states (Seed et al., 1967). The confining pressure model is given in (2-1):

$$M_R = k_1(\sigma_3)^{k_2} \tag{2-1}$$

where σ_3 is the confining pressure (psi), k_1 and k_2 are regression constants determined from experiment data that is fitting into the model.

2.2.2 Bulk Stress ($k-\theta$) Model

This model originally reported by Hicks and Monismith considers the nonlinear description of the resilient modulus and stresses the sensitivity of unbound aggregates.

This model was implemented in the AASHTO Guide for the Design of Pavement Structures. This model was commonly used among the pavement engineers (Hicks et al. 1971). The resilient modulus was given in Equation (2-2):

$$M_R = k_1(\theta)^{k_2} \tag{2-2}$$

where θ is the bulk stress which is the sum of the principal stresses $(\sigma_1 + 2\sigma_3)$, k_1 and k_2 are regression fitting parameters.

2.2.3 Uzan Model

This model originally developed by Uzan modifies the bulk stress model by including the deviator stress term to catch the softening in shear behavior in unbound aggregates (Uzan 1985). This model is defined in Equation (2-3):

$$M_R = k_1(\theta)^{k_2}(\sigma_d)^{k_3} - \tag{2-3}$$

where θ is the bulk stress which is the sum of the principal stresses $(\sigma_1 + 2\sigma_3)$, σ_d is deviator stress $(\sigma_1 - \sigma_3)$, k_1 and k_2 are regression fitting parameters.

The capability of the Uzan model appears to account for the shear softening and degradation of the resilient modulus better than the $k-\theta$ model (Adu-Osei, 2000).

Witczak and Uzan (1988) modified Equation (2-3) by replacing the bulk stress term with the first stress invariant and also the deviatoric term with the octahedral shear stress. The purpose of the stress components to non-dimensionalized changed the model to facilitate easy unit conversion. The Uzan model became favored as the universal

model by pavement engineers in application of routine pavement system analysis. The universal model is given in Equation (2-4):

$$M_R = k_1 P_a \left(\frac{I_1}{P_a} \right)^{k_2} \left(\frac{\tau_{oct}}{P_a} \right)^{k_3} \tag{2-4}$$

where I_1 is the first stress invariant (sum of principal stresses), τ_{oct} is the octahedral shear stress, P_a is the atmospheric pressure, k_1, k_2 and k_3 are model fitting parameters.

In the resilient modulus model, Equation (2-4) the term $\left(\frac{\tau_{oct}}{P_a} \right)^{k_3}$ is known as the softening component, and the term $\left(\frac{I_1}{P_a} \right)^{k_2}$ is known as the hardening component.

2.2.4 Bulk-Shear Modulus Model (K-G Models)

This model developed by Boyce (1976) shows the influence of mean normal stress (p) and the ratio of deviatoric stress to normal stress. The non-linear stress-strain behavior of unbound aggregates was developed to show the decomposition of stresses and strains in volumetric and shear components (Boyce 1976). Later, Boyce improved the resilient modeling by considering the secant bulk modulus (K) and the secant shear modulus (G) for granular materials (Boyce 1980). These developed models are given in Equations (2-5) and (2-6):

$$K = \frac{K_i p^{(1-\mu)}}{1 - \beta \left(\frac{q}{p} \right)^2} \tag{2-5}$$

$$G = G_i p^{(1-\mu)} \tag{2-6}$$

where K_i and G_i are initial values of bulk and shear moduli respectively, μ is a model constant less than 1.0, q is the deviator stress, and $\beta = (1-\mu) K_i / (6G_i)$.

In the bulk shear model, volumetric and deviatoric strains depend on the deviatoric stress ($q = (\sigma_1 - \sigma_3)$) and mean normal stress ($p = (\sigma_1 + \sigma_2 + \sigma_3)/3$). The K-G model is given in Equations (2-7) and (2-8):

$$\varepsilon_v = \left(\frac{1}{K_i}\right) p^n \left[1 - \beta \left(\frac{q}{p}\right)^2\right] \tag{2-7}$$

$$\varepsilon_q = \left(\frac{1}{3} G_i\right) p^n \left(\frac{p}{q}\right) \tag{2-8}$$

where ε_v is the volumetric strain and ε_q is the shear strain.

2.2.5 Counter Model

The Boyce (1976) model was modified by Brown and Papin (1981) to improve the earliest version of the model by extending three parameters to five parameters and accounting for the stress path effects. This model utilizes the shear and bulk moduli to characterize granular materials properties. The contour model determines the shear and the volumetric strain by the following Equations (2-9) and (2-10):

$$\varepsilon_v = \left(\frac{1}{K_i}\right) \left(\frac{p}{p_0}\right)^{k_1 - 1} \left[1 - \beta \left(\frac{q}{p_0}\right)^2\right] p \tag{2-9}$$

$$\varepsilon_q = \left(\frac{1}{3G_i}\right)\left(\frac{p}{p_0}\right)^{k_2-1} q \tag{2-10}$$

$$\Delta\varepsilon_q = \left(\frac{1}{3G_i}\right)\left[\left(\frac{p_2}{p_0}\right)^{k_2}\frac{q_2}{p_2} - \left(\frac{p_1}{p_0}\right)^{k_2}\frac{q_1}{p_1}\right]\ell^{k_3}$$

where K_i and G_i are initial bulk and shear moduli, p_0 is the reference pressure,

$\ell = \left(\Delta p^2 + \Delta q^2\right)^{\frac{1}{2}}$ is the path length between stress state 1 and stress state 2, and β, k_1, k_2 and k_3 are the statistical material constants.

The counter model provides resilient modulus accurately within a broad range of stress paths. However, β, k_1, k_2 and k_3 are statistical material constants that require calculations, and hence the analytical and laboratory test procedure may turn out to be more sophisticated for routine applications (Tutumluer, 1995).

2.2.6 Lytton Model

This model developed by Lytton uses the principles of unsaturated soil mechanics, and Lytton applied these principles to the Uzan model. Lytton included volumetric water content and a suction term to the Uzan model to capture the impact of moisture on the stiffness properties and effect of resilient properties on partially saturated granular aggregates (Lytton 1995). The Lytton resilient model is given in Equation (2-11):

$$M_R = k_1 P_a \left(\frac{I_1 - 3\theta fh_m}{P_a}\right)^{k_2}\left(\frac{\tau_{oct}}{P_a}\right)^{k_3} \tag{2-11}$$

where I_1 is the first stress invariant (sum of principal stresses), τ_{oct} is octahedral shear

stress, P_a is the atmospheric pressure, θ is the volumetric water content, h_m is the matric suction, f is the function of the volumetric water content, and k_1, k_2 and k_3 are the model fitting parameters.

The function of the volumetric water content is given in Equations (2-12) to (2-14):

Moist Soil (Wet Soil) pF>3.5 $f = 1$ (2-12)

$$f = 1 + \frac{S - 85}{15}\left(\frac{1}{\theta} - 1\right) \quad (2\text{-}13)$$

Effectively Saturated pF<2 $f = \frac{1}{\theta}$ (2-14)

where S is the degree of saturation.

2.3 Permanent Deformation Models of Unbound Aggregates

The repeated triaxial test showed that the applied energy in a sample has two types of components; the applied energy that can be recovered is resilient energy or non-recoverable energy. Most of the applied energy in unbound aggregates turns into permanent strain accumulated with the repetition and causes an increase in rutting. Permanent lateral shearing movement and volumetric compression are two parts of the rutting behavior in aggregate base courses (Adu-Osei, 2000).

The mechanistic design methods aim to control the effect of the fatigue damage by reducing the resilient strain at the bottom of the asphalt layer, and also the impact of rutting by limiting the vertical compression strain at the top of the subgrade unbound aggregate layer.

Several studies have been conducted on modeling the permanent deformation characteristics in unbound aggregate materials. The proposed model usually correlates the plastic strain to the number of load applications or a stress condition. The following section presents reviews on selected models proposed by pavement engineers to determine permanent deformation behavior of unbound aggregate materials.

2.3.1 Hyperbolic Model

This model originally developed by Duncan and Chang determines plastic deformation properties under static loading within a wide range of stress states (Duncan and Chang, 1970). The hyperbolic model was given in Equation (2-15):

$$\varepsilon_p = \frac{\sigma_d}{k_1 \sigma_3^{k_2}} \Bigg/ \left[\left(1 - \frac{\sigma_d R_f}{2\left(C\cos\phi + \sigma_3 \sin\phi\right)} \right) \frac{1}{\left(1 - \sin\phi\right)} \right] \tag{2-15}$$

where ε_p is the axial plastic strain, $k_1 \sigma_3^{k_2}$ is the relationship defining the initial tangent modulus as a function of confining pressure when k_1 and k_2 are constant values, C is the cohesion of the soil, ϕ is the angle of internal friction, and R_f is the ratio of measured strength to ultimate hyperbolic strength.

2.3.2 VESYS Model

The VESYS is a computer program that was developed with an approach to calculate permanent strain for each layer and sum the calculated rut depths to determine the total rut depth of an asphalt pavement surface. This model uses the linear elastic layered pavement model, and considers the permanent strain is proportional to the resilient strain (Kenis, 1978). The VESYS model was presented in Equation (2-16):

$$\varepsilon_p(N) = \varepsilon\mu N^{-\alpha} \tag{2-16}$$

where $\varepsilon_p(N)$ is the plastic or permanent strain due to single load or N^{th} load application, ε is the elastic or resilient strain at the 500^{th} repetition, N is the number of load repetition, μ is a parameter representing the constant of proportionality between permanent strain and elastic strain, and α is a parameter indicating the rate of decrease in permanent strain with number of load repetition.

2.3.3 Exponential or LogN Model

This approach was developed by Lent and Baladi and is one of the most commonly used method to determine the permanent strain of unbound aggregate material. This approach primarily shows that the rate of change in permanent strain is quite large in the first few loading cycles; however, this rate changes and progressively decreases as the loading cycles continue (Lentz and Baladi, 1981). The general form of this model is presented in Equation (2-17):

$$\varepsilon_p = AN^b \text{ or } \log\varepsilon_p = a + b\log N \tag{2-17}$$

where N is the number of repeated load application, ε_p is the permanent strain, α and b are experimentally determined factors, and A is the antilog of α.

2.3.4 Ohio State University (OSU) Model

This model was developed by Ohio State University and become very popular for determination of permanent strain. VESYS and OSU model were developed based on using same mathematical concept, and the OSU model was proposed to Ohio

Department of Transportation as a permanent deformation model (Majidzadeh, 1980). The OSU model is presented in Equation (2-18):

$$\frac{\varepsilon_p}{N} = AN^m \tag{2-18}$$

where N is the number of repeated load application, ε_p is the permanent strain, m is the experimental constant depending on material type, and A is the experimental constant dependent on material and state of stress conditions.

2.3.5 Tseng and Lytton Model

This model was originally developed by Tseng and Lytton to predict the permanent deformation characteristics of the unbound aggregate materials by using the three parameters model (Tseng and Lytton, 1989). The general form of the model is presented in Equation (2-19):

$$\varepsilon_p = \varepsilon_0 \exp^{-\left(\frac{\rho}{N}\right)} \tag{2-19}$$

where N is the number of repeated load application, ε_p is the permanent strain, ε_0, β and ρ are material parameters.

Three material parameters depend on unbound aggregate material types and are affected by test conditions such as confining pressure, deviatoric stress and density.

2.3.6 Rutting Rate (RR) Model

This model was introduced by Thompson and Naumann predicts the rate to rutting. The AASHTO road test data was analyzed by using the RR model to evaluate the permanent

deformation depth in the pavement system (Thompson and Naumann, 1993). The RR model is presented in Equation (2-20):

$$RR = \frac{RD}{N} = \frac{A}{N^B} \tag{2-20}$$

where N is the number of repeated load application, RR is the rutting rate, RD is the rut depth (inches), A and B are the terms that were developed from field calibration testing data and information.

2.3.7 Yield Surface Model

This model developed by Bonaquist and Witczak utilizes the yield surfaces from a flow theory model. The yield surfaces mechanism basically indicate the magnitude of permanent strain during the first loading cycle. Bonaquist and Witczak observed based on the a set of repeated load test data that yield surface shows coherence between permanent strain at a load cycle related to the permanent strain on the first cycle and also the number of load cycles (Bonaquist and Witczak, 1996). The Yield Surface model is given in Equations (2-21) and (2-22):

$$\xi_N = \frac{1}{N^{1.06}} \xi_i \tag{2-21}$$

$$\varepsilon_p = \sum \xi = \sum \left(\frac{1}{N^{1.06}} \right) \xi_i \tag{2-22}$$

where N is the number of repeated load application, ξ_N is the permanent strain for load cycle N, ξ_i is the permanent strain for the first load cycles and $\sum \xi$ is the accumulated permanent strain.

Equation (2-22) shows the sum of the accumulated permanent strain based on each loading cycles.

2.3.8 Shakedown Model

This model has developed based on the computational procedure originated from the shakedown theory. A pavement system accumulates the permanent strain under repeated load according to the shakedown theory the amplitude of the load surpassing a limit, which is known as the shakedown load. When the load repetition passes the shakedown load, the pavement yields an incremental collapse or a gradual failure. The increase in plastic strain become a smooth surface when the applied load is smaller than the shakedown limit. In the laboratory, different unbound granular materials are tested by using the repeated load triaxial test to develop a correlation between the permanent strain, the number of applied load, the stress path, and the maximum shear stress ratio for the entire pavement structure by using the principles of the shakedown theory from Lekarp and Dawson (1998). The form of the developed model is presented in Equation (2-23):

$$\frac{\varepsilon_{1,p}(\mathrm{N_{ref}})}{(L/\mathrm{P_0})} = a\left(\frac{\sigma_d}{I_1}\right)^b_{\max} \tag{2-23}$$

where $\varepsilon_{1,p}(\mathrm{N_{ref}})$ is the accumulated permanent axial strain after a given number of cycles $\mathrm{N_{ref}}(\mathrm{N_{ref}} > 100)$ number of repeated load application, L is the stress path length, I_1 is the first stress invariant (sum of principal stresses), σ_d deviator stress, a and b are material properties.

3. PERFORMANCE PREDICTION MODELS FOR BASE COURSES AND LABORATORY TESTING

3.1 Introduction

In a flexible base course system, the base course is defined as the layer that is laid between asphalt and subgrade layers. The function of the base layer is to provide the support to the covered asphalt layer and protect the subgrade from permanent deformation. When a weak bearing stress, in unbound aggregate layer, is subject to repeated traffic loads, the top asphalt pavement layer become poor from the beneath support, and hence it becomes more prone to permanent deformation (Kancherla, 2004). Therefore, the permanent deformation (rutting) characteristics of unbound aggregates play an important role in the prediction of the permanent deformation of the unbound aggregate base layer. Along with the permanent deformation, the resilient modulus of unbound aggregates has been widely recognized as the primary mechanical property of the base course required in the mechanistic-empirical design of pavement structures. The resilient modulus is defined as the ratio of the maximum cyclic stress to the recoverable resilient strain in one repeated dynamic loading cycle. It can be used to describe the response of the base layer under the traffic load.

This study provides information regarding both the resilient modulus models and the permanent deformation. A detailed explanation of the test procedures, material preparation and testing procedure is provided in a subsequent section. The next section presents the resilient modulus model sampling and testing procedure, and the subsequent section covers the permanent deformation models sampling and testing procedure. The

final section presents the Aggregate Imaging System (AIMS) test procedure and covers the analysis outcomes of the aggregates geometric characteristics index.

3.2 Resilient Modulus Test

3.2.1 Test Protocol and Procedures

The loading protocol used in the resilient modulus test was developed based on the cross-anisotropic behavior of granular materials. Although the cross-anisotropic behavior of granular materials has been well recognized, the loading protocols developed by AASHTO T 307 and NCHRP Project 1-28A still does not take it into consideration. The calculated stress responses of an aggregate layer are demonstrated in Figure 3-1.

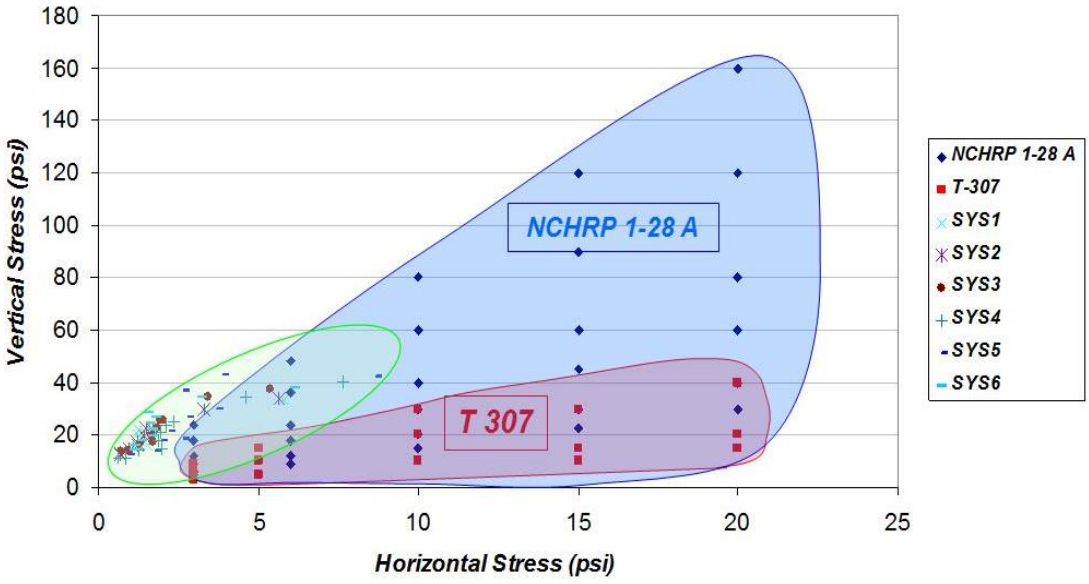

Figure 3-1 Anisotropic Stress Responses of Base Layer Test Protocols (Ashtiani, 2009)

Figure 3-1 also plots the loading level and stress envelopes for AASHTO T 307 and NCHRP 1-28A (Ashtiani, 2009). One finite element model was established to calculate the responses of aggregate layers under actual traffic loading when considering the cross-anisotropic characteristic. It is obvious that the stress envelopes for AASHTO T 307 and NCHRP 1-28A do not agree well with the responses of the finite element model. Under these circumstances, a new loading protocol is needed to cover the actual response of aggregate layers under various traffic loading types. For this purpose the new loading sequences for the resilient modulus test are shown in Table 3-1. For each loading sequence, the samples were tested at a constant confining pressure and under a specific axial cyclic stress using a haversine shape with a 0.1 second load duration and a 1.0 second cycle duration.

Table 3-1 Loading Sequences for Resilient Modulus (Epps et al., 2013)

Sequence	Confining Pressure (psi)	Contact Stress (psi)	Cyclic Stress (psi)	Maximum Stress (psi)	N_{rep}
0	15	1.5	13.5	15	500 – 1000
1	2	.4	9.6	10	100
2	2	.4	14.6	15	100
3	2	.4	19.6	20	100
4	2	.4	24.6	25	100
5	2	.4	29.6	30	100
6	4	.8	9.2	10	100
7	4	.8	14.2	15	100
8	4	.8	24.2	25	100
9	4	.8	34.2	35	100
10	4	.8	44.2	45	100
11	6	1.2	18.8	20	100
12	6	1.2	28.8	30	100
13	6	1.2	38.8	40	100
14	6	1.2	48.8	50	100
15	6	1.2	58.8	60	100
16	8	1.6	18.4	20	100
17	8	1.6	28.4	30	100
18	8	1.6	38.4	40	100
19	8	1.6	48.4	50	100
20	8	1.6	58.4	60	100
21	10	2.0	18	20	100
22	10	2.0	28	30	100
23	10	2.0	38	40	100
24	10	2.0	48	50	100
25	10	2.0	58	60	100

3.2.2 Sample Preparation

Base course aggregate specimens were prepared by using a vibratory compaction machine based on the recommendation in AASHTO T 307 sampling protocol. These granular specimens were compacted at the given moisture content and corresponding densities. In this study, the specimen dimensions are 6 in. diameter with 12 in. height. After de-molding, the specimen was wrapped in a plastic membrane to minimize moisture loss and was kept for 14 hours, or overnight, to allow the water inside the specimen to distribute uniformly. One linear variable differential transformers (LVDTs)

was attached on each side of specimen before it was placed into the triaxial chamber. The gauge length of LVDTs used to compute strain was 6 inches. Figure 3-2 shows the specimen with LVDTs before the repeated loading test started.

Figure 3-2 Sample Preparation before Resilient Modulus Test

3.2.3 Test Procedure

The resilient modulus test was conducted on cylindrical aggregate specimens using the triaxial chamber with the Material Testing System (MTS). Figure 3-3 illustrates the configuration of the resilient modulus test. Prior to the test, the chamber moved downward to seal the specimen; then, the pressure inside the chamber was increased until it reached the desired constant pressure. This confining pressure is applied directly to the sample. Then, the MTS applied an axial load to the specimen through the loading

frame. The entire testing process was controlled by a computer using programs that specified the axial load and the confining pressure. During each test, the two LVDTs measured the vertical deformations of the specimen. The test data were used to determine the recoverable and unrecoverable behavior of the granular material.

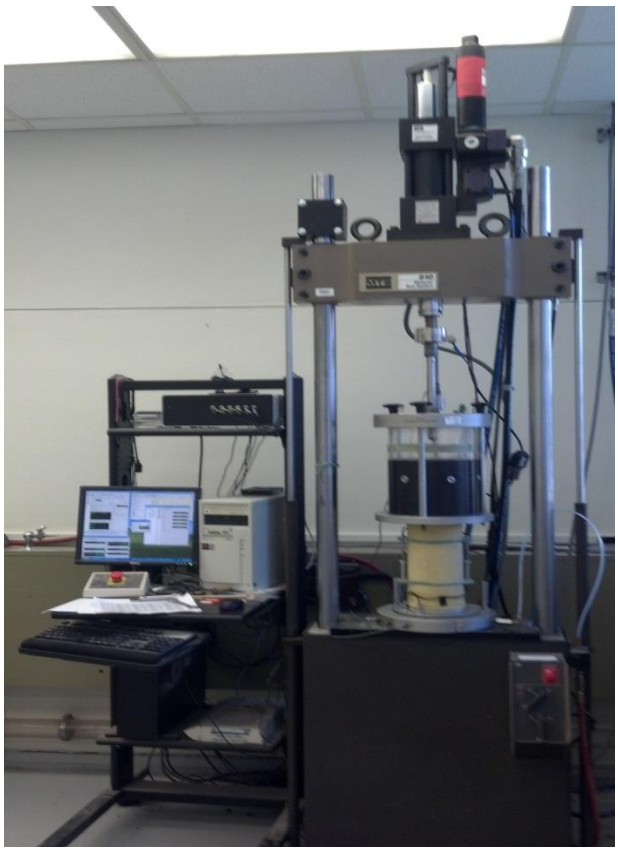

Figure 3-3 Configuration of Material Testing System Test Machine with a Mounted Sample

3.2.4 Test Results

The resilient modulus of the aggregate matrix specimen was measured from each loading sequence. Because granular material is stress-dependent, the resilient modulus

model needs to be developed to predict resilient modulus at any specific stress level. In this study, the universal model in AASHTO 2002 was used to determine the resilient modulus. The model used is presented in Equation (3-1):

$$E_y = k_1 P_a \left(\frac{I_1 - 3\theta f h_m}{P_a}\right)^{k_2} \left(\frac{\tau_{oct}}{P_a}\right)^{k_3} \quad (3\text{-}1)$$

where I_1 gives the first invariant of the stress tensor, P_a is the atmospheric pressure, θ represents the volumetric water content, h_m is the matric suction in the aggregate matrix, f yields the saturation factor, $1 \le f \le \frac{1}{\theta}$, τ_{oct} is the octahedral shear stress, and k_1 , k_2, and k_3 are material parameters that are dependent on material properties of the base course.

The base course properties used in the development of the prediction models are presented in Table 3-2.

Table 3-2 Example Resilient Modulus Test Results for Aggregate Specimen at Optimum Moisture Content

Source Type	γ_d (lb/ft^3)	pfc	k_1	k_2	k_3	Matric Suction (kPa)	Resilient Modulus (ksi)	R^2
E-06-1-13	150.7	13.2	1733	0.46	0.16	-50.1	41.47	0.89
E-06-2-6	150.4	12.3	2662.74	0.26	0.24	-39.8	47.88	0.73
E-05-Drum	140.7	21.5	689.1	1.31	-0.16	-20	46.99	0.99
E-02-1-3-4	137.1	11.4	144.1	1.48	-0.17	-100	19.06	0.99
E-02-2-3-2	136.3	13	349.6	1.1	-0.06	-100	23.89	0.99
E-04-1-3	140.2	12.7	386.2	1.44	-0.1	-125.9	49.37	0.93
E-09-1-14	136.4	13.3	1415.7	0.78	-0.01	-63.1	58.65	0.99
E-07-69-1-14	137.7	15.5	391.5	1.34	-0.12	-63.1	34.98	0.74
E-07-68-2-6	139.4	15.8	537.2	1.08	-0.1	-63.1	33.68	0.7
E-08-235-1- 12	145.8	13.3	1564.5	0.73	0.07	-39.8	53.72	0.97
E-08-2-1-6	140.4	15	1072.5	1.02	-0.08	-100	68.70	0.96
E-01-1-3-2-3	143.0	16.1	3002.5	0.27	0.06	-63.1	59.94	0.93
E-01-Drum	141.2	19.7	2496.1	0.51	0.05	-63.1	68.49	0.96
E-03-6-10-3	130.6	22.8	1835.3	0.11	0.12	-316.2	30.14	0.75

Table 3-2 provides examples of the analysis results of the resilient moduli of all aggregate samples tested at the optimum moisture content and under a confining pressure at 7 psi and a deviatoric stress at 20 psi.

3.3 Permanent Deformation

3.3.1 Permanent Deformation Models

The permanent deformation model needs to be established to accurately predict the long-term performance of granular base course materials. The vast majority of permanent deformation models found in literature were developed based on using laboratory test results. In this study, the VESYS model and Tseng-Lytton model were used to evaluate the permanent deformation behavior of aggregate materials (Zhou and Scullion, 2002; Tseng and Lytton, 1989).

3.3.2 VESYS Model

The VESYS model assumes that the relationship between permanent deformation and number of load applications is linear in a logarithm scale, which is expressed in Equation (3-2):

$$\varepsilon^p(N) = IN^s \tag{3-2}$$

By assuming the resilient strain is constant for each loading application, which can be expressed in Equation (3-3):

$$\frac{1}{\varepsilon_r}\left(\frac{\partial \varepsilon^p(N)}{\partial N}\right) = \left(\frac{IS}{\varepsilon_r}\right)N^{S-1} \tag{3-3}$$

when assuming $\mu = \frac{IS}{\varepsilon_r}$ and $\alpha = 1 - S$, Equation (3-4) can be rewritten as:

$$\frac{1}{\varepsilon_r}\left[\frac{\partial \varepsilon^P(N)}{\partial N}\right] = \mu N^{-\alpha} \tag{3-4}$$

where ε_r yields the resilient strain of the granular aggregate, ε^p represents the permanent strain of the granular aggregate, N gives the number of load cycles, μ is the parameter representing the constant of proportionality between permanent and resilient strain, and α is the parameter indicating the rate of decrease in permanent strain with the number of load applications.

3.3.3 Tseng-Lytton Model

Tseng and Lytton (1989) developed a three-parameter model to predict the relationship between the permanent strain and the number of loading cycles for the granular material, which is expressed in Equation (3-5):

$$\varepsilon_p = \varepsilon_0^p e^{-(\frac{\rho}{N})^\beta} \tag{3-5}$$

where ε_p represents permanent strain of granular material, ε_0^p is the maximum permanent strain, ρ gives the scale factor; and β is the shape factor.

In the MEPDG manual, this equation was modified to predict the permanent deformation of aggregate layers with thickness, h, using Equation (3-6):

$$\varepsilon_p = (\frac{\varepsilon_0}{\varepsilon_r}) e^{-(\frac{\rho}{N})^\beta} \varepsilon_v h \tag{3-6}$$

where ε_v is the vertical strain in the granular aggregate layer, and h gives the thickness of the aggregate layer.

3.3.4 Test Protocol and Procedures

The permanent deformation test was begun with sequence zero as the preconditioning step as shown in Table 3-3. The following sequence (sequence one) was used to determine the unrecoverable behavior of the granular material. The stress level of sequence one was determined according to the actual stress response of the aggregate layer under standard traffic loading. The static confining pressure and haversine-shaped deviator stress with 0.1 second load period and 0.9 second rest period were applied to the specimen for 10,000 cycles. The cumulative plastic strains were recorded to characterize the permanent deformation behavior of aggregate material.

Table 3-3 Example Resilient Modulus Test Results for Aggregate Specimen at Optimum Moisture Content

Sequence	Confining Pressure (psi)	Contact Stress (psi)	Cyclic Stress (psi)	Maximum Stress (psi)	N_{rep}
0	15	1.5	13.5	15.0	500 – 1000
1	7	2.0	18	20.0	10,000

3.3.5 Test Results

The two most commonly accepted permanent deformation models, VESYS model and Tseng-Lytton model, were used to analyze the permanent deformation test data. The permanent deformation test results for different materials at optimum water content are tabulated in Table 3-4.

Table 3-4 Summary of the Permanent Deformation Test Results for Aggregate Specimens at Optimum Water Content

Material Type	ε_r at 500th load application	VESYS Model Parameters		Tseng-Lytton Model Parameters		
		α	μ	ε_0	ρ	β
E-06-1-13	0.000389	0.811	0.437	8.38E-03	890	0.301
E-06-2-6	0.000307	0.769	0.294	5.04E-03	860	0.305
E-05-61-12	0.000359	0.776	0.461	9.32E-03	940	0.287
E-05-Drum	0.000406	0.727	0.888	2.72E-02	1500	0.307
E-02-1-3-4	0.000881	0.79	0.227	1.04E-02	860	0.305
E-02-2-3-2	Specimen broke during test					
E-04-1-3	0.000325	0.794	0.284	4.86E-03	940	0.292
E-04-2-6	0.000385	0.675	0.363	1.23E-02	970	0.293
E-09-1-14	0.000312	0.823	0.137	1.98E-03	820	0.310
E-07-69-1-14	0.000423	0.767	0.909	2.19E-02	900	0.300
E-07-68-2-6	0.000482	0.684	0.526	2.24E-02	1230	0.304
E-08-235-1-12	0.000361	0.711	0.349	9.19E-03	950	0.302
E-08-2-1-6	0.000228	0.647	0.196	4.50E-03	980	0.310
E-01-1-3-2-3	No permanent deformation observed					
E-01-Drum	0.000192	0.944	0.108	1.42E-03	980	0.100
E-03-6-10-3	0.000395	0.458	0.006	8.57E-04	1530	0.305

3.4 Unbound Aggregate Characteristics Measurements

3.4.1 Test Procedure

The Aggregate Image Measurement System (AIMS) is a computer integrated laboratory test device to analyze aggregate properties. The AIMS device measures aggregate shape, angularity, and texture that affect the engineering properties of the unbound aggregate layers. Therefore, the AIMS test results provide material properties that are utilized to design a base course layer through the aggregate characteristics of shape, angularity, and texture. The AIMS device is a system comprised of a computer, image acquisition hardware, a high-resolution camera, microscope, aggregate tray, and lighting system shown in Figure 3-4.

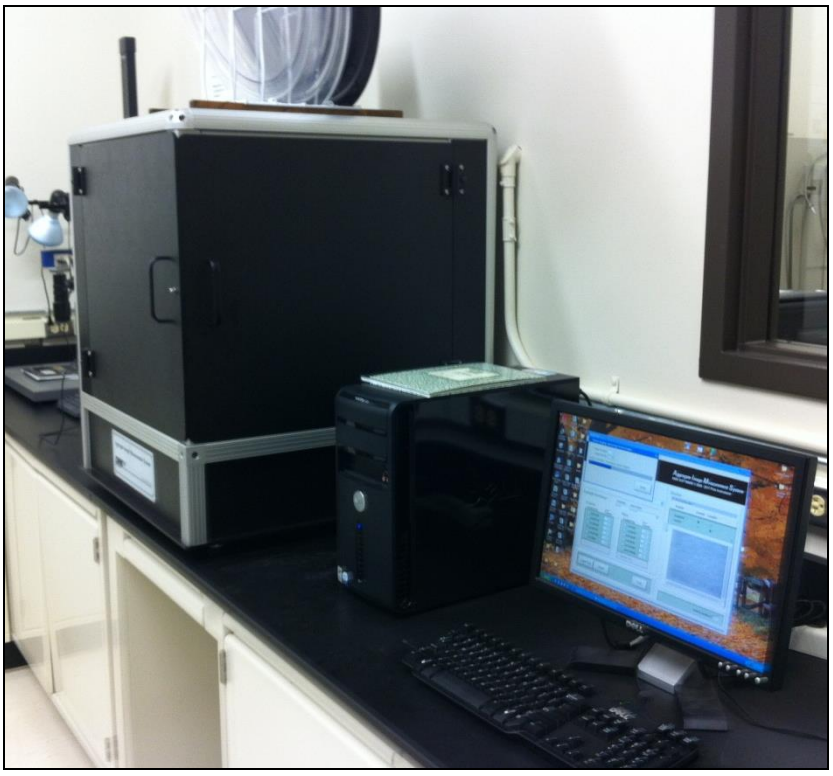

Figure 3-4 A Test Set up of AIMS Device along with a Supported Computer System

The AIMS device is capable of analyzing the aggregate materials in the size range from 0.075 mm to 37.5 mm. The aggregates with a size larger than 4.75 mm are considered coarse aggregates. The aggregates with a size smaller than 4.75 mm are considered fine aggregates.

The AIMS test was conducted on base aggregate from various quarries throughout Texas. The coarse aggregates analysis requires aggregates to be washed and separated based on three sieve sizes. The coarse aggregates are separated by retaining materials on 1/2 in., 3/8 in., and No. 4 sieves. The washed and dried coarse aggregates are placed in separate trays. Each tray rotates in the AIMS device, and an image of each

aggregate particle is captured under controlled lighting using a camera. The AIMS software analyzes shape, texture, and angularity data and outputs the analysis in the MS Excel spreadsheets.

3.4.2 Develop Weibull Distributions of Measured Gradation, Angularity, Shape, and Texture of Each Aggregate Type

Coarse aggregates from nine different quarries were tested using the AIMS device. Three representative sieve sizes (1/2 in, 3/8 in., and No. 4) were employed to analyze aggregate geometric characteristics. Angularity, shape, and texture are particle geometric characteristics that are fitted to a Weibull distribution. The Weibull distribution provides a reasonable fit to both particle size and shape properties. The Weibull distribution contains two parameters: shape parameter (α) and scale parameter (λ). These distribution parameters for each aggregate quarry are given tabulated in Table 3-5 and Table 3-6.

Table 3-5 Weibull Distribution Parameters Shape, Form, and Texture Index

Source	Sieve No.	Angularity		2D Form		Texture	
		Shape Parameter	Scale Parameter	Shape Parameter	Scale Parameter	Shape Parameter	Scale Parameter
E-05	1/2	4.07	3207.77	4.56	7.33	2.39	163.21
	3/8	3.79	3291.5	3.96	7.75	2.12	165.78
	#4	3.27	3272.77	4.12	8.59	1.78	94.17
E-06	1/2	3.81	3325.83	3.61	9.3	3.04	180.43
	3/8	4.76	3327.99	4.44	8.86	2.93	174.63
	#4	4.66	3481.14	4.2	8.66	2.08	107.76
E-02	1/2	4.35	3068.61	3.89	8.54	2.03	198.85
	3/8	5.09	3113.11	4.11	8.56	2.51	194.07
	#4	7.12	2949.7	5.54	8.6	2.44	137.12
E-09	1/2	3.91	3468.47	3.44	8.52	1.63	202.54
	3/8	3.75	3228.12	4.48	7.6	1.75	205.47
	#4	4.13	3005.48	3.89	7.86	1.61	102.08
A-42	1/2	4.03	3457.8	3.37	8.4	3.69	264.07
	3/8	4.38	3336.93	4.66	8.19	3.16	287.58
	#4	3.95	3490.31	4.43	7.95	2.66	180.7
E-07	1/2	4.12	3099.27	3.28	7.61	1.76	159.81
	3/8	4.53	3210.45	4.63	7.97	1.86	138.83
	#4	4.17	3192.53	3.88	7.89	2.27	98.44
E-08	1/2	3.77	3314.52	4.11	8.26	1.76	161.21
	3/8	4.99	3342.81	3.63	8.72	1.48	205.58
	#4	4.14	3266.97	3.65	8.33	1.82	115.4
E-04	1/2	4.07	3100.49	3.69	7.96	2.02	164.42
	3/8	5.1	3072.87	3.65	8.03	1.96	171.51
	#4	4.15	3135.33	3.81	8.17	2.25	106.75
E-03	1/2	3.18	3389.92	3.18	7.95	2.58	258.74
	3/8	3.25	3633.44	4.27	8.15	2.87	253.88
	#4	4.02	3613.27	4.5	8.69	2.61	167.2

Table 3-6 Weibull Distribution Parameters of Gradation, Angularity, Shape, and Texture

Source	Code No.	Gradation		Angularity		Shape		Texture	
		Shape Parameter (a_G)	Scale Parameter (λ_G)	Shape Parameter (a_A)	Scale Parameter (λ_A)	Shape Parameter (a_S)	Scale Parameter (λ_S)	Shape Parameter (a_T)	Scale Parameter (λ_T)
E-06	2-6	0.6652	9.585	4.76	3327.99	4.44	8.86	2.93	174.63
E-06	1-13	0.7279	10.61	4.76	3327.99	4.44	8.86	2.93	174.63
E-05	61-12	0.8761	11.28	3.79	3291.5	3.96	7.75	2.12	165.78
E-02	1-3-4	0.8663	14.57	5.09	3113.11	4.11	8.56	2.51	194.07
E-02	2-3-2	0.8555	15.67	5.09	3113.11	4.11	8.56	2.51	194.07
E-04	2-6	0.9297	12.65	5.1	3072.87	3.65	8.03	1.96	171.51
E-04	1-3	0.9278	10.32	5.1	3072.87	3.65	8.03	1.96	171.51
E-07	68-2-6	0.852	13.07	4.53	3210.45	4.63	7.97	1.86	138.83
E-07	69-1-14	0.8467	12.69	4.53	3210.45	4.63	7.97	1.86	138.83
E-08	235-1-12	0.884	10.81	4.99	3342.81	3.63	8.72	1.48	205.58
E-08	2-1-6	1.016	13.14	4.99	3342.81	3.63	8.72	1.48	205.58
E-01	1-3-2-3	0.8783	8.31	4.38	3336.93	4.66	8.19	3.16	287.58
E-03	6-10-3	0.747	9.859	3.25	3633.44	4.27	8.15	2.87	253.88
E-05	drum	0.717	10.36	3.79	3291.5	3.96	7.75	2.12	165.78
E-09	1-14	0.9048	11.33	3.75	3228.12	4.48	7.6	1.75	205.47
E-01	drum	1.018	11.02	4.38	3336.93	4.66	8.19	3.16	287.58

3.5 Development of the Design Parameters in Pavement Performance Models

3.5.1 Resilient Modulus Parameters

Multiple regression analysis is performed using the JMP software to investigate the correlation between the *k* values and the base course properties, including the dry density (γ_d), moisture content (w), methylene blue value (MBV), percent fines content (*pfc)*, and aggregate gradation, angularity, shape and texture in terms of the shape parameter (a) and the scale parameter (λ) in the Weibull distribution. These selected base course properties, compared to plasticity index, liquid limit and $P_{200,}$ are much more directly related to pavement performance (Pan et al. 2006).

A stepwise multiple regression analysis is performed by using the JMP software to detect the significant base course material properties for modeling k_1, k_2, and k_3. The prediction models for k_1, k_2, and k_3 from the regression analysis are presented in Equations from (3-7) to (3-9), respectively:

$$\ln k_1 = -224.87 + 15.94\ln(\gamma_d) + 13.18\ln(\lambda_A) - 0.75\lambda_S + 1.55\ln(\lambda_T) \quad (3\text{-}7)$$

$$k_2 = 100.01 + 0.09\,pfc - 12.67\ln(\lambda_A) - 0.37\alpha_T + 0.33\lambda_S \quad (3\text{-}8)$$

$$k_3 = -20.03 - 0.03\,pfc - 0.02\lambda_G + 2.52\ln(\lambda_A) + 0.07\alpha_T \quad (3\text{-}9)$$

where k_1, k_2, and k_3 are coefficient in resilient model, γ_d is the dry unit weight of soil, λ_A is the angularity index scale parameter, λ_S is the shape index scale parameter, λ_T is the texture index scale parameter, α_T is the texture index shape parameter, pfc is the percent fines content.

It is noted that the gradation, shape, angularity and texture of the aggregates, and the percent fines content (pfc) are playing an important role in the proposed models. The prediction of these performance-related base course aggregate properties are precise, faster and more reliable in the prediction model.

3.5.2 Permanent Deformation Parameters

Based on the determined permanent deformation properties and base course properties, multiple regression analysis is performed by using the JMP software to investigate the correlation (Sall, 2005). The base course properties used in the development of these models include the dry density (γ_d), moisture content (w), MBV, *pfc*, and aggregate gradation, angularity, shape and texture in terms of Weibull distribution parameters. A stepwise regression analysis is performed to identify the significant performance-related properties of the base course for predicting α , μ , ε_0 , ρ , and β in the permanent deformation models (Nazzal, 2010). The list of the prediction models for α , μ , ε_0 , ρ , and β are given in Equations (3-10) to (3-14), respectively:

$$\ln \alpha = 4.91 + 1.23 \ln \gamma_d - 0.02 MBV + 0.59 a_G - 1.91 \ln \lambda_A + 0.17 a_T \quad (3\text{-}10)$$

$$\ln \mu = -54.68 + 16.89 \ln \gamma_d + 0.06 pfc + 3.34 a_G - 7.60 \ln \lambda_A - 3.72 \ln \lambda_T \quad (3\text{-}11)$$

$$\ln \varepsilon_0 = 10.24 - 0.03 MBV + 0.10 pfc + 0.88 a_A - 3.95 \ln \lambda_T \quad (3\text{-}12)$$

$$\ln \rho = 6.74 + 0.02 MBV + 0.04 pfc - 0.85 a_G + 0.03 \lambda_G - 0.13 a_T \quad (3\text{-}13)$$

$$\ln \beta = 10.17 - 2.75 \ln \gamma_d - 0.05 pfc - 2.00 a_G - 1.61 \ln \lambda_A - 0.34 a_T \quad (3\text{-}14)$$

where μ and α are permanent deformation properties in VESYS model , ε_0^p, ρ and β are permanent deformation properties in the Tseng-Lytton model, γ_d is the dry unit weight of soil (chosen unit is kg/m^3), *MBV* yields the methylene blue value (mg/g), *pfc* gives the percent fines content, λ_A is the angularity index a scale parameter, λ_T is the texture index a scale parameter, λ_G is the gradation index a scale parameter, α_T is the texture index a shape parameter, α_G is the gradation index a shape parameter, α_A is the gradation index a shape parameter.

It is shown in the prediction models that maximum dry density, MBV, shape parameter of gradation, scale parameter of angularity index, shape parameter of texture, and scale parameter of texture are significantly influential variables to predict the parameters in the VESYS model. It is also suggested that MBV, *pfc*, shape parameter of angularity index, shape parameter of texture, and scale parameter of texture are significantly influential variables to predict the parameters in the Tseng-Lytton Model.

3.6 Closure

This part of the study covers the development of two important models for unbound aggregates. This study proposes accurate and efficient methods to estimate the resilient modulus and permanent deformations properties of unbound aggregate. The test procedure for the resilient modulus and permanent deformation test, and AIMS test are given, and the sample preparation protocols were also explained in detail. The major observations associated with both the resilient modulus model and permanent deformation models were highlighted and summarized. The repeated load triaxial test is

used with new loading sequences to evaluate the moisture susceptible of the resilient modulus model. This proposed resilient model incorporates both the stress dependence and moisture dependence. Therefore, a matric suction term was integrated to consider the effect of the moisture under various conditions. It is also noted that matric suction is a significant parameter to reflect the moisture dependence of resilient modulus. A multiple regression analysis was performed to predict the *k* coefficient in the resilient model. It was concluded that the gradation, shape, angularity and texture, percent fines content and dry unit weight are playing important roles to predict the *k* coefficient. VESYS and Tseng-Lytton models were investigated, and it was noted that both models can be used to characterize the permanent deformation behavior of unbound aggregates. A good agreement is observed between the predicted permanent deformation properties and the measured ones. This indicates that the proposed regression models predict the permanent deformation behavior very accurately. The multiple regression analysis is performed to develop the prediction models for parameters α, μ, ε_0, ρ, and β in the permanent deformation models using a set of performance-related base course properties. The index parameters for angularity, shape and surface texture indices were measured by using the AIMS machine. These index parameters are used to characterize the coarse aggregate properties. There is a good agreement using the cumulative Weibull distribution to fit the measured distributions. The shape parameter and scale parameter from the Weibull distribution can characterize the measured distribution quantitatively. Along with index parameters the MBV is a good indicator to evaluate the variability of material production for the quarry.

4. DEVELOP A METHODOLOGY TO DETERMINE PERCENT CLAY CONTENT USING THE METHYLENE BLUE TEST

4.1 Introduction

This part of the study describes an experimental investigation of the methylene blue test (MBT) and particle size distribution analyzer (PSDA) that are used to determine the fraction of fines in soils. The MBT is employed to detect the methylene blue value (MBV) and assess the amount of percent clays. The PSDA test machine is used to generate a percent distribution curve for fine materials passing through No. 200 sieve. The outcomes of the both tests have been used to find a correlation between MBV and percent clays in fines content, and this correlation along with the improved sampling and testing protocol are presented in following section.

4.2 Background

Engineering properties of soils and aggregates are strongly influenced by the clay fraction in the mixture (Neshvadian Bakhsh, and Zollinger, 2014). It is known from experience and extensive laboratory testing that the engineering characteristics of aggregate mixtures are significantly influenced by the amount and characteristics of the fines in the mixture. Because of this, there is a need to determine engineering properties of these aggregate mixtures by analyzing the fines content of the mixtures, including both clay and non-clay fines. The physical properties of clays depend on the clay mineralogy. Methylene blue is an essential test method that has been validated to assess

clay mineralogy changes with cation exchange capacity (CEC) and specific surface area (SSA).

The methylene blue has a large polar organic molecule $C_{16}H_{18}N_3S^+$ that can be adsorbed onto the negatively charged surfaces of clay minerals. The amount of adsorbed methylene blue depends on the amount of the surface area of the clay particles. The cation exchange capacity (CEC) and specific surface area (SSA) change with clay characteristics and mineralogy. The more methylene blue adsorbed by the clay particles, the brighter the methylene blue solution will be. The adsorbed methylene blue is able to be quantified by assessing the color change of the methylene blue solution. Hence, the amount of adsorbed titrated methylene blue solution represents the surface area of a clay mass (Phelps and Harris, 1967). Furthermore, it is considered that the titration of the methylene blue has a capability of giving a measurement of CEC (Fairbairn and Robertson, 1957; Nevins and Weinritt, 1967).

The clay potential of the soil has been determined by using the methylene blue solution with various methods. One of the methods is ASTM C 837, which is a standard test method for a methylene blue test. The test method is used to determine amount of methylene blue dye adsorbed by clay particles. The test method determines the methylene blue index (MBI). The bias of the test method is not known because the MBI is not directly related to any clay characteristics. Another standard test method is the qualitative detection of harmful clays in the smectite group of aggregates in AASHTO 330-07. This method identifies the presence of harmful clays by employing methylene

blue dye. The method gives the methylene blue value in mg per g of passing No. 200 sieve material.

Recently, a new test method proposed by W.R. Grace Inc., to assesses the MBV value of soil by using the methylene blue solution with a colorimeter device. The MBV represents the amount of fines content in the aggregate mass. The advantage of this test method is to be relatively simple, inexpensive and repeatable. However, the limitation of the test method does not allow a direct measurement of fines content (Sahin, 2014). Furthermore, the MBV measurement range is limited to non-clay particles, and hence it does not properly measure the soil with higher clay contents in aggregate mixtures.

4.3 Methylene Blue Test

The W.R. Grace has proposed a test to determine the methylene blue value in aggregate mixes. The MBV is an indicator that represents the solution concentration of percent fines in the mixture. This is a quite rapid test method to measure the MBV. However, the test method was not established to measure directly the amount of active clays in an aggregate mixture. Therefore, the W.R. Grace test protocol was evaluated, and a new test protocol was prepared at Texas A&M University to enable its use for different types of aggregate to determine the percent fines content in the mixture. In addition, this test method is further modified to represent a direct relation between the MBV and percent fines content in any type of aggregate mixture.

4.3.1 Material Selection

The unbound base course aggregate materials were collected from nine-(9) various pits throughout Texas. These quarries were chosen to capture the geographic, mineralogical, and production volume diversity of typical sources used for TxDOT projects. Table 4-1 summarizes the sources used in the sampling and testing program. The aggregate samples were subjected to an extensive laboratory testing program at the Texas A&M Transportation Institute laboratory. This test program uses the portion of the aggregate mixture passing through No. 4 sieve (minus #4 and finer).

Table 4-1 Sources of Material for Sampling and Laboratory Testing

Source	Rock Type	Production Size
E-01	Limestone	Medium
E-02	Sandstone	Large
E-03	Caliche	Small
E-04	Limestone	Small
E-05	Limestone	Large
E-06	Limestone	Large
E-07	Limestone	Large
E-08	Limestone	Large

4.3.2 Experiment Apparatus

The W.R. Grace methylene blue test employs a few devices to perform the experiment. Figure 4-1 shows a set of the equipment employed to perform the methylene blue test. Because the MBT utilizes an uncomplicated and transportable set of experiment kits, this advantage makes the MBT a test that is capable of determining the fines fraction of an

aggregate system in an unbound aggregate mixture in both the laboratory and outside the laboratory environment.

The colorimeter device provides an objective way to assess the color change of the methylene blue solution according to the principle of Beer's Law, which is shown in Equation (4-1):

$$\mathrm{A} = \log\left(\frac{l_i}{l_t}\right) = abc \tag{4-1}$$

where A is absorption of sample, l_i is amount of light entering a sample, l_t is amount of light leaving a sample, a is molar absorptivity of the sample, b is curvature of the sample's container, c is molar concentration of the sample.

Figure 4-1 The W.R. Grace Methylene Blue Test Measurement Apparatus

Figure 4-1 shows a Hach DR 850 brand colorimeter, a timer, a plastic tube of 45 mL, a micropipette with tip ranging nearly 500 microliters, a plastic syringe, a filter with 0.20 micrometers size, an eyedropper with a capacity of 7.50 mL, plastic tube with volume of 1.4 mL, and a portable scale with 0.01 gram sensitivity. Furthermore, the double distilled water and a bottle of methylene blue solution are required items to perform the test.

4.3.3 Experimental Test Procedure

The methylene blue test utilizes an anhydrous form of the chemical. The chemical formulation of the methylene blue concentration is calibrated to 0.5 percent by weight before starting the test. This procedure must be done for each new methylene blue bottle as it is opened. The modified methylene blue test method described here is used to sample the size of the portion of the soil that passes through No.4 sieve. The recommended starting amount of the sample is 20.00 g. The initial sample size may vary based on the MBV reading at the end of the test. The 20.00 g sample is added into 30.0 mL of calibrated methylene blue solution in a plastic tube. The mixture is shaken for 1 minute and rested for 3 minutes and shaken again for 1 minute. Then, the solution is filtered through a 2.0 μm filter by using a syringe. The sample passing the 2.0 μm size is used for the rest of the experiment. 130 mL of the filter solution is taken into a plastic tube and filled with distilled water until total of 45.00 g is collected. The new mixed solution is placed in a small glass tube, which fits into the colorimeter device. The MBV value is read through the colorimeter device. This process is shown in in Figure 4-2.

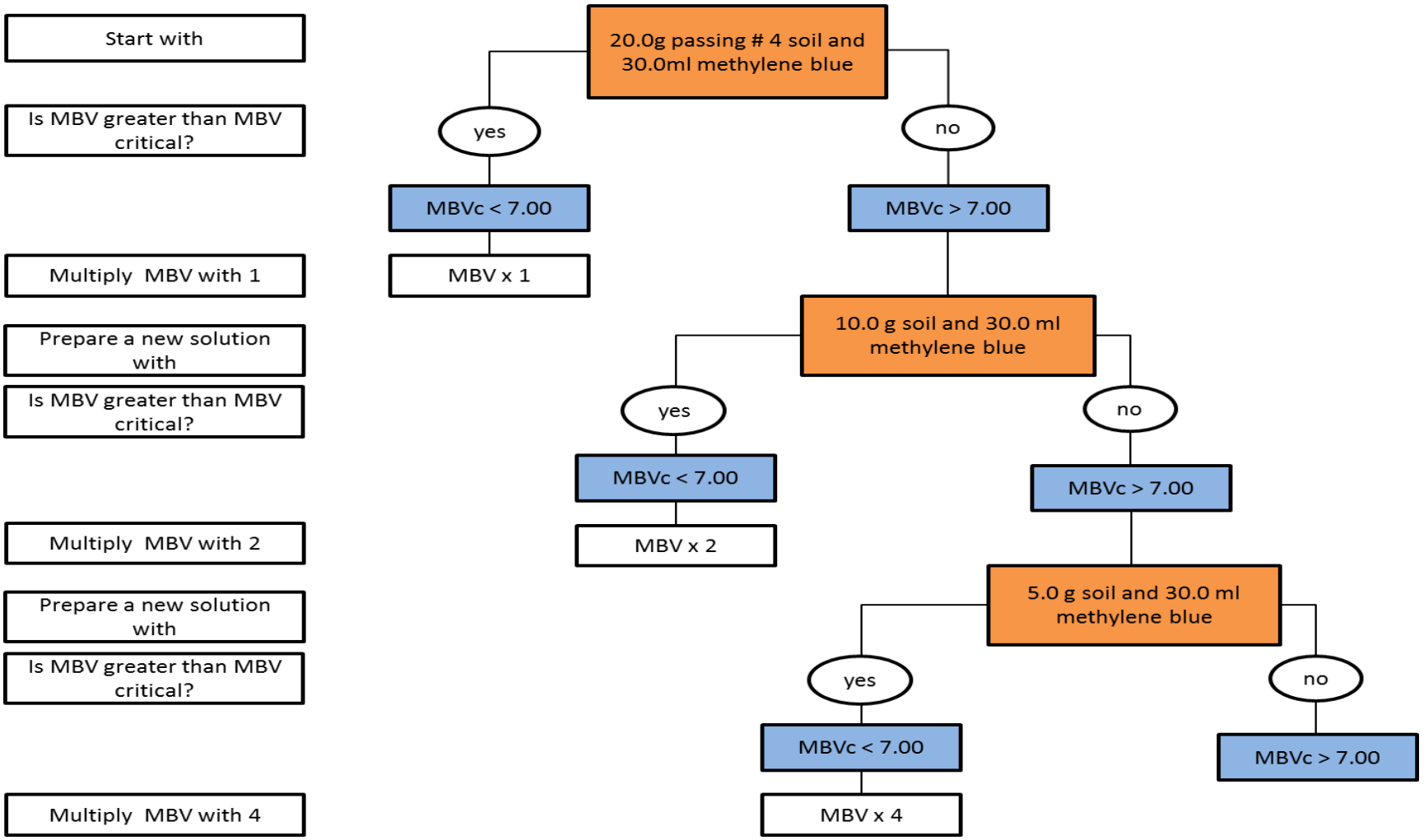

Figure 4-2 A Schematic of the New Sampling Method based on Shifting Sample Size with Characteristics of Material Used

If the MBV reading is smaller than 7.0 mg/g, it is considered a valid reading and hence 20.00 g is considered a valid sample size. If the MBV is higher than 7.00 mg/g then the sample size must be cut in half to 10.00 g, and test procedure will be repeated. The total test time for a reading takes less than 10 minutes. The test procedure is also presented in Figure 4-2 to show the process of changing the sample size used with clay mineralogy and characteristics.

A number of various aggregate samples have been compiled from various sources and tested to determine the MBV values. The sample size changes from 20.00 g to 4.00 g based on the composition of the aggregate type. Furthermore, the methylene blue has a range change based on the sample amount used and clay mineralogy. A new methylene blue scale is developed, ranging from 2.0 to 28.0. At the end of the test the MBV is calculated by given Equation (4-2):

$$MBV = S_c x(MBV_{reading} + CF) \tag{4-2}$$

$$S_c = \frac{20}{n} \tag{4-3}$$

where $MBV_{reading}$ is the methylene blue value reading from the colorimeter device (mg/g), MBV is the methylene blue value after applying two correction factors, CF is the correction factor for the concentration due to dilution, S_c is the sample correction factor based upon the size of the sample used, and n is sample size used in grams.

The methylene blue test protocol along with a step by step testing procedure is given in Appendix A.

4.4 Percent Fines Content (*pfc*) Test by Using the Horiba Particle Size Distribution Analyzer

4.4.1 Material Selection

The same set of samples used for the methylene blue tests are also tested to determine the percent fines content portion directly. However, if the material size is changed for this test, the maximum size of the material used is the No. 200 sieve (minus 75 micrometers sample). For this purpose, the Horiba PSDA test device is employed to determine the all of the samples fines particle fraction.

4.4.2 Experiment Apparatus

The Horiba Laser Scattering Particle Size Distribution Analyzer is a laboratory test device, which is produced by Horiba Instrument Inc., and that is employed to analyze fine particle size distribution. The device version of LA-910 is shown in Figure 4-3. It operates by using an optical light source and a large lens measures the entire range of the particle size down to $0.02\,\mu m$. The device completes the measurements in less than10 minutes with significant accuracy and repeatability. The LA-910 calculates the particle size distribution in less than one minute, and the results are displayed as a histogram graph.

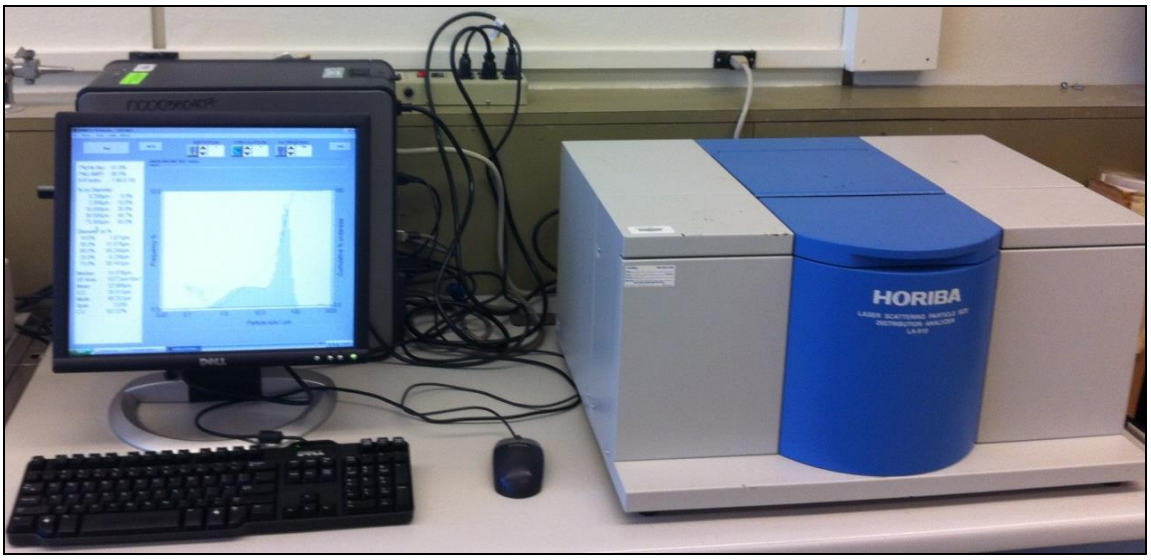

Figure 4-3 Configuration of the Horiba LA-910 Particle Size Distribution Analyzer

4.4.3 Experiment Procedure

The sample portion, which passes through the No. 200 (minus75 μm) sieve, is taken to determine percent of the 2 μm size in the aggregate mixture. This device has a pre-sample preparation, which includes an ultrasonic bath with a disintegrating stirrer. The sample is prepared by mixing with distilled water in the unit to have a viscous flow solution and then performs the measurement. The soil water mixture in a viscous form flows through a light beam to detect particle scattering in the mixture. The soil particles are suspended in the solution in a proper concentration during the measurement.

The histogram graph demonstrates the entire range of small particles in the viscous flow. The LA-910 irradiates the particles from different angles and then the scattered distribution is analyzed. The Horiba LA-910 uses the Mie theory to determine particle size distribution analysis (Horiba Manual, 1995). The sample is processed in

four states: the first is agitation of the sample with the distilled water; second, the ultrasonic dispersion process; third, the circulation of viscous flows, and the last is measurement of the concentration.

The right amount of prepared soil sample is agitated with the distilled water in a water bath and an ultrasonic dispersion is applied to the sample. The sample in the liquid state flows through the laser beams to measure the scattering. The result shows the percentage of 2 μm size in the sample. The amount of the 2 μm size is the known percent fines content in a soil mixture and is denoted by *pfc*, and it is given in Equation (4-4):

$$pfc = \frac{\%-No.2 \text{ micron}}{\%-No.200 \text{ sieve}} \times 100 \tag{4-4}$$

where *pfc* is percent fines content, $\%-No.2$ micron is the percent passing number 2.0 microns size, and $\%-No.200$ sieve is percent passing No. 200 sieve.

The soil classification systems separate soil particles into two major divisions that are coarse grained (gravels and sands) and fine (silts and clays) grained particles. The American Association of State Highway and Transportation Officials (AASHTO), American Society for Testing Materials (ASTM, 1980) and the Unified Soil Classification System (USCS) (U.S. Bureau of Reclamation, 1974; U.S. Army Engineer WES, 1960) are the only commonly used systems in civil engineering practice (Holtz and Kovacs, 1981). According to AASHTO, ASTM and USCS soil classification and the particle size distribution curve, the coarse particle sizes are down to 75 μm, and the fines sizes are smaller than 75 μm (Al-Hussaini, 1977). The silts are classified from 75

μm and 2 μm, the clays are considered smaller than 2 μm. Therefore, the percent fines content concept (*pfc*) originated based on the AASTHO, ASTM and USCS classification systems.

4.5 Correlation between Methylene Blue Value and *pfc*

The percent fines content and the methylene blue value are determined on the same set of the base course aggregate sources. It was determined that the test results show a general relationship between the methylene blue value and the percent fines content. These test results are expressed in a mathematical form and, based on that, a mathematical model is developed. The presentation of the developed MBV-vs-pfc relationship is given in Figure 4-4.

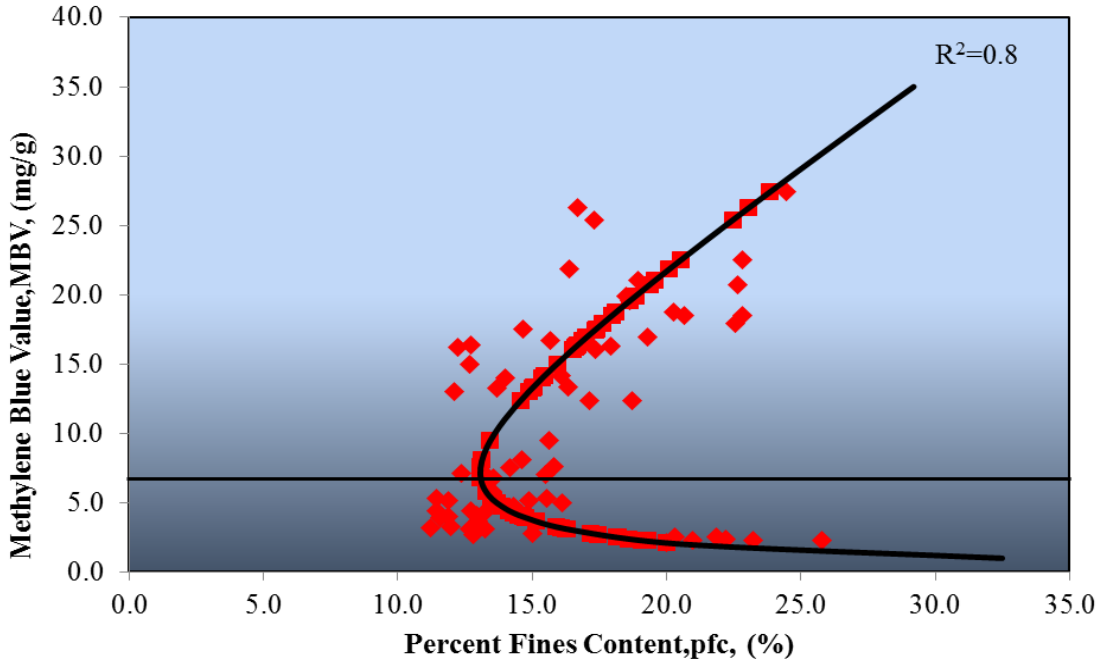

Figure 4-4 The Curved, Relationship between Methylene Blue Value and Percent Fines Content, Represents the Developed Model (Sahin, 2013)

Figure 3 shows a "C" shaped curve that covers the entire methylene blue range for base course aggregate materials. The methylene blue range reaches MBV 28.0 at the 5.0 g sample. This curve is divided into two zones. The methylene blue value of 7.0 mg/g is considered the critical point ($MBV_{critical}$). The value below the 7.0 mg/g is considered a low methylene blue value of the soil, which has a lower cation exchange capacity or is a relatively non-plastic soil. The MBV below 7.0 mg/g represents the lower liquid limit (LL) and plasticity (PI) value. The value above the MBV 7.0 mg/g is a soil with higher plasticity and cation exchange capacity. Thus, zone II represents the higher plasticity index (PI) and liquid limit (LL) values.

Based on considering all the test results, a mathematical model is proposed for the *pfc* to present the relationship between the methylene blue value and percent fines content. Since the determined C-shaped curve is similar to the specific energy diagram in fluid mechanics, the form of specific energy equation is used to obtain the mathematical correlation model. This is not a direct fitting curve, in fact this is a mechanistic equation that has been used in open channel flow in the field of water resource engineering to determine critical height with respect to energy in the energy diagram (Chaudhry, 2008). Originally, the specific energy equation and diagram have been derived from the Bernoulli equation that is the most common equation used to determine the hydraulic gradient of fluid flow. In this study, the specific energy equation was modified and applied in this specific case to determine *pfc* and the MBV correlation. The mathematical form of the developed equation is presented in Equation (4-5) as follows:

$$pfc = \frac{a_m}{\left(MBV\right)^{n_m}} + b_m\left(MBV\right) \tag{4-5}$$

The *pfc* depends on a function of the methylene blue value. The critical methylene blue value ($MBV_{critical}$) of methylene blue is also formulated. The $MBV_{critical}$ is given in Equation (4-6) as follows:

$$MBV_{critical} = \left(\frac{n_m a_m}{b_m}\right)^{\frac{1}{(n_m+1)}} \tag{4-6}$$

where MBV represents the methylene blue value, $MBV_{critical}$ is the critical methylene blue value, which occurs at the "nose" of the curve where the pfc is at a minimum. It is

normally about 5.0 to 7.0 mg/g. The *pfc* gives percent fines content; $a_m, b_m,$ and n_m are three distinct fitting parameters that control the shape of the curve, and they change with clay mineralogy, characteristics, and clay fractions. Thus, each pit may have different or similar three fitting parameters.

4.6 Quality Index Charts of the Grace Methylene Blue Value and AASHTO

Methylene blue is a standard test method for the qualitative detection of harmful clays of the smectite group in aggregates used in AASHTO T 330-07. A greater reading of the methylene blue value shows that a larger amount of active fines or organic materials exists. A scaled relationship of the expected performance of the materials, and the methylene blue value is presented in Figure 4-5.

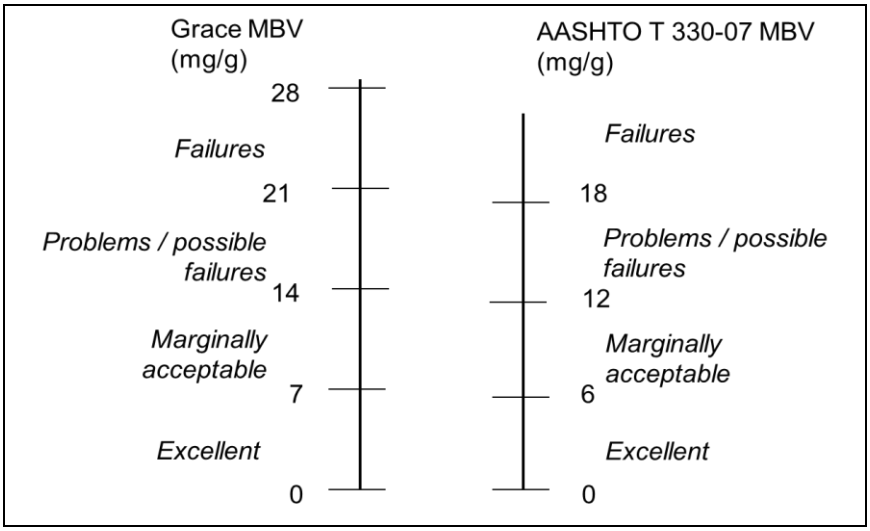

Figure 4-5 Comparison of Grace MBV and AASHTO T 330-07 Methylene Blue Values

Figure 4-5 illustrates that the AASHTO T330-07 MBVs range from 0.0 to 18.0 to show expected performance. The scaled values are divided into four groups; excellent, marginally acceptable, problems, and failure. The improved W.R. Grace methylene blue test, which was modified by the Texas A&M Transportation Institute (TTI), values are scaled from 0.0 to 28.0. Figure 4-5 illustrates that the improved W. R. Grace MBV and AASHTO T330-07 are significantly related. The mathematical form of the relationship is shown in Equation (4-7):

$$MBV_{\text{Improved Grace TTI}} = 1.667 MBV_{AASHTO\ T330} \tag{4-7}$$

where $MBV_{\text{Improved Grace TTI}}$ represents the methylene blue value based on the Texas A&M University improved Grace method and $MBV_{AASHTO\ T330}$ yields the methylene blue value provided according to AASHTO T330.

4.7 Presenting the Relationship between the MBV and *pfc* from Variety of Aggregate Sources in Texas

The multiple soil samples from nine-(9) separate aggregate sources are analyzed to assess the *pfc* values. Each aggregate quarry has a unique relationship between the methylene blue value and the percent fines content. Furthermore, each pit has an estimated mathematical equation that make it possible to calculate the *pfc* value for a given MBV.

MBV and *pfc* Equation (4-5) has three distinct parameters, and hence the three parameters change with the material characteristics of the pit. Thus, three parameters are determined for various sources, and typical values of them at each pit are shown in Table 4-2. A general three-parameter is determined for all of the pits located in Texas and it is noted as "General" and shown in the first column of the table.

Table 4-2 Three Parameters Showing for Nine Various Aggregate Sources

Source		**General**	**E-01**	**E-02**	**E-03**	**E-04**	**E-05**	**E-06**	**E-07**	**E-08**	**E-09**
Parameters	a_m	27.60	27.60	19.74	30.67	28.04	28.29	27.60	27.60	28.01	27.68
	b_m	1.55	1.553	0.948	0.552	0.410	0.456	1.553	1.553	0.813	1.135
	n_m	0.92	0.924	0.675	0.448	0.534	0.355	0.924	0.924	0.629	0.953
R^2		0.79	0.82	0.83	0.67	0.76	0.76	0.82	0.82	0.77	0.91

The generated method showed a unique relationship for each of the nine quarries throughout Texas. The three parameter correlations depend on the clay mineralogy in each of the pits thereby showing unique relationships. The 90 percent confidence levels

are determined for each pit, and two boundary lines are plotted to show the minimum and maximum accepted values. The confidence level may be used for quality control and quality assurance of the aggregate source in the production processes.

Two examples of MBV vs. *pfc* curves are given in Figure 4-6 and Figure 4-7 to show relatively a higher quality material and relatively lower quality material. Figure 4-6 shows a higher quality material with lower plasticity and less active clay. Figure 4-7 shows a lower quality of material due to high plasticity clays. The variety of quality change is also illustrated from Figure 4-8 to Figure 4-12 in all of the collected aggregate materials in Texas.

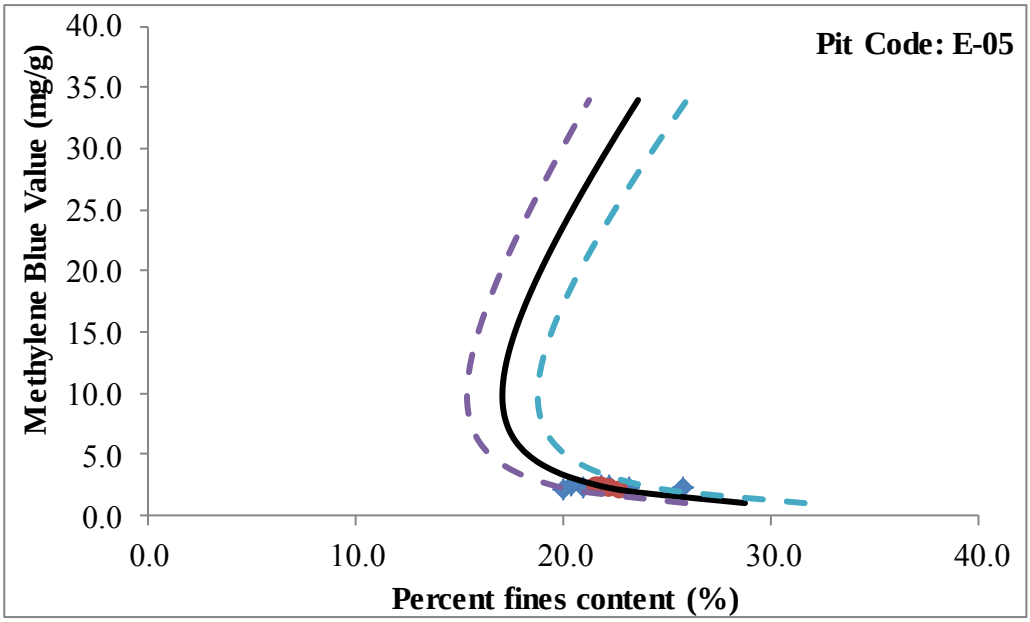

Figure 4-6 MBV vs. *pfc* Showing for a Higher Quality for E-05 Aggregate Source

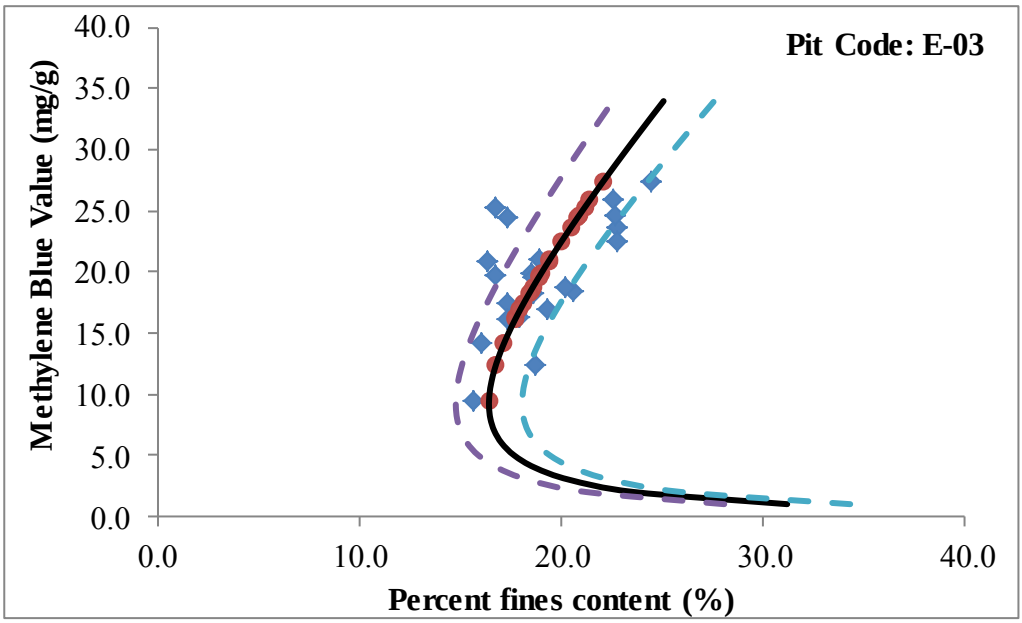

Figure 4-7 MBV vs. *pfc* Showing for a Lower Quality for E-03 Aggregate Source

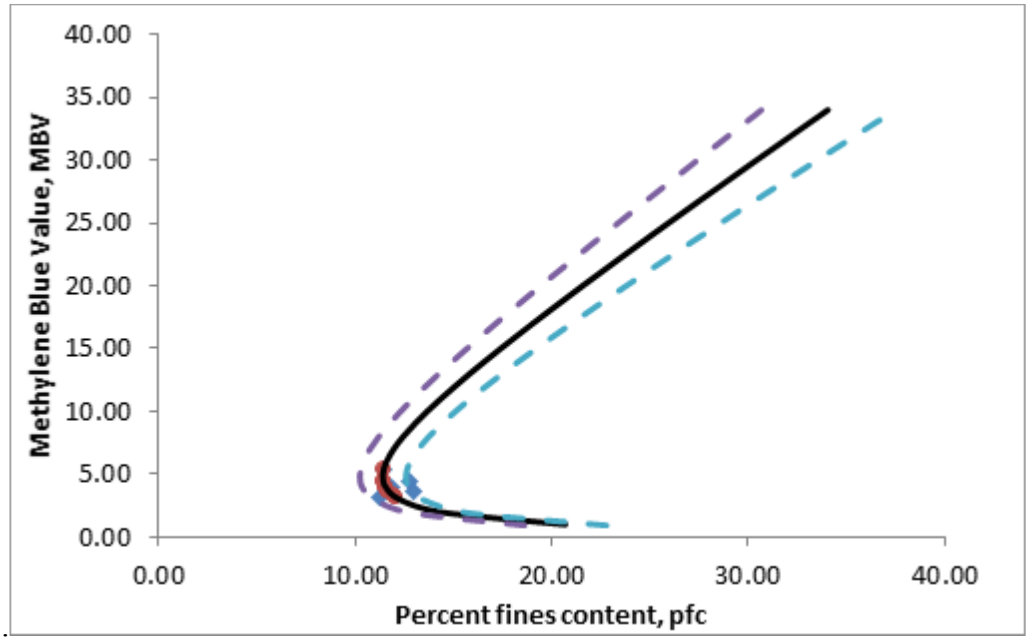

Figure 4-8 MBV vs. *pfc* Correlation Showing for E-02 Aggregate Source

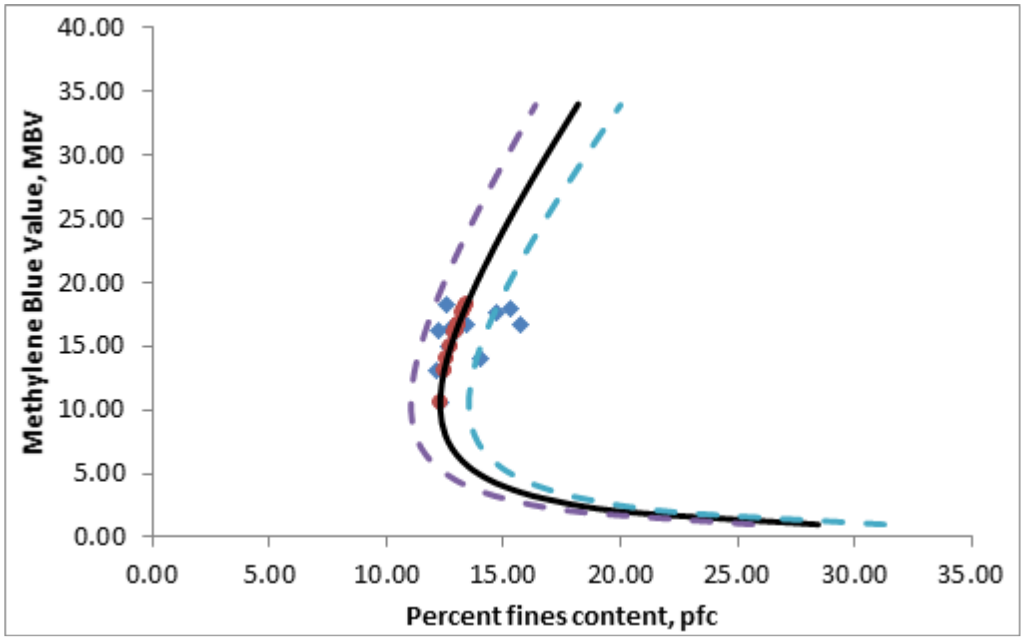

Figure 4-9 MBV vs. *pfc* Correlation Showing for E-04 Aggregate Source

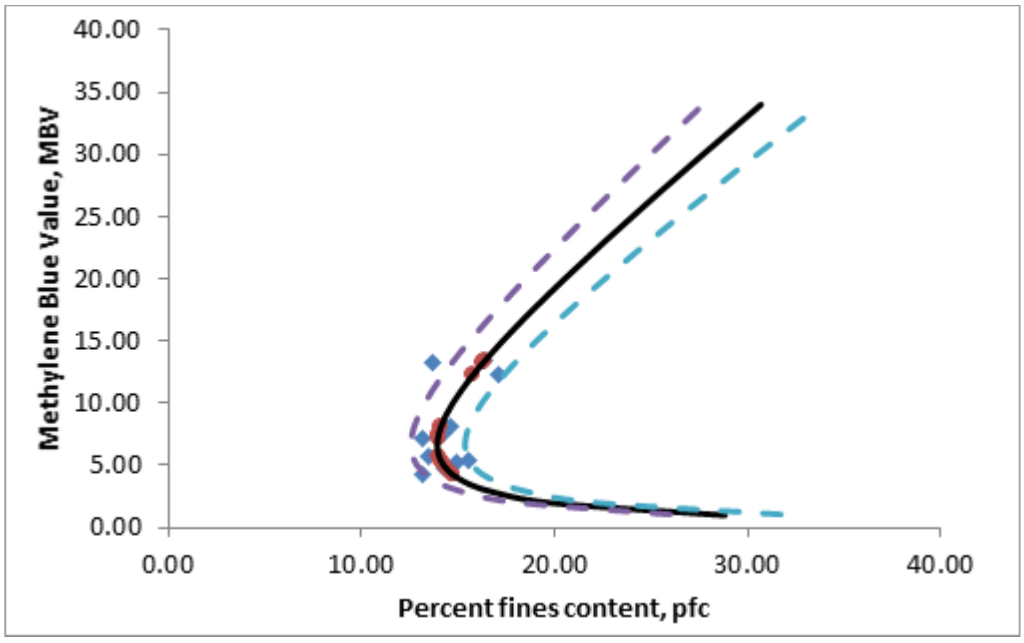

Figure 4-10 MBV vs. *pfc* Correlation Showing for E-06 Aggregate Source

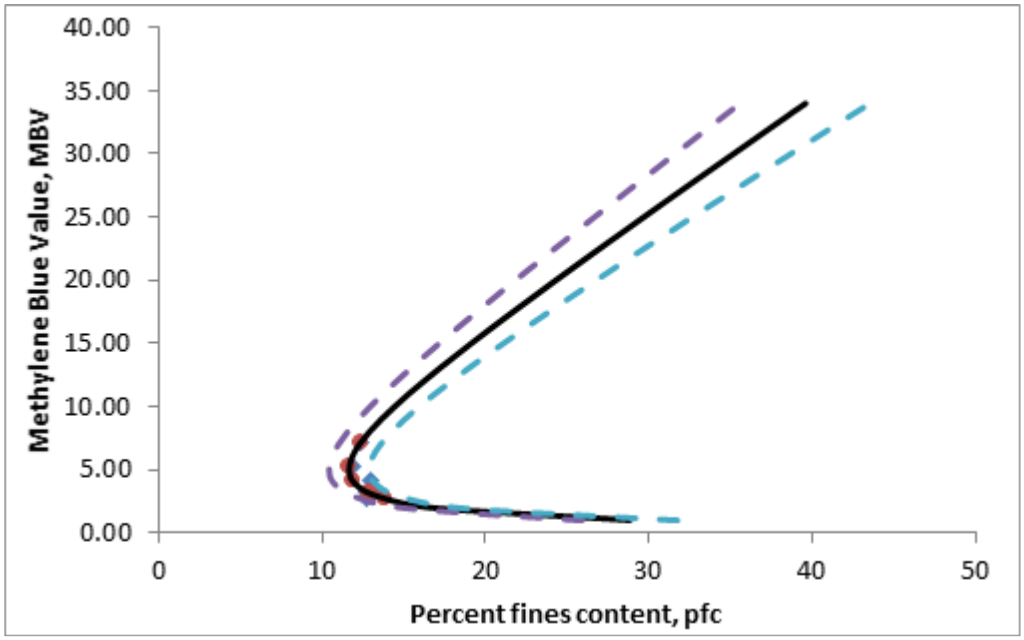

Figure 4-11 MBV vs. *pfc* Correlation Showing for E-09 Aggregate Source

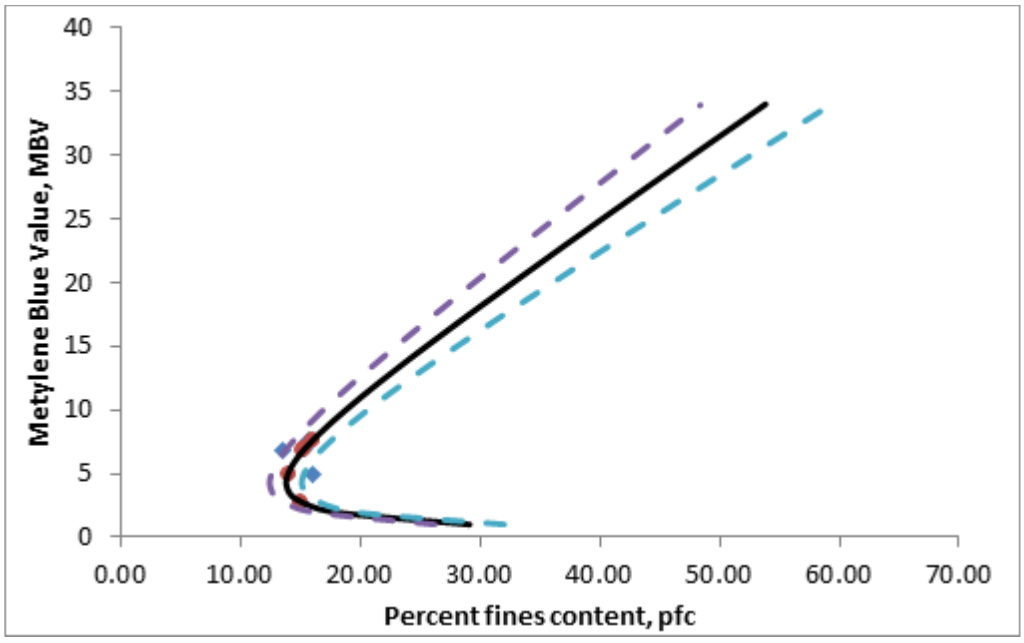

Figure 4-12 MBV vs. *pfc* Correlation Showing for A-42 Aggregate Source

A statistical analysis of the test results is very important to validate the accuracy and precision level of the test method. Therefore, the width of the 90 percent confidence level bands is an indicator of the variability of the sources of the aggregate.

The methylene blue test provides a highly reliable and useful investigation method for using the separate quality of poor and good performing unbound aggregate materials.

4.8 Closure

Based on the present study, the methylene blue test is a proven test method that has been used in detecting the qualitative of clays for the last two decades. The experimental procedure was improved significantly based on the sampling method used to perform test and a new correlation was also found to show the graphical presentation of the resulting data from the test. The first improvement is to decrease the amount of the sample used for the test. The new method uses 3-(three) levels of sample preparation based on the sample size. The sample that is used decreases with increasing plasticity of the soil. The second improvement is to develop a relationship between the methylene blue value and the percent fines contents. The data has a unique distribution of data points, and the only way to gather data under the one model is to use a “C” shaped curve.

In addition to the traditional methylene blue test, the improved W.R. Grace methylene blue test is a significantly more rapid, reproducible and simple method to estimate the percent fines content. This new test method is improved to assess a

relationship between the adsorbed methylene blue value and the percent fines fraction, especially in aggregate mixes. This improvement warrants the assessment of the methylene blue value for samples using the fraction smaller than No. 4 sieve size, rather than the size smaller than 2 mm. Additionally, the test method is applicable both in the laboratory and in field applications because the test method requires fewer experimental tools.

This method is capable of measuring clay percentage rather than using other methylene blue test methods that require a more extensive laboratory experimental program and time. The methylene blue value could help observe and monitor the activity of fines with better test precision and turnaround time than the current methods. Therefore, this is a promising method beyond the current status to assess the amount of fines fraction of a mixture in road construction. These improvements help in estimating performance through index tests that may allow the development of a QC/QA program that truly relates to the performance measures used in design.

5. DEVELOPMENT SOIL DIELECTRIC CHARACTERISTICS CURVE (SDCC) MODEL FOR BASE COURSE MATERIALS

5.1 Introduction

The base course moisture is one of the most important parameters, especially during the construction stage of the base course aggregate because engineering characteristics such as stiffness, modulus and compaction are highly dependent on the degree of moisture content (w). The moisture content, which is a variable that changes in both time and space, is required to measure frequently for quality control and quality assurance purposes, especially at the construction site. On the other hand, highly labor intensive traditional methods determine gravimetric moisture content or volumetric water content (θ), regardless of a need to replace the traditional method with contemporary electrical devices that calculate the moisture condition of the base course in shorter time with higher precision.

A percometer is a non-destructive test instrument to make simultaneous measurements of the base course aggregate dielectric constant (ε_r), electrical conductivity and temperature. The percometer test device is used to assess the dielectric constant both in the laboratory and in-situ conditions. In this study, a percometer device is utilized in the laboratory environment to determine the soil suction of the base course aggregates.

The percometer determines the dielectric constant, and the filter paper test provides soil suction h_m, measurements. The relationship between the base course

material suction and the dielectric value is investigated by using the percometer and the filter paper test. These measurements are used to develop a unique suction-dielectric constant correlation, which gives the whole range of suction change with the material dielectric constant. The outcome of this correlation is an S-shaped curve, representing the correlation between soil suction (h_m) and dielectric constant (ε_r).

The following section introduces the sampling and testing protocol to measure the dielectric constant experiment. The subsequent section presents the correlation developed between the soil suction and dielectric constant. The final section gives the method of developing the fitting parameters used in this correlation based on the methylene blue and percent fines content introduced in the past chapters.

5.2 Percometer Test

5.2.1 Experiment Devices

The percometer is an instrument that measures simultaneously dielectric constant (ε_r), electrical conductivity (J), and temperature (T) at the surface of a material. The word "percometer" is originated from the words permittivity (per), conductivity (co), and meter (meter). The percometer is used to measure soil dielectric permittivity and conductivity in soil studies (Yoe and et al., 2012). The percometer is a frequency domain device, which measures at a frequency of 50 kHz. The accurate definition of dielectric constant (ε_r) is the real part of the relative complex electric permittivity, which is directly related to the moisture content in the soils (Saue and et al., 2008).

The percometer is a non-destructive test instrument that can be used both in the laboratory and for in-situ testing. It is highly accurate and reliable, lightweight, user friendly, and presents the results in less than 5 seconds per reading. One of the most extensively used percometer devices is the Adek brand percometer manufactured in Estonia. A percometer device central unit and a supplementary surface probe are shown in Figure 5-1.

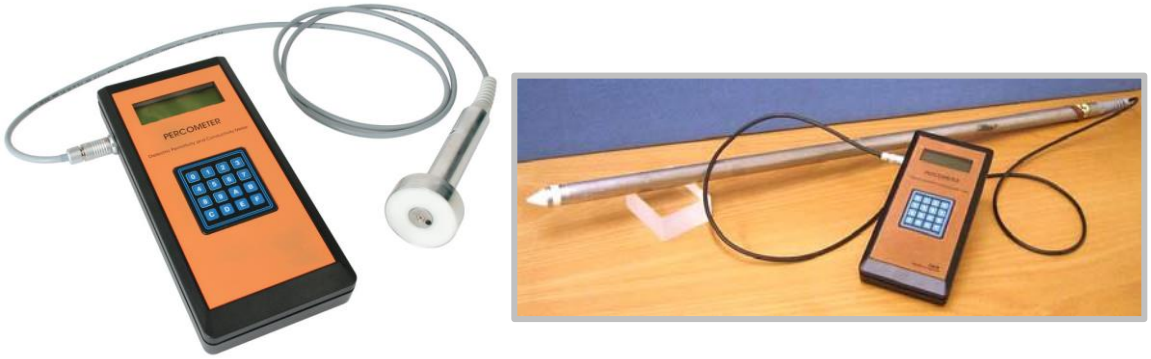

Figure 5-1 A Standard Adek Percometer^{TM} Device Including Surface Probes and Tube Probes (roadscanners.com)

The percometer permits the use of multiple types of probes with the same central unit. One type of probe is the surface probe that is designed to measure aggregate samples, tile walls, and liquids. Although the percometer probe is a non-destructive approach to making measurements, it has an effective penetration depth of 2-3 cm, and this depends on the medium of the materials. In this study, a surface probe SF model with a diameter (D) of 60 mm has been utilized in measurements because the compacted samples used, which have very smooth surfaces, thereby allowing the surface

probe to have good contact and have precise readings. The second type is the tube probe, which is designed as a cylindrical shaped and manufactured with various length (L) for inserting into softer medium material. It requires minimum depth of 10 cm to perform an accurate reading because of these features, and it is an ideal probe to make measurement on soft soils, vertisol soils with less granules and road subgrade layers. The various types of percometer probes along with the accuracy ranges and recommended application use areas are given in Table 5-1.

Table 5-1 Various Probe Types and Specified Areas of Application (roadscanners.com)

Probe Type Description	**Dielectric Constant** ε_r	**Electrical conductivity** $\mu S/cm$	**Temperature** $^{\circ}C$	**Recommended applications**
Surface Probe SF (D=60mm)	1 to 40 with an accuracy of $\pm$ (0.1 + 1%)	0 to 9999	-40 to +80	Laboratory use, Tube Suction Test, detection of moisture in structures with even surfaces
Surface Probe SV (D= 60 mm)	1 to 200 with an accuracy of $\pm$ (0.25 + 2%)	0 to 9999	-40 to +80	Laboratory use (high ε_r)
Short Tube Probe TFS (L = 18 cm)	1 to 15 with an accuracy of $\pm$ (0.05 + 1%)	0 to 9999	-40 to +80	Laboratory tests, e.g. triaxial testing of aggregates
Short Tube Probe TVS (L = 18 cm)	1 to 90 with of an accuracy $\pm$ (0.25 + 2%)	0 to 9999	-40 to +80	Percostation laboratory tests
Long Tube Probe TVL (L = 100 cm)	1 to 90 with an accuracy of $\pm$ (0.25 + 2%)	0 to 9999	-40 to +80	Field measurements (high ε_r)
Long Tube Probe TFL (L = 100 cm)	1 to 15 with an accuracy of $\pm$ (0.05 + 1%)	0 to 9999	-40 to +80	Field measurements
Surface Probe SF1 (diam = 60 mm)	1 to 200 with of an accuracy $\pm$ (0.1 + 1%)		-40 to +80	Laboratory use

The dielectric permeability is considered as complex number function with real and imaginary units. The complex function is shown in Equation (5-1):

$$\varepsilon^* = \varepsilon' - i\varepsilon'' \tag{5-1}$$

where ε^* is the dielectric permittivity, ε' is the real part and is the ratio of the dielectric field storage capacity of free space, ε'' is the imaginary part of the dielectric and is usually expressed in terms of dielectric losses, and where i is the imaginary component ($i^2 = -1$) of the function (Martinez and Byrnes, 2001).

The dielectric constant varies with the material type, and hence each material has a unique dielectric constant value. Some of the materials might have a dielectric range/interval instead of single value. Over the past years, several studies have documented the measurement of frequency dependent dielectric constants, which are given in Table 5-2, based on the most commonly used construction materials (Nguyen et al., 1997; Wensink, 1993; Knoll, 1994; Curtis, 1995).

Table 5-2 Typical Highway Construction Materials with Corresponding Dielectric Constants

Material	**Dielectric Constant (ε_r)**
Air	1.0
Vacuum	1.0
Water	81.0
Asphalt	4.0-6.0
Asphalt concrete	5.0-7.0
Concrete	8.0-12.0
Clay	4.0-40.0

The dielectric constants are presented in Table 5-2 for the materials, all of which are primary components in road construction in the pavement and base course layers.

5.2.2 Sample Preparation

Soil sample preparation is an important part of the testing procedure because the accuracy and consistency of the outcomes between the samples are highly dependent on the sampling producer. Therefore, soil samples material passing through the No. 4 sieve size fractions are compacted at the optimum moisture content by following the standard compaction test procedure given in Tex-114. The samples prepared in cylindrical geometric shapes with 1.5 in. high and 3 in. diameter, two identical soil samples are prepared from each pit. The dielectric readings are taken on each identical sample at the same moisture content. The compacted soil samples are placed into a 100 percent relative humidity environmental room shown in Figure 5-2, and the moisture content losses were monitored in every 24 hours.

Figure 5-2 A Set of Compacted Soil Samples in 100 Percent Humidity Monitored for Moisture Reduction

5.2.3 Test Procedure

When the sample moisture content approached 2 percent the dielectric readings were taken at this stage, immediately before starting the filter paper test. The dielectric constant readings were taken carefully from five different points on the surface of the samples, and this process is shown in Figure 5-3. Immediately after dielectric readings, samples were prepared to begin the filter test paper and then to determine soil matric suction.

Figure 5-3 Adek Percometer Measuring the Dielectric Constant of Compacted Soil Samples

5.2.4 The Complex Refraction Index Model (CRIM)

Volumetric models show the dielectric properties of the soil media based on the relative ratio of the soil components in the media and based on the dielectric characteristics of each component. All inputs consist of solid matter, void space, and volumetric water

content (van Dam et al., 2005). A number of volumetric models have been proposed over the years such as Arithmetic Average, Harmonic Average, Liechtenecker-Rother, and Time-Propagation (Martinez and Byrnes, 2001). The complex reflective Index model (CRIM) is based on the Liechtenecker-Rother model, which is the most widely used model (Hilhorst et al., 2000; Birchak et al., 1974; Dobson et al., 1985).

The dielectric value (ε_r) of a base course is a composite of the dielectric values of the components of the base course: solids, water, and air. Theoretical developments supported by laboratory and field measurements have shown that the composite dielectric is weighted by the volume concentration of the components. The CRIM model for a material with *k* components can be written as the following Equation (5-2):

$$\varepsilon_r^n = \sum_{i=1}^{k} \varepsilon_{ri}^n c_i \tag{5-2}$$

where c_i is the volume concentration of the ith component of a mixture, ε_r is the dielectric constant of the ith component, n is an empirical exponent, which theoretically may vary between -1.0 to 1.0. However, multiphase mixtures, such as a soil, values between 0.4 and 0.8, which gives the CRIM a semi-imperial nature. The n of 0.5 is the most commonly accepted value (Roth et al., 1990; Bohl and Roth, 1994; 22 37 -42).

The complex refraction index model is used to determine the dielectric value of the aggregate mix, and the dielectric constant of the solids ε_s value for aggregate mixture is calculated in a two-step procedure. Since the dielectric value (ε_r) of the base course is measured by using the percometer, it is a known parameter along with the relative dielectric value of the water (ε_w) 81 in Equation (5-3). The first step is to

determine the volumetric solid content (θ_s), and the volumetric water content (θ_{sat}) by using a known parameter ε_w, and the parameters γ_w, γ_d, and G_s, which are properties of the base course aggregate. Then, the dielectric value of the solids is calculated because it is the only unknown parameter in Equation (5-3). The second step is to determine the saturated dielectric value of the material by using Equation (5-4). In the first step, the saturated volumetric water content (θ_{sat}) and the volumetric solid content (θ_s) were determined. The calculated volumetric water content is used in the second step because the volumetric solid fraction is the same value, which does not vary with change in the moisture content. Next, the dielectric value ε_r can be calculated by using both θ_{sat} and θ_s in Equation (5-4). The two CRIM dielectric values are given in Equation (5-3) as follows:

$$\sqrt{\varepsilon_r} = \left[\left(\sqrt{\varepsilon_s} - 1 \right) \theta_s + \left(\sqrt{\varepsilon_w} - 1 \right) \theta_w + 1 \right] \tag{5-3}$$

The saturated dielectric value is calculated in Equation (5-4):

$$\left(\sqrt{\varepsilon_r} \right)_{sat} = \left[\left(\sqrt{\varepsilon_s} - 1 \right) \theta_s + \left(\sqrt{\varepsilon_w} - 1 \right) \theta_{sat} + 1 \right] \tag{5-4}$$

where ε_r is the measured dielectric value, ε_s gives the dielectric value of solid, ε_w is the dielectric value of water, θ_s represents the volumetric solids content, θ_w is the volumetric water content, and θ_{sat} yields the saturated volumetric water content.

The micromechanics self-consistent model is another widely used model to determine dielectric value based on the moisture content and the dry density of soil

mixture (Lee et al., 2009). In this regards, this model considers the moisture content as soil component and is used to determine the dielectric value of the soil. Therefore, this model takes more fundamental approaches into account for every component element along with the contribution of the moisture in the composite media. The micromechanics self –consistent model is given in Equations (5-5) to (5-7):

$$\sum_{i=1}^{n} \theta_i \left[\frac{\varepsilon_i - \varepsilon_r}{\varepsilon_i + 2\varepsilon_r} \right] = 0 \tag{5-5}$$

$$\left(\frac{\gamma_d}{G_s \gamma_w} \right)_s \left(\frac{\varepsilon_s - \varepsilon_r}{\varepsilon_s + 2\varepsilon_r} \right) + \theta_w \left(\frac{\varepsilon_w - \varepsilon_r}{\varepsilon_w + 2\varepsilon_r} \right) + \left(1 - \frac{\gamma_d}{G_s \gamma_w} - \theta_w \right) \left(\frac{1 - \varepsilon_r}{1 + 2\varepsilon_r} \right) = 0 \tag{5-6}$$

The term $\gamma_d / G_s \gamma_w$ represents the volumetric solid of soil media and thus it can be substituted with θ_s term:

$$\theta_s \left(\frac{\varepsilon_s - \varepsilon_r}{\varepsilon_s + 2\varepsilon_r} \right) + \theta_w \left(\frac{\varepsilon_w - \varepsilon_r}{\varepsilon_w + 2\varepsilon_r} \right) + \left(1 - \theta_s - \theta_w \right) \left(\frac{1 - \varepsilon_r}{1 + 2\varepsilon_r} \right) = 0 \tag{5-7}$$

where γ_d is the dry density of soil, G_s gives the specific gravity of soil, γ_w is the unit weight of water, and all other inputs are defined above.

5.2.5 Calculations

The weight relationship between the moisture content and the unit weight is given in Equation (5-8) and (5-9), respectively:

$$w = \frac{W_w}{W_s} \tag{5-8}$$

$$\gamma = \frac{W}{V} \tag{5-9}$$

where w is the gravimetric water content, W_w is the weight of water (g), W_s is the weight of solids (g), W is the total weight of the mixture, γ is the unit weight (g/cm^3), and V is the volume of the sample (cm^3).

To calculate the volumetric water content, a relationship among moisture content and unit weight should be identified clearly from the volume-weight phase diagram of the sample. The phase diagram is given in Figure 5-4, in which the volume equation is given in term of void ratio (e).

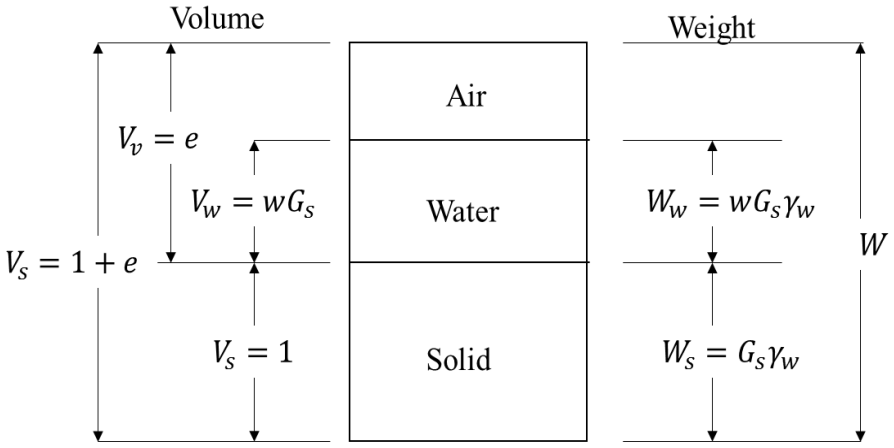

Figure 5-4 Soil Volume and Weight are Represented in the Phase Diagram with Volume Equal to 1

The volume of the water is expressed in Equation (5-10):

$$V_w = \frac{W_w}{\gamma_w} = wG_s \tag{5-10}$$

where γ_w is the unit weight of water (g/cm^3), G_s is the specific gravity of solids and the dry density of soil can be written as in Equation (5-11):

$$\gamma_d = \frac{W_s}{V} \tag{5-11}$$

where γ_d is unit weight of soil (or dry density g/cm^3)

Thus, the volumetric water content, which can be expressed in terms of the unit weight of the water, dry density, and gravimetric water content, is presented in (5-12):

$$\theta_w = \frac{V_w}{V} = \frac{\gamma_d}{\gamma_w} w = \frac{W_w \gamma_d}{W_s \gamma_w} = \frac{Se}{1+e} \tag{5-12}$$

where θ_w is the volumetric water content, S is the degree of saturation, and e is the void ratio.

This part of the chapter, which is about the experimental study, covered the sample preparation and measurement of the dielectric constant by using the percometer device. The calculated saturated dielectric value will be used to generate a soil suction-vs- dielectric constant correlation. A detailed procedure of the correlation will be presented in the following section.

5.3 Suction Dielectric Characteristic Curve (SDCC)

The dielectric constant of base course aggregate can be used directly to measure the soil suction. The percometer, the probe measurements are a part of empirical study, can be utilized to measure suction from 0 kPa to 10^6 kPa. In order to measure the soil suction, a general model is carried out between the matric suction and dielectric constant value. This model delivers the direct value of the soil suction as a function of the dielectric

constant. Here, the model is presented for the first time and is defined as the Soil-Dielectric Characteristic Curve and is denoted as *SDCC*.

The mathematical form of the *SDCC* model is derived based on the approach developed by Juarez-Badillo (1981;1983;1985). The general philosophic principle are used to obtain the changes in the dielectric constant under defined boundary limits with respect to the soil suction change from zero suction to the maximum suction value of 10^6 kPa. A schematic illustration presents the boundary conditions for each defined function in Figure 5-5.

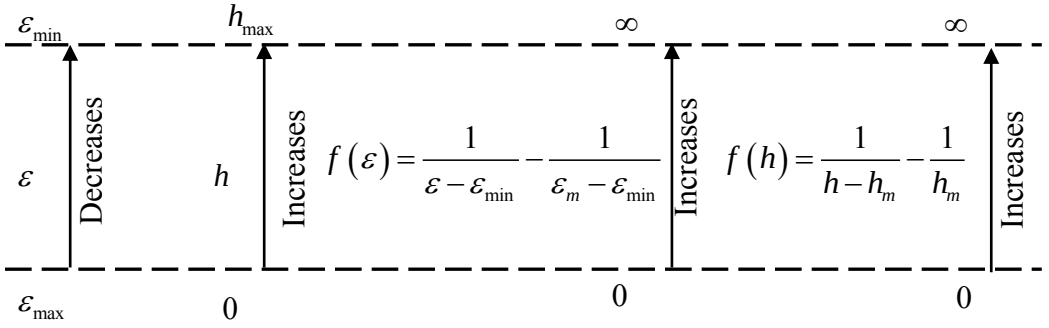

Figure 5-5 Schematic Presenting the Boundaries with the Functions

The domain for dielectric is from ε to ε_m, and the defined function changes that is f(ε)=0 for $\varepsilon=\varepsilon_m$ and f(ε)=∞ for $\varepsilon=\varepsilon_{min}$. Similarly, defined f(h) function changes f(h)=0 for h=0 and f(h)=∞ for h=∞. The defined functions f(ε) and f(h) are connected with γ, which is a non-dimensional parameter of proportionality. Defined parameters are expressed in Equation (5-13):

$$\int_{\varepsilon_1}^{\varepsilon} \frac{df(\varepsilon)}{f(\varepsilon)} = \gamma \int_{h_1}^{h} \frac{df(\mathrm{h})}{f(\mathrm{h})} \tag{5-13}$$

Equation (5-13) was integrated to obtain following:

$$\ln\left[\frac{\frac{1}{\varepsilon-\varepsilon_{\min}}-\frac{1}{\varepsilon_m-\varepsilon_{\min}}}{\frac{1}{\varepsilon_1-\varepsilon_{\min}}-\frac{1}{\varepsilon_m-\varepsilon_{\min}}}\right] = \gamma \ln\left[\frac{\frac{1}{h_m-h}-\frac{1}{h_m}}{\frac{1}{h_m-h_1}-\frac{1}{h_m}}\right] \tag{5-14}$$

Equation (5-22) was simplified and rewritten:

$$\ln\left[\frac{\left(\varepsilon_m-\varepsilon_{\min}-\varepsilon+\varepsilon_{\min}\right)}{\left(\varepsilon-\varepsilon_{\min}\right)\left(\varepsilon_m-\varepsilon_{\min}\right)} * \frac{\left(\varepsilon_1-\varepsilon_{\min}\right)\left(\varepsilon_m-\varepsilon_{\min}\right)}{\left(\varepsilon_m-\varepsilon_{\min}-\varepsilon_1+\varepsilon_{\min}\right)}\right] = \gamma \ln\left[\frac{\left\lfloor h_m-\left(h_m-h\right)\right\rfloor h_m\left(h_m-h_1\right)}{\left(h_m-h\right)h_m\left[h_m-\left(h_m-h_1\right)\right]}\right] \tag{5-15}$$

$$\ln\left[\frac{\left(\varepsilon_m-\varepsilon\right)}{\left(\varepsilon-\varepsilon_{\min}\right)}\frac{\left(\varepsilon_1-\varepsilon_{\min}\right)}{\left(\varepsilon_m-\varepsilon_1\right)}\right] = \gamma \ln\left[\frac{h}{\left(h_m-h\right)}\frac{\left(h_m-h_1\right)}{h_1}\right] \tag{5-16}$$

$$\left[\frac{\left(\varepsilon_m-\varepsilon\right)}{\left(\varepsilon-\varepsilon_{\min}\right)}\right] = \left[\frac{\left(\varepsilon_m-\varepsilon_1\right)}{\left(\varepsilon_1-\varepsilon_{\min}\right)}\right]\left[\frac{\left(h_m-h_1\right)}{h_1}\right]^{\gamma}\left[\frac{h}{\left(h_m-h\right)}\right]^{\gamma} \tag{5-17}$$

An r term is defined in Equation (5-18):

$$r = \left[\frac{\left(\varepsilon_m-\varepsilon_1\right)}{\left(\varepsilon_1-\varepsilon_{\min}\right)}\right]\left[\frac{\left(h_m-h_1\right)}{h_1}\right]^{\gamma}\left[\frac{h}{\left(h_m-h\right)}\right]^{\gamma} \tag{5-18}$$

Equation (5-18) is inputted in Equation (5-19):

$$\varepsilon = \frac{\varepsilon_m+\varepsilon_{\min} r}{1+r} \tag{5-19}$$

An α term is defined in Equation (5-20):

$$\alpha = \left[\frac{(\varepsilon_m - \varepsilon_1)}{(\varepsilon_1 - \varepsilon_{\min})}\right]\left[\frac{(h_m - h_1)}{h_1}\right]^{\gamma} \tag{5-20}$$

Equation (5-19) is rewritten with α :

$$\varepsilon = \frac{\varepsilon_m + \varepsilon_{\min}\alpha\left[\frac{h}{(h_m - h)}\right]^{\gamma}}{1 + \alpha\left[\frac{h}{(h_m - h)}\right]^{\gamma}} \tag{5-21}$$

The general form of the Suction Dielectric Characteristic Curve is presented in Equation (5-22):

$$\varepsilon_r = \left[\frac{\varepsilon_{sat} + \varepsilon_{\min}\alpha\left[\frac{h}{\left(1.45x10^5 - h\right)}\right]^{\gamma}}{1 + \alpha\left(\frac{h}{1.45x10^5 - h}\right)^{\gamma}}\right] \tag{5-22}$$

where ε_{sat} is the saturated dielectric value, ε_r gives the soil dielectric value, $\varepsilon_{\min}$ is the minimum dielectric constant, h_m is the maximum suction (1.45x10^5 psi), α and γ are the soil parameters change with the soil characteristics.

The minimum dielectric constant is given in Equation (5-23):

$$\sqrt{\varepsilon_{\min}} = 1 + \theta_s\left(\sqrt{\varepsilon_s} - 1\right) \tag{5-23}$$

where all the variables are defined above.

The *SDCC* is an S-shaped curve and requires the input of the saturated dielectric constant, suction, and two parameters. Two soil fitting parameters control the major mechanism to govern the change in the shape of the *SDCC*. The effect of the parameter α is given in Figure 5-6.

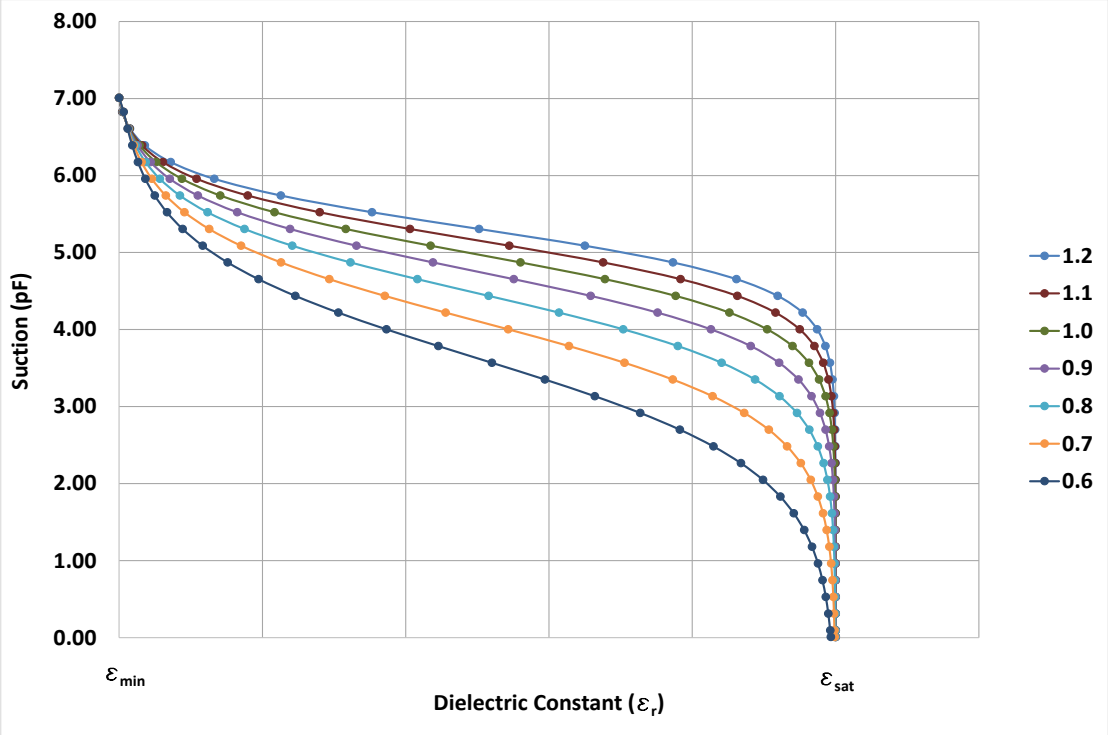

Figure 5-6 Effect of Variation of the Parameter α on *SDCC*

Figure 5-6 shows that when the parameter α increases, the suction value, the same as the dielectric constant, increases as well. This parameter governs the shape of the *SDCC* range at which the suction values are lower range.

The second parameter γ also has an effect on the *SDCC* shape. The influence of the parameter γ is given in Figure 5-7.

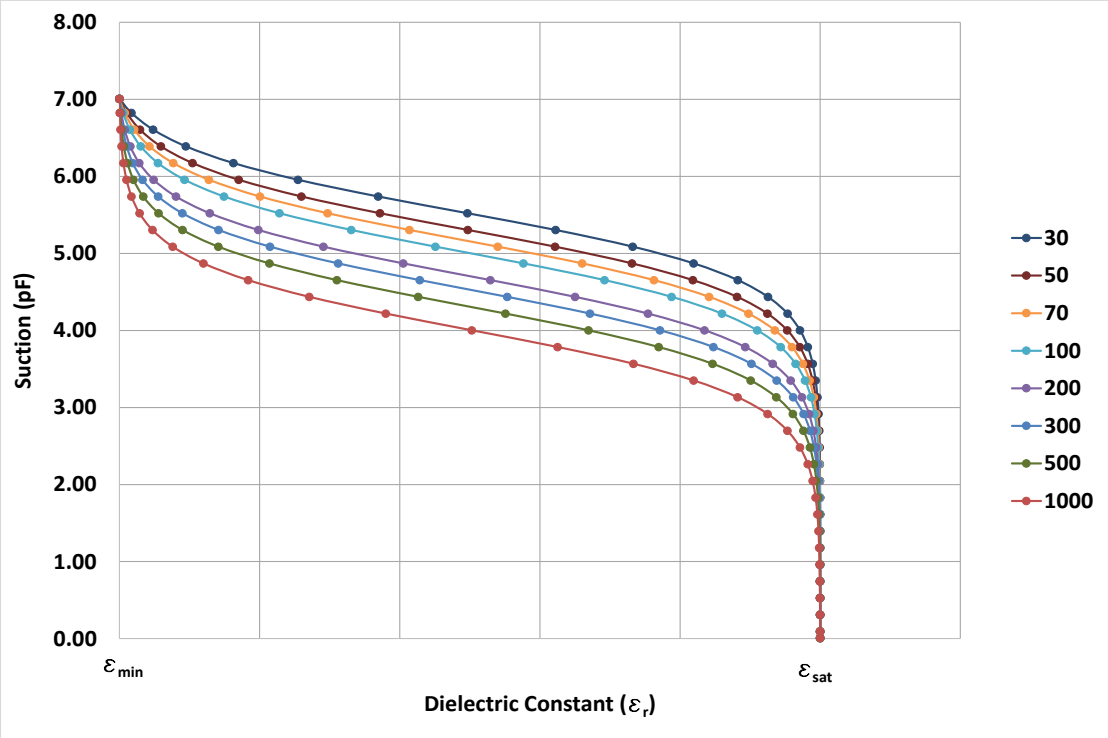

Figure 5-7 Effect of Variation of the Parameter γ on *SDCC*

Figure 5-7 shows that when the γ parameter decreases, the suction increases at the same dielectric constant. The shape of the *SDCC* at a higher suction level is governed by parameter γ to provide a smoother fit with the data. It is important to note that the proposed *SDCC* model is capable of calculate accurate suction both in the psi and kPa unit. Figure 5-7 and Figure 5-6 presented above are calculated and plotted based on the psi unit.

This proposed *SDCC* method is applied to a set of the unbound base course aggregate materials. Three parameters, ε_{sat}, α and γ, are utilized to obtain a *SDCC* that covers the entry suction range. These three parameters vary with the base course aggregate sources/pits.

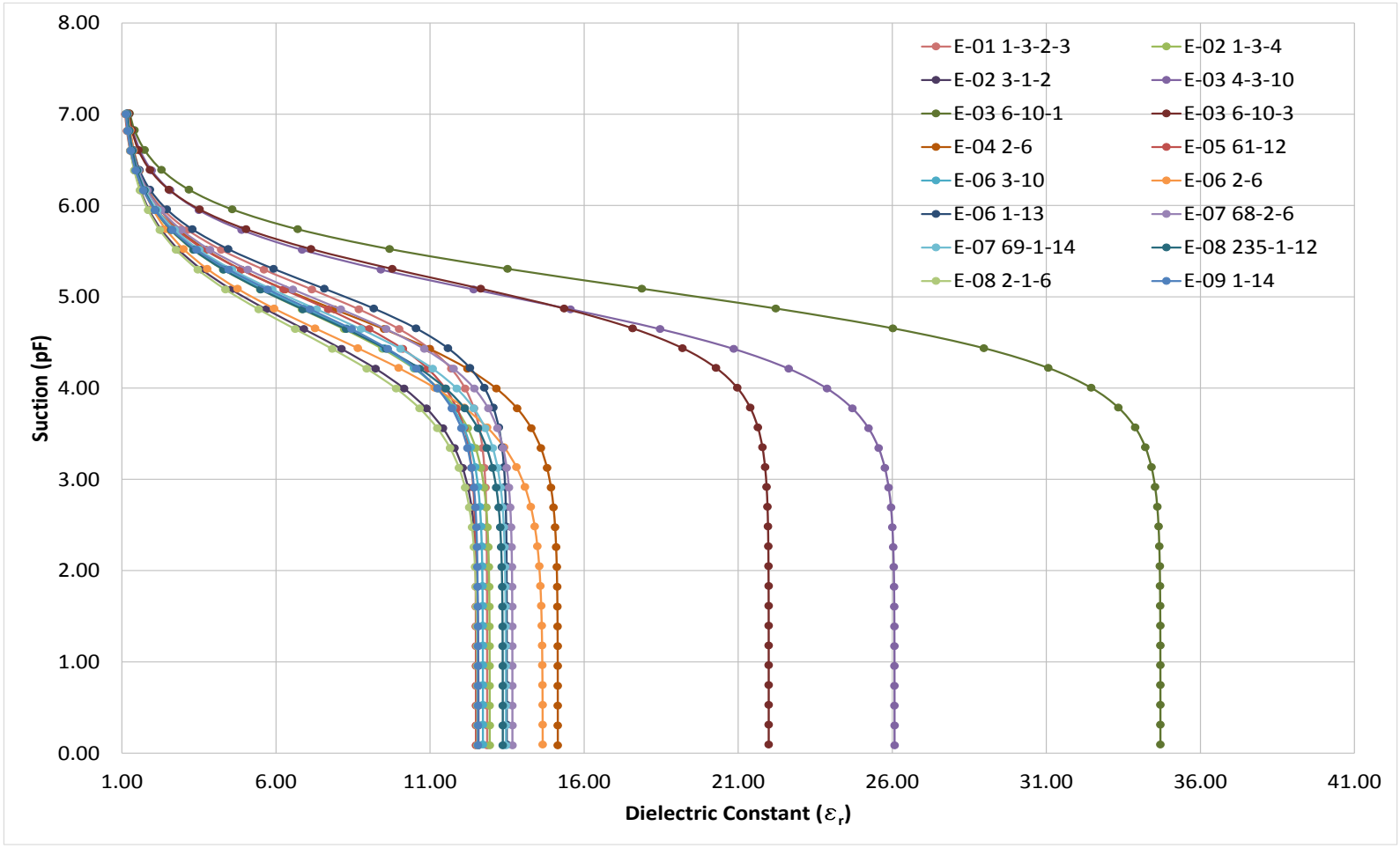

Figure 5-8 A Family of the Generated *SDCC* Curves for Various Material from Nine Pits

A family of plotted *SDCC*s with respect to the dielectric constant value for nine-(9) different aggregate pits are illustrated in Figure 5-8. These 9 pit names are collected from various locations in Texas, and these pits are listed by using label codes as E-01, E-02, E-03, E-04, E-05, E-06, E-07, E-08 and E-09. The first two numbers give the pit name, and the extension numbers represent materials that are sampled multiple times for the same pit.

It can be observed from Figure 5-8 that all of the materials from various pits have a unique *SDCC* curve, and the shape of the curve is specifically defined for each material. The reason behind this phenomenon is that each *SDCC* has a specific saturated dielectric constant value, air entry value, and a slope angle, all of which reflection of the material characteristic at the production time in the pits. This phoneme is controlled by only two parameters; therefore it is required to determine the two fitting parameters α and γ.

An efficient methodology has developed to determine the two parameters for base course material. This methodology uses the methylene blue value and percent fines content to provide a unique value. The details of this methodology are explained in the following section.

5.4 Development of Curve Fitting Method Two Fitting Parameters

Two critical steps are involved to generate the *SDCC*s using the fitting parameters method. The first one is to assess the two parameters using the curve fitting method. The

other one is to establish correlations between determined two parameters and methylene blue value based on the regression analysis. These methods explained as follows.

5.4.1 Curve Fitting Method

The curve fitting methodology utilizes the regression analysis to identify two fitting parameters α and γ. In order to run regression analysis, three points must be calculated, and these points are shown in Figure 5-9. The *Point-A* represents a point where the suction is pF 7.0, and at this point the corresponding dielectric value is considered approaching to $\varepsilon_{\min}$. Thus, the dielectric value (ε) at *Point-A* is considered at $\varepsilon_{\min}$. *Point-B* represents a point at which the dielectric measurements are taken and suction is determined through the filter paper test. At this point the dielectric value (ε_r) is measured directly from the soil sample prepared for the filter paper test. *Point-C* represents a point at which suction approaches to zero when the sample is reaching the saturated state. When a sample is fully saturated with water, the suction approaches to zero and the saturated dielectric value (ε_{sat}) is determined based on the CRIM model.

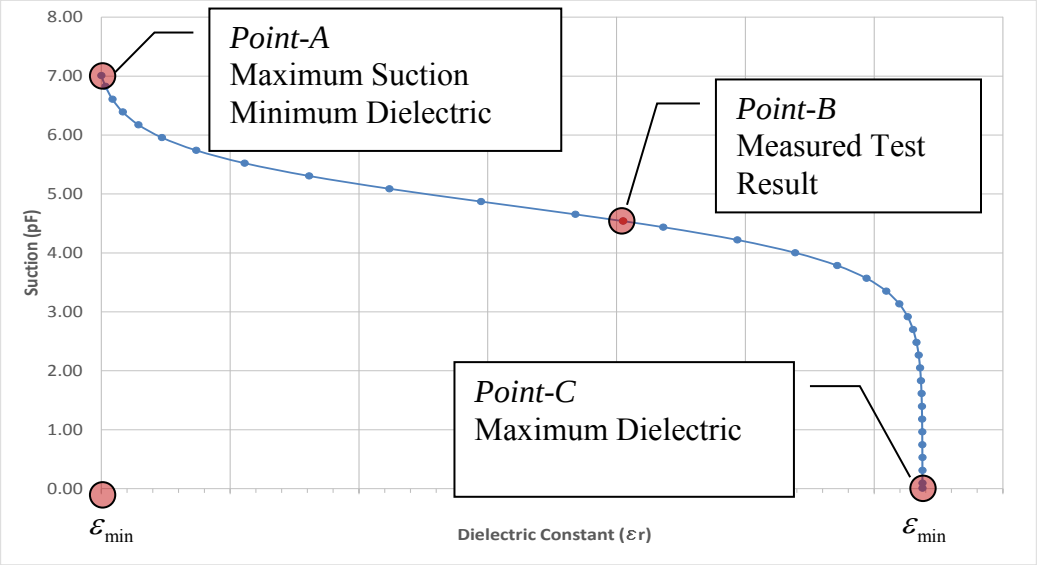

Figure 5-9 A Schematic Illustrate the Three-Point Method at the *SDCC*

The curve fitting method aims to minimize the difference between the measured dielectric constant at Point-B and the curve fitted to the dielectric value. The best fitting curve for the predicted dielectric constant gives the two fitting parameters. This analysis process is repeated for each of the materials twice to find the best fitting curve by using the *MS Excel Solver* function.

5.4.2 Regression Analysis

The regression analysis is performed to investigate the correlation between the determined two fitting parameters and methylene blue value and percent fine content. The regression analysis has executed by using the JMP statistical software program. This software constructs a neural network analysis database based on the input values. Then JMP executes a systematic stepwise regression analysis to find the perfect correlation that represents the data set, which passes through the predicted fitting. This analysis

process was repeated a number of times to find the most realistic and rational mathematical correlation between the input and the prediction model. The second concern in this regression analysis is to generate a good correlation with highest accuracy. Thus, in order to provide the highest accuracy, the pre-calculated steps are construed by using the hidden layer approach in the neural analysis process. As a result, the two fitting parameter correlations are assessed with a significantly higher accuracy.

The parameter α consists of two hidden layers, and these two layers are functions of the percent fines content and the methylene blue value. These hidden layers are given in Equations (5-24) and (5-25). The predicted parameter α is presented in Equation (5-26):

$$H_{1\alpha} = \text{TANH}(0.5(-0.478027\ (\text{MBV}) - 0.034582\ (\text{pfc}) + 8.923868)) \tag{5-24}$$

$$H_{2\alpha} = \text{TANH}(0.5(-0.207206\ (\text{MBV}) + 0.334387\ (\text{pfc}) + -8.088245)) \tag{5-25}$$

$$\text{Predicted}\,\alpha = 6.3772003\left(\text{H}_{1\alpha}\right) - 46.1404624\left(\text{H}_{1\alpha}\right) + 53.363999 \tag{5-26}$$

where α is the fitting parameter, $H_{1\alpha}$ and $H_{2\alpha}$ are hidden layer functions employed in the pre-calculation steps, *MBV* gives the methylene blue value and *pfc* is the percent fines content.

The validation of the real parameter α values and the predicted parameter α values based on the *MBV*, and *pfc* are presented in Figure 5-10.

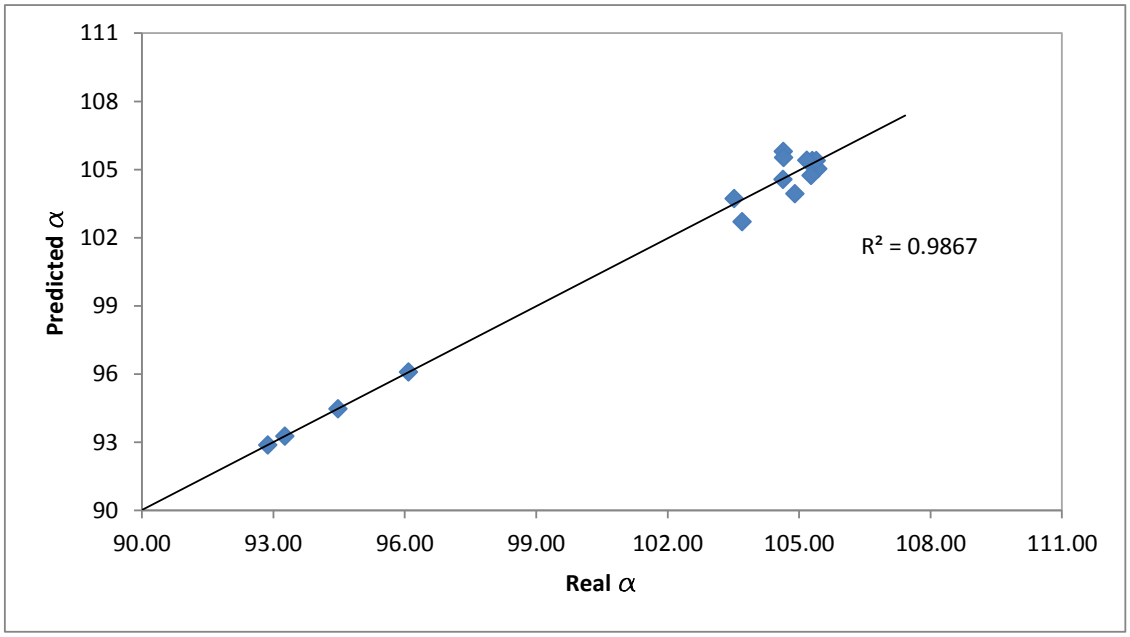

Figure 5-10 The Correlation between Predicted and Real Values of Parameter α

The second fitting parameter γ consists of three hidden layer functions and these three layers totally depend on the percent fines content and methylene blue value. These hidden layers are expressed in Equations (5-27) and (5-29). The predicted parameter γ is given in Equation (5-30):

$$H_{1\gamma} = \text{TANH}(0.5(0.0897001(MBV) - 0.1597119(\text{pfc}) + 0.69592558)) \quad (5\text{-}27)$$

$$H_{2\gamma} = \text{TANH}(0.5(-0.0968849(\text{MBV}) - 0.020036(\text{pfc}) + 1.1379340)) \quad (5\text{-}28)$$

$$H_{3\gamma} = \text{TANH}(0.5(0.0668142(\text{MBV}) + 0.2112468(\text{pfc}) - 4.4814587)) \quad (5\text{-}29)$$

$$\text{Predicted}\,\gamma = 3.0066674(\text{H}_{1\gamma}) + 4.212358(\text{H}_{2\gamma}) + 3.211806(\text{H}_{3\gamma}) + 3.045290 \quad (5\text{-}30)$$

where γ is the fitting parameter, $H_{1\gamma}$, $H_{2\gamma}$ and $H_{3\gamma}$ are hidden layer functions employed in the pre-calculation steps, *MBV* is the methylene blue value, and *pfc* is the percent fines content.

The parameter γ depends on both the *MBV* and *pfc* values, all of which can be calculated by using the methylene blue test. The correlation between the real and predicted the parameter γ is given in Figure 5-11.

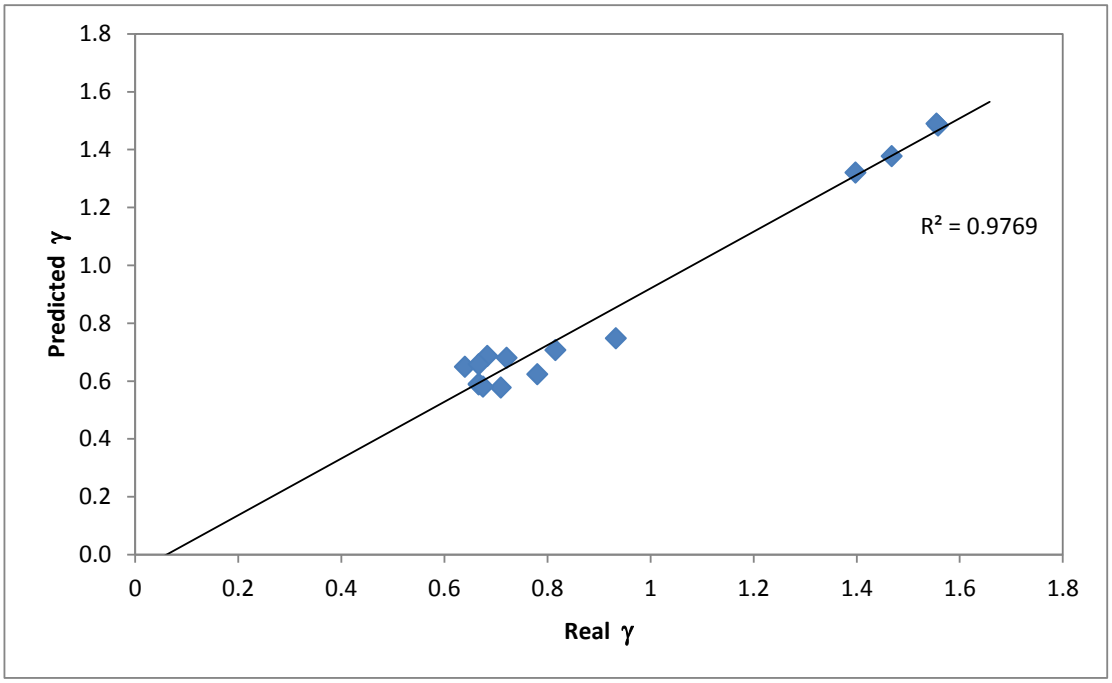

Figure 5-11 The Correlation between Predicted and Real Values of Parameter γ

5.4.3 Maximum and Minimum Dielectric Values

The maximum dielectric constant (ε_{sat}) of the soil, which is expressed as the saturated dielectric constant is explained earlier. The parameter ε_{sat} represents the maximum dielectric constant holding capacity of unbound base course aggregate at the minimum possible suction. The value of ε_{sat} must be calculated in order to determine the *Point-C*, which was explained previously and was presented in Figure 5-9. The saturated dielectric constant parameter is presented in Figure 5-12.

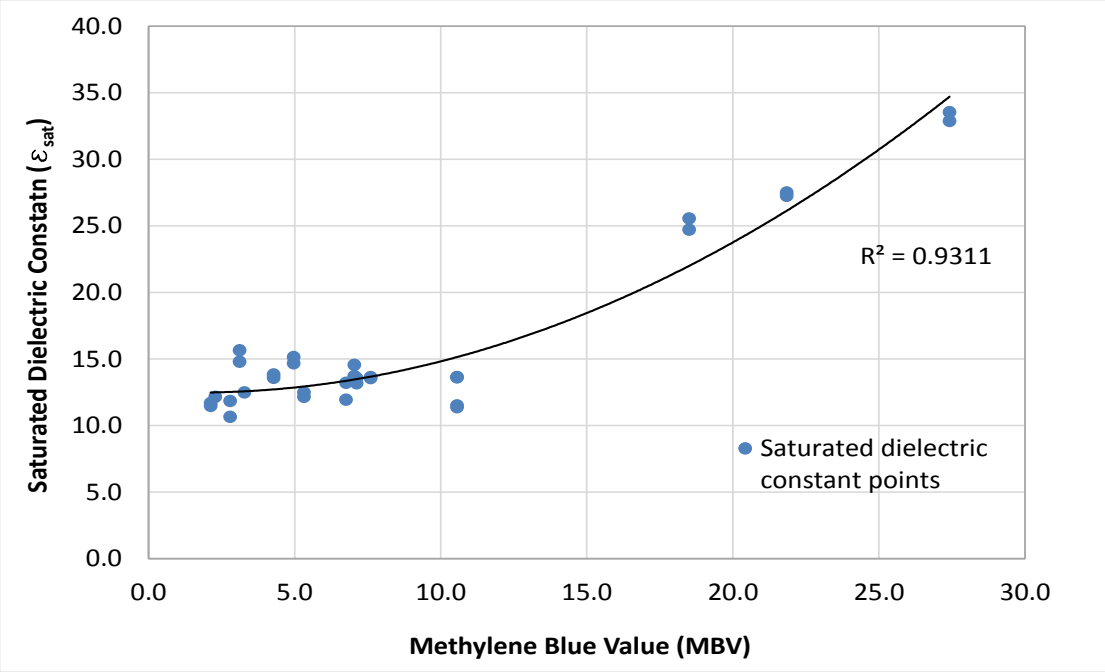

Figure 5-12 The Correlation between Methylene Blue Value and Saturated Dielectric Constant

The form of the ε_{sat} expression is presented in Equation (5-31):

$$\varepsilon_{sat} = 0.0334\left(MBV^2\right) - 0.1086\left(MBV\right) + 12.569 \quad (5\text{-}31)$$

where ε_{sat} is the saturated dielectric constant value, and *MBV* is the methylene blue value.

Equation (5-31) gives a simple second order polynomial expression and the value of the parameter ε_{sat} depends merely on the *MBV*.

The value of ε_{min} also must be determine in order to calculate the minimum dielectric constant at *Point-A*, which was explained previously and was presented in Figure 5-9. The saturated dielectric constant parameter is presented in Figure 5-13.

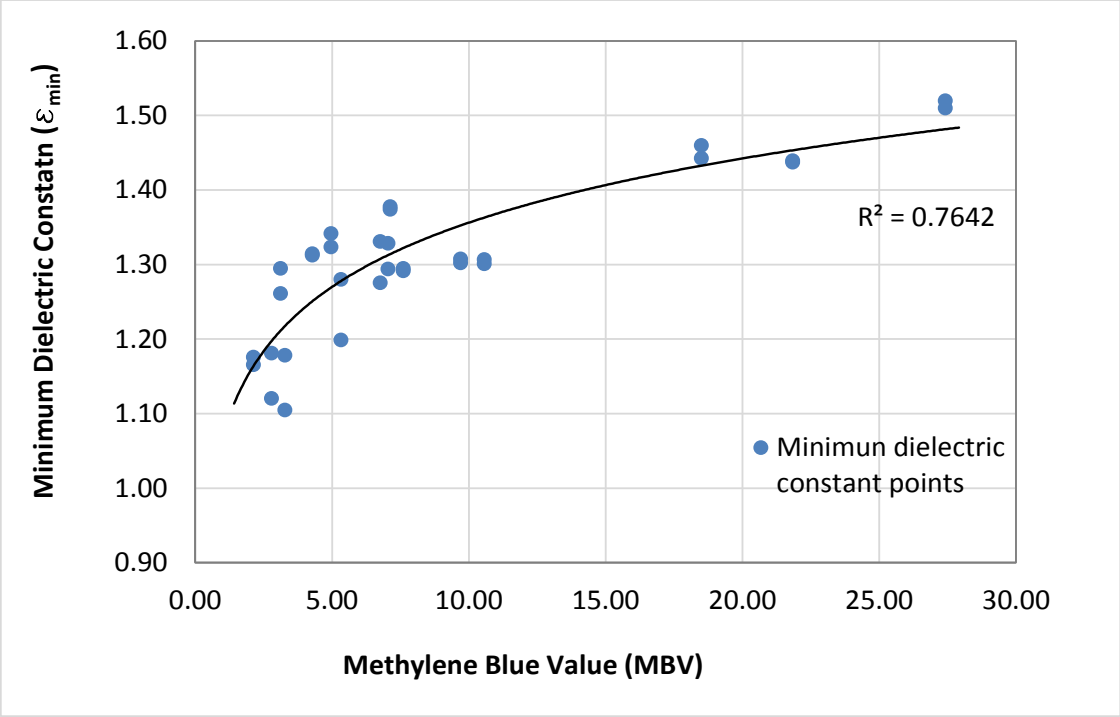

Figure 5-13 The Correlation between Methylene Blue Value and Minimum Dielectric Constant

The form of the ε_{min} expression is presented in Equation (5-32):

$$\varepsilon_{\min} = 0.1243\log(MBV) + 1.0668 \tag{5-32}$$

where $\varepsilon_{\min}$ is the minimum dielectric constant value, and *MBV* is the methylene blue value.

Equation (5-32) represents a logarithmic correlation, which total depends on the MBV. Therefore, performing the methylene blue test on a base course material is very important in determining the *SDCC* characteristic of the material.

In the previous section, two important dielectric models CRIM and Self-consistent were introduced, which are used to determine the dielectric value of a composite media. The CRIM is utilized to calculate dielectric constant, specifically the maximum dielectric constant of the base course aggregate materials. The results of a comparison between these two models is shown in Figure 5-14.

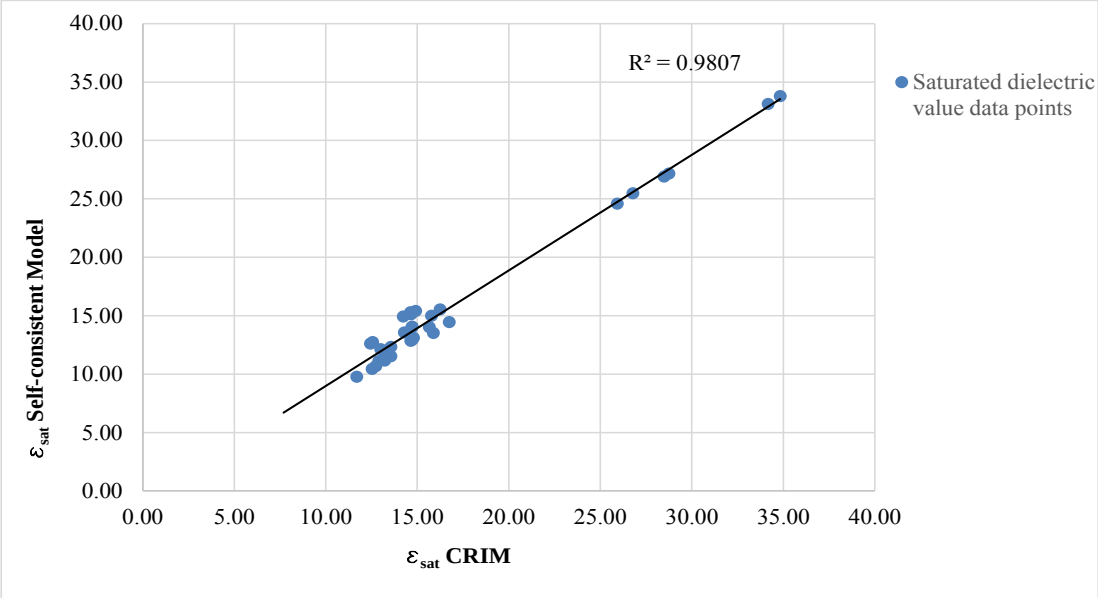

Figure 5-14 A Comparison of Saturated Dielectric Constants based on the Two Models

It is important to evaluate the quality of both the CRIM and Self-consistent models based on the calculated ε_{sat} parameter. Figure 5-14 shows that both models show a consistency to determine the dielectric constant. There is a good agreement between these models with an R^2 0.98. Thus, both models can be used in calculation of ε_{sat} but in this study, the presented calculations in the *SDCCs* were made based on the CRIM model.

5.5 Closure

This part of the study covers the empirical method to determine the dielectric value and provides the information about new approaches that are used to analyze the test results to determine a new mechanistic dielectric constant model. The percometer test procedure was explained in detail, including the dielectric constant concept, the soil sample preparation method and dielectric measurement. Additionally, a correlation was carried out between soil dielectric constant value and soil suction for unbound base course aggregate materials. A soil-dielectric characteristic curve (*SDCC*) method was proposed to determine soil suction with respect to dielectric constant value. A family of nine distinct pits were used to determine the soil suction by using the proposed *SDCC* model. It is noted that *SDCC* is capable of providing the suction value and each selected pit showed different geometric shape and characteristics.

The reason behind the unique curve is that only two fitting parameters control the shape of the *SDCCs* .The predicted correlation showed that these parameters change with the mineralogical characteristic of the pits. In fact, these parameters totally depend

on the percent fines content and methylene blue value of the pits. Therefore, the correlations were determined between the two-fitting parameters and *pfc*, *MBV*. The outcomes of the regression analysis was expressed in two mathematical relationships for the fitting parameters.

All of these improvements have shown that the *SDCC* is a simple and accurate method to determine soil suction of the base course aggregate. This method utilizes non-destructive test techniques to determine the dielectric constant, and it is also well applicable to use in both laboratory and in-situ measurements.

These advances give a capability of finding the soil suction by using the *SDCC* and provides a connection to soil suction water characteristic curve (*SWCC*), which is one of the fundamental soil properties. This advance enables the proposed *SDCC* method to reliably determine the volumetric water content by using the percometer device. This improvement will be discussed in following sections.

6. DEVELOPMENT SOIL WATER CHARACTERISTIC CURVE (SWCC) METHODOLOGY FOR BASE COURSE MATERIALS

6.1 Introduction

Information about the stiffness and other critical material characteristics of the aggregates are essential and hence they must be taken into account while designing the unbound base course layer. The presence of fines and their characteristics, combined with the aggregate mineralogy, affect the base performance and contribute significantly to moisture susceptibility and other similar distresses. The softening effect that builds up results in increased permanent deformation in pavement systems when subjected to heavy repeated loading due to high traffic volumes and also induces a drop in the suction. While the importance of suction in unsaturated soil mechanics has been well recognized over the last several decades and various suction theories have been modified and improved, the implementation of the theories has not been widespread in geotechnical and pavement engineering applications.

The important engineering properties of aggregate base courses, such as stiffness, shear strength, permeability, and diffusion shear strength are directly related to the soil water characteristic curve (*SWCC*). Generating the *SWCC* curve and determining matric suction is extremely important in order to measure such engineering properties. The *SWCC* and soil matric suction values are determined based on the soil properties. This research effort aims to determine the *SWCC* based on the soil characteristics and the methylene blue value.

A study that is developing a correlation between the methylene blue test and the fines particle size distribution is presented in the following section, and a new methodology that is used to determine the *SWCC* based on the *MBV* is described in detail. The *MBV* is correlated to the four important *SWCC* parameters.

6.2 Background

The soil water characteristics curve represents a relation between soil moisture and suction. This relationship occurs between either suction and water content or suction and degree of saturation. Every soil has a unique *SWCC* shape. The reason is that the *SWCC* is generally affected by soil type, mineralogy formation of the soil, amount of fines content, soil gradation and the percent passing through the No. 200 sieve.

There are several laboratory test devices, such as pressure plates, which are employed to generate the *SWCC* . The experimental procedure takes from two days to a week. Thus, the experimental method takes a longer time to predict a *SWCC* curve due to its limitations. Consequently, developed mathematical models have been proposed to build up the *SWCC* in a shorter time.

A number of experimental studies have shown that the shape of the *SWCC* is an S-shape or sigmoidal curve. Furthermore, several studies have demonstrated that the sigmoidal shape is the fit compared to the other curve types. Among the various types of models developed, Fredlund and Xing's (1994) model has shown the best fitting relationship to their equation based on a study conducted by Zapata (1999).

The Fredlund and Xing (1994) model is one of the most commonly used *SWCC* models and is given in Equations (6-1) and (6-2):

$$\theta_w = C(h) \times \left[\frac{\theta_s}{\left[\ln\left[\exp(1) + \left(\frac{h}{a_f} \right)^{b_f} \right] \right]^{c_f}} \right] \tag{6-1}$$

$$C(h) = \left[1 - \frac{\ln\left(1 + \frac{h}{h_r} \right)}{\ln\left(1 + \frac{10^6}{h_r} \right)} \right] \tag{6-2}$$

where a_f is a function of the air entry value of the soil in kPa, b_f is a function of the rate of water extraction from the soil once the air entry value is exceeded, c_f is a function of the residual water content, h_r is a function of the suction at the residual water content in kPa, θ_w is the volumetric water content, and θ_s is the saturated volumetric water content.

Currently, there are two popular approaches to determine the *SWCC* for a soil: the first one is an experimental method by conducting the filter paper test or pressure plate test to measure the suction values at different moisture contents; the other is an estimation method on the basis of the *SWCC* method.

6.3 Problems Related to Methods Used to Determine SWCCs

Problems related to unsaturated soil and expansive clays are significant; therefore, a recent research has focused on developing new analysis methods and models that will mitigate the problems associated with the clay. The *SWCC* gives the matric suction, which is one of the most important unsaturated soil mechanics properties, associated with the fundamental engineering properties related to shear strength, compressibility, and fluid flow (Perera 2005). For instance, the stress sensitivity depends on the suction and moisture level. The stress sensitivity requires knowledge of the SWCC because the water content-suction relationship is controlled by the finer fraction of the aggregate mix.

The measurement of an *SWCC* requires a special set of laboratory equipment, experienced labor, longer experiment time, and specific testing program. In order to eliminate the difficulties of a laboratory experimental program, the methylene blue test method was established as an efficient alternative approach in predicting the four fitting parameters. The prediction of the shape of the *SWCC* curve is determined by using the methylene blue test, and verification is completed by using the filter paper method.

One of the pioneer studies correlating the fitting parameters in the Fredlund and Xing equation with the analytical equation was conducted by Zapata (2000). Later, several studies elaborated on this research through finding new correlations for the fitting parameters developed based on D_{10}, D_{60}, plasticity index and the No. 200 sieve (Perera et al., 2005; Houston, 2006). These pioneering correlations are a solid basis from which to develop a new method based on other soil index properties, such as percent

fines amount and methylene blue value. The idea to develop the new approach reported here was suggested by the following limitations of the plasticity index and P_{200} approach: (a) errors involved in performing the plasticity index tests can be significant due to human intervention, test equipment sensitivity, and other such factors; (b) plasticity index may not be available to validate the sample and to calculate the parameters at all times, especially in the field; (c) in field applications, explicitly in quality control management, it might be necessary to determine the plasticity index quicker, or to predict the PI at a specific spot/location.

Also, it is noted in all geotechnical engineering textbooks and reference books that the percent fines content has been used for decades as an indicator of the activity of clay minerals. In a recent study, the *SWCC* fitting parameters were predicted by using the four new analytic fitting models, based on the percent fines content and methylene blue value, and proposed for expansive soils by Sahin (2011). This new approach overcomes the limitation in the previous methods.

The multi regression analysis is performed on each set of data to determine the four parameters based on the MBV. The four fitting parameters are provided on the S-shaped curve based on the Fredlund and Xing (1994) equation. Thus, the derived equations are useful to generate the *SWCC* s whenever testing time is limited.

6.4 Filter Paper Test

6.4.1 Sample Preparation

The unbound base course aggregate materials are selected based on the material testing program explained in Chapter 3. The materials delivered from each pit are tested based on the weekly production schedule. The material fraction passing through the No. 4 sieve from the sieve analysis is used to prepare a compacted sample, which is used for the filter paper test.

The standard filter paper test was used to measure the matric suction of the material passing through the No.4 sieve. Two compacted aggregate samples are prepared by using the standard compaction method in ASTM D 698. The size of the compacted specimens is 1.5 in. high and 3 in. in diameter. The compacted soil samples are kept in a 100 percent humidity room until they dry down to 2 percent moisture content. When the samples have reached the desired moisture content, they are taken from the environmental room and immediately placed in the filter paper test.

6.4.2 Test Procedure

The soil suction using the filter paper test is a common method that has been used in unsaturated soil mechanics for many years. Both total and matric suction can be determined by using the filter paper test method. In the matric suction measurement, filter paper is placed in between two identical compacted soil samples. When equilibrium is achieved, suction in the sample and filter papers will reach the equivalent phase. A schematic representation of the test setup is illustrated in Figure 6-1. In this

project, the prepared base mixture (complete gradation or just fines) was used to estimate suction at a given moisture content.

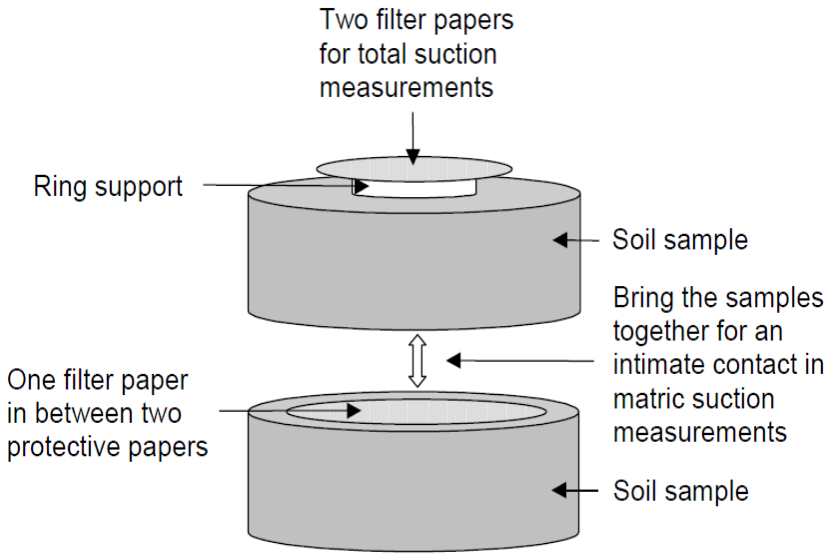

Figure 6-1 Soil Samples and Filter Papers for Matric and Total Suction (Lytton et al., 2004).

One filter paper is placed in between two compacted samples to measure matric suction. Then, the samples are placed in a jar and sealed with electrical tape. Two filter papers are placed on top of the sample to measure total suction level and then sealed again. The samples are kept for 7 days in the sealed jar. Then the jar is opened, and the suction values are measured by using moisture content based on the placement of the filter papers. The filter paper test procedure is given in ASTM D 5298 and an updated version used in this study is in TTI report 4518 in volume 2. The entire testing protocol for a compacted base course sample is shown in Figure 6-2.

(a)

(b)

(c)

(d)

(e)

(f)

(g)

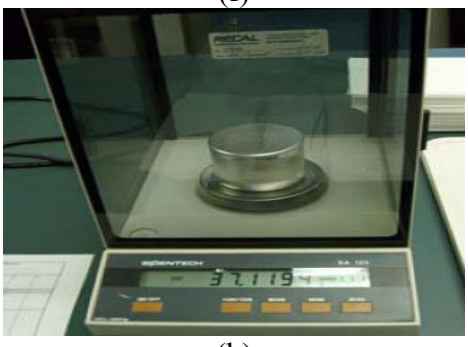

(h)

Figure 6-2 Filter Paper Suction Test Procedure Steps

Figure 6-2 shows that (a) compacted identical base course samples, (b) one filter paper in between two samples and one filter paper on top of the samples, (c) two filter papers placed on top of a plastic ring, (d) the process of placing samples in a jar and sealing it, (e) storing the sealed jar in a chest box, (f) after equilibrium period, opened the seal jar and weigh the wet filter papers along with the tin, (g) place tin with wet the filter paper in a hot oven, and (d) weigh the tins along with the dry paper.

The soil suction value for engineering practices is generally calculated in pF units (Schofield, 1935). The unit suction in pF equals $\log_{10}\left|suction\ in\ cm\ of\ water\right|$. The soil suction is also presented in the $\log kPa$ system (Fredlund and Rahardjo, 1993). The unit suction in $\log kPa$ is equal to the $\log_{10}\left|\text{suction in kPa}\right|$. The unit conversion correlation between these two systems is that *suction* in logkPa equals *suction* in pF-1 (Bulut, 2001).

6.5 Curve Fitting Methodology

The curve fitting process is a combination of a two-step process as described herein. The first step, which utilizes the filter paper suction test, investigates to find the best fitting curve based on the measured filter paper and the Fredlund and Xing (1994) equation. In the second step, predicted fitting curves are utilized to determine a correlation related to methylene blue test. These procedures are explained as follows:

6.5.1 Curve Fitting Method

In a previous study, the four parameters a_f, b_f, c_f and h_r and the soil suction value h_m are used to find the best fitting curve through the statistical multi regression analysis (Zapata 2010). This regression analysis aims to minimize the difference between the Fredlung and Xing equation and estimated points by changing the four fitting parameters on a plotted *SWCC* . It is usually enough to fit a curve only using three points, and hence three estimated points are used in the regression analysis. These points are illustrated in Figure 6-3.

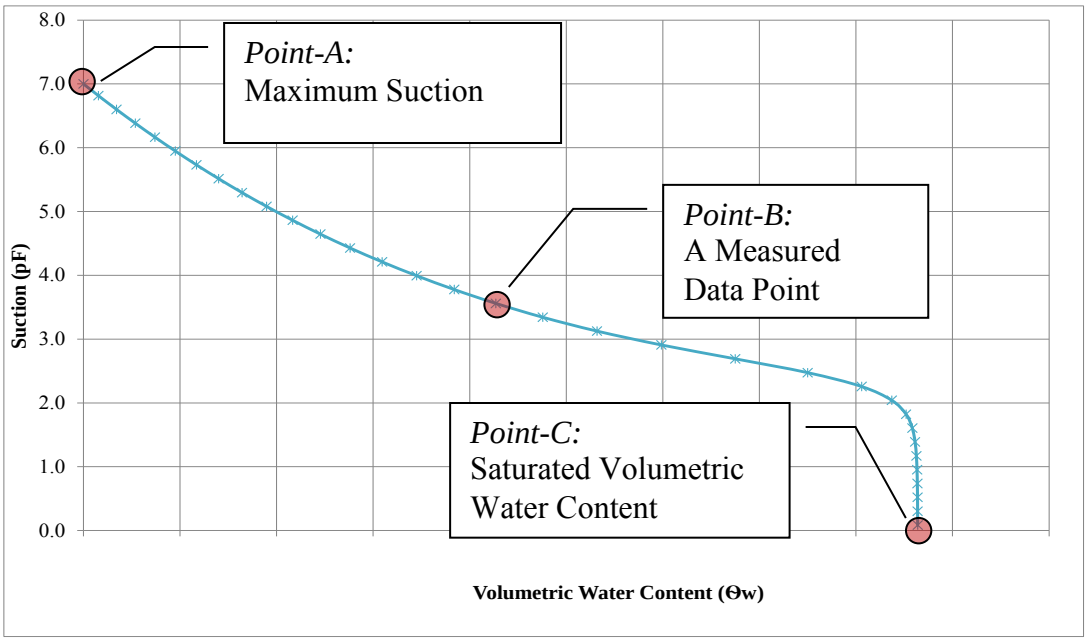

Figure 6-3 A Schematic Illustration of the Three-Point Method at the *SWCC*

Figure 6-3 shows *Point-A, Point-B,* and *Point-C,* each of which represent basically a state of the moisture content in the unit phase diagram of a soil media. *Point-*

A represents a state at which soil suction reaches the maximum level of pF 7 (10^6 kPa; 1.45 10^5 psi), and at this state moisture content approaches zero. *Point-B* represents the measured matric suction and the measured volumetric water content from the filter paper test. *Point-C* represents the saturated volumetric water content, which is the maximum moisture-holding capacity of the soil. Also, this point shows that the soil suction is at the minimum level.

The regression analysis was repeated several times by using these estimated points, which are calculated for each pit and the material sampled from the same pit at different times. The *Point-A* and *Point-C* sets were calculated and tabulated for all the collected materials, and the corresponding *Point-B* sets are measured by the experiment. Once these points are determined on the *SWCC* , the MS Excel Solver program is used to execute the analysis. This analysis determines the four parameters that provide the best possible fitting curve that passes through the matric suction data points. For this purpose, the minimum squared error was sought between the determined points and the *SWCC* equation by iterating the fitting parameters. This process was repeated for each material several times to find the best-fitting parameters, and a set of estimated fitting parameters were collected. These parameters are used in the following analysis.

6.5.2 Regression Analysis

These estimated four fitting parameters are tabulated with respect to the corresponding methylene blue values for each pit. A correlation was investigated between each fitting parameter and the measured MBV. The analysis showed that there is good agreement between the fitting parameters and the MBV. Thus, this successful approach enables

MBV to determine the *SWCC* for any unbound aggregates by calculating the fitting parameters. The four correlations between the fitting parameters a_f, b_f, c_f, and h_r, and the measured MBV are represented in Figure 6-4, Figure 6-5, Figure 6-6, and Figure 6-7 respectively. Along with these correlations, the agreements between the MBV and four fitting parameters are expressed from Equation (6-3) to (6-6).

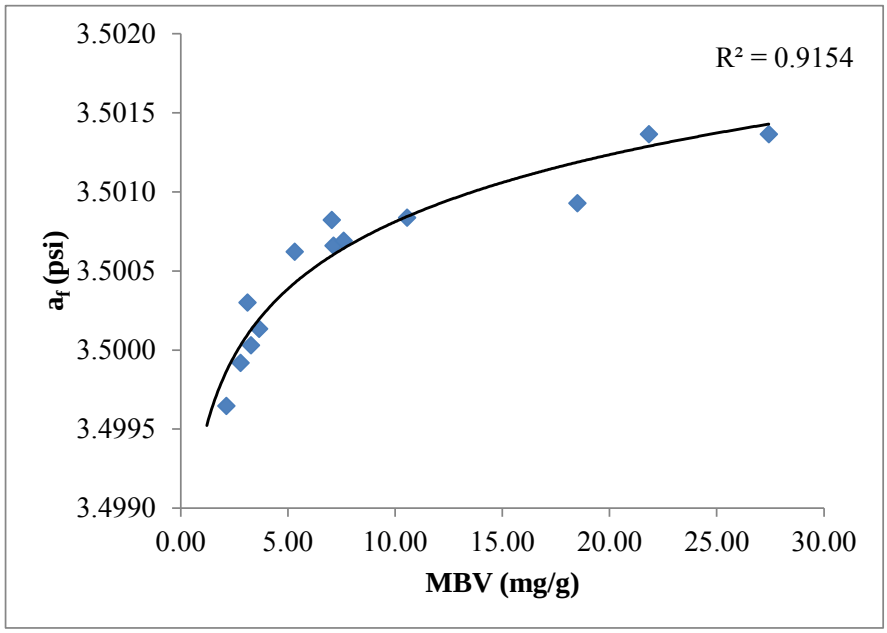

Figure 6-4 Change in a_f with respect to the Methylene Blue Value

The air entry value of the unbound base course aggregate (a_f) is formulated based on the MBV, and it is given in Equation (6-3):

$$a_f = 3.4994 MBV^{0.0002} \tag{6-3}$$

where all of them are defined above.

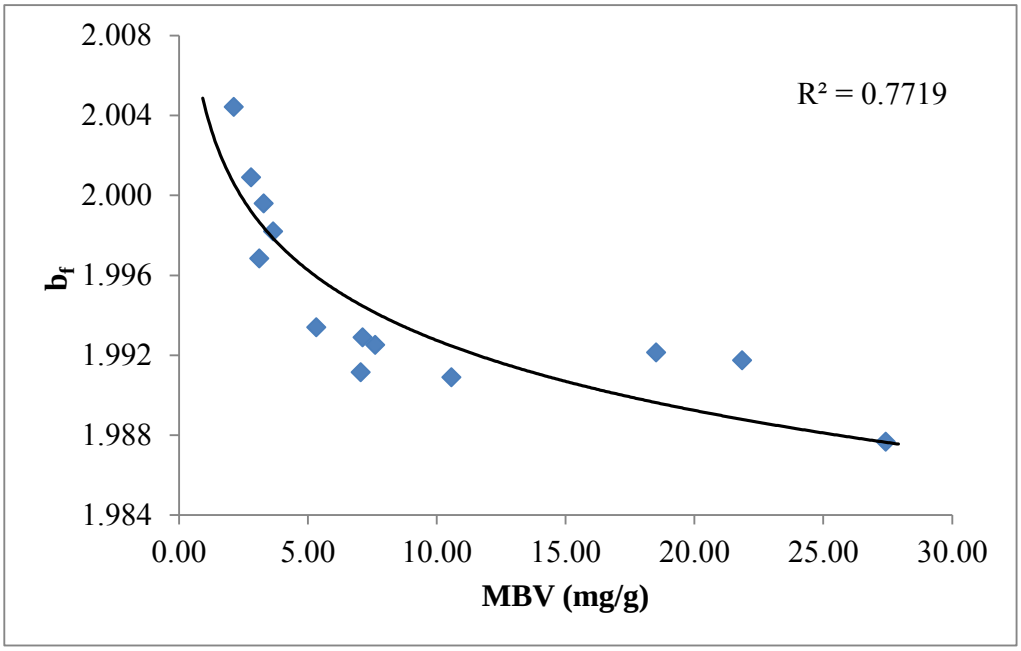

Figure 6-5 Change in b_f with respect to the Methylene Blue Value

The rate of water extraction of the unbound base course aggregate after exceeding the air entry value (b_f) is formulated in Equation (6-4):

$$b_f = 2.0044 MBV^{-0.003} \tag{6-4}$$

where all of them are defined above.

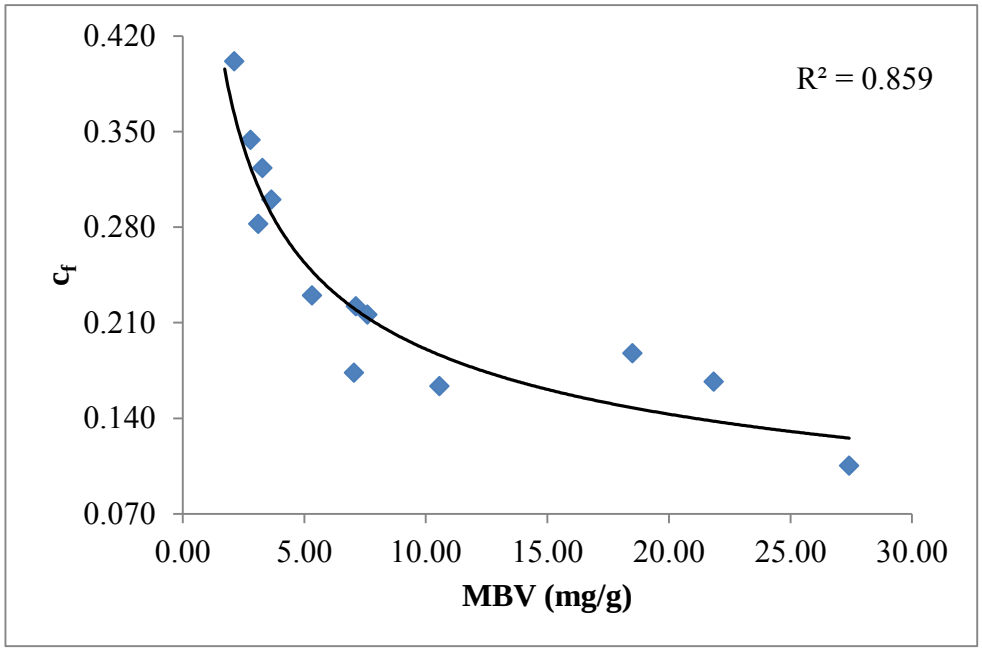

Figure 6-6 Change in c_f with respect to the Methylene Blue Value

The mathematical formulation for the residual water content of the unbound base course aggregate (c_f) is given in Equation (6-5):

$$c_f = 0.4956 MBV^{-0.415} \tag{6-5}$$

where all of them are defined above.

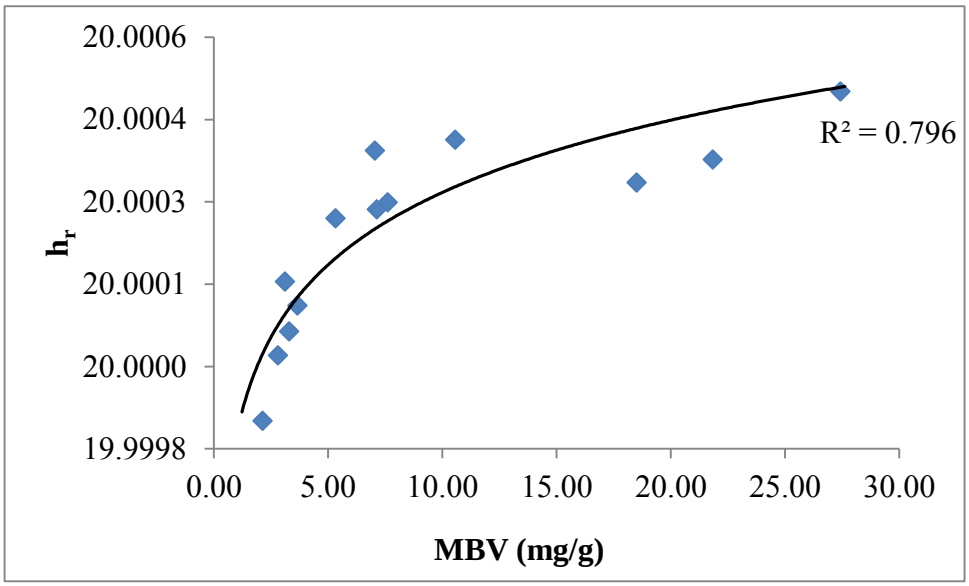

Figure 6-7 Change in h_r with respect to the Methylene Blue Value

The mathematical formulation for the residual suction value, at which the residual water content occurs (h_r) is given in Equation (6-6):

$$h_r = 20.00 x MBV^{9.5E-06} \tag{6-6}$$

where all of them are defined above.

6.5.3 Saturated Volumetric Water Content

The *Point-C* represents the saturated volumetric water content (θ_{sat}) as was mentioned earlier in Figure 6-3. The *Point-C* also shows the quantitative value of the maximum volumetric moisture content when the suction is at zero.

The saturated volumetric water content is numerically equal to the porosity of soils, which is the ratio of the volume of voids to the total volume, in the saturated state where all of the air voids are filled with water. It has been proven that porosity can be

used to represent the saturated volumetric water content by Houston (2006). In this regard, the saturated volumetric water content can be calculated in Equation (6-7).

$$\theta_{sat} = \left\lfloor 1 - \frac{\gamma_d}{(G_s \gamma_w)} \right\rfloor \tag{6-7}$$

where θ_{sat} is the saturated volumetric water content, γ_d gives the maximum dry unit weight of the soil, G_s is the specific gravity of the soil, and γ_w represents the unit weight of water.

In order to perform a regression analysis, three required points are employed, including a single measured suction point, a maximum suction value (pF=7.0) and a fully volumetric saturated point (pF=1). The volumetric water content of full saturation is equal to the porosity. Each one of the base course aggregates is a type of granular materials that are used in this study with various gradations. Therefore, the porosity of each material is calculated for further calculations.

The saturated volumetric water contents (θ_{sat}) are determine along with the four fitting parameters. A stepwise regression analysis was performed by using the JMP statistical software program. This software is capable of running the stepwise neural connections as it investigates the rational correlations. This analysis resulted in a correlation that shows the relationship between the saturated volumetric water content and the MBV, *pfc* and G_s. This neural modeling consists of three hidden layers that increase the accuracy of the neural model. The predicted θ_{sat} and the calculated θ_{sat} values, which is calculated by using Equation (6-7), are presented in Figure 6-8.

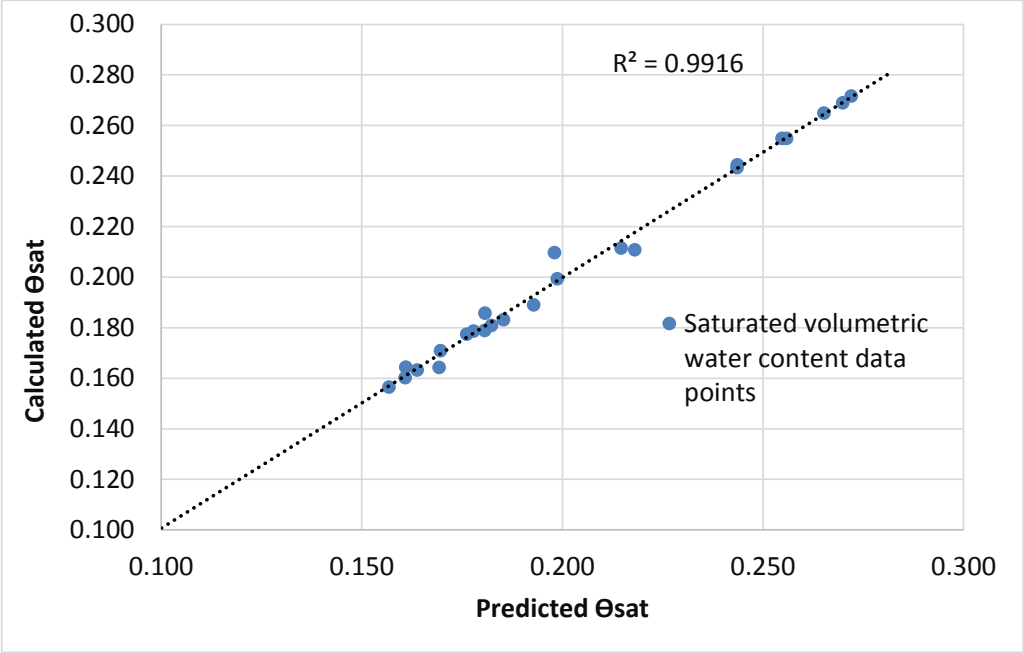

Figure 6-8 A Comparison of the Predicted and Calculated Saturated Volumetric Water Contents

The saturated volumetric water content gives the maximum moisture holding capacity of the soil media, and the θ_{sat} is a very significant parameter. The predicted θ_{sat} is given in Equations from (6-8) to (6-11).

$$\theta_{sat} = 0.214926485H_{1\theta_{sat}} + 0.27640261H_{2\theta_{sat}} - 0.12511932H_{3\theta_{sat}} + 0.30045553 \quad (6\text{-}8)$$

$$H_{1\theta_{sat}} = \tanh[0.5(0.1353107MBV + 0.14124964pfc - 2.67159193Gs + 4.689449)] \quad (6\text{-}9)$$

$$H_{2\theta_{sat}} = \tanh[0.5(0.42673905MBV + 0.4791957pfc - 14.5836317Gs + 28.3844308)] \quad (6\text{-}10)$$

$$H_{3\theta_{sat}} = \tanh[0.5(0.65761429MBV + 1.56633384pfc - 39.54978185Gs + 79.178564)] \quad (6\text{-}11)$$

where θ_{sat} is the saturated volumetric content, $H_{1\theta_{sat}}$,$H_{2\theta_{sat}}$,$H_{3\theta_{sat}}$ represent hidden layers, MBV is the methylene blue value, *pfc* gives the percent fines content, and G_s is the specific gravity of soil.

6.5.4 MVB Shape Effects on SWCC

The Fredlund and Xing (1994) equation is adapted in this work to generate the *SWCC* curves for unbound aggregate base courses. This equation includes four fitting parameters, which were investigated during this study and found to be related to the

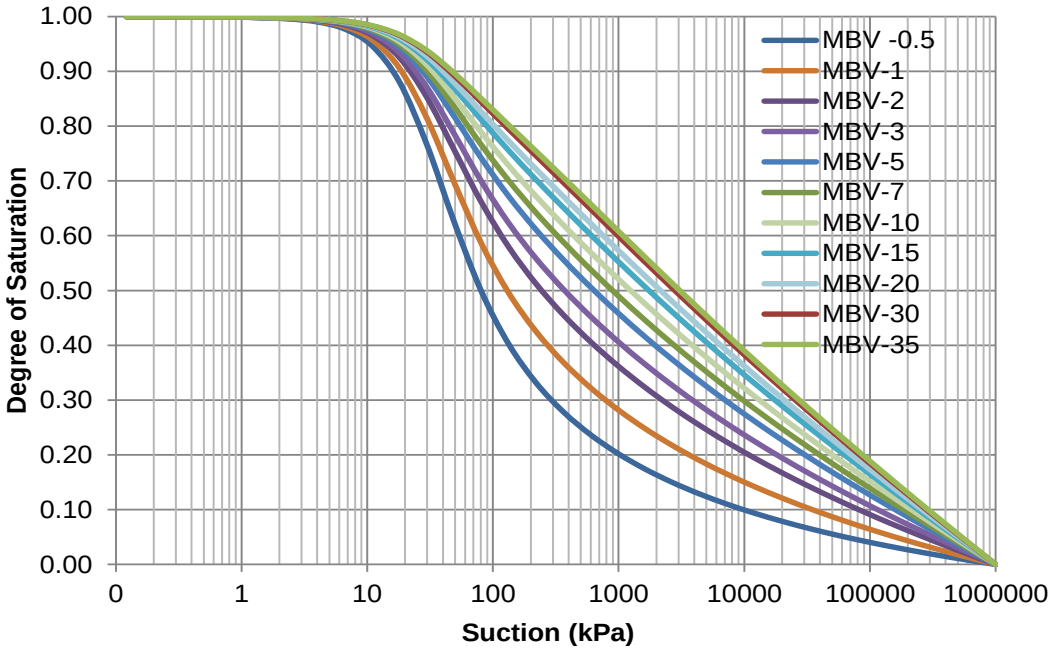

Figure 6-9 The MBV Effect on the Shape of the SWCC

MBV. Based on that, a parametric study was conducted to illustrate the effect of the MBV on the constructed SWCC when the MBV range changes from 0.5 to 35. This effect is shown in Figure 6-9.

Figure 6-9 shows the suction change in the *SWCC* with degree of saturation. It was assumed in the parametric study that all of the material are fully saturated at 100 percent. After that, eleven different MBV values are calculated and plotted together to compare the shape effect due to MBV. It is noted that the lower the MBV shows the lowest suction value; on the other hand, the higher the MBV shows the higher suction at the same degree of saturation. As was mentioned earlier in Chapter 4, the lower MBV values are associated with lower plasticity material and the higher MBV are associated with higher plasticity materials.

The equations above are provided to determine a unique curve for each of the aggregate materials based upon the sources. Because clay mineralogy and accordingly the *SWCC* will change based on the aggregate quarry, and hence it is recommended to measure the MBV for each quarry at each time. For this purpose, as was mentioned earlier, the methylene blue test was performed on the various aggregates from all of the pits. The four fitting parameters are determined for each of the aggregate sources based on the measured MBV. Lastly, a family of *SWCC* curves is demonstrated for these pits collected shown in Figure 6-10.

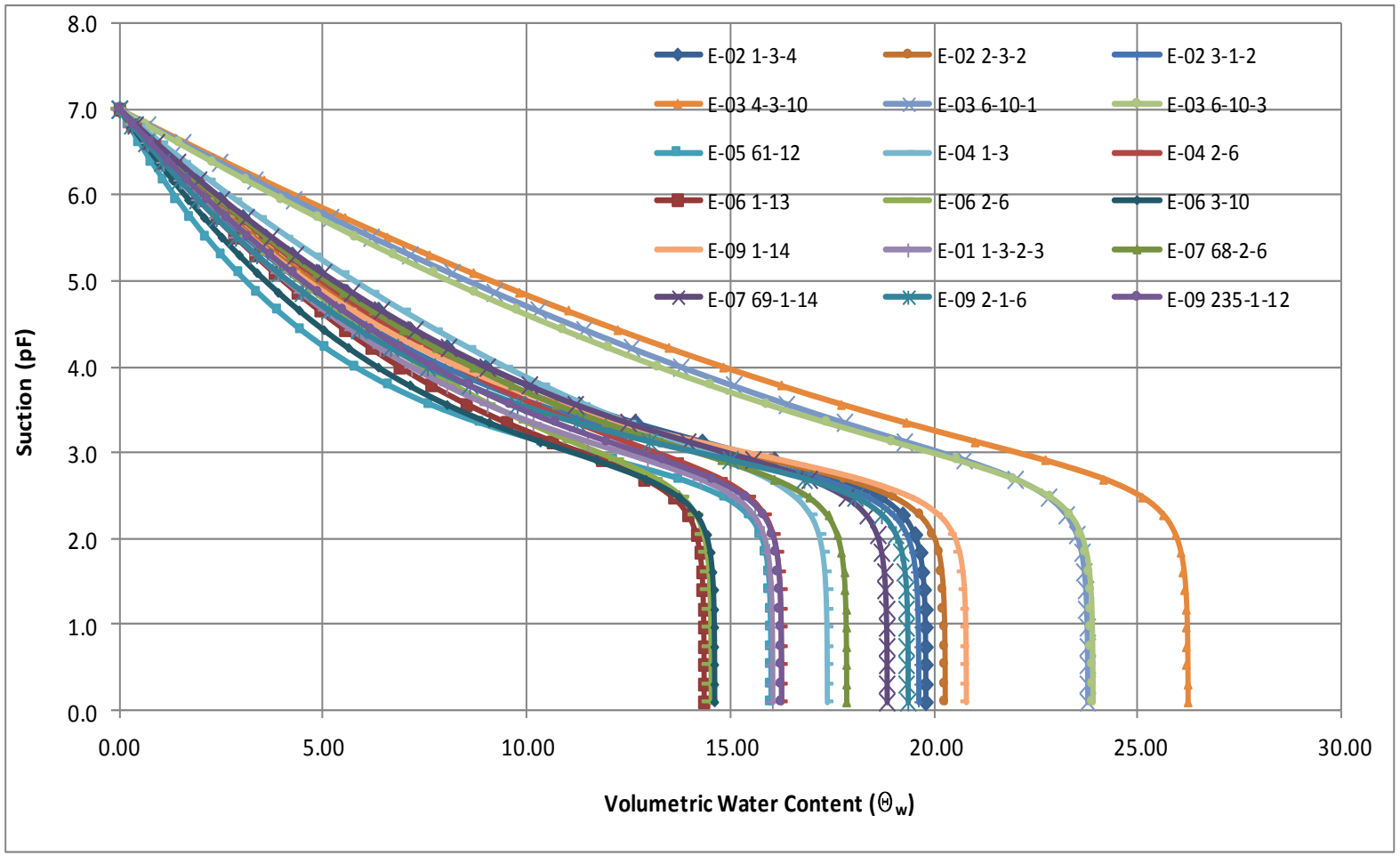

Figure 6-10 A Family of Calculated *SWCC* s for Nine Pits with Various Aggregate Samples

Figure 6-10 shows that each pit has a different shape of the *SWCC*. This differentiation is the result of the specific clay quantity, quality, and characteristics effect on the shape of *SWCC*. It is noted that the methylene blue test is alone a sufficient test to assess the fitting parameters and generate any type of *SWCC*.

The accuracy of the proposed fitting parameters equations are evaluated in the following section.

6.6 Validation of the Four-Parameter

The accuracy of the *SWCC* is evaluated with measured matric suction by using the filter paper test. It is important to compare with an experimental method that is capable of directly measuring suction. The filter paper is an ideal test method for this purpose, and it is performed on the same set of samples that are used for the methylene blue test to estimate the MBVs. By using the multi regression analysis, each of the curves is required to pass through the measured matric suction point. The best fitting models, representing the correlation between the MBV and fitting parameters, are expressed earlier in Equations (6-3) to (6-6). The new generated curve uses the data from these equations. The comparison of the suction values are given in Figure 6-11.

Figure 6-11 shows a validation line between the measured and calculated suction values with a significant correlation. Hence, calculating the suction through the four parameters based on the MBV is a very reliable method.

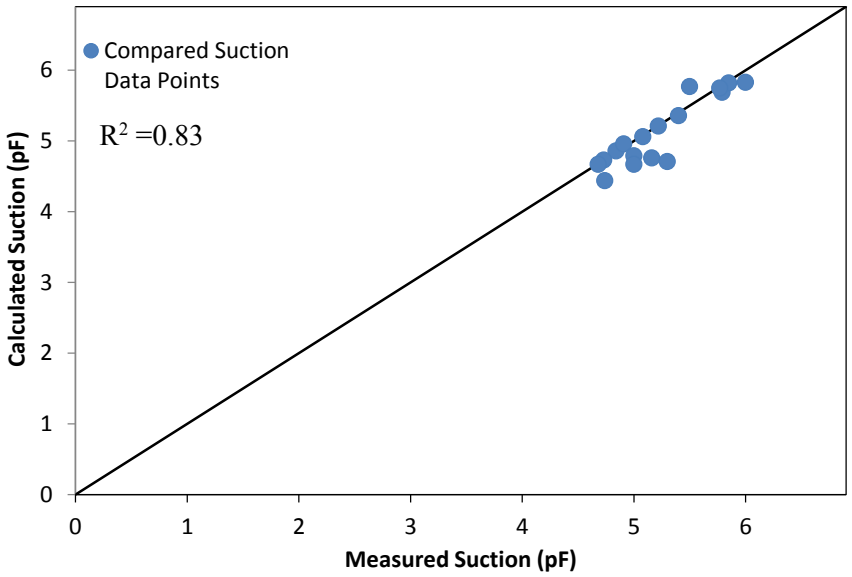

Figure 6-11 Measured versus Calculated Suction Value for Various Aggregate Samples

6.7 Closure

In this chapter, the improved methylene blue test methodology is used to generate the soil water characteristic curve (*SWCC*) for unbound aggregate materials. The principles of unsaturated soil mechanics are taken into account to develop four models to determine relationships for the fitting parameters in the Fredlund and Xing (1994) equation. An efficient method was developed by using the methylene blue test to determine the four parameters, which are a significant essential basis for the *SWCC* equation. The methylene blue test (MBT) allows MBV to generate the *SWCC* quicker than previous techniques, and this includes even in the field. These improvements widen the range of methylene blue test applications and enable the MBT to be the standard test to construct the *SWCC* without using difficult laboratory experiments. These proposed models

simplified the process to develop the $SWCC$ s without using the difficult test devices and lengthy laboratory testing procedures. Because of this, the amount of time spent in the laboratory for experimental study and labor can be decreased significantly.

The saturated volumetric water content is a very important parameter in the $SWCC$ equation. The previous studies have been focused only on the fitting parameters, and hence there is no research study that has aimed to determine a model for the θ_{sat}. Yet this study was undertaken to determine a reliable method to predict the θ_{sat}. As a result, the correlation was carried out to prove that the θ_{sat} can be predictable based on only the MBV, *pfc*, and dry unit weight.

The proposed techniques are capable of determining both the total and matric suction by using the same approach. The total suction has a different set of four-parameter equations than matric suction but developing a total suction equation is not the primary purpose of this study.

The prediction models and methods presented in this study are particularly worthwhile to determine four parameters and the $SWCC$ for the base course aggregate materials. Both the models and methods are powerful tools, especially in the field implementation purposes because these methods directly use the fundamental base course aggregate material properties. These approaches adapt unsaturated soil mechanics theories to field applications in a highly practical way. The method can be used in the quality control and quality assurance process during the base course layer construction.

7. DEVELOPMENT OF A MOISTURE DENSITY RELATIONSHIP MODEL

7.1 Introduction

This chapter describes an empirical investigation as a replacement for current methodology to estimate the dry density of base courses as an in-situ test. The empirical investigation will present a relationship between material properties and the dry density curve. Within the experiment program, nine pre-selected pits with various soil characteristics were investigated to build a precise and reliable correlation. This study presents a direct measurement method because currently no reliable replacement method exists for this purpose. This chapter covers an experimental process and a modeling methodology of the correlation.

Soil compaction is an optimization process of air, water and density. The compaction effort increases the soil density through decreasing the air void ratio until there is no significant change in the volume of the soil. In general, the higher the degree of compaction the higher the shear strength will be; therefore, achieving a maximum dry density will increase the soil strength significantly. The degree of the compaction is measured in terms of dry unit weight.

The compaction properties of the unbound base course aggregates are determined in the laboratory by using a compaction machine. The sample is placed in a cylindrical mold, and then a standard compaction effort is applied. A standard compaction procedure is applied on each soil layer separately to reach maximum dry density. After the sample compaction is completed, the water content is determined. After that, the dry

density is calculated by using the value of the moisture content. This process is repeated at least three or four times, by which the water content is increased at each time.

The dry unit weight is plotted against the water content. This plot is used to fulfill a general dry density vs. water content curve or determined an optimum moisture curve at a maximum dry unit weight. This curve represents a curvilinear relationship, and a typical one is shown in Figure 7-1.

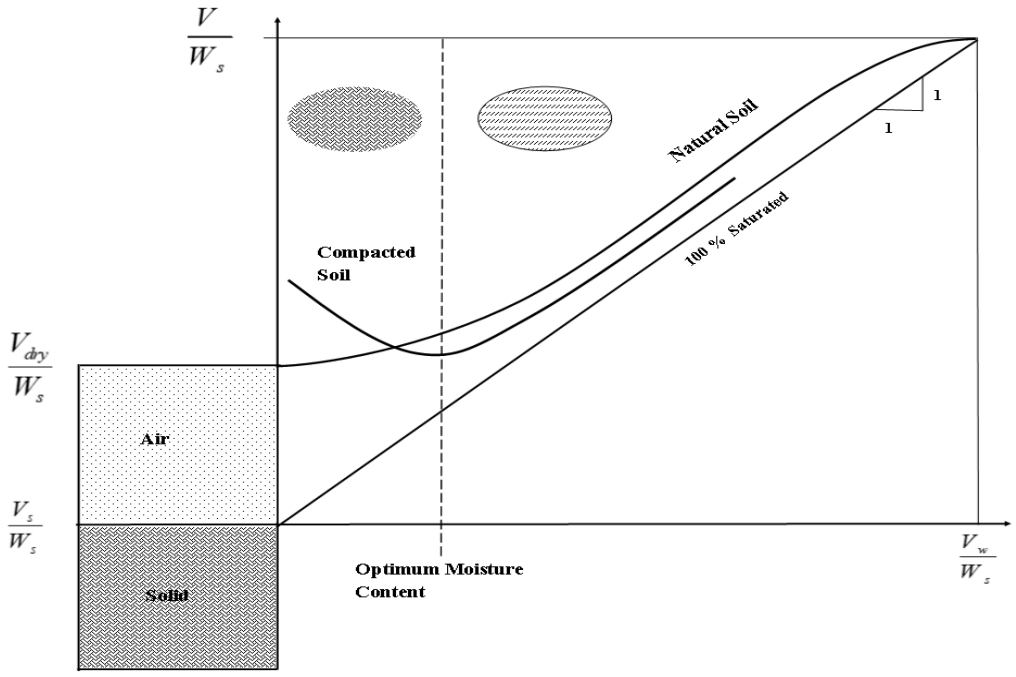

Figure 7-1 A Schematic Illustration of Dry Density Curve along with the Degree of Saturation Lines

Figure 7-1 shows a schematic of the dry unit weight and water content relationship from the unsaturated soil mechanics perspective. In this illustration, the air voids filled with the moisture with respect to change in the maximum density in the soil media. The lowest point of the curve occurs at a particular value of moisture content, which is the optimum moisture content.

The optimum moisture content is a significant value because the soil media reaches its maximum compaction state at that moisture content. At a lower moisture content, the soil tends to be firm, and hence it is difficult to compact. In contrast, at a higher moisture content voids become filled with water, which makes it nearly incompressible. Therefore, the soil media loses most of its strength due to the excess moisture that fills the majority of the voids. Hence, the higher the moisture the lower the density will be, after excessed the optimum moisture content. If all the voids in a soil media are filled with the moisture, this becomes the saturated state for the soil media.

An alternative current test method is the nuclear density-moisture gage (NDG) that is one of the apparatus required by AASHTO T 310. This test method provides the in-place density and moisture of the soil and unbound aggregate. Although the NDG has been used to determine moisture and density for a long time, there are some concerns associated with this device, such as certification and transportation of a nuclear device. Furthermore, the current pavement design procedures are based on more mechanistic methods that considers the modulus of pavement layer as opposed to the dry density (Nazarian et al., 2007). The NDG method uses a technique that measures the present hydrogen atoms in a material tested because hydrogens are usually associated with water

molecules. However, hydrogen molecules naturally exist in the chemical structure of the aggregate/soil material as well, some of which are mica, lime, fly ash, cement, organic materials, gypsum, coal, and phosphates. Therefore, a false low density measurement can occur due to these circumstances (Evett, 2000).

By taking account all of the considerations mentioned above, a model is needed to be developed to determine dry unit weight of an aggregate mixture in a quick, simple, and accurate fashion. This model finds a relationship between the dry unit weight and the moisture content of a measured compaction curve by using the material properties. The model uses the unsaturated soil mechanics and macro mechanistic approaches for the dry unit weight curve, which is in an unsaturated condition.

This chapter is organized as follows. The next section explains the testing and sampling protocol used during the study. The subsequent section introduces the developed model, including the curve fitting methodology and applied regression analyses. The final section shows the effect of transportation on the dry density curve.

7.2 Optimum Moisture Content Test

7.2.1 Sample Preparation and Testing Procedure

The research objective is to capture production variability; therefore, base course materials were sampled by calendar day and the collected information are relevant to daily, weekly and monthly variability. This objective increases the number of tests that are run for each pit to determine the moisture-density relationship within four calendar

months. The selected base material sources were explained in detail and the material types based on the source were tabulated in Chapter 3.

The base course materials are compacted a mold that is 6 in (152.4 mm) in diameter and 8 in. (203.2 mm) high, and are molded in four layers using a 10 lb. (4.53 kg) rammer. The rammer drops from a height of $18 \pm 1/2$ in. (457 ± 12.7 mm) until the total compactive energy of 750.0 (ft-lbs) is delivered equally to each layer, which is determined by using the soil compactor analyzer (SCA) device per layer. To reach the total energy, the total number of blows is $50 \pm$ 5 drops. This test procedure covers the material passing through the 1-3/4 in (45 mm) sieve, and the test is performed on using a 7/8 in. (22.6 mm) sieve to separate the aggregate retained on the 7/8 in. sieve from the aggregate passing the 7/8 in. sieve. The separated materials both retained and passing on the 7/8 in. (22.6 mm) are distributed equally based on size, shape, and number of particles into four separate layers. This process is repeated four times with different moisture contents to obtain a well-defined moisture content vs. dry density curve.

Figure 7-2 Compaction Equipment when Molding a Specimen by Using a SCA

After compacting specimens at four different moisture contents, dry unit weights and moisture contents at the end of the test was determined to construct an experimental compaction curve, which ideally includes at least two performed tests in both sides of the optimum moisture content.

The standard test procedure Tex -113 E is followed to perform the compaction test on each of the collected samples to obtain the compaction characteristics and the moisture-density relationship of base materials. The detail of the instruction can be found in the following test procedure.

7.2.2 Test Result Displaying

The mathematical expression for the dry unit weight in an unsaturated condition is as follows:

$$\gamma_d = \frac{G_s \gamma_w}{1 + wG_s} \tag{7-1}$$

where γ_d is the dry unit weight of base course material (lb/ft^3), γ_w is the unit weight of water (lb/ft^3), and G_s is specific gravity of the solids, and w is moisture content (%).

After compaction is completed, the water content of the soil is determined and the dry unit weight is calculated by using Equation (7-1). This process was repeated at least four times, by which increasing the water content each time, and the moisture content is plotted against to dry unit weight. The plotted compaction curve is shown in Figure 7-3.

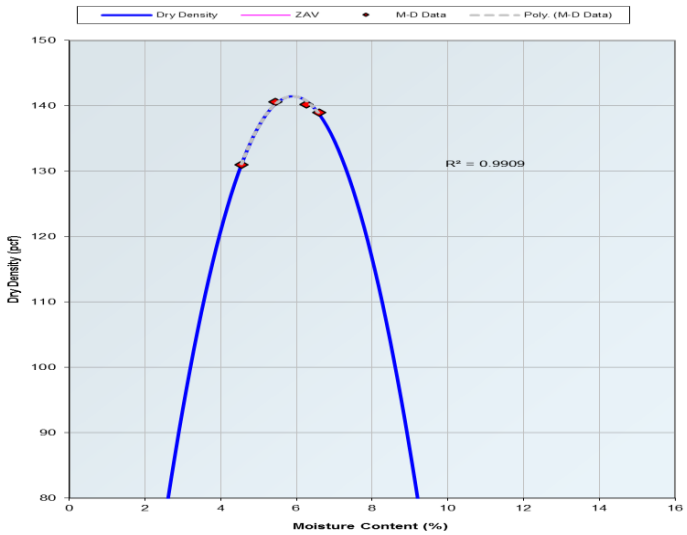

Figure 7-3 A Moisture-density Relationship Plot for Base Course E-05

Figure 7-3 shows a typical compaction curve that is constructed directly from the obtained experimental data.

7.3 Compaction Curve Methodology

7.3.1 Compaction Curve Model Equation

The results of the moisture content vs dry density tests are analyzed to investigate the moisture-density relationship, which is called compaction curve model (CCM). For this purpose, all of the collected aggregate sources are utilized because they consist of various mineralogical characteristics. This investigation resulted by deriving a CCM model that is quite capable of representing the experimental data. Furthermore, the model determines the dry unit weight of the base course materials not only at a particular point of the maximum dry unit weight but at any moisture content. The form of a typical compaction curve is generally a C-shaped curve; therefore, the same mathematical models used to determine the percent fine content equation, which was introduced in Chapter 3, has been modified to apply to the CCM. A new equation was derived based on the introduced concept. The mathematical formulation of the CCM is given in Equation (7-2):

$$\left(\frac{\gamma_d}{\gamma_w}\right) = a_d\left[\operatorname{csch}\left(\frac{\theta_w\theta_{sat}}{G_s\left(\theta_{sat}-\theta_w\right)}\right)\right]^{n_d} - b_d\left[\operatorname{csch}\left(\frac{\theta_w\theta_{sat}}{G_s\left(\theta_{sat}-\theta_w\right)}\right)\right] \qquad (7\text{-}2)$$

where γ_d is the dry unit weight of base course material, γ_w is the unit weight of water, θ_w is the volumetric water content, θ_s is the saturated volumetric water content, and where a_d, b_d, and n_d are three parameters, which change with an aggregate source (pit).

This model was derived with the idea of embedding the fundamental material properties in Equation (7-2). This model consists of three parameters (a_d, b_d, n_d) that

are dependent on the degree of saturation, the specific gravity and the unit weight of water.

The compaction curve model (CCM) was validated by using the laboratory test results. In order to do that, the laboratory compaction and the modeled compaction curves were plotted in a same figure to possess an understanding of the curve-fit comparison. The two plotted compaction curves for same aggregate pit are shown in Figure 7-4.

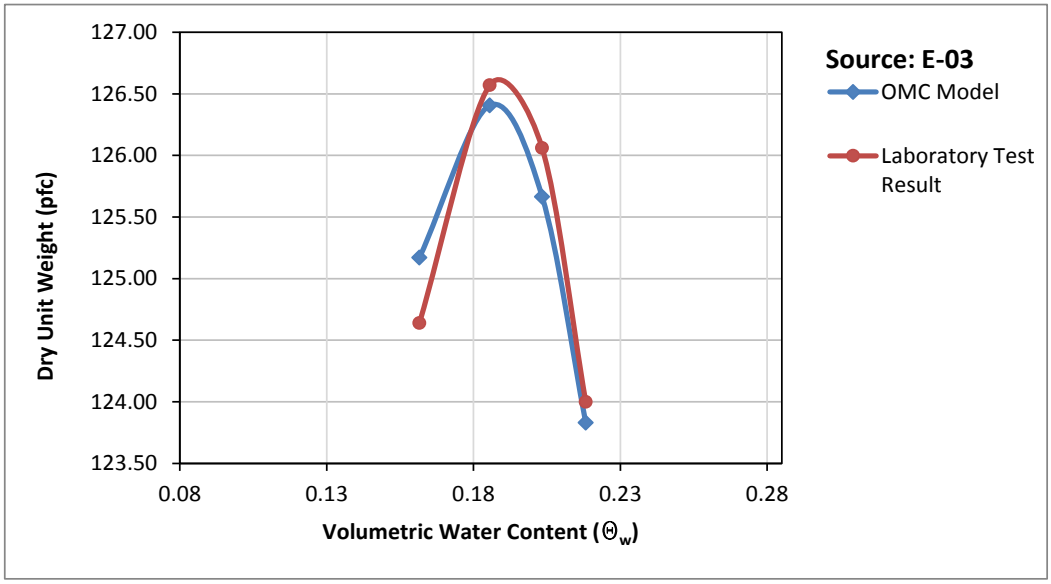

Figure 7-4 A Comparison of the Moisture-density Relationship Curves for Pit E-03

Figure 7-4 demonstrates that the developed CCM follows a very similar pattern to that which the experimental compaction curve follows. It is also noted that the four calculated points, by using the compaction model, are significantly closer to each of the

four points measured by the experiment. The minimum density difference between the two curves occurs at the maximum dry density point. The three parameters in the developed compaction model must be identified in order to build up a compaction curve, and for this purpose a regression analysis has been conducted and is explained thoroughly in following section.

7.3.2 Curve Fitting Method

The CCM consist of three parameters: a_d , b_d ,and n_d . In order to determine fitting parameters an *MS Excel* macro program was established to repeat the require computation. Table 6-1 shows an example and a simplified version of the *MS Excel* computation set-up. The *MS Solver* function was used to optimize the nonlinear relationship. The *Solver* function investigates to calculate the least square value of the dry unit weight points, which were determined by the compaction model and the laboratory test. The four measured points are commonly used as input value, and the two of the points are usually located below the optimum moisture content and the other two are located above the optium moisture content. The *Solver* function yields more an accurate outcome if the selecected initial values are close enough to mimic the real CCM. Furthermore, the selected initial fitting parameters must be kept the same with no change even though the aggregate sources are changed within the analyisis. For this study, The initial value was chosen as a_d =2.0, b_d =0.05, and n_d =0.30. The *Solver* function was repeated until it obtained a least square error.

Table 7-1 A Regression Analysis Template Used for Calculating the Four Points on a Compaction Curve and Calculating Dry Unit Weight

$(\gamma_d)_{lab}$ (lb/ft^2)	$\left(\frac{\gamma_d}{\gamma_w}\right)_{lab}$	θ_w	θ_{sat}	$f(\theta)$	csch(θ)	n_d	b_d	a_d	$\left(\frac{\gamma_d}{\gamma_w}\right)_{cal}$	$(\gamma_d)_{cal}$ (lb/ft^2)
126.60	2.028	0.186	0.264	0.228	4.330	0.111	0.052	1.911	2.024	126.31
124.64	1.997	0.156	0.264	0.138	7.183	0.111	0.052	1.911	2.005	125.17
126.57	2.028	0.180	0.264	0.205	4.836	0.111	0.052	1.911	2.025	126.40
126.06	2.020	0.198	0.264	0.286	3.447	0.111	0.052	1.911	2.013	125.66
124.00	1.987	0.213	0.264	0.395	2.461	0.111	0.052	1.911	1.984	123.83

Experiment

Regression Analysis

Model

Table 7-1 shows a regression analysis template and the regression calculation sequence. The terms used in Table 7-1 are explained as follows. The red rectangular area shows the input data assessed from the conducted *experiment*. The green rectangular area represents three parameters data calculated by the executed *regression analysis*. The blue rectangular area gives the calculated dry unit weight data *model* based on the regression analysis. The term $(\gamma_d)_{lab}$ represents the dry unit weight measured experimentally. The term $(\gamma_d/\gamma_w)_{lab}$ shows the ratio between experimental dry unit weight and the unit weight of water. The $f(\theta)$ is equal to the significant part of the CCM equation $\left(\frac{\theta_w\theta_{sat}}{G_s(\theta_{sat}-\theta_w)}\right)$. The csch(θ) gives the calculated csch (f(θ)) term. The parameters a_d, b_d and n_d are the shape fitting parameters. The $(\gamma_d/\gamma_w)_{cal}$ gives the ratio of the calculated dry unit weight and the dry unit weight of water. Lastly, the $(\gamma_d)_{cal}$ is the calculated dry unit weight.

7.3.3 JMP Regression Analysis

The determined fitting parameters are obtained from the *MS Solver* analysis. A regression analysis is conducted on the fitting parameters by using the JMP statistical software program. Because the JMP software is focused on exploratory data analysis to investigate sophisticated data, and also is designed to drill down or up for exploring the data and visual representations (Jones and Sall, 2011; Carver, 2010). Conducting a systematic, stepwise neural statistical regression analysis is one of the most important features in the JMP program. The link between unbound aggregate materials and the estimated fitting parameters are investigated by JMP program. Eventually, the modeled and measured results fit significantly well. The neural data analysis gives the hidden layers to increase the accuracy of the final calculation, and thus these estimated models have hidden layers. The parameters a_d, b_d and n_d were found to be highly dependent to material properties as explained herein.

The a_d is given in the following equation with three hidden layers H_{1a}, H_{2a}, H_{3a}, all of which are depend on MBV, *pfc*, and G_s:

$$a_d = -0.7255499645H_{1a_d} + 0.2397642438H_{2a_d} + 0.8786388739H_{3a_d} + 1.88831833 \quad (7\text{-}3)$$

$$H_{1a_d} = \tanh[0.5(0.40877300MBV + 0.21113984pfc - 8.72963215Gs + 16.336761)] \quad (7\text{-}4)$$

$$H_{2a_d} = \tanh[0.5(-0.27242731MBV + 0.38117451pfc + 4.81581562Gs - 15.246911)] \quad (7\text{-}5)$$

$$H_{3a_d} = \tanh[0.5(0.65761429MBV + 1.56633384pfc - 39.54978184Gs + 79.17856)] \quad (7\text{-}6)$$

where a_d is one of the fitting parameters, H_{1a_d},H_{2a_d}, and H_{3a_d} are hidden layers, MBV is methylene blue value, pfc, percent fines content, and G_s specific gravity of soil. An error analysis gives the accuracy of the model and it is shown in Figure 7-5.

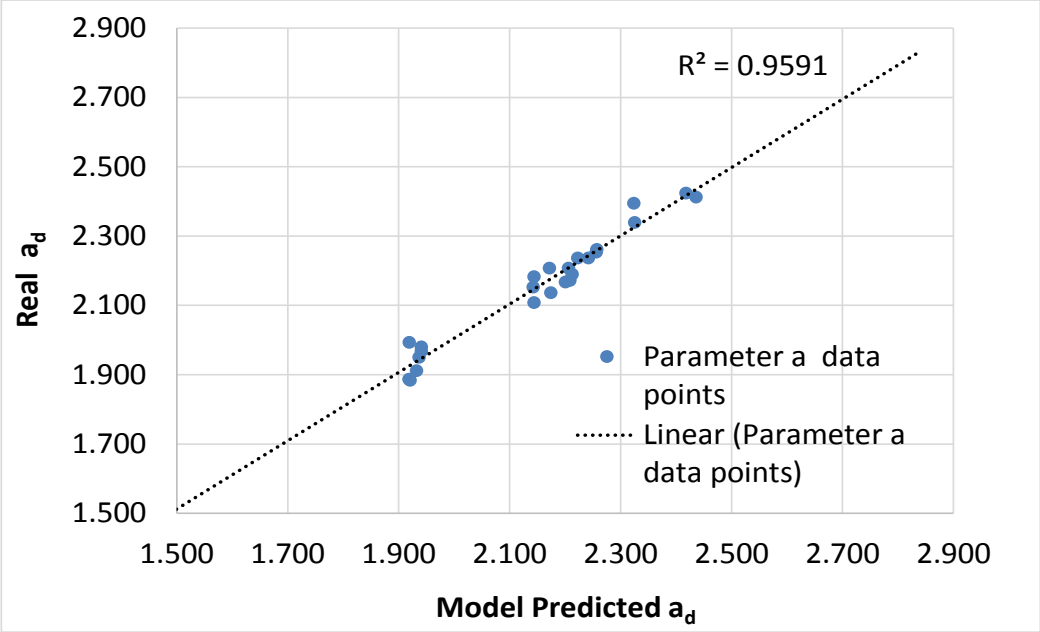

Figure 7-5 An Error Analysis of Real Versus Calculated a_d Values

The b_d is given in the following equation with three hidden layers H_{1b},H_{2b},H_{3b}, all of which are depend on MBV, *pfc*, and Gs:

$$b_d = 0.108053941H_{1b_d} - 0.166763132H_{2b_d} + 0.160133497H_{3b_d} + 0.122496083 \quad (7\text{-}7)$$

$$H_{1b_d} = \tanh[0.5(0.30481277MBV + 0.4712751pfc - 23.51993211Gs + 52.840434)] \quad (7\text{-}8)$$

$$H_{2b_d} = \tanh[0.5(-0.05056449MBV - 0.11228127pfc + 27.55907692Gs - 71.931755)] \quad (7\text{-}9)$$

$$H_{3b_d} = \tanh[0.5(-0.13331382MBV - 0.36012434pfc + 29.23482354Gs - 72.562443)] \quad (7\text{-}10)$$

where b_d is one of the fitting parameters, H_{1b_d},H_{2b_d}, and H_{3b_d} are hidden layers, MBV is methylene blue value, *pfc*, percent fines content, and G_s specific gravity of soil. An error analysis gives the accuracy of the model and it is shown in Figure 7-6.

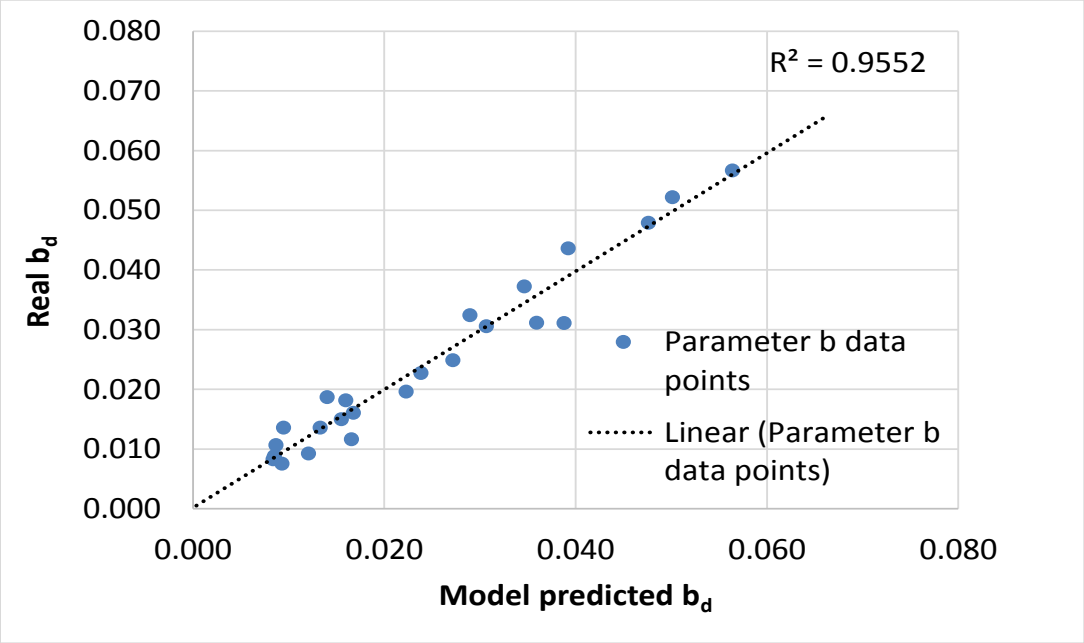

Figure 7-6 An Error Analysis of Real versus Calculated b_d Values

The n_d is given in the following equation with three hidden layers H_{1n},H_{2n},H_{3n}, all of which are depend on MBV, *pfc*, and G_s:

$$n_d = -0.013073056H_{1n} - 0.045526936H_{2n} + 0.013674419H_{3n} + 0.058352963 \quad (7\text{-}11)$$

$$H_{1n_d} = \tanh[0.5(-0.26235498MBV + 0.47405037pfc - 71.58187117Gs + 189.223422)] \quad (7\text{-}12)$$

$$H_{2n_d} = \tanh[0.5(-0.78480185MBV + -0.75914733pfc + 56.24092591Gs - 133.107727)] \quad (7\text{-}13)$$

$$H_{3n_d} = \tanh[0.5(-0.23889927MBV - 0.87246044pfc - 84.01782691Gs + 246.667662)] \quad (7\text{-}14)$$

where n_d is one of the fitting parameters, H_{1n_d}, H_{2n_d}, and H_{3n_d} are hidden layers, MBV is the methylene blue value, pfc is the percent fines content, and G_s is the specific gravity of soil.

An evaluation analysis that gives a direct comparison of the n_d model by JMP and the estimated real n_d values is presented in Figure 7-7.

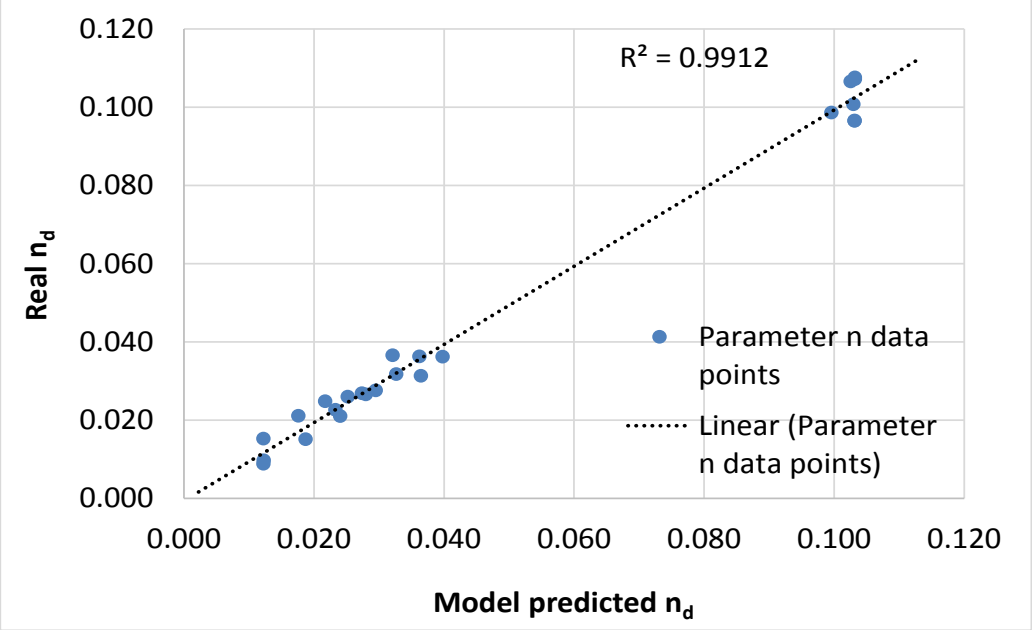

Figure 7-7 An Error Analysis of Real versus Calculated n_d Values

The regression analysis yields the three parameters a_d, b_d and n_d. The quality of the statistical analysis methodology used in the JMP program to determine the prediction parameters reflect, eventually, the accuracy of the compaction model. Therefore, the JMP program was well utilized to obtain the highest possible correlation and the minimum error between the real and predicted. As a result, the coefficient of determination (R^2) values for a_d, b_d, and n_d were 0.9591, 0.9559 and 0.9912, respectively.

Table 7-3 shows the a_d, b_d, and n_d fitting parameters for each pit, which consist of several optimum moisture contents at each base at the time of sampling. The values presented in Table 7-3 are average calculated values of all samples are in each pit as well as to show the variation between pits.

Table 7-2 Typical Parameters a_d, b_d, and n_d Values for each Pit Showing along with Material Properties

Source	a_d	b_d	n_d	γ_{dry} **(lbc)**	θ_w	θ_{sat}	G_s	*MBV*	*pfc*
E-01	2.2104	0.0090	0.0243	142.10	0.1377	0.1838	2.79	7.52	16.45
E-02	2.1325	0.0177	0.0347	136.93	0.1587	0.2106	2.78	4.08	11.70
E-03	1.9392	0.0428	0.1020	128.08	0.1728	0.2575	2.76	21.47	19.73
E-04	2.1901	0.0117	0.0260	142.10	0.1366	0.1808	2.78	10.56	12.29
E-05	2.1951	0.0166	0.0315	141.10	0.1347	0.1732	2.74	6.57	19.86
E-06	2.4104	0.0098	0.0113	150.43	0.1318	0.1629	2.88	8.99	15.62
E-07	2.2450	0.0267	0.0228	139.10	0.1589	0.1780	2.71	4.67	14.00
E-08	2.2557	0.0128	0.0208	143.10	0.1456	0.1677	2.76	4.80	15.19
E-09	2.2072	0.0306	0.0317	136.40	0.1727	0.1993	2.73	3.26	12.68

It is noted that in Table 7-3, each pit has a typical a_d, b_d or n_d value specifically defining a pit. Furthermore, each material source can have multiple exclusive defined sets of fitting parameters because they depend on the specific gravity (G_s), especially methylene blue value , percent fines content (*pfc*). Thus, it is very essential to perform a methylene blue test to measure the methylene blue value precisely for the required material source when it is needed. In other word, when two samples come from the same material source but are sampled at different times within the production period, it is most likely to have two different a_d, b_d and n_d values. The reason is that the variation in the production causes changes in the fitting parameters to some degree, and these changes are reflected to the maximum dry unit weight of that specific material at that specific moment of the production. Therefore, the change in the dry unit weight does not come from the method; the variation comes from the fines content, fines mineralogy and fines type. Furthermore, this method is sensitive enough to catch any changes in base course aggregate material. This unique feature shows that this method is significantly capable to monitor the dry unit weight variation due to changes in the aggregate material.

7.3.4 Error Analysis and Precision

The dry unit weight and the moisture content for the various aggregate sources are calculated to develop a mathematical relationship based on the empirical data. The developed relationships for both the laboratory data and the data estimated based upon the compaction prediction models. These calculated and measured maximum dry unit weights from the laboratory test as well as the error between the predicted and measured for each of the aggregate sources are presented in Table 7-3 .

Table 7-3 Tabulated Test Results that Compare the Laboratory and Measured Dry Unit Weight Results and Three Parameter Coefficients for Each Source

Source	Code	W_{opt} (%)	γ_{dry} (cal)	γ_{dry} (lab)	Error (%)
E-01	1-3-2-3	5.82	142.60	143.00	0.28
E-01	DM	6.41	138.84	141.20	1.67
E-02	1-3-4	7.20	135.24	137.10	1.35
E-02	2-3-2	7.34	133.79	136.30	1.84
E-02	3-1-2	7.44	136.70	137.40	0.51
E-03	1-10-2	9.07	127.71	125.90	1.44
E-03	1-10-5	9.42	122.15	125.00	2.28
E-03	2-10-3	8.04	132.96	128.80	3.23
E-03	4-3-10	9.38	124.14	126.60	1.94
E-03	6-10-1	7.86	126.50	130.90	3.36
E-03	6-10-2	7.47	129.60	128.80	0.62
E-04	2-6	6.14	138.87	142.10	2.27
E-05	61-12	6.15	138.18	141.50	2.34
E-05	DM	5.93	140.27	140.70	0.30
E-06	2-6	5.60	150.58	150.40	0.12
E-06	1-13	5.41	150.60	150.70	0.07
E-06	3-10	5.39	150.59	150.20	0.26
E-07	68-2-6	7.12	138.68	139.40	0.51
E-07	69-1-14	7.39	137.98	137.70	0.21
E-07	DM	6.90	140.35	140.20	0.10
E-08	2-1-6	6.67	136.88	140.40	2.51
E-08	235-1-12	6.18	146.44	145.80	0.44
E-09	1-14	7.87	137.03	136.40	0.46

Table 7-3 presents the calculated and the empirical maximum dry unit weight data that show significantly reliable parallel structures to each other. It is noted that the errors between the empirical and model maximum dry unit weight range from 0.07% to 3.36%. The amount of errors are reasonably small, and hence it can be considered that

this is a tolerable and minor error due to human interventions or the test equipment within the sampling and compaction process.

The highest degree of the error comes from the material source E-03 in Table 7-3. The reason is because, E-03 is historically known to be a poor quality material. This statement was proven based on the experimental results. Furthermore, E-03 has very active clays mineralogy and also the materials characteristic significantly varies within the production. This result confirms the experience that E-03 is considered a lower consistency material source.

The maximum dry unit weight, based on experiment results and the compaction model calculated, are compared to understand the error tolerance between the two methods. This comparison is given in Figure 7-8.

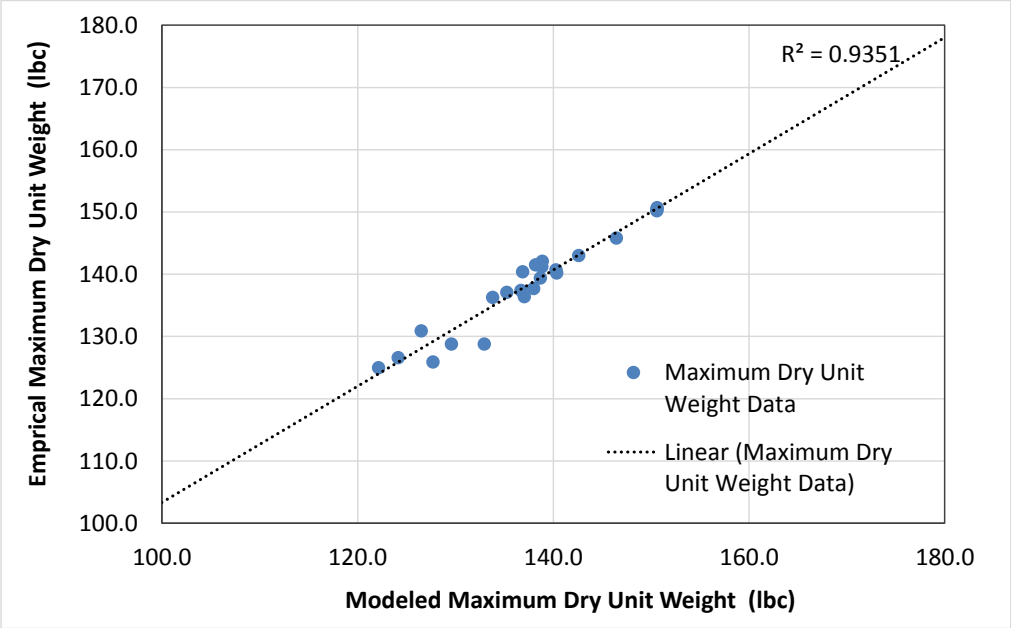

Figure 7-8 An Error Analysis for the Maximum Dry Unit with Comparison for Calculated versus Laboratory Outputs

Figure 7-8 shows a comparison of method. It is observed that the calculated maximum dry unit weights are significantly reasonable and accurate when compared to the measured maximum dry unit weights. The estimated R-squared values is 0.935. Thus, it can be concluded that the compaction model is a very robust technique, determining the maximum dry unit weight at any volumetric water content of a base course materials.

7.4 Determine Optimum Moisture Content

The optimum moisture content represents the amount of water at the maximum dry unit weight. To determine the maximum dry unit weight, it is first necessary to calculate the

optimum moisture content. For this purpose, the derivate of optimum moisture content calculation is given briefly in following.

The form of the compaction curve model (CCM) is given in Equation in (7-2). The equation for the optimum moisture content is determined by taking the first derivative of the compaction curve with respect to volumetric water content and setting the result equal to zero:

$$f'(\theta_w) = \frac{d}{d\theta_w}\left(a_d \left[\operatorname{csch}\left(\frac{\theta_w \theta_{sat}}{G_s(\theta_{sat} - \theta_w)} \right) \right]^{n_d} - b_d \left[\operatorname{csch}\left(\frac{\theta_w \theta_{sat}}{G_s(\theta_{sat} - \theta_w)} \right) \right] \right) = 0 \quad (7\text{-}15)$$

The derivation of Equation (7-15) is given in Equation (7-16) is solved for θ_w:

$$\begin{aligned} & b_d \left(\frac{\theta_{sat}}{G_s(\theta_{sat} - \theta_w)} + \frac{\theta_{sat}\theta_w}{G_s(\theta_{sat} - \theta_w)^2} \right) \operatorname{Coth}\left[\frac{\theta_{sat}\theta_w}{G_s(\theta_{sat} - \theta_w)} \right] \operatorname{Csch}\left[\frac{\theta_{sat}\theta_w}{G_s(\theta_{sat} - \theta_w)} \right] - \\ & a_d\, n_d \left(\frac{\theta_{sat}}{G_s(\theta_{sat} - \theta_w)} + \frac{\theta_{sat}\theta_w}{G_s(\theta_{sat} - \theta_w)^2} \right) \operatorname{Cosh}\left[\frac{\theta_{sat}\theta_w}{G_s(\theta_{sat} - \theta_w)} \right] \operatorname{Csch}\left[\frac{\theta_{sat}\theta_w}{G_s(\theta_{sat} - \theta_w)} \right]^{1+n_d} = 0 \end{aligned} \quad (7\text{-}16)$$

The solution of the Equation (7-16) gives the point at which the volumetric water content is equal to the optimum moisture content (θ_{opt}):

$$\theta_w = \theta_{opt} = \left(\frac{G_s \theta_{sat} \ln\left[\frac{1}{2}\left(1 + \sqrt{1 + 4\left(\frac{2^{1-n_d} b_d}{a_d n_d} \right)^{\frac{2}{-1+n_d}}} \right) \left(\frac{2^{1-n_d} b_d}{a_d n_d} \right)^{\frac{1}{-1+n_d}} \right]}{\theta_{sat} + G_s \ln\left[\frac{1}{2}\left(1 + \sqrt{1 + 4\left(\frac{2^{1-n_d} b_d}{a_d n_d} \right)^{\frac{2}{-1+n_d}}} \right) \left(\frac{2^{1-n_d} b_d}{a_d n_d} \right)^{\frac{1}{-1+n_d}} \right]} \right) \quad (7\text{-}17)$$

When Equation (7-17) is substituted in Equation (7-18) that is will provide the maximum dry density ($\gamma_{d\max}$) at the optimum moisture content:

$$\frac{\gamma_{d\max}}{\gamma_w} = a_d \left[\operatorname{csch}\left(\frac{\theta_{opt}\theta_{sat}}{G_s\left(\theta_{sat} - \theta_{opt}\right)} \right) \right]^{n_d} - b_d \left[\operatorname{csch}\left(\frac{\theta_{opt}\theta_{sat}}{G_s\left(\theta_{sat} - \theta_{opt}\right)} \right) \right] \qquad (7\text{-}18)$$

Equation (7-18) gives the maximum dry density and the three parameters a_d, b_d, and n_d. These parameters are the same numerical numbers that are given in Equation (7-2). The method of calculation of these parameters are expressed above. As it noted that the maximum dry density model, which uses the volumetric water content in calculation. Therefore, the volumetric water content must be converted to gravimetric water content in order to plot a typical compaction curve. The conversion can be made by using the following equation:

$$w = \frac{\theta_w \gamma_w}{\gamma_d} \qquad (7\text{-}19)$$

where w is gravimetric water content, θ_w is the volumetric water content, γ_w is the unit weight of water (~62.40 psi, ~1.0 g/cm^3, ~9.80 kN/m^3), and γ_d is the dry unit weight of soil.

7.5 A Family of the Optimum Moisture Content Curves

The Ohio Department of Transportation (ODOT) laboratory has collected moisture content and dry density information throughout Ohio State in 1935. In 1937, Woods and Litehiser published a paper presenting the generalized outcomes of these experiments

determined from about 1088 samples. In 1949, the collected soil sample data reached over 10,000, and these samples were compacted by using the Standard Proctor test (ASTM D698).In 1959, Joslin published the research to show a family of typical moisture density compaction curves. The published curves are shown in Figure 7-9.

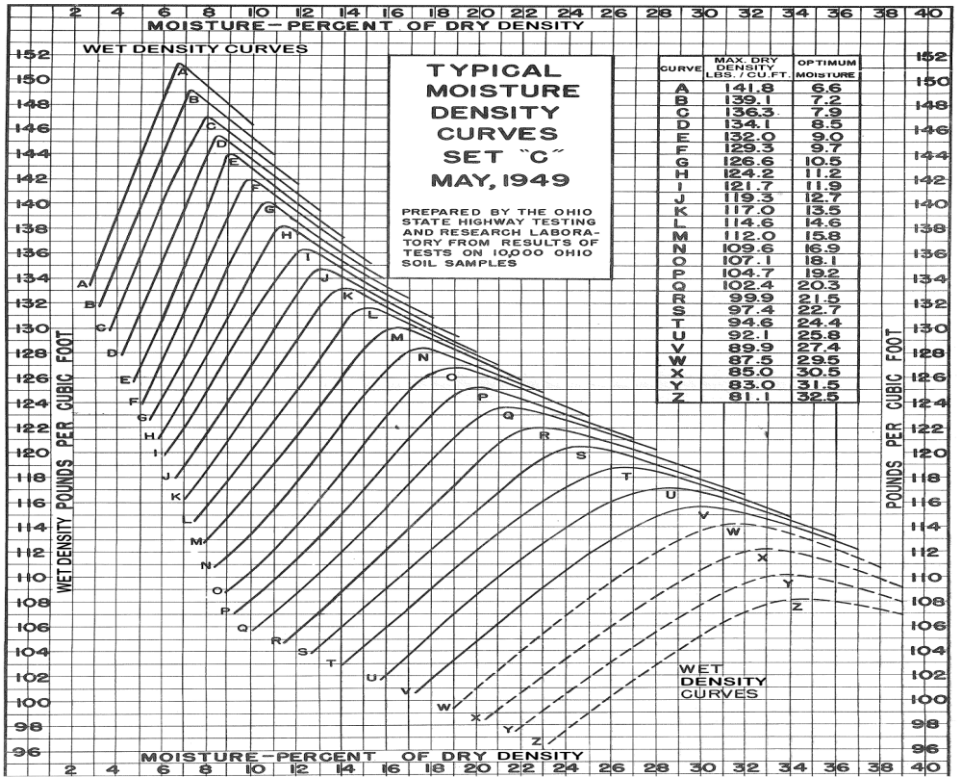

Figure 7-9 A Family ODOT of Moisture Density Curves (after Joslin1959).

The ODOT set of compaction family curves followed a pattern: as the moisture content decreases the maximum dry density increases. Also, at the lower moisture content, the dry density curves have shaper curves but at the higher moisture contents the dry density curves are wider.

This part of the study illustrates the dry density curves that are generated using the developed compaction model. The generated curves represent a good mix of a variety of samples that have various moisture contents, maximum dry density, as well as different shapes of the dry density curves. The family of optimum moisture content curves are presented in Figure 7-10.

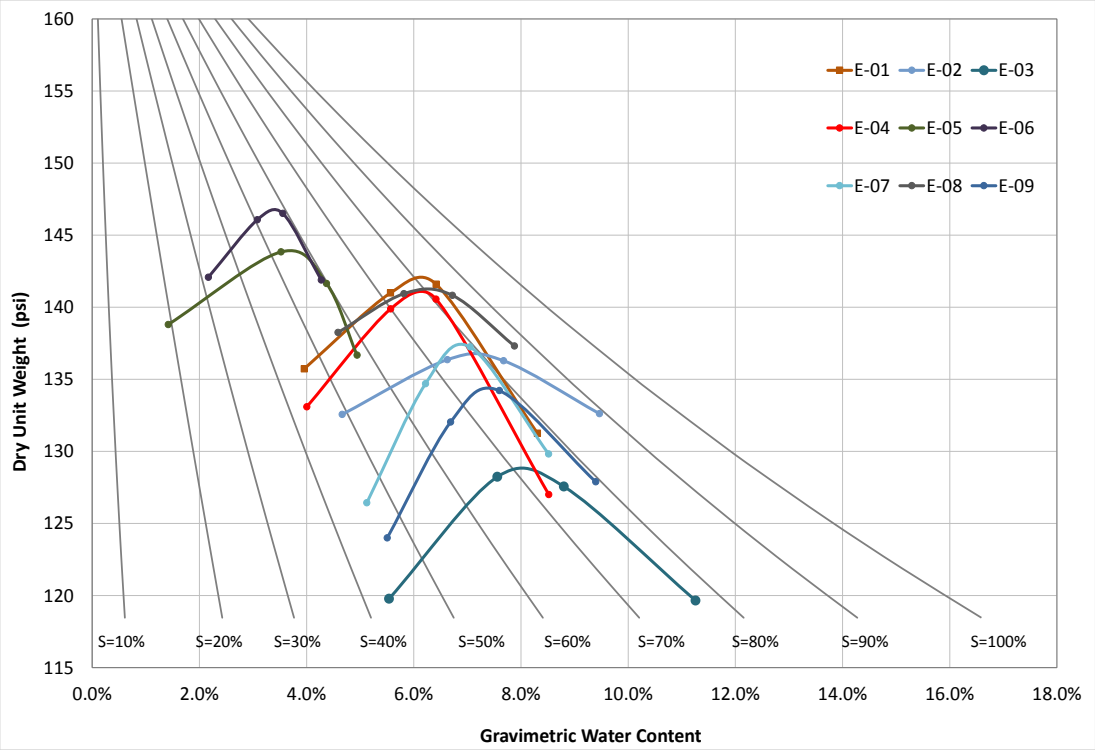

Figure 7-10 A Family of Generated CCM Curve for All the Collected Aggregate Materials along with Degree of Saturations

Figure 7-10 shows the changes with gradation in the material and the resulting the optimum moisture content variation. The gradation variation is usually affected by

the fines amount in the mixture. It has been known that the greater the amount of fines the lower the maximum dry density.

The specific gravity used for calculation is 2.77 and the degree of saturation lines were plotted from 10% to 100%. The plotted compaction curves represent the nine aggregate sources, which have variety of maximum dry densities. One of the important things about the sources is that each of the sources has unique material characteristics. Therefore, it can be seen the plotted curves show various maximum densities and the pits with similar characteristics showing similar or close maximum dry densities.

The variation of compaction curves and maximum dry density will be studied to determine the change by using the MBV in the fines materials.

7.6 Haul Effects on Compaction Curves

The unbound aggregate materials are usually carried out from a quarry to a stockpile, and then are transported to a construction site. In each of these phases, unbound aggregates materials are consistently subject to dumping, reloading, and crushing, which are direct or internal impacts. All of these factors cause internal frictions between aggregate materials; therefore, the amount of fine particles increases in the aggregate. The total amount of fines, at the final destination, is different than in the original gradation, which was transported from the aggregate source. Furthermore, each of loading process to a truck and unloading from a truck, as well as the transporting process by a truck, which causes internal friction and breakage, and increases the fine fraction. As was explained in earlier sections, fine materials have an effect on the unbound

aggregate base course layer. They are initially related to the maximum dry unit weight and permanent deformation, as well as the stiffness and modulus. Therefore, the fines content must be detected in the field at the construction site. Based on the detected *pfc*, the maximum dry unit weight, and the optimum moisture content must be determined constantly. This is because, when the percent fines content changes, the optimum moisture content and the density will also be changed.

The methylene blue test is a very effective method to determine fines content in the field. Since the MBT has a significant accuracy, it can detect the changes in fines. If the MBT is performed both at the material source and the field, this will allow the MBV to compare how much variation was generated between the original aggregate source and the construction site.

The amount of fine particles changes with the methylene blue value. If the material is above the critical MBV 7.00 mg/g, when the MBV increases, the percent fines content will increase as well. If the material is below the critical MBV, when the MBV increases, the percent fines content will decrease. Figure 7-11 illustrates the *pfc*-MBV correlation, and the effect of hauling and handling.

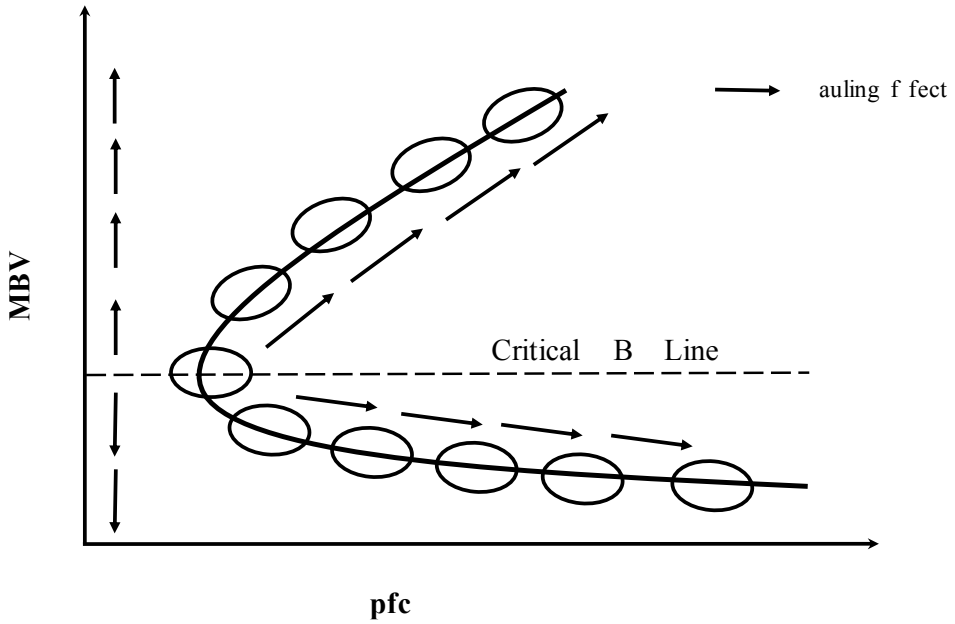

Figure 7-11 The Schematic of Hauling Effect from the *pfc*-MBV Curve Perspective

To investigate the effect of hauling on fines particles, a case study was conducted on one aggregate source. Aggregate material was sampled from a quarry, at which three points were chosen for sampling, to obtain a unified sample and eliminate the sampling errors. The same sampling process was also conducted on a location, where trucks bring and dump on the aggregate on a roadway construction on state highway SH-77 in Texas. The methylene blue test was conducted at the quarry and roadway to measure the change on methylene blue value and percent fines content. This discovery highlights the importance of the hauling effects, and the findings are shown in Table 7-4. The measurement showed that the selected aggregate quarry is located below the critical

MBV 7.00 mg/g zone. Hence, as it is illustrated in Figure 7-11, the MBV decreases as *pfc* increases in this lower MBV zone.

Table 7-4: Variation of the MBV and Dry Density due to Hauling Effect

Sampled Location	**Quarry**			**Roadway**		
Sample ID	**1-12**	**13-24**	**25-36**	**1-12**	**13-24**	**25-36**
Methylene Blue Value	5.46	5.41	5.66	4.87	5.03	4.57
Percent Fines Content	14.231	14.202	4.353	13.956	14.016	13.877
Maximum Dry Unit Weight	141.682	141.503	142.411	139.703	140.210	138.822

Table 7-4 shows that the average *MBV* value in the quarry is greater, and the percent fines content is lesser than in the roadway site. The effect of hauling was detected by using the MBT. The effect of these variations on the compaction curves was also investigated. The compaction curves in both quarry and roadway are plotted in Figure 7-12.

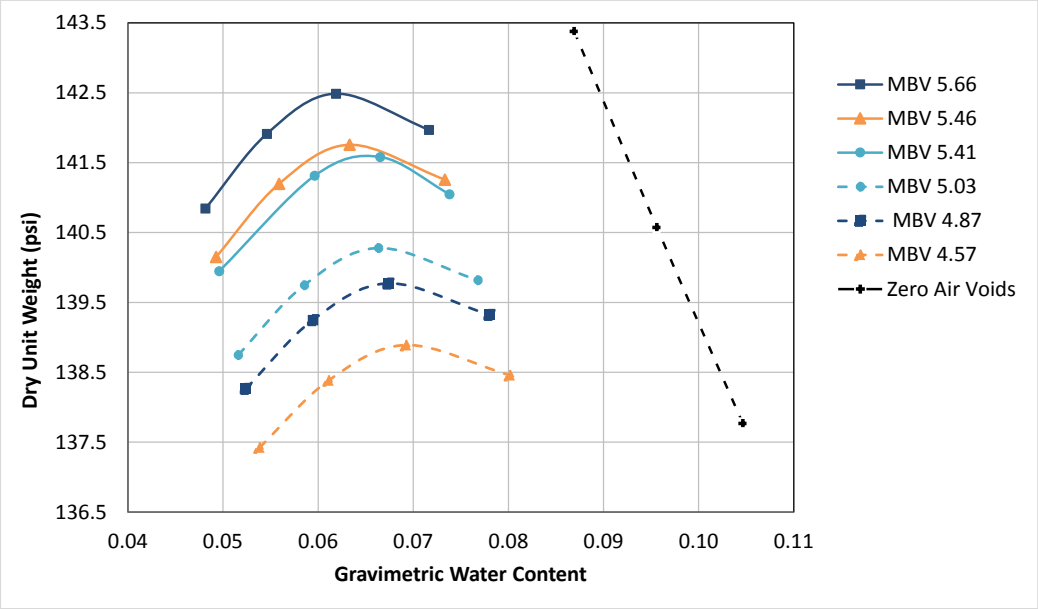

Figure 7-12 MBV Shifts due to the Hauling and MBV Making Effect on Compaction Curves

Figure 7-12 illustrates that compaction curves in the quarry and roadway are different. This leads a conclusion that hauling due to various transportation processes causes the maximum dry density to decrease. Therefore, the compaction curves measured by experimentally in the laboratory, and the compaction curves model (CCM), which is used in the design calculations, may not be the same maximum dry unit weight due to third party effect, such as a hauling.

7.7 Closure

This chapter covers a study of determining the dry density and moisture content relationship for unbound base course aggregate material. The laboratory compaction tests and the methylene blue test outcomes are integrated to find a model that is capable

of predicting dry density of unbound aggregates. The developed model determines the maximum dry density along with optimum moisture content. The compaction model has three fitting coefficients a_d, b_d and n_d, all of which depend on the methylene blue value, the percent fines content, and the specific gravity of soil. Therefore, when the MBV, *pfc* and G_s are known, the compaction model easily predicts the optimum moisture content, and also correlates it to a determined maximum dry density. This model is designed to use in the field to determine the maximum dry density; however, there is no limitation to use this method in the laboratory to determine the density moisture correlation curve as well. This method can be used in the laboratory because the tolerable error between the measured and predicted dry density are less than 3 percent. The proposed compaction model should not replace the current controlled laboratory tests; however the model can be used safely in the laboratory.

The compaction curve well utilizes the MBT that is a significant method to measure the methylene blue value and detect the percent fines content. The MBT eliminates the complexity of existing methods to compare aggregate materials in a quarry and a construction site. The aggregate materials are prone to get finer in the processes of hauling, transportation, loading, unloading and surfacing and even compaction. This variation can be effectively determined by only using the methylene blue test as well as the change in the maximum dry unit weight due to fine particles. Therefore, this part of the study proposes a novel approach for quality management. By using this approach, the quality control and quality assurance can be simpler, cheaper, and faster with significant accuracy right on the construction site.

8. DEVELOPMENT OF A DIFFUSIVITY MODEL

8.1 Introduction

Pavement performance is the record that shows the degree of pavement deterioration by both load and non- load related distresses. Load related distress includes fatigue cracking in both concrete and asphalt pavements, rutting and stripping in asphalt pavements, joint faulting and spalling in concrete pavements, and base course erosion and pumping in both types of pavements, among others. Non-load related distress includes roughness due to expansive soils and frost heaving soils, thermal cracking, transverse cracking due to the thermal shrinkage of base course materials and longitudinal cracking due to shrinkage of supporting subgrade soils among others. In all of these types of distress, the distress is accelerated by the effect of the moisture that either enters or is drawn out of the base course material (Sahin, 2013). The influx or efflux of water from the base course is an unsaturated diffusion process, which is governed by the parabolic partial differential equation proposed by Mitchell (1979); Lytton, et al., (2004):

$$\frac{\partial u}{\partial t} = \alpha \frac{\partial^2 u}{\partial z^2} \tag{8-1}$$

where u is the pF of the base course; α is the unsaturated diffusivity of the base course material (typical units cm^2/sec).

The diffusion coefficient rate (α) is defined by Lytton as the rate of infiltration of surface moisture into a soil layer, and this process is controlled by diffusion (Lytton, et al., (2004). Diffusion rates can be measured by an experimental method in the

laboratory. Other than the experimental method, the diffusion rates can be determined by using the empirical correlation and index properties.

In this study, an empirical method will be introduced and a correlation that uses percent fines content to estimate the diffusion coefficient rate for base course layers will be covered.

8.2 Test Procedure

The soil diffusion rate alpha (α) for each quarry was determined based on the water weight loss test data. The test results have shown that there is a relationship between the percent fines content and the diffusion rate. To determine the soil diffusion two pieces of a soil sample are compacted at the optimum moisture content and placed in a 100 percent relative humidity environment room at 23°C temperature and the daily moisture loss was recorded.

The aggregate samples are compacted as two pieces for the diffusion test. The portion of aggregates smaller than the No. 4 sieve is used to prepare an aggregate mixture. The mixture is compacted at optimum moisture content by using the standard compaction method in ASTM D 698 (2012). The compacted sample is placed in a cylindrical mold with a radius of 2 in. and height of 1.5 in. Two cylindrical soil samples are obtained by compaction and their shapes are shown in Figure 8-1.

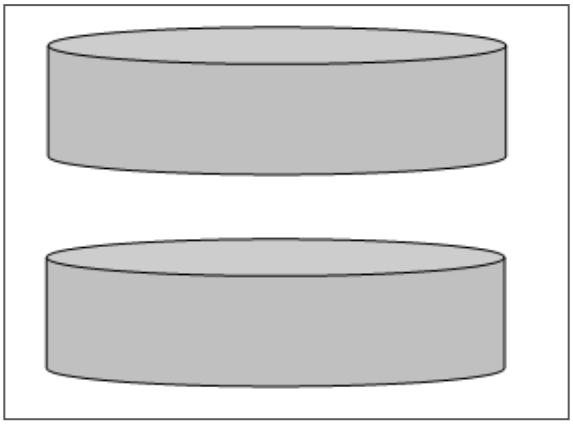

Figure 8-1 A Schematic Showing the Two Pieces Compacted Soil Samples

The environment room provides a stable air condition for soil samples to lose moisture under uniform conditions. The moisture decreases as the soil samples are monitored daily, and the sample moisture contents are calculated. The samples are kept in the environmental room until they reach a moisture content of 2 percent. Two of the soil samples placed in the environment room are shown in

Figure 8-2. It was observed that the sample surface must be shielded from direct contact with liquid water drops while the samples remain in the environment room.

Figure 8-2 Two Compacted Soil Samples in an Environment Room

The daily monitored data was evaluated to determine the diffusion rate. A mathematical function was derived from Equations (8-2) and (8-3):

$$W(t) = Wo(1 - e^{\frac{-12Dt}{d^2}}) \tag{8-2}$$

$$\frac{dW(t)}{dt} = -W_o e^{\frac{-12Dt}{d^2}} - \frac{12Dt}{d^2} = \frac{12Wo}{d^2} e^{\frac{-12Dt}{d^2}} \tag{8-3}$$

The final form of the diffusion equation is given in Equation (8-4):

$$\ln\left[\frac{dW(t)}{dt}\right] = \ln\left(\frac{12WoD}{d^2}\right) - \left(\frac{12D}{d^2}\right)t \tag{8-4}$$

where D is the diffusion rate of soil in (cm^2/sec), t is the time since the moisture loss began in seconds, W_o is the maximum weight lost in grams, W(t) is the weight of the sample with time as water is lost in grams, and d is the thickness of the sample (in).

8.3 Test Results

The diffusivity value of each quarry was determined for selected samples during the three month production period. The percent fines content was also determined by using the Horiba particle size distribution analyzer device for the selected soil samples. The diffusion test results and the corresponding *pfc* results are tabulated in Table 8-1.

Table 8-1: Tabulated Diffusivity and the Corresponding *pfc* Values Given for Each Quarry

Source ID	Diffusion Material Code	Diffusivity Rate (cm^2/sec)	*pfc* (%)
E-03	4-3-10 A	1.8777E-06	16.36
E-03	4-3-10 B	2.7257E-06	16.36
E-03	6-10-1 A	6.6559E-07	24.45
E-03	6-10-1 B	8.8873E-07	24.45
E-03	6-10-3 A	1.9972E-06	20.26
E-03	6-10-3 B	1.5147E-06	20.26
E-04	2-6 A	3.4490E-06	12.71
E-04	2-6 B	2.7810E-06	12.71
E-06	1-13 A	2.6279E-06	14.21
E-06	1-13 B	2.5869E-06	14.21
E-07	68-2-6 A	2.4181E-06	15.81
E-07	68-2-6 B	2.8264E-06	15.81
E-07	69-1-14 A	2.5811E-06	15.48
E-07	69-1-14 B	2.1952E-06	15.48
E-06	2-6 A	3.3075E-06	12.28
E-06	2-6 B	2.7810E-06	12.28
E-06	3-10 A	3.1727E-06	13.21
E-06	3-10 B	3.1228E-06	13.21
E-09	1-14 A	3.3075E-06	13.25
E-09	1-14 B	3.3362E-06	13.25
E-01	1-3-2-3 A	2.8440E-06*	16.10
E-01	1-3-2-3 B	2.4539E-06*	16.10
E-08	2-1-6 A	1.5003E-06	15.03
E-08	2-1-6 B	1.5800E-06	15.03
E-08	235-1-12 A	2.9712E-06*	15.55
E-08	235-1-12 B	3.0604E-06*	15.55

Table 8-1. Continue

Source ID	Diffusion Material Code	Diffusivity Rate (cm^2/sec)	*pfc* (%)
E-02	1-3-4 A	3.0696E-06	11.43
E-02	1-3-4 B	2.9957E-06	11.43
E-02	2-3-2 A	2.4649E-06	12.97
E-02	2-3-2 B	2.1689E-06	12.97
E-02	3-1-2 A	2.4889E-06	11.96
E-02	3-1-2 B	2.6616E-06	11.96
E-05	61-12 A	8.4818E-07	19.90
E-05	61-12 B	1.0301E-06	19.90
** Additional weight was lost by friable particles.*			

8.4 Diffusivity Dependence on Percent Fines Content

The diffusivity values and the percent fines content were plotted together, and it showed that there is a good correlation between the two variables. The soil samples that are used in the diffusivity tests were separated into two groups based on whether the MBV values are above or below 7.00 mg/g. The percent fines content in the two different MBV groups were compiled to find a correlation with the diffusivity. The graph of the two relationships is given in Figure 8-3.

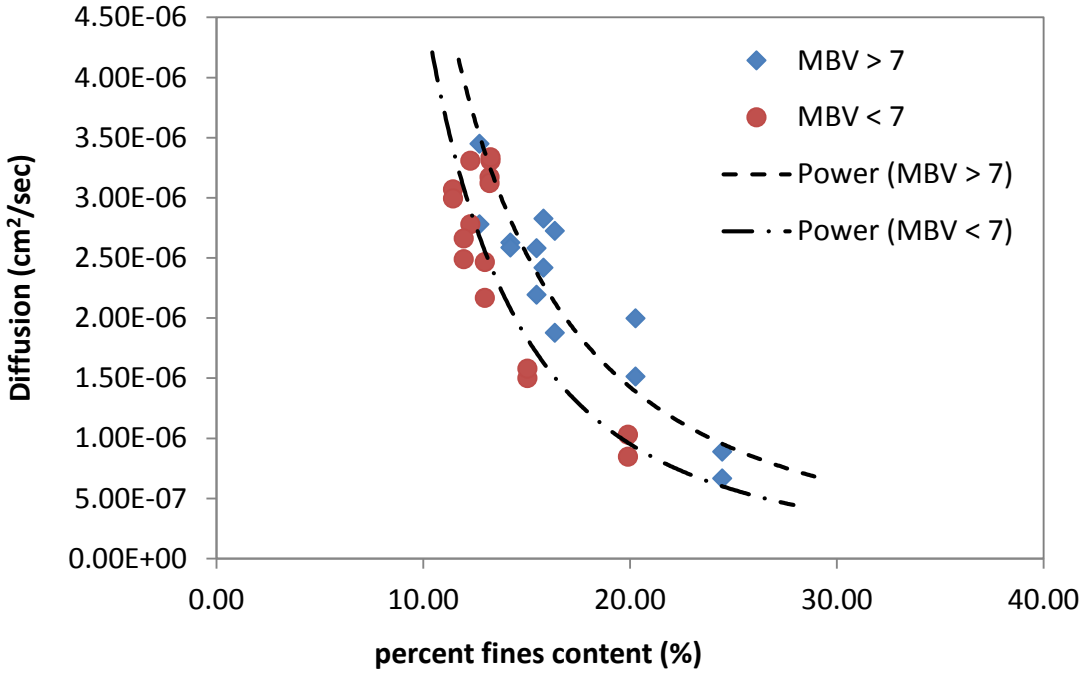

Figure 8-3 Two Empirical Relations between Percent Fines Clay and Diffusivity for both Low and High Plastic Samples

The test results illustrate two trends between the diffusivity values and the percent fines content and these relations are formulated as power equations. The results were divided into two groups: the MBV is greater than 7.00 mg/g and smaller than 7.00 mg/g. The forms of the diffusion equations based on the MBV levels are given in Equations (8-5) and (8-6):

$$D = 5.63E^{-0.4}(pfc)^{-2.00} \text{ for MBV is greater than 7.00 mg/g} \quad (8\text{-}5)$$

$$D = 8.88E^{-0.4}(pfc)^{-2.28} \text{ for MBV is smaller than 7.00 mg/g} \quad (8\text{-}6)$$

where D is the diffusion rate of the soil in (cm^2/sec), pfc is the percent fines content, and MBV is the methylene blue value.

8.5 Closure

Many more examples could be presented of how the performance of a pavement depends upon the unsaturated properties of the materials in those layers. This study illustrates only a few of the relationships that demonstrate the dependence of pavement performance on the unsaturated properties of the supporting layers. Among these dependencies the most significant one is the matric suction, which controls the resilient modulus, permanent deformation, and diffusivity properties of the base course and the subgrade.

The determination of the diffusion rate of the alpha enables researchers to determine the rate at which moisture moves in to the base course layer in horizontal and vertical directions.

9. DEVELOPMENT OF MODELS FOR ATTERBERG LIMITS AND SPECIFIC GRAVITY

9.1 Introduction

In this part of the study, correlations between the methylene blue and both the liquid limit and plasticity index will be investigated. Furthermore, the specific gravity of soil will be studied to determine a relationship with the Atterberg limits. This chapter aims to find quick correlations that can be used when time is limited to determine liquid limit, plasticity index and specific gravity. Additionally, other than the time limitations, usually it is a challenge to obtain these values in construction sites due to limited equipment. This chapter will present a solution to these challenges, especially for the quality control and quality assurance related demands.

9.2 Relationship between MBV and Liquid Limit

Atterberg limits consisting of liquid limit, plastic limit and plasticity index are among the most extensively used soil index properties that create with the engineering properties of soils. There are standard laboratory test procedures to determine the Atterberg limits. These standard test procedures require a certain amount of laboratory work and waiting time. For instance, in the traditional Atterberg limit method, assessment of the soil moisture is very labor-intensive. In order to determine Atterberg limits, the moisture content must be determined. According to the standard test manual, drying takes at least 12 hours by using a standard oven to measure water content. On the

other hand, finding the Atterberg limit is possible in less than 10 minutes, a significantly shorter time, by only employing the improved methylene blue test.

The liquid limit defines a state at which the soil flows and is defined based on the moisture content. The liquid limit test is a standard test method in ASTM D 4318. The liquid limit value is determined by using a standard laboratory test device, which helps to measure the moisture content in the liquid state.

The methylene blue test value and soil liquid limit are correlated. The correlation between liquid limit (LL) and methylene blue value (MBV) is shown in Figure 9-1.

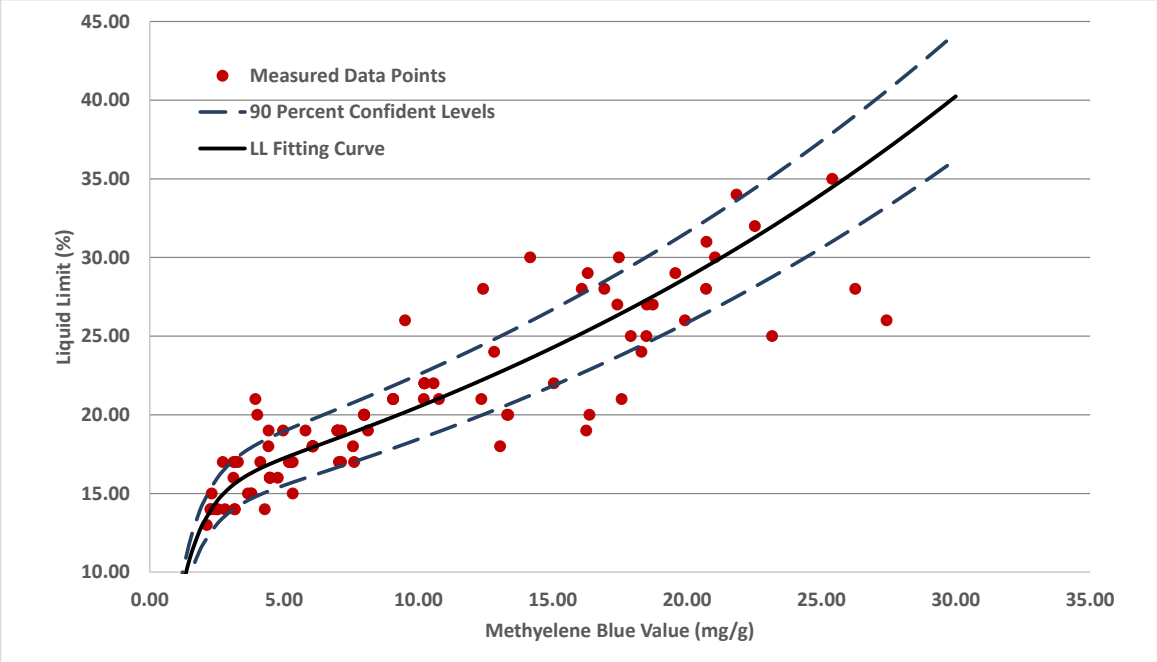

Figure 9-1 A Correlation between Liquid Limit and Methylene Blue Value

The methylene blue value increases proportionally to the liquid limit (LL). The fitting gives a good R-square value of 0.8422, indicating that there is a significant correlation. The 90 percent confidence boundary lines are also shown in Figure 9-1. This correlation is expressed in Equation (9-1):

$$LL = 14.64\,e^{(0.03371MBV)} - 24.99\,e^{(-1.149MBV)} \quad (9\text{-}1)$$

where LL is the liquid limit value of the soil and MBV is the methylene blue value of the soil.

9.3 Relationship between MBV and Plasticity Index

The plastic limit (PL) is the boundary between the plastic state and semi-solid state. Plastic limit is defined as the moisture content at this boundary. The plastic limit test is a standard test method in ASTM D 4318. The test requires a certain amount of lab work and also requires a waiting time to measure moisture content. If a conventional oven is used, the time is around 12 hours.

The plasticity index is also calculated by the difference between liquid limit and plastic limit test results. The methylene blue test also has a good relationship with the plasticity index (PI) as shown in Figure 9-2.

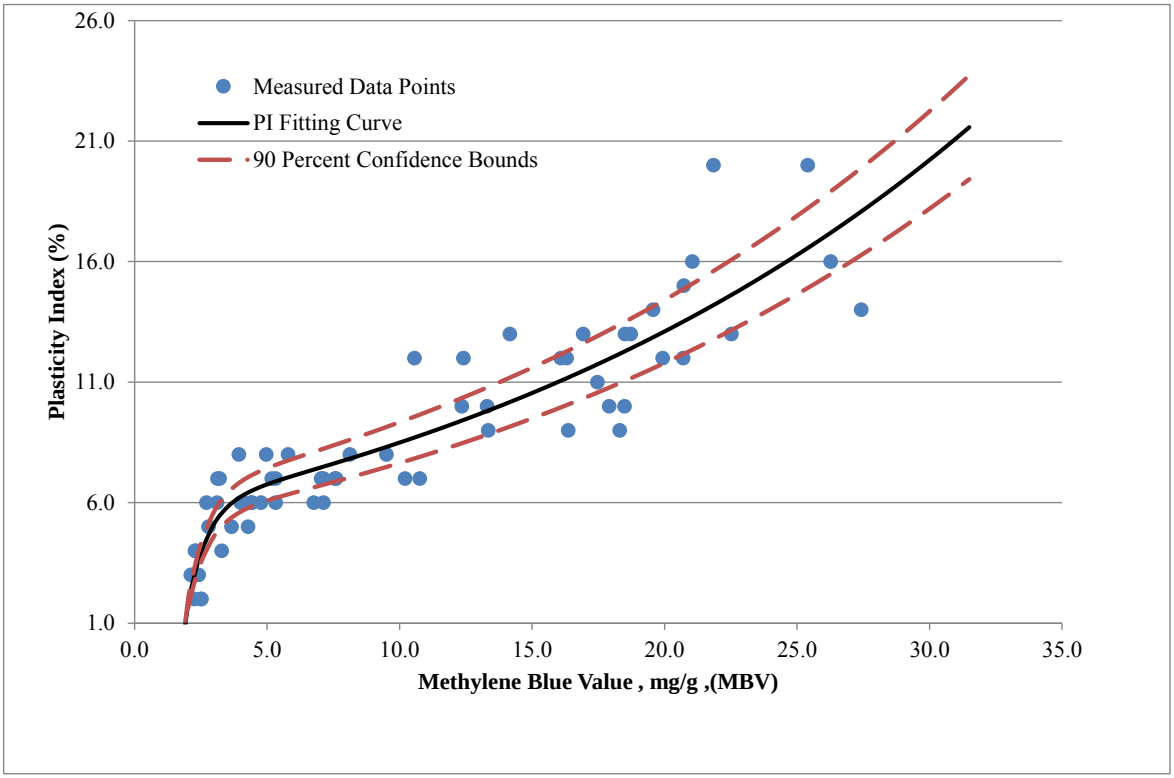

Figure 9-2 A Correlation between Plasticity Index and Methylene Blue Value

Figure 9-2 shows the relationship between MBV and PI value with an R-square value 0.8295 for base course aggregate material. The 90 percent confidence level boundaries are also shown in Figure 9-2. The PI can be estimated using the following Equation (9-2):

$$PI = 5.503e^{(0.04337MBV)} - 62.37*10^{-5}\, e^{(-1.331MBV)} \quad (9\text{-}2)$$

where *MBV* is the methylene blue value and PI is the plasticity index value.

The plasticity index (PI) and liquid limit (LL) values are determined based on Texas Department of Transportation Standard test procedures of Tex-104-E and Tex-106-E. The percent fines content (*pfc*) is determined by using the Horiba particle size

distribution analyzer. The plasticity index and liquid limit are divided by percent fines content, and the results are denoted as PI/pfc and LL/*pfc*. The fraction of PI/pfc is the Activity Ratio (Ac). The test results have demonstrated that a correlation exists between activity ratio (Ac) and the Liquid limit/ *pfc* ratio, and the results are shown in Figure 9-3.

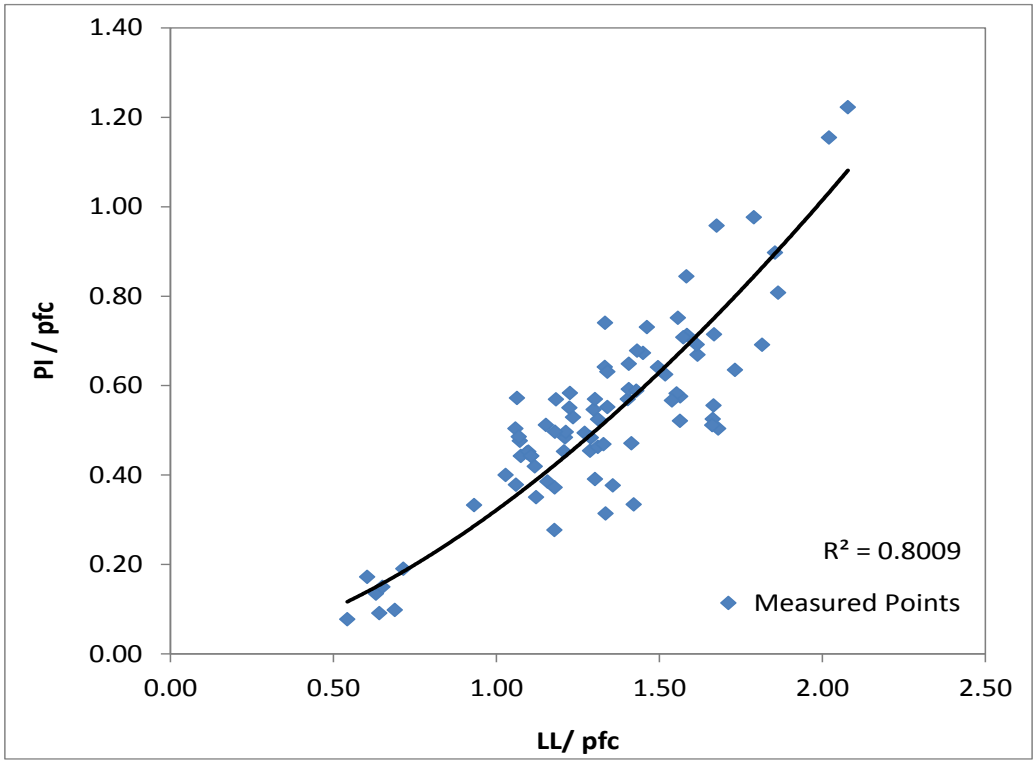

Figure 9-3 A Demonstration of Activity Ratio Correlation with LL/pfc

There is an equation that relates this correlation given in Equation (9-3):

$$\frac{\mathrm{PI}}{pfc} = 0.2994\left(\frac{LL}{pfc}\right)^{1.7039} \tag{9-3}$$

where all of the variables are defined above.

9.4 Specific Gravity Correlation

The specific gravity of soil is an important soil parameter. This is used in many equations, involving the weight-volume calculations in soil mechanics. It is important to note that specific gravity of soil solids refers only to the solid phase in in the phase diagram, and it does not include water and air phases. This is defined as the ratio of soil solids to the density of distilled water at 20 degrees centigrade. This is expressed in Equation (9-4):

$$G_s = \frac{\gamma_{\text{substance}}}{\gamma_{\text{water}}} = \frac{W_s / V_s}{\gamma_{\text{water}}} \tag{9-4}$$

Table 9-1 Specific Gravity of Some Important Soil Minerals (USDA, 1986)

Mineral	**Specific Gravity**
Dolomite	2.87
Quartz	2.66
Kaolinite	2.6
Illite	2.8
Montmorillonite	2.65-2.8
Halloysite	2.0-2.55
Potassium feldspar	2.57
Sodium and calcium feldspar	2.62-2.76
Chlorite	2.6-3.0
Biotite	2.8-3.2
Muscovite	2.76-3.1
Hornblende	3.0-3.47
Limonite	3.6-4.0
Olivine	3.27-3.7

Quartz is usually a primary component of gravel and sand, and hence a value of 2.66 is usually assumed to be the specific gravity for sands and gravel. A soil with higher percent silt usually has a specific gravity of about 2.68. The reason is that other than quartz, a small amount of clay in the soil increases the specific gravity. In general, the clay minerals have a specific gravity range from about 2.60 to 2.80. Soils with a high amount of micaceous flakes, hematite, or magnetite may have a specific gravity ranging from about 2.75 to 3.3 (USDA, 1986).

The specific gravity is calculated in a laboratory with the standard test method for solids, by using a pycnometer ASTM D845 (ASTM, 2002). This test procedure is applicable for soils composed of particles smaller than the No.4 (4.75mm) sieve based on the USA sieve size.

A direct measurement of the specific gravity is obtained using AASHTO T100 and this test is executed in conjunction with a consolidation test in AASHTO T180 for base course unbound aggregates.

A laboratory test can be conducted to estimate the specific gravity of the soil solids. However, this test may not be performed in some field investigations because of time limitations. Therefore, a quicker estimate is crucial to be used in such situations. In order to meet this need, an alternative to the laboratory experiment method should be used to determine specific gravities. For this purpose, a correlation was proposed by using the plasticity index and the sieve analysis in the MEPDG Design Guide in the environment report (MEPDG, 2004). This specific gravity equation was developed to be used in computations in the EICM (The Enhanced Integrated Climatic Model), a

software program, which is a part of the design software. The proposed specific gravity equation is given in Equation (9-5):

$$G_s = 0.041\left(P_{200}PI\right)^{0.29} + 2.65 \tag{9-5}$$

where G_s is the specific gravity, P_{200} is the percent of aggregate passing through the No.200 sieve, and PI is the plasticity of the soil. The P_{200} can be obtained from the grain size distribution analysis in AASHTO T 27, and PI is determined from an Atterberg limit test in AASHTO T 90.

Even though Equation (9-5) is very simple and provides an accurate estimate of specific gravity, it has limitations in certain field investigations. Usually, during the quality assurance and quality control process, the P_{200} and PI test results may not be in hand to determine the specific gravity. Therefore, an equation was derived to estimate the specific gravity by using only the plasticity index and liquid limit. The required parameters can be obtained by using the methylene blue Equations (9-1) and (9-2) given in the previous section.

Juárez-Badillo (1981; 1985) formed of an equation with boundary conditions, which was used to derive the relationship between the specific gravity and plasticity index and liquid limit, is given in Equation (9-6):

$$\int_{g_1}^{g} \frac{df(\mathrm{g})}{f(\mathrm{g})} = \gamma \int_{p_1}^{p} \frac{df(\mathrm{p})}{f(\mathrm{p})} + \delta \int_{l_1}^{l} \frac{df(\mathrm{l})}{f(\mathrm{l})} \tag{9-6}$$

Equation (9-6) was integrated to obtained Equation (9-7):

$$\ln\left[\frac{\frac{1}{g_m-g}-\frac{1}{g_m-g_o}}{\frac{1}{g_m-g_1}-\frac{1}{g_m-g_o}}\right]=\gamma\ln\left[\frac{\frac{1}{p_m-p}-\frac{1}{p_m-p_o}}{\frac{1}{p_m-p_1}-\frac{1}{p_m-p_o}}\right]+\delta\ln\left[\frac{\frac{1}{l_m-l}-\frac{1}{l_m-l_o}}{\frac{1}{l_m-l_1}-\frac{1}{l_m-l_o}}\right] \tag{9-7}$$

Equation (9-7) was simplified and rewritten in Equation (9-8):

$$\left(\frac{g-g_o}{g_m-g}\right)\left(\frac{g_m-g_1}{g_1-g_o}\right)=\left[\left(\frac{p-p_o}{p_m-p}\right)\left(\frac{p_m-p_1}{p_1-p_o}\right)\right]^{\gamma}\left[\left(\frac{l-l_o}{l_m-l}\right)\left(\frac{l_m-l_1}{l_1-l_o}\right)\right]^{\delta} \tag{9-8}$$

The β is defined in Equation (9-9) and is substituted as.

$$\beta=\left(\frac{g_1-g_o}{g_m-g_1}\right)\left(\frac{p_m-p_1}{p_1-p_o}\right)^{\gamma}\left(\frac{l_m-l_1}{l_1-l_o}\right)^{\delta} \tag{9-9}$$

$$\left(\frac{g-g_o}{g_m-g}\right)=\beta\left[\left(\frac{p-p_o}{p_m-p}\right)\right]^{\gamma}\left[\left(\frac{l-l_o}{l_m-l}\right)\right]^{\delta} \tag{9-10}$$

Equation (9-10) was solved for g:

$$g=\frac{g_o+g_m\beta\left[\left(\frac{p-p_o}{p_m-p}\right)\right]^{\gamma}\left[\left(\frac{l-l_o}{l_m-l}\right)\right]^{\delta}}{1+\beta\left[\left(\frac{p-p_o}{p_m-p}\right)\right]^{\gamma}\left[\left(\frac{l-l_o}{l_m-l}\right)\right]^{\delta}} \tag{9-11}$$

The final form of the Juárez-Badillo equation is expressed in Equation (9-12):

$$G_s=\frac{G_o+G_m(\beta)\left(\frac{PI-P_o}{P_m-PI}\right)^{\gamma}\left(\frac{LL-L_o}{L_m-LL}\right)^{\delta}}{1+G_m(\beta)\left(\frac{PI-P_o}{P_m-PI}\right)^{\gamma}\left(\frac{LL-LL_o}{LL_m-LL}\right)^{\delta}} \tag{9-12}$$

where G_s is the specific gravity, G_o is the minimum specific gravity, G_m is the maximum specific gravity, PI is the plasticity index, P_o is the minimum plasticity index, P_m is the maximum plasticity index, LL is the liquid limit, L_o is the minimum liquid limit, L_m is the maximum plasticity index, and where β is a parameter, γ is an exponent for plasticity indexes, δ is an exponent for liquid limit.

The specific gravity of most of the minerals are within a range from 2.60 to 2.90 (Das, 2012) Therefore, the minimum and maximum specific gravity range is considered to cover most of the commonly used minerals in engineering practice. The specific gravity of soil depends on the type of soil mineralogy and the composition of the soil grain size. The composition of a soil can be utilized to estimate a value for the specific gravity (USDA 1986). The Atterberg limits can be estimated in a simple way by using the introduced MBV method; therefore, Atterberg limits were chosen to use in the developed specific gravity equation. The final form of the equation is in Equation (9-13):

$$G_s = \frac{2.55 + 2.91(2.43)\left(\frac{PI-1}{22-PI}\right)^{0.3076}\left(\frac{LL-1}{40-LL}\right)^{-0.3525}}{1+(2.43)\left(\frac{PI-1}{22-PI}\right)^{0.3076}\left(\frac{LL-1}{40-LL}\right)^{-0.3525}} \tag{9-13}$$

where Gs is the specific gravity, PI is the plasticity index, and LL is the liquid limit.

The proposed specific gravity equation is evaluated by comparison with the specific gravity equation given in the MEPDG report. A comparison based on a set of calculated specific gravity values is shown in Figure 9-4.

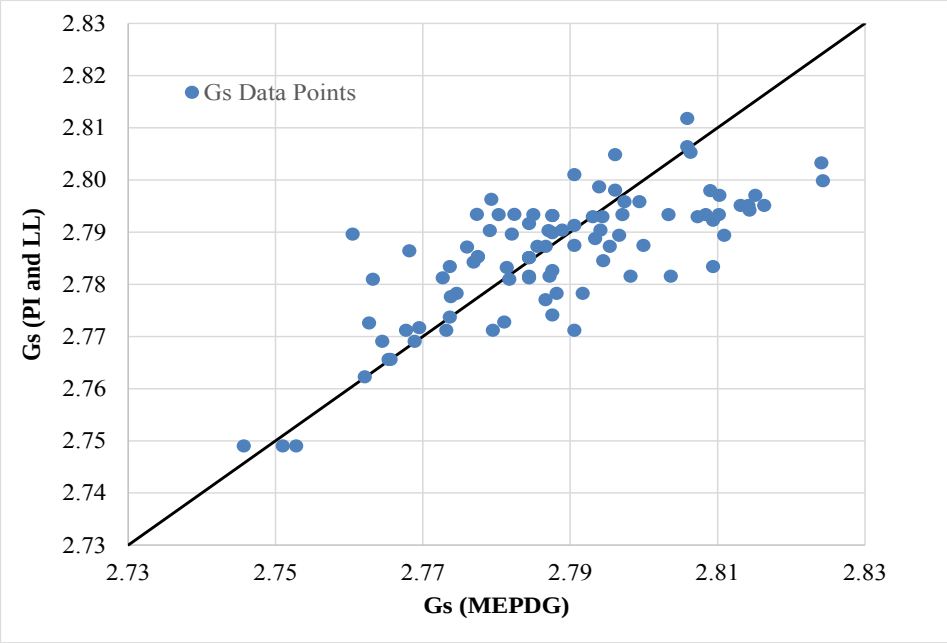

Figure 9-4 A Comparison of Specific Gravities based on the MEPDG and New Methods

An experimental study was conducted on the nine aggregate sources to determine specific gravity. The standard test procedure ASTM D 854 was followed in this study. These laboratory test results were compared with the developed specific gravity Equation (9-13) and tabulated in Table 9-2.

Table 9-2 Tabulated Laboratory and Calculated Results of Gs for Nine Aggregate Sources

Code Producer	Gs Model	Experimental	Error (%)
E-01	2.79	2.79	0.00
E-02	2.79	2.78	0.36
E-03	2.79	2.78	0.36
E-04	2.80	2.78	0.71
E-05	2.76	2.77	0.36
E-06	2.82	2.87	1.77
E-07	2.79	2.71	2.87
E-08	2.79	2.77	0.72
E-09	2.79	2.73	2.15

Table 9-2 shows that there is a good correlation between in the empirical and calculated results. In addition, the developed Gs model is sensitive enough to capture the change in the specific gravity due to material characteristics and properties that affect the Atterberg limits.

9.5 Closure

In this section, there unique soil correlations of liquid limit, plasticity index and specific gravity was investigated to find correlation with the methylene blue value (MBV). The investigation found that there is a good agreement between them. A general equation was determined to be used in laboratory and in field investigations.

The first correlation is that the liquid limit (LL) can be predicted by using the methylene blue test. This correlation is defined by using an S-shaped equation. It is correlated entirely to the methylene blue values.

The second one is the plasticity index (PI), which is also determined to be of the same form of equation as the liquid limit equation. The PI is only dependent to the MBV. The 90 percent confidence limits are determined for both liquid limit and plasticity index.

These two correlations for the LL and PI showed that the methylene blue test is significant to determine the Atterberg limits.

The last correlation is the specific gravity of soil. A general specific gravity equation was presented in this study. A significant specific gravity was modeled according to the Juarez-Badillo form of equation. The specific gravity equation uses the liquid limit and plasticity index as input values. It highlights the significance of the Atterberg limits value. Other than that, the Atterberg limits can be predicted by using the methylene blue test so the prediction of the specific gravity depends on the MBT as well.

These models mainly aim at being used for the quality control and quality assurance purposes in the field investigations where a quick simple method is needed to find the results.

10. A FIELD VERIFICATION BY USING NONDESTRUCTIVE TESTS

10.1 Introduction

This part of the study will cover the most commonly used nondestructive test methods in pavement management and pavement design. In addition, a case study conducted with these methods will be analyzed to evaluate the condition of a pavement. This study uses the methods developed in the previous sections in this case study as well.

The predictions of the pavement layer properties are determined from historical records but these records are either not very accurate or not available. Therefore, currently acceptable test methods used in predicting the pavement properties are grouped into two classes: destructive and nondestructive. The destructive method usually requires extracting a core sample and testing this sample in the laboratory. Although extracting a sample provides sufficient data about the pavement properties, it has many obvious disadvantages. These disadvantages include pavement structure being subject to damage by the cores taken, being unable to provide real time measurements, and traffic disruptions. However, the advantages of nondestructive test are many: include real time condition assessment of pavement, rapid measurement and quantitative evaluation of the condition, no sample disturbance, and no traffic service delay due to coring.

A ground penetrating radar (GPR) is a nondestructive testing device used to determine the dielectric constant and the layer thickness of pavements. The knowledge of the layer dielectric and structural information are used to identify the presence of the layers' wetter areas, which are more susceptible to permanent deformation. GPR

presents the collected data in a colored map analysis system. A falling weight deflectomer (FWD) is also an important nondestructive test device that is utilized for research and design. The FWD unit mimics the pavement response under the passing traffic loads. The FWD can be used in a variety of pavement analysis methods, including the in network level pavement management and project design. The typical output data of a GPR is usually considered the source of the input data in a FWD analysis. The philosophy of the study conducted in this section is organized based on the scheme presented Figure 10-1.

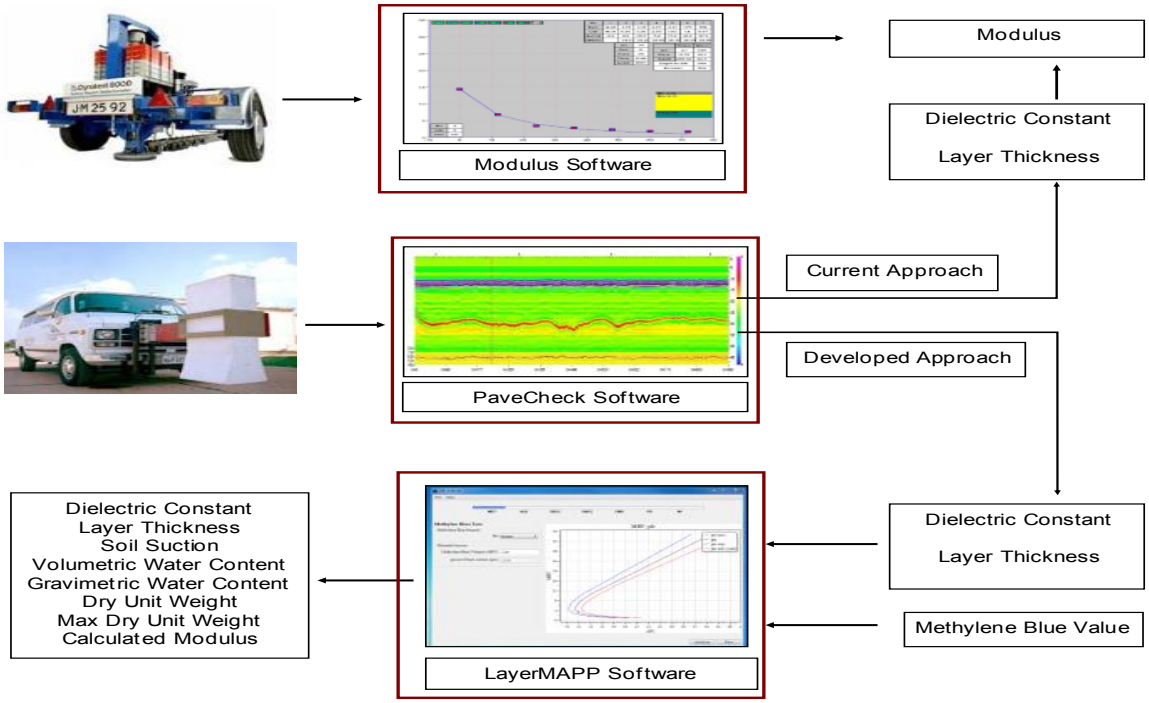

Figure 10-1 Schematic Flow Charts Showing the Philosophy of the Study Conducted

This section will begin with an introduction of the case study test location. It will continue with a review of the principles in the GPR and FWD systems, explaining the background information regarding theories and operation philosophies, respectively. In addition, the GPR section covers the PaveCheck program, and the FWD section covers the MODULUS program. The LayerMAPP is new analysis software program designed for Measurement and Analysis of Pavement Performance (MAPP). It will present the quantification of pavement properties based on the case study on the pavement section, and subsequent section test results and findings will be summarized.

10.2 A Case Study: Survey Location

The data examined in this study was collected from one construction site that is selected by Texas Department of Transportation (TxDOT) for investigations in Delta County in Texas. The data was collected by using an air coupled GPR system mounted on a van. The ambient temperature during data collection was mid-90^{o} F. There was no rainfall prior the surveying. In fact, the county had not received precipitation for more than a month. The total length of the project was 6.43 miles including 6.19 miles of roadway and 0.242 miles of bridges. The location of the construction site is shown in Figure 10-2.

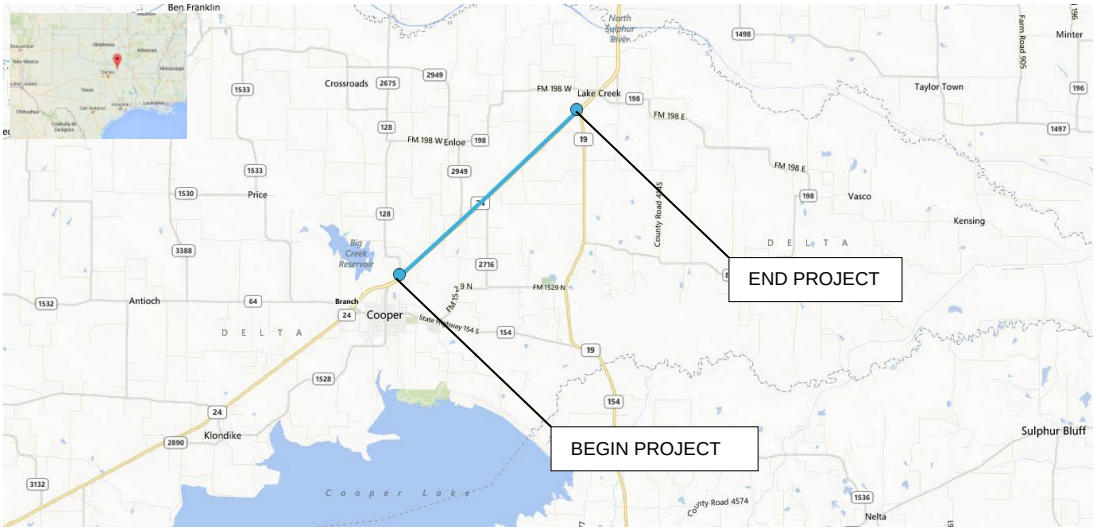

Figure 10-2 SH 24 Road in Cooper Town in Delta County (ArcGIS map)

The data analyzed in this study was taken from the west bound lane of the site of the construction. The collected data has a length of 4.5 miles from the beginning section of the project. The GPR van collected the data on a routine basis from the site for forensic investigations by TxDOT. This project was completed in 2008. When the measurements were conducted, it was a recently constructed pavement.

The pavement system as-built configuration in SH24 was determined from the GPR survey conducted. A summary of pavement thickness and the properties of the pavement system are presented in Figure 10-3. This pavement system consists of three main layers; asphalt concrete top layer, an unbound aggregate base layer over stabilized subgrade on top of the local vertisol soil.

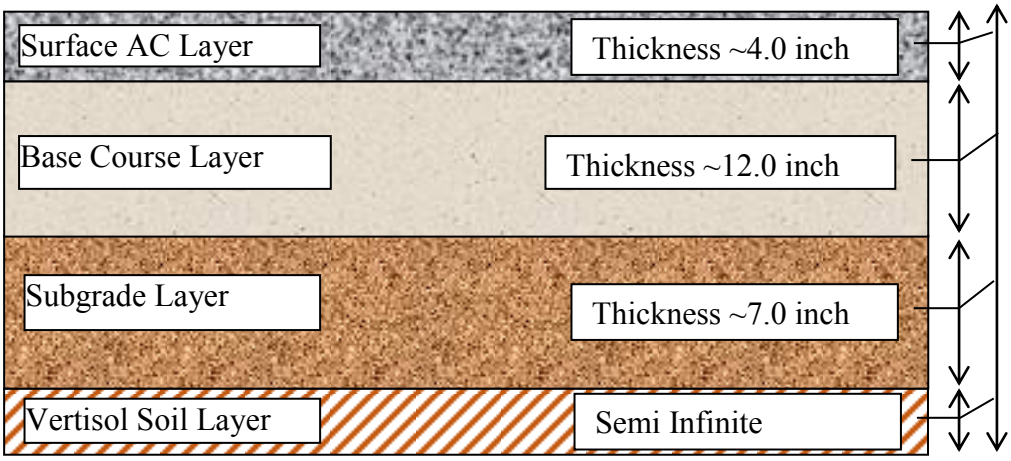

Figure 10-3 General Layer-structure Design of the Pavement System

Two core samples were taken from the unbound aggregate materials used to construct the base course layer. The base course material type is sandstone, and it was transferred to the Delta County from a quarry in Sawyer, Oklahoma. The particle size analyses results from the extruded samples based on the Tex-110-E are given in Table 10-1.

Table 10-1 A Laboratory Sieve Analyses Results for Oklahoma Material (Dry Sieved).

Sieve Sizes	Individual Wt. Retained (g)	Cumulative Retained (%)	Individual Retained (%)	Cumulative Retained (%)
1 3/4	0	0	0.00%	0.00%
7/8	1205.7	1205.7	18.56%	18.56%
3/8	1632.6	2838.3	25.14%	43.70%
No.4	793.8	3632.1	12.22%	55.92%
No.40	1618	5250.1	24.91%	80.83%
Sum:	--	6495.1	0.00%	100.00%

The gradation analysis is within the master grading. Also, according to TxDOT specification referring to Item 247, this master grading is a coarse graded as Grade-I.

According to laboratory test results, the base course aggregate shows a low plasticity index. The plasticity index is in range of about 3.2. The laboratory compaction curve provides the optimum moisture content range of about 6.9 (%) and the maximum dry unit weight range of about 137.3 (lb/ft^3).

An air launched GPR was used to survey the location where forensic investigation was conducted. GPR antenna emits electromagnetic waves to the subsurface of the pavement. The arrival time and magnitude of the reflected waves are received from the interface of each pavement layer. The dielectric constant represents the electric properties of the layer and also determines the relative magnitude of the reflected wave pulse. The dielectric constant of materials are unique with material type

and were calculated from the reflected GPR wave data that were collected. Approximately 24,000 GPR traces were analyzed.

10.3 Ground Penetrating Radar

10.3.1 General

The ground penetrating radar (GPR) is one of the nondestructive geophysical tools used to detect the underground layer properties and monitors the variations in the layer beneath the surface layer. It is has been adapted and was successfully applied to predict the pavement layer system characteristics by pavement engineers. The basic principle of the GPR operation system is that it emits the electromagnetic (EM) pulses and receives the reflected signals through an antenna and measures in the time of arrival of each wave. The magnitude of the signals amplitudes changes are based on the dielectric properties of each layer (Annan, 2003). The mechanics of the radar sending energy and the reflection from each layer interface is shown in Figure 10-4.

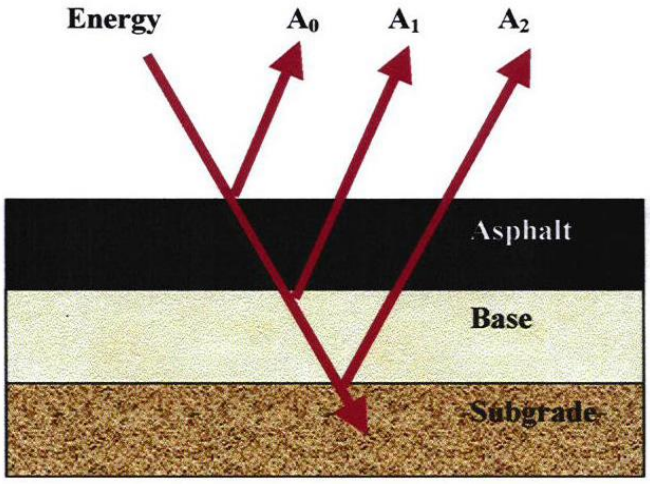

Figure 10-4 A Typical Received Radar Signal from a Pavement Structure

The GPR technology offers a high speed data collection and assessment of the continued dielectric profile. A transmitter antenna transmits a high-frequency mono-pulse electronic signal, which travel through each layer and reflects at the interface between the two layers of the materials with different dielectric properties. This high-frequency signal is received by the antenna and transmitted to a signal acquisition unit to convert them to relatively lower signal pulses. A typical plot of a received radar signal versus time for one pulse is shown in Figure 10-5. The first amplitude A_o is the reflection from the lower end of the antenna and the second amplitude is reflected signal from the pavement surface.

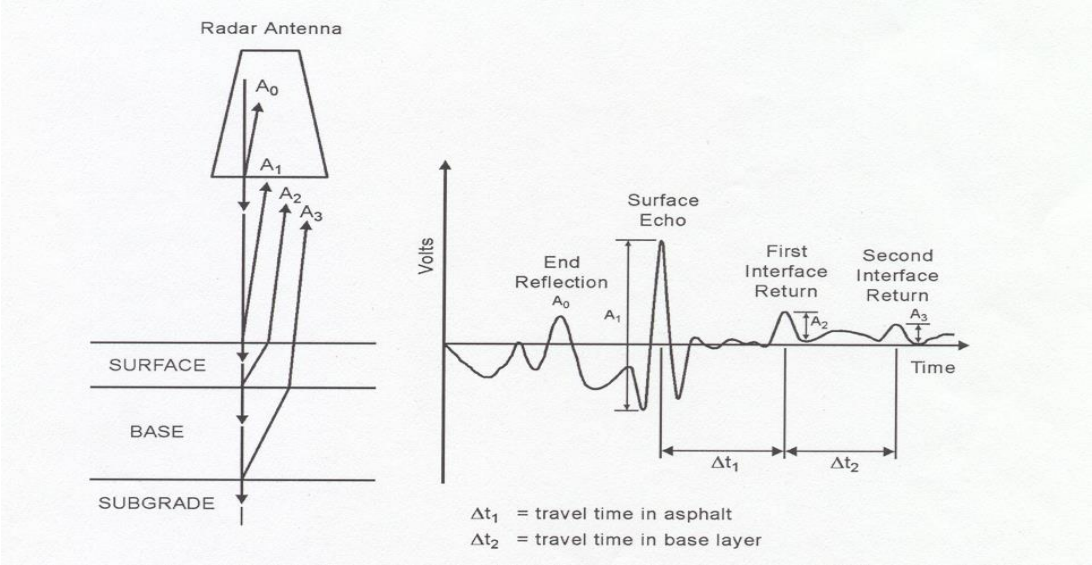

Figure 10-5 Radar Operation System Principals of a Typical Emitted and Received Radar Signal Schematic

Figure 10-5 shows that the incident wave is reflected at each layer interface and plotted as return voltage against time of arrival in nanoseconds. The amplitude A_1

represents the pulse energy from the surface of the pavement, amplitude A_2 and A_3 represent the reflection from the surface of the base and subgrade, respectively. These signals are received by a receiver and are converted in a low frequency and digitized by an A/D converter and then sent to a host computer to data process and display. A radar system moves along the survey location and received waves displayed in a 2-D pseudo color strip map by the host computer.

A radar system is usually carried by a van, and the radar antenna is mounted on the front bumper. An air launched ground penetrating radar unit is shown in Figure 10-6.

(a)

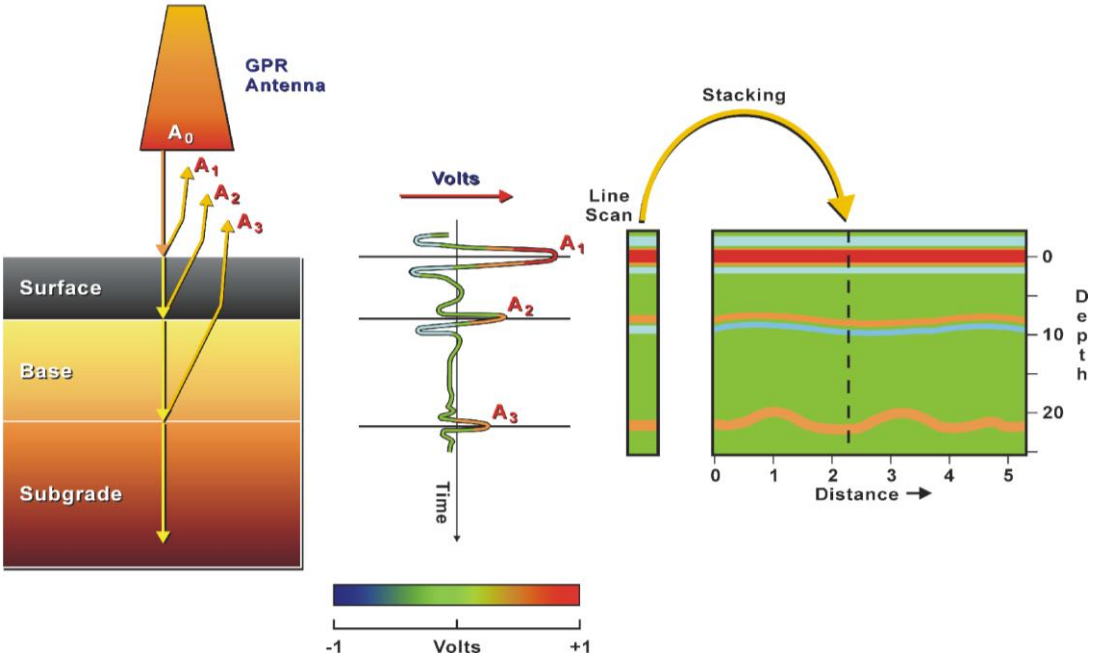

(b)

Figure 10-6 A GPR Equipment (a) and Mechanics of Signal Operation System (b)

This particular GPR van operates at a highway speed of 60 mph and can effectively collect the data. This unit is capable of emitting and receiving 50 pulses per second in penetrating to a depth of 2 feet. In Figure 10-6, A_o is the incident amplitude; A_1 is the amplitude of the GPR wave that is reflected from the surface; A_2 is reflected from the interface between the surface layer and the base course; A_3 is reflected from the interface between the base course and the subgrade.

The GPR uses a very sophisticated system and most advanced technology. The main component of a GPR is a high speed pulse generator, high speed data acquisition, real time data processing, and wireless communication systems. Displaying data is a synchronized process in the GPR unit. This system was adapted by the state transportation departments and agencies: likewise, TxDOT and TTI have the GPR vans.

10.3.2 Principal of Ground Penetrating Radar System

The dielectric constant and the layer thickness can be calculated by using the measured amplitudes (volts) and time delays (ns). The general form of the equations are summarized below. The surface layer dielectric equation is given in Equation (10-1):

$$\varepsilon_a = \left[\frac{1 + A_1 / A_m}{1 - A_1 / A_m} \right]^2 \tag{10-1}$$

where ε_a gives the dielectric of the surface layer, A_1 is the amplitude of surface reflection (volts), A_m is the amplitude of reflection from a large metal plate in volts (this represents the 100% reflection case).

The top layer thickness is presented in Equation (10-2).

$$h_1 = \left\lfloor \frac{c\Delta t_1}{2\sqrt{\varepsilon_a}} \right\rfloor \tag{10-2}$$

where h_1 shows the thickness of the top layer, c is the speed of electromagnetic wave in air (5.9 ins/ns two way travel), Δt_1 is the time delay between peaks A_1 and A_2 (in ns).

The dielectric value of base course layer is presented in Equation (10-3).

$$\sqrt{\varepsilon_b} = \sqrt{\varepsilon_a}\left[\frac{1-\left(\frac{A_1}{A_m}\right)^2 + \left(\frac{A_2}{A_m}\right)}{1-\left(\frac{A_1}{A_2}\right)^2 - \left(\frac{A_2}{A_m}\right)} \right] \tag{10-3}$$

where ε_b yields the dielectric value of the base course aggregate andA_2 is the amplitude of reflection (volts) from the top of the base course layer.

The thickness of the base course layer is estimated in Equation (10-4):

$$h_{base} = \frac{c\Delta t_2}{2\sqrt{\varepsilon_b}} \tag{10-4}$$

where h_{base} yields the thickness of the base and Δt_2 is time delay (ns) between A_2 and A_3

The given equations from (10-1) to (10-4) provide a summary that are derived to calculate the pavement layer dielectric values and thickness. In this particular study, the base course thickness and dielectric constant will be utilized in the analysis process. This study is discussed in the following section in detail.

10.3.3 PaveCheck Program

PaveCheck is a software program that is used to analyze the GPR survey data. The data set used in this section demonstrates the results of PaveCheck. This section describes the data analysis by using the PaveCheck program but a detailed description and user manual are available in a PaveCheck user manual (Liu and Scullion, 2006).

The GPR van collects both the pavement dielectric constant along with video images on the survey section. The GPR radar data is processed, including a color map, a signal trace analysis, and the video image screens and are shown in Figure 10-7.

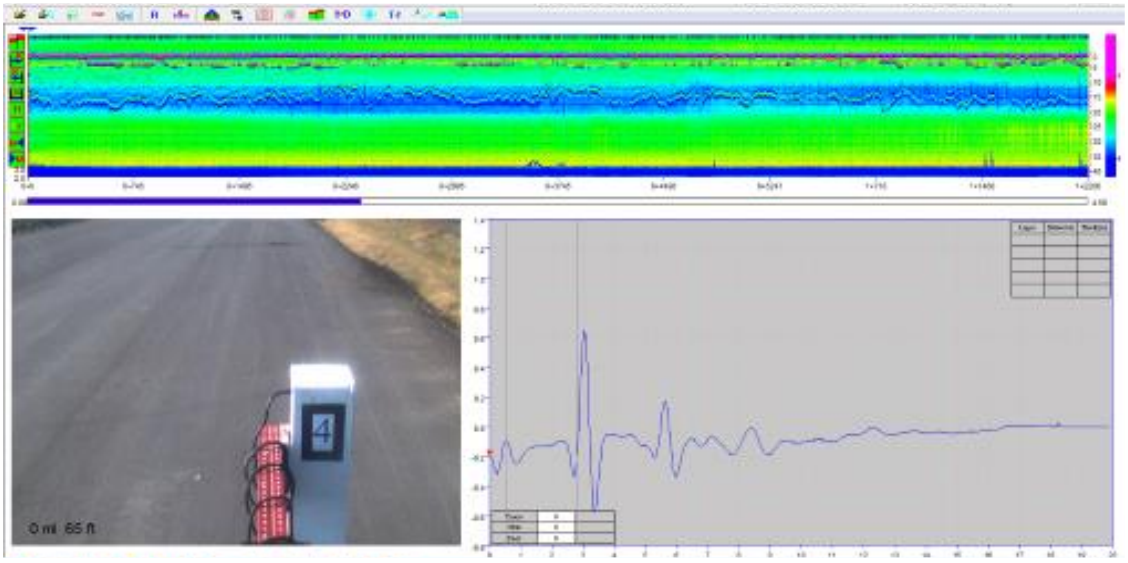

Figure 10-7 PaveCheck Program Data Processing Display

Figure 10-7 shows a spot on the pavement surface, which is captured at 65 ft away from the survey beginning section. This screen shows a video image of a surveyed point in feet units. The box next to it shows the trace of the reflected signal at the

surveyed point and thickness of the layers at the imaged point. A color map with the layer thickness properties are shown in Figure 10-8.

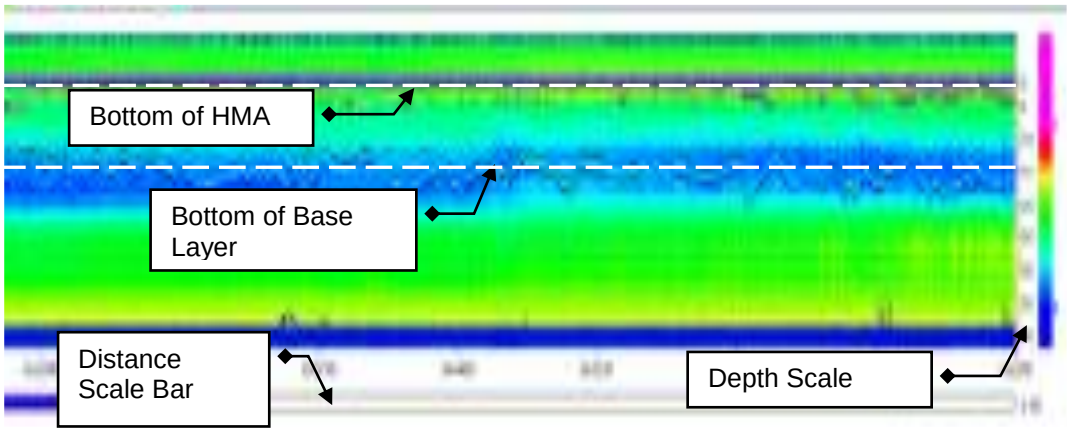

Figure 10-8 A Color Coded Map Screen

Figure 10-8 shows a typical displayed map presenting the survey location and the pavement structure system. This display is taken from a section of newly constructed asphalt layer. The layer interfaces are red and blue colored lines. Both the HMA and base layer boundaries are shown in Figure 10-8. The distance scale shows the survey distance in mile or feet units, and the distance bar is the total survey length. The dielectric constant value is used to calculate the depth scale by converting the measured time scale to a depth scale.

The GPR data are loaded in the PaveCheck program and the data are processed. Then, the GPR data is utilized to the obtain color map. The boundaries of the layer interface are identified by using a right click on a mouse and selecting the pen option. Carefully mark the entire base course layer interface boundaries. Especially in this

project, it is slightly difficult to differentiate these layers, and the bottom of the base course layer changes by fluctuating in every several feet.

When all the sections are marked, the selected markers are saved by clicking on the output button. This saved file can be opened with an MS Excel document to organize the calculated data. Based on this, the dielectric constant and the base course layer thickness of the survey section were determined.

10.3.4 Data Analysis

The PaveCheck program feeds the survey results into an MS Excel program. The results are organized to determine the layer thickness and the dielectric constant of the base course layer. The predicted results are turned into strip maps to display the variation of these along the length of the survey section.

The measured data showing in Figure 10-9 to Figure 10-14 are analyzed in following order: (i) Refine the dielectric value from the radar survey by using the PaveCheck program. (ii) Predict the base course thickness along the survey section. (iii) Dielectric measurements is an input in the *SDCC* curve, and it was explained in an earlier chapter. Therefore, the dielectric values are employed to determine the suction at each corresponding dielectric reading. The *SDCC* curve parameter alpha and gamma are determined based on the MBV and pfc. (iv) The calculated matric suction values are used as inputs in the *SWCC* curve. The form of the *SWCC* curve enables the calculating of the volumetric water content at each suction reading (indirectly each dielectric constant). The four parameters are used to estimate the shape of the *SWCC*, which was calculated before this step.

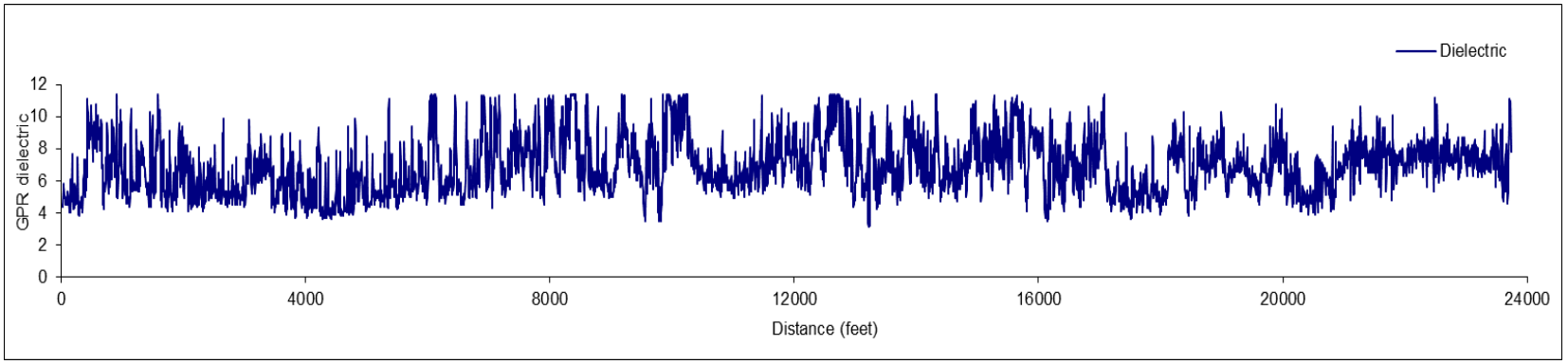

Figure 10-9 Dielectric Value Presented in Colored Strip Map

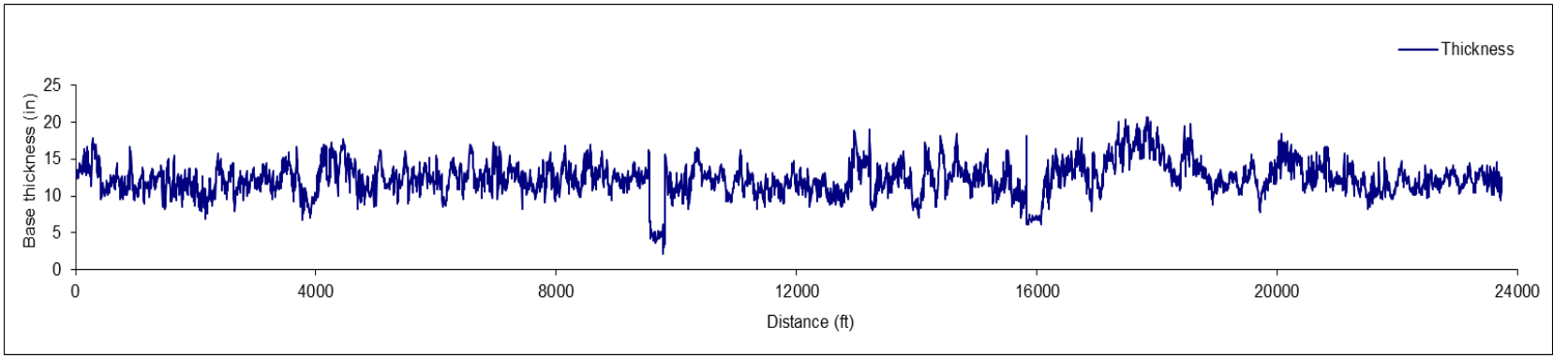

Figure 10-10 Base Course Layer Thickness Presented in Colored Strip Map

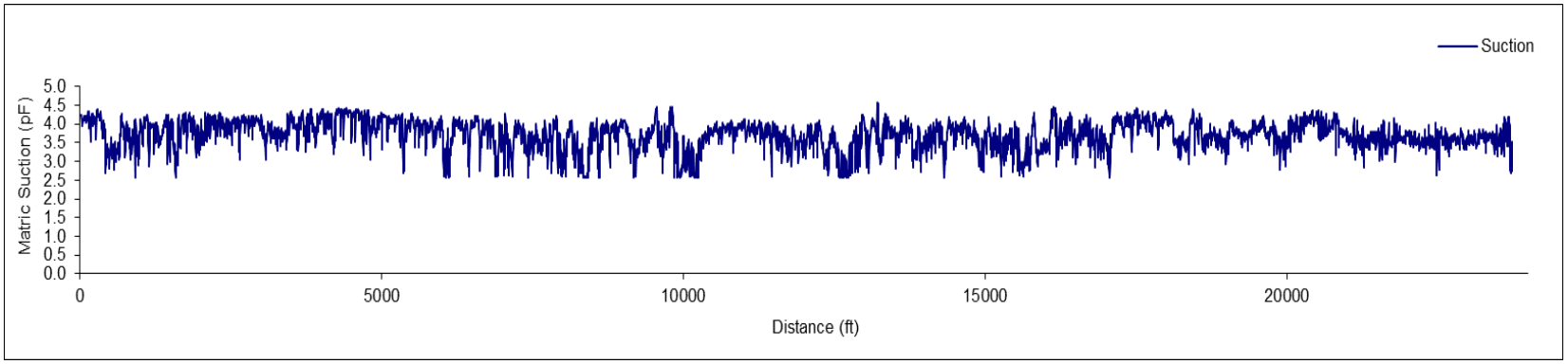

Figure 10-11 Matric Suction Presented in Colored Strip Map

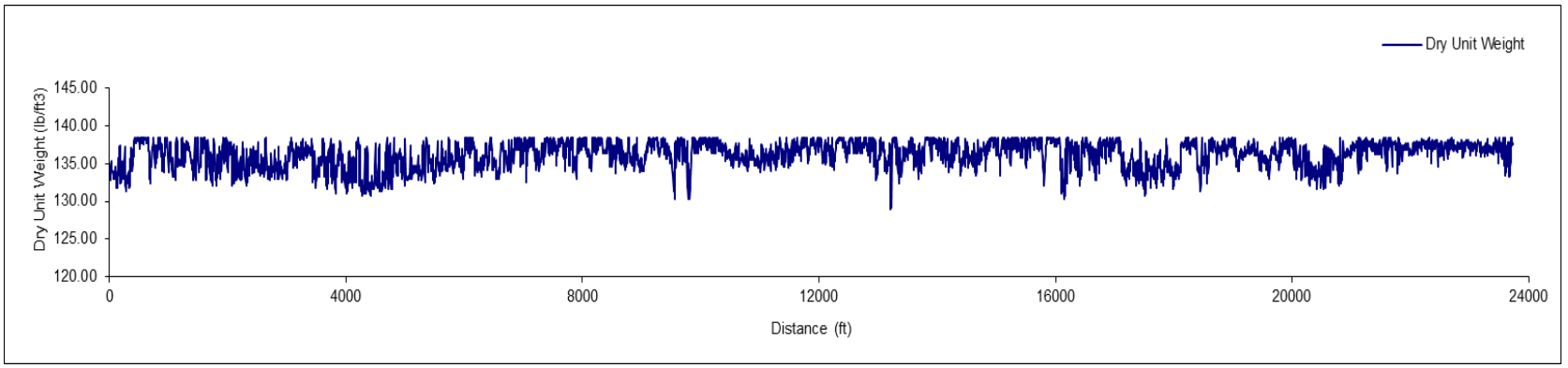

Figure 10-12 Dry Unit Weight Presented in Colored Strip Map

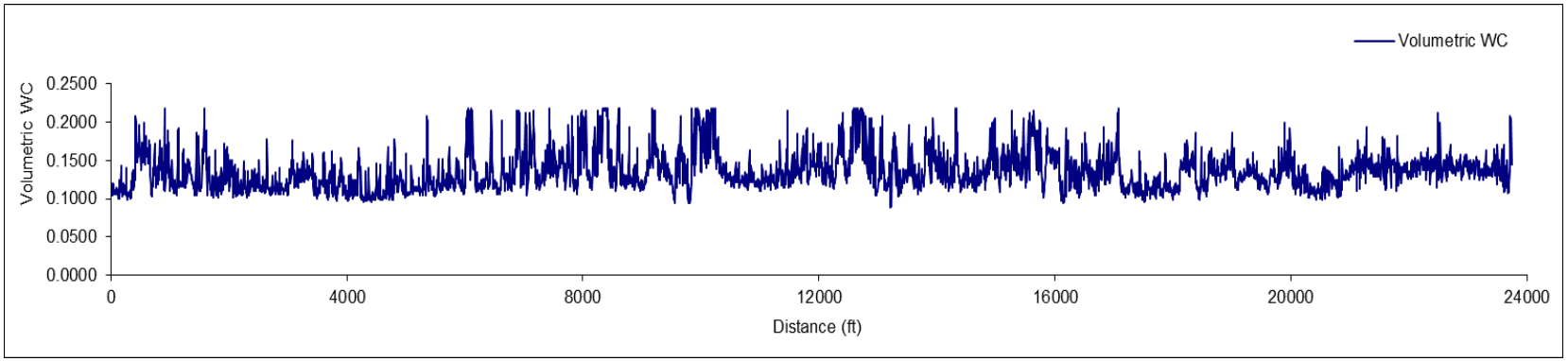

Figure 10-13 Volumetric Water Content Presented in Colored Strip Map

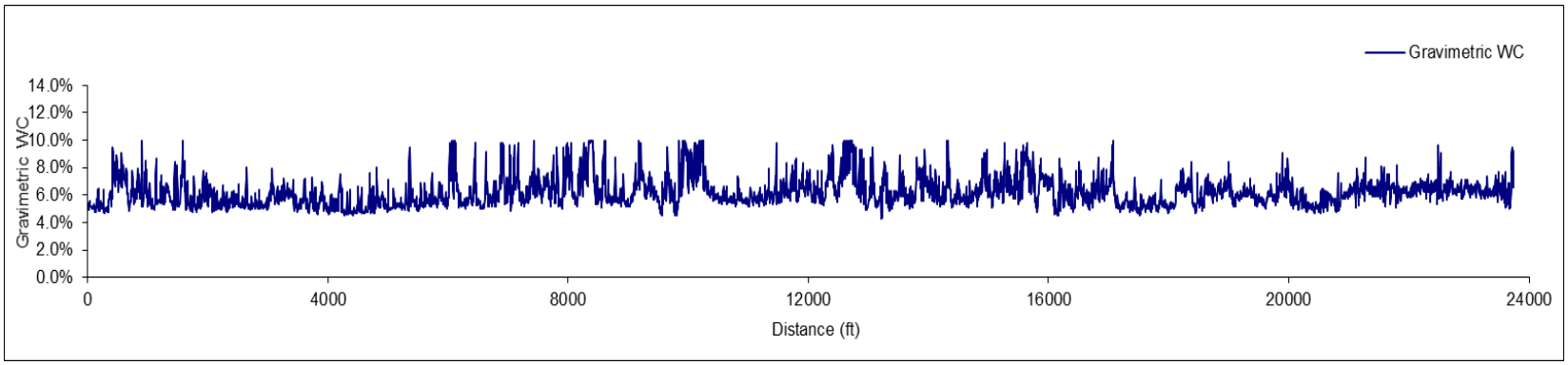

Figure 10-14 Gravimetric Water Content Presented in Colored Strip Map

(v) These are a well-known equations, which are shown in a previous chapter, to estimate the gravimetric water by using the volumetric water content. (vi) The dry density equation was presented in Chapter 7 and the steps used to calculate the dry unit weight was explained thoroughly. There are three parameters a_d, b_d, and n_d, which govern the dry unit weight curve. These three parameters are calculated and then the dry unit weight was predicted by using the calculated gravimetric water content. The gravimetric water content showed that the base course materials are not at the optimum moisture content. The outcomes of these six-steps are presented in Figure 10-9 to Figure 10-14, respectively.

Figure 10-9 shows that the dielectric constant value is determined directly from the GPR measurements. Figure 10-10 gives the base course layer thickness variation, and it was determined by using the PaveCheck program. This program allows users to select the boundary of the pavement layers in the pavement system as well as to calculate the layer thickness for not only the base course but also the HMA. Figure 10-11 shows the matric suction, which is calculated based on the *SDCC* approach. It is clearly seen that the matric suction changes and is not a constant value in the entry measurement section. This calculation was performed in very accurate fashion because it directly uses the measured dielectric constant from the GPR. Figure 10-12 represents the dry unit weight value along the length of the survey section. The maximum dry unit weight for this material is about 137.3 (lb/ft^3). Therefore, the measured dry unit weight values are below the maximum dry unit weight values, which act as a limit in the strip map. It is also noted that some the measurements are far below the maximum dry unit

weight. Figure 10-13 gives the volumetric water contents that are calculated directly from the predicted matric suction. Figure 10-14 shows the gravimetric water content, and it changes along the survey section. The change in the gravimetric water content affects the values in the dry unit weight. Each of the calculations was performed at one foot intervals in the 23,760 feet total survey suction.

The significance of the presented data is to assess the important information regarding the pavement layer properties. These figures present the essential supplementary information that can be used in pavement quality management. For instance, the change in the dry unit weight is easily identified by using the Figure 10-12. The poorly compacted locations can be observed from the figure. A detailed dry unit weight representation of the selected pavement spots are highlighted in Figure 10-15.

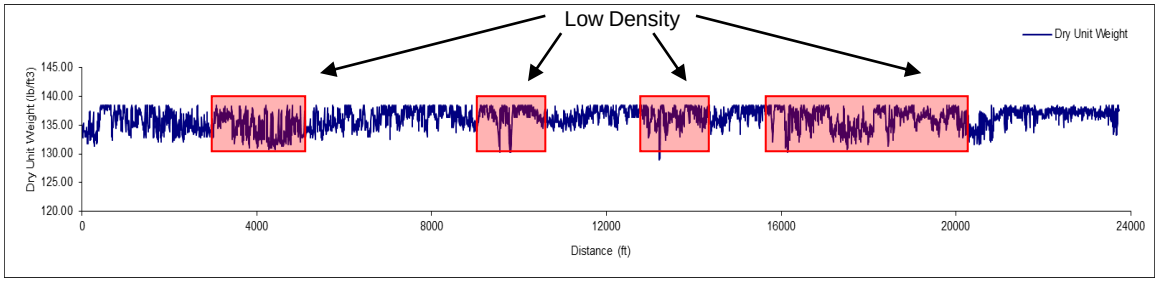

Figure 10-15 Highlighting the Poorly Compacted Spots

Figure 10-15 shows small locations where the dry unit weight is significantly lower than maximum dry unit weight. The quality control protocols defines the minimum acceptable limit for the dry unit weight. Therefore, if a spot or area is poorly compacted and needs re-compaction, it can be determined and raised to an acceptable

compaction limit before covering it with HMA. By this means, the future problem is defined quickly and eliminated before occurs while the construction is under way.

This section shows that there is a possible method to determine suction, gravimetric and volumetric water content, and dry unit weight by using the dielectric constant and the methylene blue value. Therefore, the significance of these six figures is for the first essential base course characteristics are presented, which are calculated by using the developed methods.

The knowledge of pavement layer thickness and properties is important because layer thickness data is fed into pavement management network to improve the pavement performance and rehabilitation priorities. Furthermore, in a construction phase, accurate layer thickness can be used precisely to determine the asphalt concrete layer design (Fernando and Maser, 1992). The most importantly, the knowledge of accurate GPR data is incorporated with the Dynaflect and FWD test results in predicting the modulus of a layer thickness. Next section will discuss surveying, data analysis, and the principle of the FWD test, which is associated with the case study.

10.4 Falling Weight Deflectometer

10.4.1 General

A falling weight deflectomer (FWD) is non-destructive test (NDT) equipment designed to simulate the deflection of a pavement surface due to a passing traffic load. Figure 10-16 shows a typical FWD unit. The FWD is a widely accepted non-intrusive test device to evaluate pavement characteristics. Furthermore, the significance of the FWD is

that is both rapid and repeatable in obtaining pavement layer moduli in the in-situ conditions. The estimated moduli are used in pavement management networks to choose

Figure 10-16 A Typical Falling Weight Deflectomer Unit

the best pavement maintenance and rehabilitation strategies.

The FWD unit applies dynamic load on the pavement surface layer through dropping a load mass from a specific height. The applied loads simulate the duration and magnitude of a single wheel vehicle load. A transient impulse load is transmitted to pavement surface by a 300 mm diameter plate, and the pavement responses are measured by a series of geophone sensors. The deflection on the surface measurement by using a series of geophones is shown in Figure 10-17.

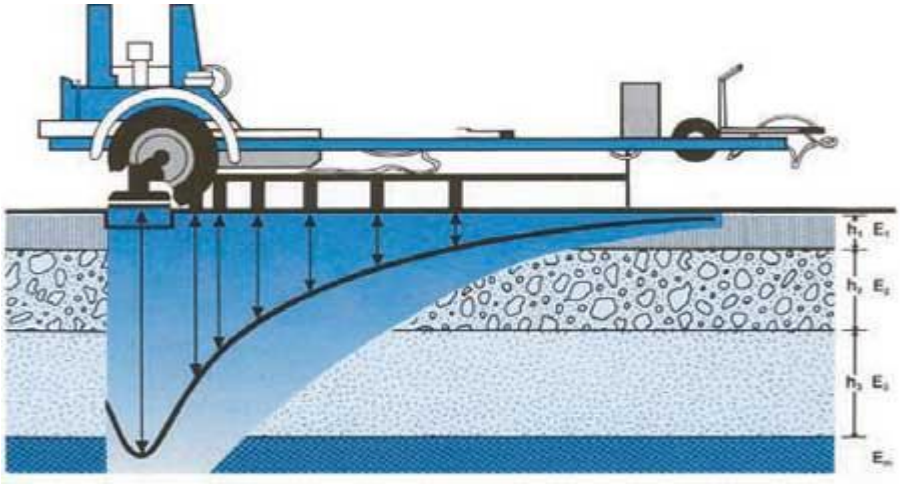

Figure 10-17 FWD Applying Load and Deflection Measurement (Cornell, 2014)

The shape of measured deformation profile is envisioned as a deflected basin from the side view. The deformations under the different geophones are collected by FWD equipment, and this test is completed in less than 2 minutes. This collected data is analyzed to determine the moduli of the pavement layers by using different theoretical constitutive models. The backcalculation routines assume a different modulus value for each layer and then a specific algorithm predicts the deflection. When the predicted deflection matches well with the measured deflection, this corresponding moduli are defined as the moduli of the pavement layers (Puppala, 2008).

This unit is a fast-moving trailer, which usually is pulled by another vehicle. This equipment applies dynamic loads. Before conducting a FWD in-situ testing, the vehicle must be at a full stop and traffic must be controlled. A series of seven geophones spaced away from the load plate at 12 in. increments measure the surface deflection, generating

a “deflection bowl”. The load plate should lay on a flat surface; the load plate and all geophones should lie on the same side of any visible cracks. Temperature data collected at the time of testing is necessary for all flexible pavements since the modulus of bituminous materials are temperature dependent. The raw deflection file, pavement layer thicknesses, layer Poisson ratios, probable layer moduli ranges, and asphalt temperatures at the time of testing are all required inputs to perform the backcalculation.

10.4.2 Mechanics of Deflection Prediction

Modulus of each pavement layer is predicted by using a complex iterative backcalculation method. Therefore, the backcalculation is usually conducted by computer software programs. The method that used in the iteration process is to backcalculate the elastic properties of the pavement layers and subgrade soils (Von Quintus 2002).

A deflection versus time history of a FWD measurement from the geophones is shown in Figure 10-18. The load time history curve describes the induced deflection by the applied dynamic load with respect to time. The dynamic load travels from the center of the applied load in a radial direction and is attenuated as it travels outward. The highest magnitude of deflection is the peak at the center of the loading plate, and the level of deflection decreases with radial distance. The deflection curve is defined by using more than 300 point, and only the peak point is utilized in backcalculation in the elastic program, MODULUS®.

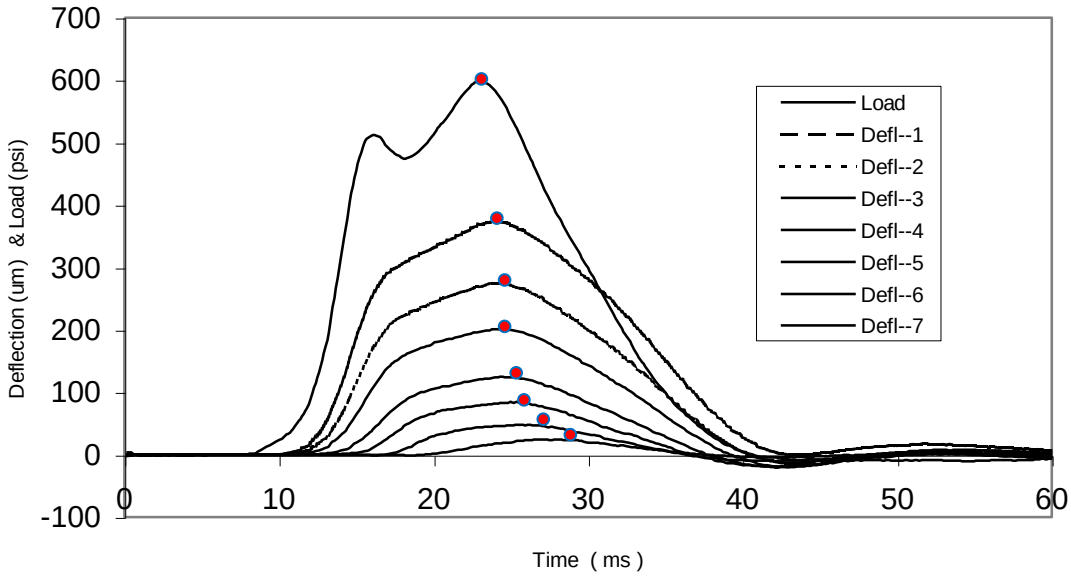

Figure 10-18 A Typical FWD the Deflection History versus Time

Uzan (1989) extensively describes the general procedure for back calculating the pavement layer moduli based on the FWD data and a summary of this study is presented below.

The ultimate purpose is to fit the pavement material properties to the measured deflection data. The perfect fit between measured and predicted data will be achieved by reducing the errors to a minimum. An objective function used to minimize the errors is expressed in Equation (10-9):

$$\in^2 = \sum_{i=1}^{s}\left[\sum_{j=1}^{d}\left(\frac{w_{ij}^m - w_{ij}^c}{w_{ij}^m}\right)\right]^2 we_i \qquad (10\text{-}5)$$

where $\in^2$ is the squared error, w^m is the measured deflection, w^c is the computed deflection, i is the sensor number sequence, j is the test number sequence, we_i is a weighting factor of sensor i.

The simple form of the error expression is given in Equation (10-6):

$$\in^2 = \sum_{i=1}^{s} \left[1 - \frac{w_i^c}{\overline{w}_i^m} \right]^2 we_i \tag{10-6}$$

where $\overline{w}_i^m$ is the average measured deflection at sensor i.

Different techniques are also available to use for defining the error function but the software program uses the Hooke-Jeeves algorithm, which is also a known local minimum (Letto, 1968).

The Modulus program is specialized to perform the computation based on the linear-elastic analyses. The calculated deflection at the radial distance i is expressed in Equation (10-11):

$$w_i^c = f_i\left(E_k, v_k, h_k, r_i, O\right) \tag{10-7}$$

where E_k, v_k are the modulus of elasticity and Poisson's ratio of layer k, h_k is the thickness of layer k, and O is other variables such as pressure, contact area radius, interference condition, etc.

All of the parameters in the backcalculation except E_k is either a predicted or is a known variable. The computed surface deflection under the condition of being a circular contact and using linear elasticity can be expressed in Equation (10-12):

$$w_i^c = \frac{pa}{E_{sg}} f_i\left(\frac{E_1}{E_{sg}},...,\frac{E_k}{E_{sg}},....,\frac{E_n}{E_{sg}}\right) \quad (10\text{-}8)$$

where p is the pressure, a is the radius of the contact area, and E_{sg} is the subgrade modulus of elasticity.

The modulus E_{sg} is inversely proportional to deflection and also a modular ratio function, for which the database is required for comparison with each measured deflection bowl. The properties of the linear elastic solution are used to process a database, which are modulus ratio to modulus values. This database generating and pattern search algorithm with the interpolation scheme are computed by the MODULUS® computer program. The Modulus is a microcomputer program that is designed to compute the layer modulus by performing a backcalculation. The detail explanation is given following section.

10.4.3 Modulus Program

MODULUS® is a computer software program developed by Texas Transportation Institute (TTI) to backcalculate the FWD deflection data. This program is capable of computing in extreme cases a four-layer system of unknowns in several seconds. The required Modulus program inputs are surface deflection, structural layer thickness, material Poisson's ratio for each layer, and the range of moduli, including minimum and

maximum moduli values for each layer. The subgrade layer (lowest layer) modulus can be calculated accurately using the deflection that is farthest form the load. Apart from these major inputs, the temperature at the time of field testing must be considered for any asphalt concrete layer.

The FWD data are processed with the Modulus analysis program, which uses the TxDOT backcalculation software. There is a sequential data combination process between the Pavecheck results and the Modulus inputs. For instance, in order to perform Modulus analysis at a given location, the layer thickness of the selected location must be determined. These thickness are typically determined form the PaveCheck program based on the radar data.

Pavement layer thickness data are given in a previous section. The recorded air temperature is 79^{o} F and pavement temperature is 98^{o} F. The Poisson's ratio for AC concrete is 0.38; base course is 0.33, and subbase is 0.35. The Modulus program is designed to be very user friendly, the major inputs of layer characteristics are asked in the first window screen, such as layer thicknesses, layer materials, Poisson's ratios and minimum and maximum modulus range for each layer. When the program is executed to run the iteration process, the outcome data will be displayed in several seconds. The FWD data results analyzed by using the Modulus program are presented in Figure 10-19 and Figure 10-20.

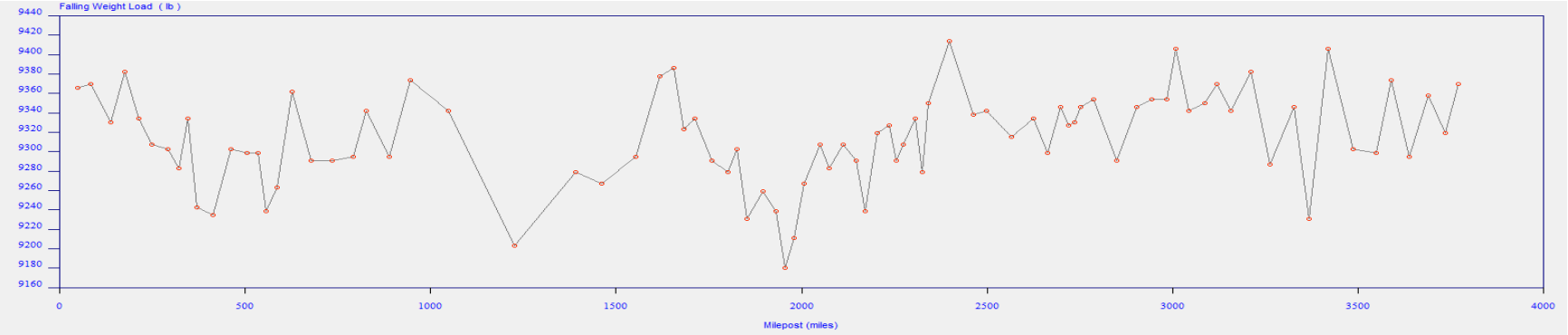

(a)

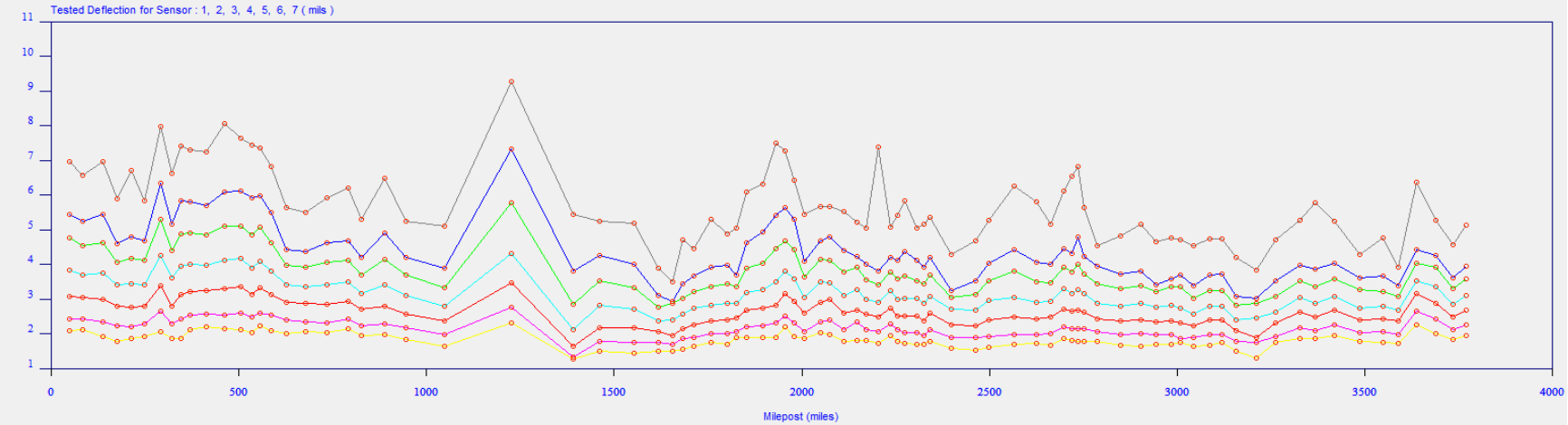

(b)

Figure 10-19 FWD Data by Applied Load (a) and Measured Deflection for Each Geophone (b) at the Stations

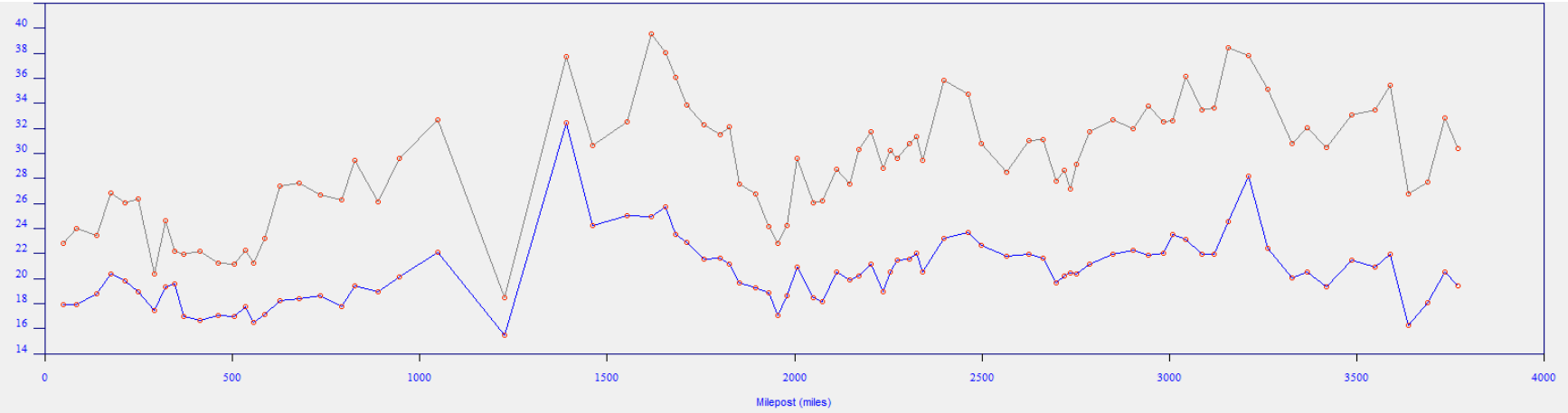

(a)

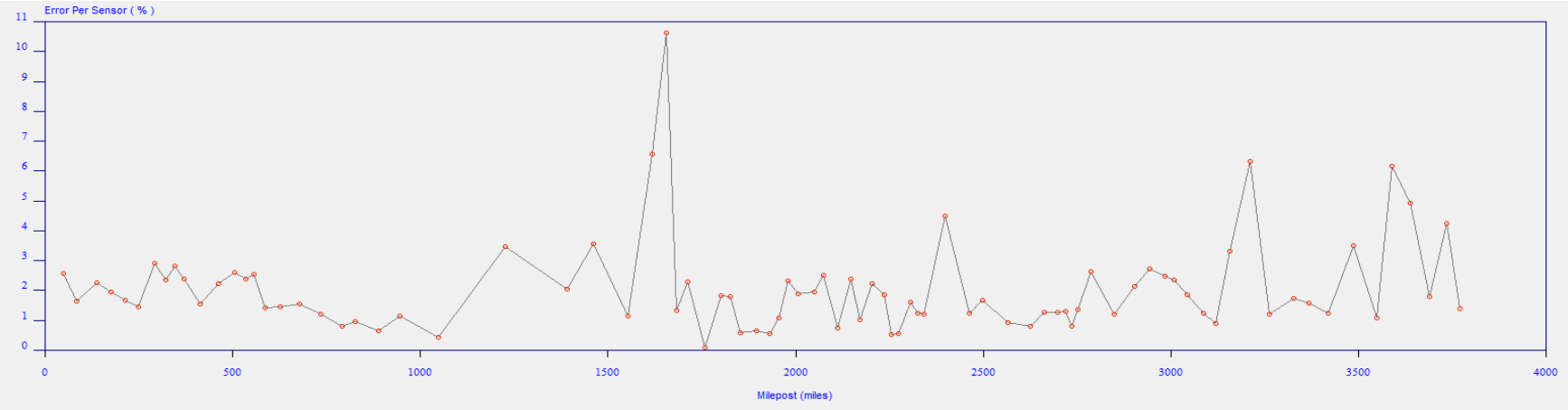

(b)

Figure 10-20 FWD Data by Applied Load (a) and Measured Deflection for Each Geophone (b) at the Stations

Figure 10-19 (a) shows the load in pound units applied by the FWD to the pavement surface at each station, and (b) presents the response of the pavement deformation measured by the geophones. There are seven geophones that measures the deflection and are placed 12 inches apart, and the highest deformation is the closest to the load center. Figure 10-20 (a) shows the iterated backcalculated modulus for each station in ksi units and (b) illustrates the error, which occurs in the iteration process in percent at each station.

10.4.4 Data Analysis

This section gives mechanics that are used to predict the resilient modulus of the base course layers. The methods and approaches used in this section are continuation of the previous chapters. For instance, the unbound base course aggregate layer modulus is calculated by using the proposed approach in Chapter 3. This approach was incorporated with the radar and material characteristics results.

The equation for the resilient modulus is given in Equation (10-9):

$$E_y = k_1 P_a \left(\frac{I_1 - 3\theta f h_m}{P_a}\right)^{k_2} \left(\frac{\tau_{oct}}{P_a}\right)^{k_3} \tag{10-9}$$

where I_1 is the first invariant of the stress tensor, P_a gives the atmospheric pressure, θ is the volumetric water content, h_m represents the matric suction in the aggregate matrix, f is the saturation factor $\left(1 \le f \le \frac{1}{\theta}\right)$, τ_{oct} yields the octahedral shear stress, and where k_1 , k_2 and k_3 are material parameters that are dependent on material properties of the base course.

The parameters k_1 , k_2, and k_3 are functions of shape and scale parameters calculated based on the AIMS test analysis. In addition, these parameters also require the dry unit weight, *pfc*, and MBV, which are explained previous sections. The predicted k_2 and k_3 values are given as 0.709 and -0.254, respectively. The value of k_1 depends on dry unit weight and hence k_1 will vary along the section, which is calculated along the survey section for every foot.

The assumed value of the atmospheric pressure (P_a) is 101.325 kPa. The defined value of the saturation factor (f) at an 80 percent degree of saturation is 1.0. The value of the matric suction in the base course aggregate layer is determined based on the radar analysis outcomes, which is also given in the previous section in detail.

Boussinesq (1883) theory predicts the stress produced at any point below the surface in a half space medium as the result of a single point load. The vertical stresses are radial and circumferential at a depth and horizontal distance away from the center of load applied (Craig 2004). The Boussinesq theory was applied to obtain the value of first invariant of the stress tensor, and octahedral shear stress. The component of the stress tensors are calculated in Equation (10-10) to Equation (10-12):

$$\sigma_r = \sigma_\theta = \sigma_z = -\frac{P}{2\pi(1-\upsilon)z^2}(1-2\upsilon) \tag{10-10}$$

$$I_1 = \sigma_r + \sigma_\theta + \sigma_z \tag{10-11}$$

$$\tau_{oct} = \frac{1}{3}\sqrt{2(\sigma_r - \sigma_z)^2} \tag{10-12}$$

where σ_r is the radial stress, σ_θ is the circumferential stress, σ_z is the vertical stress, z presents the half depth of the base layer, υ is Poisson ratio, P is point load, I_1 yields the first invariant of the stress tensor, and τ_{oct} gives the octahedral shear stress.

This approach enables one to obtain the stress tensors based on the GPR analysis. The depth of base course layer is predicted and is shown in a previous section. It varies along the selected survey section, and hence these tensor invariants are calculated at each foot throughout the section. Both the calculated and measured resilient modulus strip maps are given in Figure 10-21. The effect of the suction on the base course layer modulus is presented in Figure 10-22. The data validation of predicted and measured resilient modulus are presented in Figure 10-23.

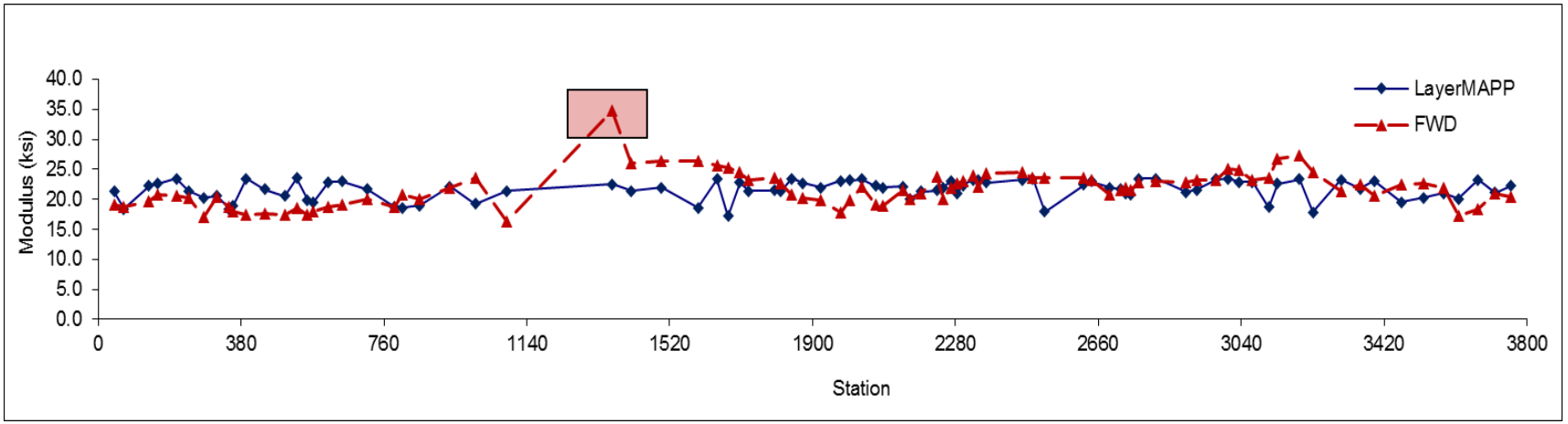

Figure 10-21 Comparison of the Unbound Aggregate Layer Resilient Modulus Strip Map

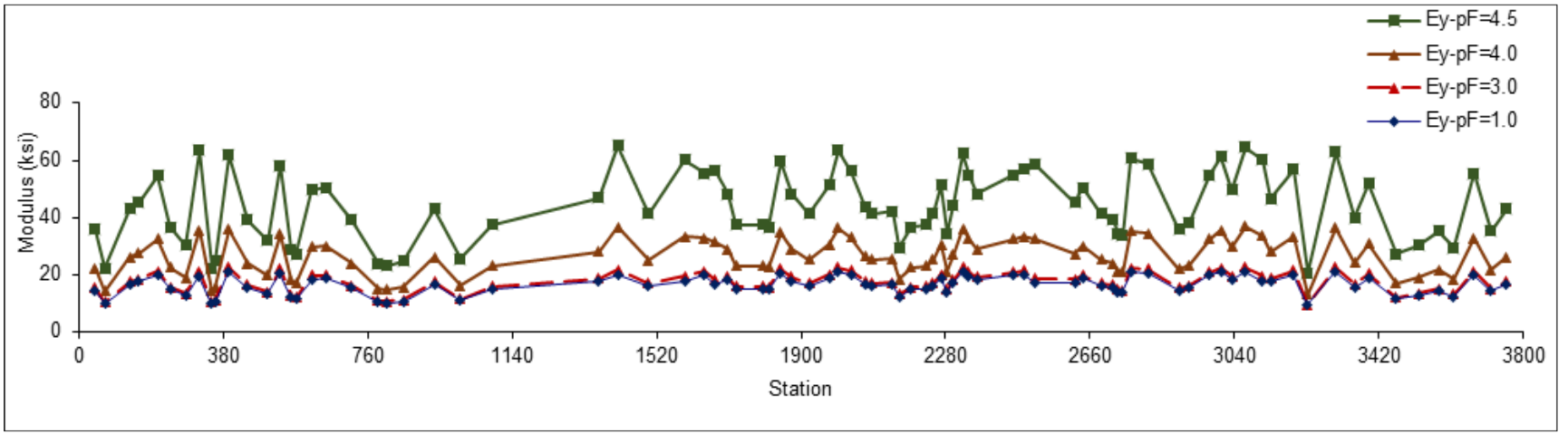

Figure 10-22 Comparison of the Unbound Aggregate Layer Resilient Modulus Strip Map

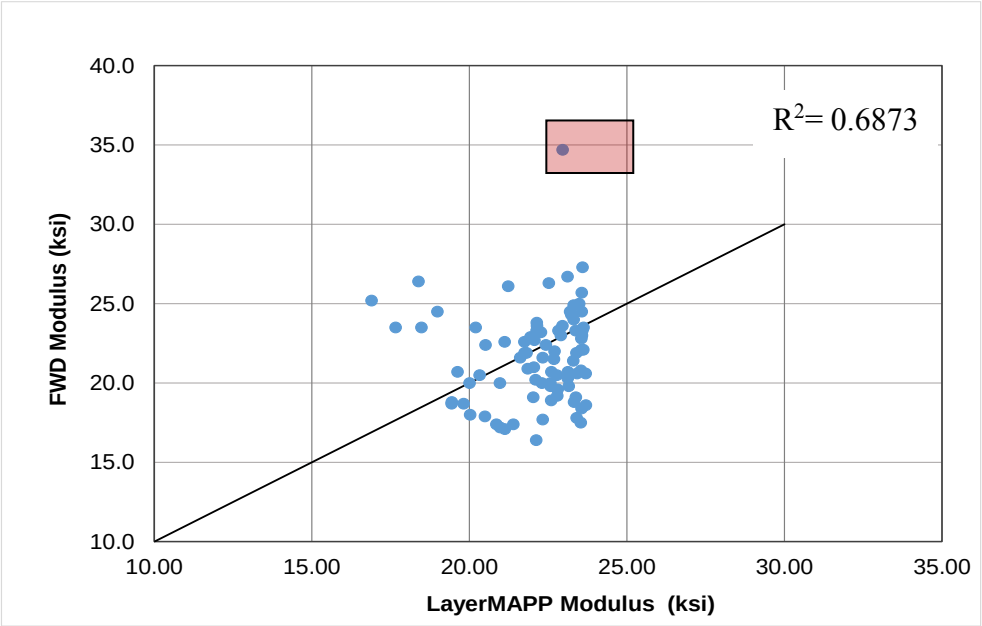

Figure 10-23 Comparison of the Unbound Aggregate Layer Resilient Modulus Strip Map

Figure 10-23 shows the produced color map of the resilient modulus in the survey section. The measured modulus data are calculated based on the back calculation method from the FWD, and the predicted moduli are determined for the base course layer using the GPR data using the program LayerMAPP. This color map clearly demonstrates the fluctuation/variation in the as-built resilient modulus. This approach allows the design modulus to compare with the constructed layer modulus. In addition, it is also possible to predict the modulus along the length of the construction section.

The objective of the following study is to investigate the effect of the suction on the resilient modulus. The findings are presented in Figure 10-22. The matric suction was allowed to vary in this study. Having the values of pF=1.0, pF=3.0, pF=4.0 and

pF=4.5 in order to determine the effect of suction at each location. On this basis, a new modulus was calculated at each of the four selected suction levels. The results show that the suction value has a significant contribution to the modulus. This demonstrates that an increase in the suction impacts the modulus and causes an increase in the calculated modulus as well.

Figure 10-23 shows a comparison between calculated FWD and the moduli predicted by Layer MAPP. It is noted that there is good agreement between the calculated and the predicted data. There is only one higher outlier point coming from the FWD modulus. At the same point the modulus is calculated lower by the LayerMAPP. It may have an unknown stiff object that was embedded underground before the FWD measurement was taken, that causes the false reading.

A new developed LayerMAPP software program was used to predict the layer modulus. The next section of this chapter introduces the LayerMAPP software program.

10.5 Closure

This part of the study covered a case study by using the ground penetrating radar and falling weight deflectomer. Both nondestructive test methods were explained to provide background information about the data collection as well as the data analysis procedures. Additionally, the pavement layer properties were determined by using a new developed method. The analysis results compared both the GPR and FWD results.

A case study, which was conducted to validate the developed model, was used to determine the characteristics of a pavement system. A field test using the GPR and FWD was conducted on a selected road section located in Delta County in Texas.

The first part of this study, the GPR system provided the dielectric constant value automatically for the asphalt, base, and subbase layers along with the layer thickness. These data were evaluated by using the PaveCheck software program. A new software program LayerMAPP was also used to determine pavement characteristics for the same data. The PaveCheck analysis result of base course dielectric constant values were utilized as input to the LayerMAPP program. It computed the base course layer matric suctions, the volumetric and the gravimetric water contents, and the dry unit weights for the entire test section.

The developed technological approach can be used in either a construction quality control or a quality management process. Currently, nuclear density gauges (NDG) have been used to determine the dry density of the pavement layers as final compaction device. The LayerMAPP program can be also used as a final compaction control method to determine the dry unit weight by using only the dielectric constant and the MBV values. The limitation with the NDG is that there are strict rules regarding with the certification and transportation of nuclear gauges. In addition to these concerns with the NDG, it has been known that the accuracy of the readings by NDG may be offset when the base course aggregate materials contain fly ash, coal, clays, gypsum, lime, phosphates, and organic materials, which contain neutron or bound hydrogen. For example, a layer with the gypsum, which includes water molecules in its crystalline

structure, that causes a false high moisture content NDG reading and hence a false low dry density NDG reading. However, there is no such limitation associated with either the GPR or dielectric constant. The accuracy of the dielectric reading on different materials is well proven.

In the second part of this study, the resilient modulus of the base layer was predicted by using the LayerMAPP program. The data computed in the first part is also used to predict the modulus along with the index properties: shape, texture, angularity and gradation indexes. The FWD field test data is also analyzed by using the MODULUS software program. These two test results are compared along the length of the test section. It was demonstrated that these two data are in good agreement on the modulus in most parts of the test selection.

It is also demonstrated that the effect of the suction on modulus is significant because a change in the suction has a large and direct impact on the modulus. Therefore, the suction value is an indispensable parameter for the performance prediction of the unbound base course.

It is also noted that resilient modulus of the base layer fluctuates and the dry unit weight fluctuates along the survey section. However, the resilient modulus does not change in proportion to the dry unit weight change. In existing applications, the dry unit weight is used as basis for quality control. However, as is presented here, the resilient modulus is influenced by the dry unit weight but is controlled by the suction.

The use of the thickness information is obvious to use for either quality control of new construction or structural evaluation of existing structures. Inaccuracy of the

layer thickness may cause a large error at the final result of the backcalculated layer modulus. The layer thickness is a significant parameter and hence the accuracy of the thickness is a major concern because the layer thickness is usually not constant throughout the project. Therefore, it is important to perform a GPR survey to obtained layer thickness along the length of the project section. The obtained layer thicknesses are used as inputs in the LayerMAPP analysis system to compute the resilient modulus for not only a single point but also along the entire project.

It must be emphasized that the LayerMAPP program can process the collected GPR data and display the pavement layer characteristics for any field project. The LayerMAPP is capable of conducting all of the layer property in real time. Furthermore, the LayerMAPP program approach enables one to display the results as a strip map (a color map) to present the results graphically, digitally, and clearly. The predicted modulus displayed on a color map provides one more advantage for quality control because it shows the as-built modulus. The color map clearly presents the higher and lower modulus subsections. The color map generated not only the resilient modulus but also the soil suction, the gravimetric and the volumetric water content, and the dry unit weight of the base course.

11. DEVELOPMENT A NEW PERFORMANCE PREDICTION SOFTWARE PROGRAM

11.1 Introduction

LayerMAPP is a software program for Measurement and Analysis of Pavement Performance (MAPP). LayerMAPP program is a quality control (QC) and quality assurance (QA) supporting layer analysis tool used to estimate pavement performance characteristics. It is capable of estimating the clay content, Atterberg limits, diffusion, matric suction, compaction curve along with maximum dry density and the optimum moisture content, the permanent deformation, and the resilient behavior of the base course layer of unbound aggregates and vertisol soils by using Methylene blue test, the AIMS test and the Percometer.

A review of the properties that are necessary to measure in the field showed that the moisture content, soil suction, and percent fines content are significant properties and they must be determined by using the MBV relationship. Rapid and accurate field QC/QA methods were developed and described in the previous chapters. A new software program was developed to show the connection between all the proposed models. This chapter is organized to introduce this software and to provide a user manual for it.

11.2 Mechanics of LayerMAPP

In the field, these measurements can be performed and evaluated by using a software program. A software program, which was written and programmed to be used as a base course design tool. This will increase the speed of the test process and reduce the

analysis time of the outcomes in the field and laboratory as well. A schematic presentation of the software is outlined in Figure 11-1.

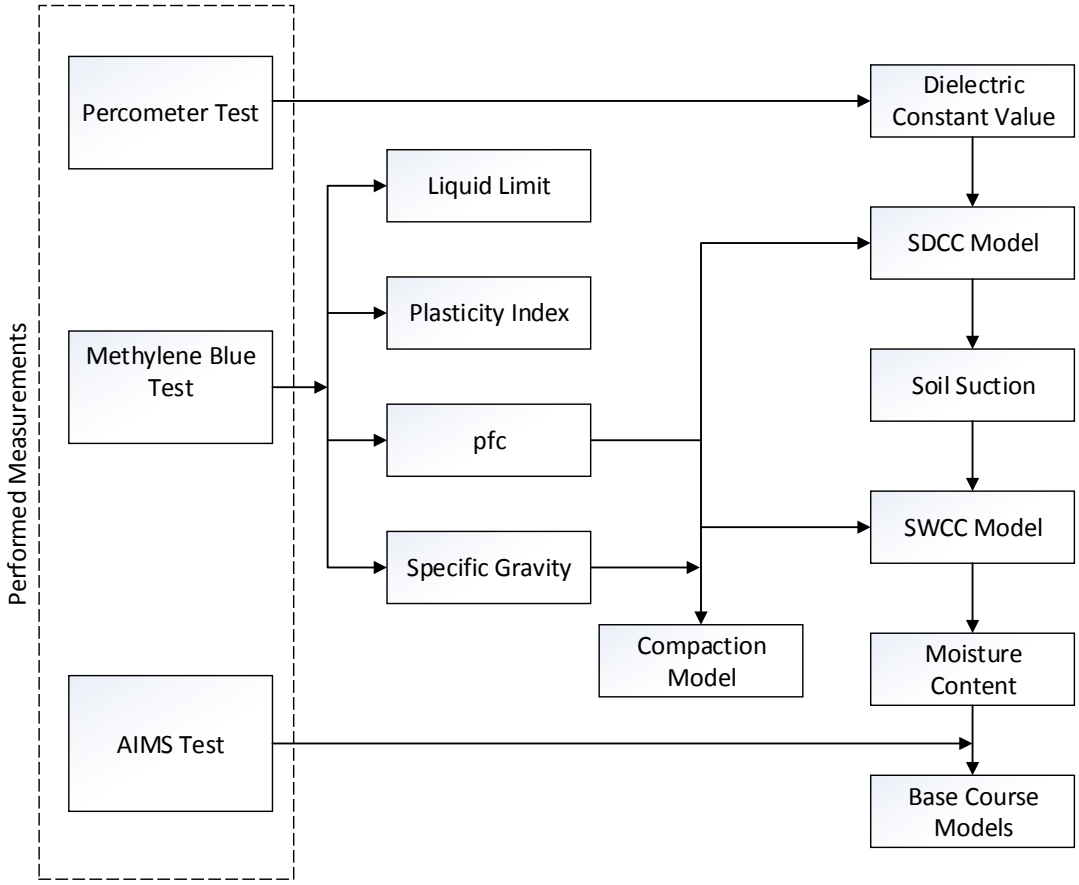

Figure 11-1 A Data Flow Chart with the Models Demonstrates the Steps Determining the Base Course Layer Properties

Figure 11-1 illustrates the entire measurement flow chart from the beginning to the final result. This whole measurement process begins with the methylene blue test, and involves a percometer reading and the last phase the AIMS analysis results are taken into account to determine the base course performance characteristics.

This software will be a very useful tool to calculate the base course modulus and it will determine the performance of the base course materials in as-built condition. Since the field measurements are simple and quick enough to provide outcomes immediately with this method, this new software will promptly calculate the performance characteristics of the base materials at any desired location/spot. A user manual of the LayerMAPP program is given in the following section.

11.3 LayerMAPP User Manual

The LayerMAPP software is a user friendly program and in the following and it is explained how to input the measured data and execute the analyses.

The LayerMAPP analysis process begins with the methylene blue test. The first part is given under the MBT tab. In this tab, select the material source that is tested by using the methylene blue (MB) device. Next, enter the measured MBV. After that, click on the analysis button to calculate the percent fines content for the measured MBV. This is shown in Figure 11-2.

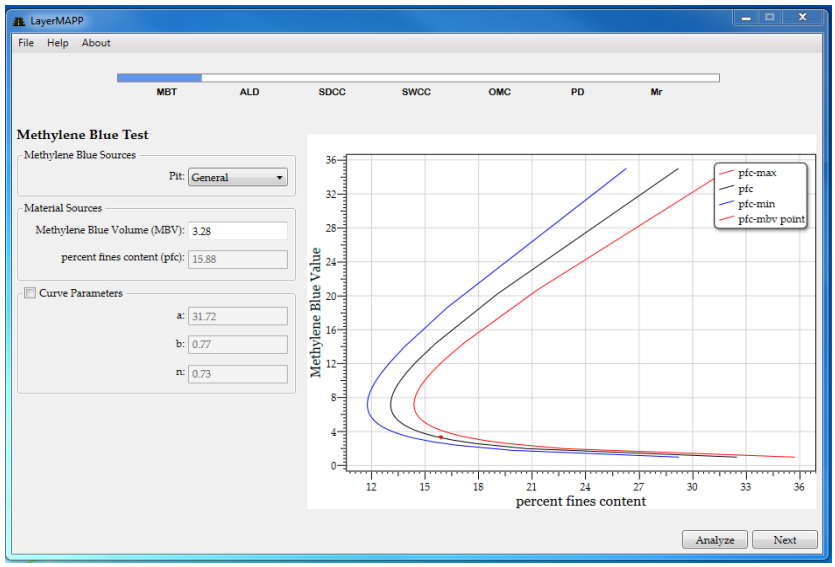

Figure 11-2 MBV and *pfc* Correlation Curve Display Screen

Figure 11-2 shows an estimated C-shaped curve along with 90 percent confidence limit curves as well. The three fitting parameter a_m, b_m, and n_m are also displayed, which can be changed by entering another set of three fitting parameters. This option makes it possible to include a new material by clicking on the small box in the fitting parameter part, and type the calculated values for the new material. This alternative to enter the three parameters is provided because the software is designed for the materials located in Texas, and it may not cover all types of base course pits in the software database. Click on the next button to continue.

The next window computes the Atterberg Limits and Diffusivity, which are shown under the ALD tab. In this window, there are no input values required because all of the needed inputs are calculated previously in the MBT tab window. The calculated correlation between the diffusivity and percent fines content is shown in Figure 11-3.

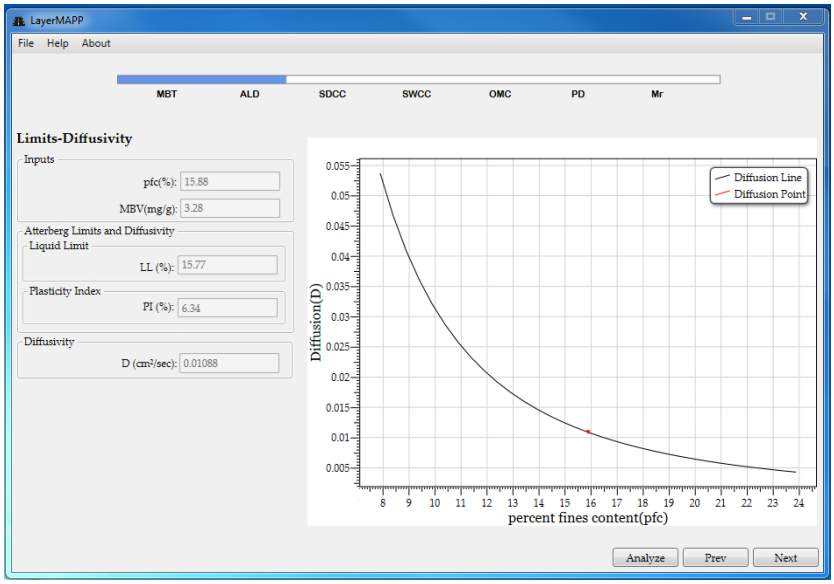

Figure 11-3 MBV and *pfc* Correlation Curve Display Screen

The calculated diffusivity is based on the calculated percent fines content and is displayed in Figure 11-3. In addition to diffusivity values, Atterberg limits, liquid limit and plasticity index, are also determined and shown under the Atterberg limits part. Click on the next button to continue.

The next window calculates the suction dielectric characteristics curve (*SDCC*). This window is denoted as the *SDCC* tab. The *SDCC* generation process requires a Percometer measurement. Once the dielectric constant is assessed, it is ready to execute the analysis because all of the other input values are estimated by LayerMAPP. Next, press the analysis button to generate an *SDCC* plot, which is shown in Figure 11-4.

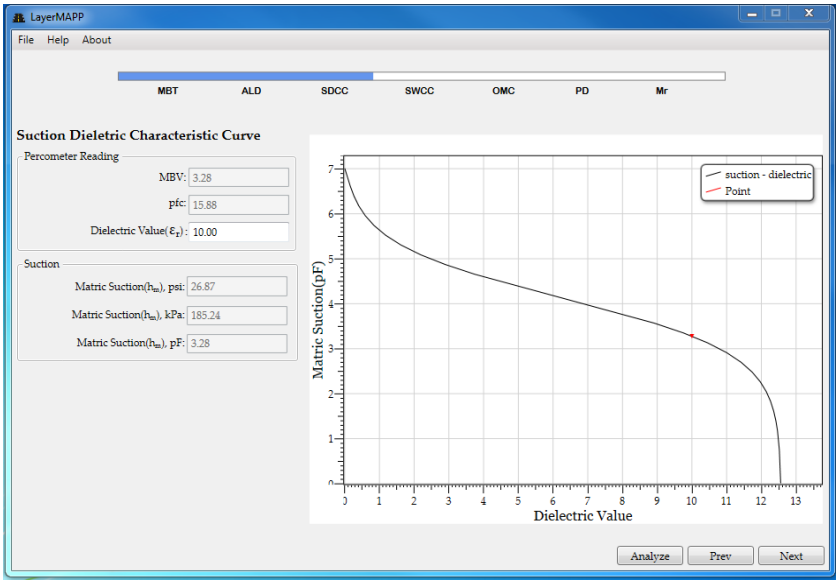

Figure 11-4 A Generated *SDCC* Plot Display Screen

Based on the previous MBV and *pfc* results an *SDCC* curve is plotted. Figure 11-4 shows the full range of the dielectric curve for all suction values. The measured dielectric value is shown with the red-color point where the *SDCC* curve reflects the calculated suction value. Furthermore, in order to avoid unit conversion, the determined suction value is shown in kPa and psi units rather than in pF units.

The suction water characteristics curve is located under the *SWCC* tab button window. There is no additional information asked in the *SWCC* window because all of the needed information are collected in the previous tabs. Press the analysis button to perform the calculations. LayerMAPP generates the entire *SWCC* plot, which is shown in Figure 11-5.

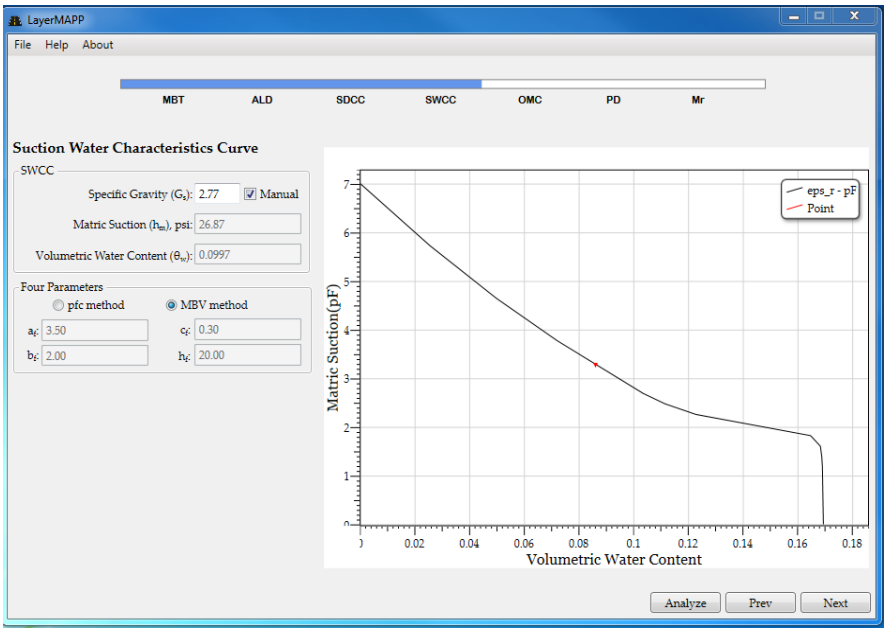

Figure 11-5 A Generated SWCC Plot Display Screen

Figure 11-5 shows the *SWCC* constructed with the MBV but it is possible to predict the *SWCC* based on the *pfc*, as well. This selection depends on the material. For instance, if the material is highly active with an MBV greater than 7.0 mg/g, then the *pfc* gives more accurate results; however if the material has less active minerals MBV gives more accurate results. There is no additional input or measurement required in this part other than specific gravity. Therefore, an essential feature is incorporated into the LayerMAPP to assess the specific gravity of the soil. If specific gravity is known beforehand it can be used for the calculation. If it is not known, then the LayerMAPP can calculate it. There is a box next to the specific gravity window called manual, which means that the value will be entered by the user. If the box has a check mark in it, the user will enter the value. Lastly, a calculated suction and corresponding volumetric

water content based on the previously measured dielectric constant value is also displayed in red-color point on *SWCC* curve.

In the next tab, the maximum dry unit weight and optimum moisture content curve is determined under the *OMC* tab window. There is no additional value required to input. This window shows the dry unit weight versus gravimetric water content curve. An advantage of the LayerMAPP is that it provides the entire range compaction curve instead of showing a single point. This feature enables one to see the change in dry unit weight with respect to change in moisture content. In addition, the zero air voids curve, which shows the saturated state of the aggregate base course without air voids, is also plotted against the dry unit weight by using the CCM. The calculated compaction and zero air void curves are presented in Figure 11-6.

The gravimetric water content is also calculated based on the previously measured dielectric constant and suction value in the *SDCC* tab. The corresponding gravimetric water content shows the amount of gravimetric water content present in the base course mixture.

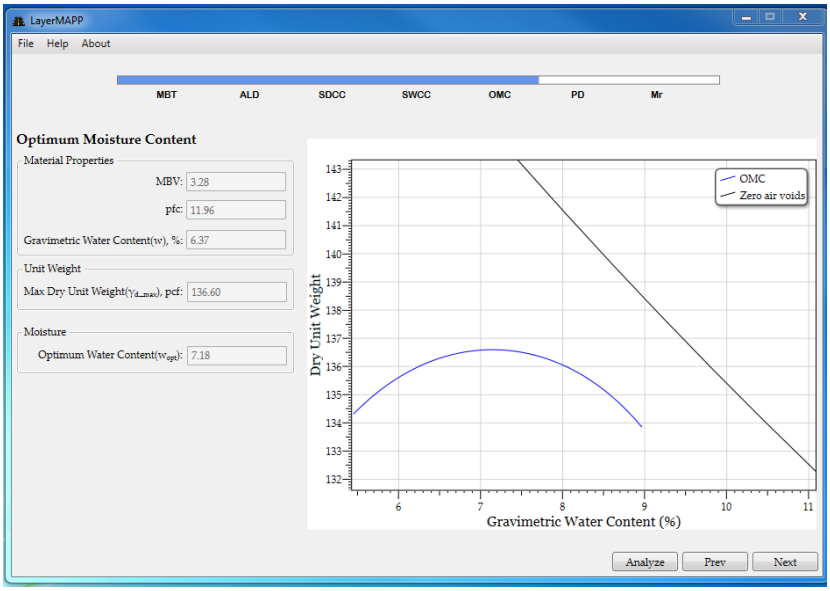

Figure 11-6 A Calculated Compaction Curve and Zero Air Voids Curves Display Screen

The PD tab represents the permanent deformation (PD) calculation. This section shows the PD prediction based on two approaches VESYS and Tseng-Lytton. In this section, the aggregate shape, texture and angularity index parameters are needed as input based on the AIMS analysis. Other than these index properties, all of the required parameters in this step are determined in previous steps.

The PD calculation is performed and displayed for both the VESYS and Tseng-Lytton method by choosing the box at the PD model part. The LayerMAPP program gives the PD up to 10000 load repetitions. A calculated permanent strain curve is shown in Figure 11-7.

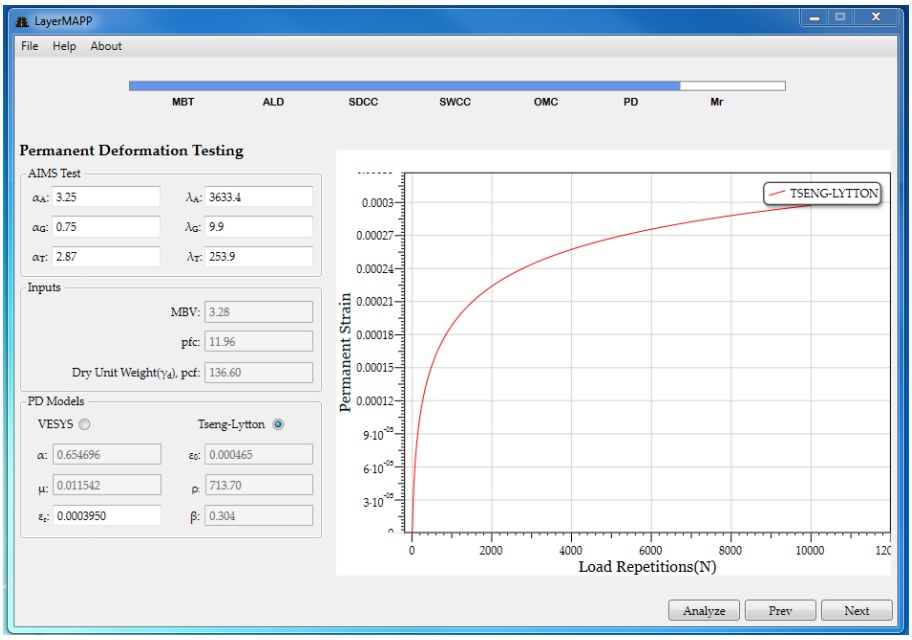

Figure 11-7 A Calculated PD Curve Display Screen

The next section gives the resilient modulus (Mr) of an unbound aggregate layer and shown under the Mr tab. This section only requires inputs that are already determined cumulatively in previous windows. Thus, in this window, only two input values are required regarding the material properties and loading cycles. One needed input is λs, the shape scale index from AIMS analysis, and the second one is f, the saturation factor.

In the parameters part, the σ_1 vertical stress and σ_3 confining pressures are two principal stresses that must be estimated because they are used to calculate the resilient modulus at three desired load levels. The τ_{oct} octahedral shear stress and I_1 first stress invariant are determined based on the stresses σ_1 and σ_3 at each of the three load levels.

The last material properties to be calculated, and the resilient modulus is calculated at the three loading levels (desired loading stress) and is based on the input material properties is shown in Figure 11-8.

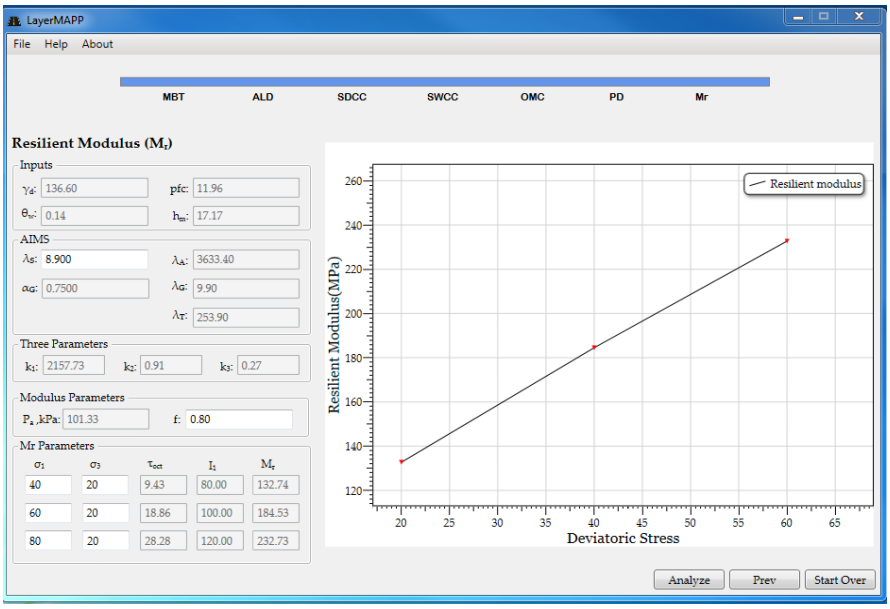

Figure 11-8 Resilient Modulus Changing with Respect to Deviatoric Stress Curve Display Screen

Figure 11-8 shows that the three parameters k_1, k_2, and k_3 are calculated based on the previous input along with the scale and shape index parameters. These parameters cannot be input or changed by the user. The atmospheric pressure Pa is also given in kPa units.

Resilient modulus results are presented with the change in the deviatoric stress at each loading level. Three resilient modulus points in MPa units are plotted against the deviatoric stress in kPa units.

11.4 Closure

A new software program called LayerMAPP is developed during this study with the aim of providing a feasible method of using the products of this research for quality control and quality assurance purposes. The LayerMAPP program uses the material properties to calculate the desired outcomes for quality control management. The outcomes are determined in real time at a construction site and hence this is a simple and easy method that can be used in all types of field investigations. The mechanisms used in this program are based on well-defined and accepted material properties, such as the amount of fines content, liquid limit, plasticity index, specific gravity, optimum moisture content, and also the geometric characteristics indexes of aggregate shape, texture, and angularity.

This is user friendly software because most of the unknown parameters will be calculated by the software itself. Furthermore, it allows users to compare known available values as well. For instance, specific gravity can be calculated by the LayerMAPP program, and there is an option to input a measured Gs value.

The LayerMAPP program can be incorporated to use Ground Penetrating Radar to determine layer properties of a base course layer. In this version of the LayerMAPP program, the results of the GPR readings are needed to be input manually but an upcoming version of this process will be automatically executed by LayerMAPP.

12. SUMMARY

The study presented in this thesis uses the fundamental unbound base course aggregate materials properties. Unbound base course aggregate samples were collected from various pits throughout the Texas. The aggregate samples were subjected to an extensive laboratory testing program in project TxDOT 0-6621. The material properties are correlated to determine the important base course models that contribute significantly to predicted performance of the pavement. Knowing these as-built criteria in the construction phase of the base course are especially useful in quality control (QC) and quality assurance (QA). The following section summarizes the important base course models and significant unbound aggregate base course findings.

- The engineering characteristics of the unbound aggregates are strongly influenced by the presence of fine-grained soils especially including the clays, which can be highly expansive (shrink and swell) in nature. Therefore, it is of the utmost importance to determine the fraction of clay content in the unbound base course aggregate mixture.
- A stepwise multiple regression analysis has performed to determine the correlation between the k_1, k_2, and k_3 parameters in the resilient modulus model and the base course aggregate material properties. This analysis shows a good correlation and defines equations for the parameters k_1, k_2 and k_3 based on the aggregate properties.

- The VESYS and Tseng-Lytton models of permanent deformation were investigated and characterized using the material properties of the unbound aggregate material. The prediction models for the parameters α, μ, ε_0, ρ, and β in the VESY and Tseng-Lytton models were developed using multi regression analysis.
- The base course index properties of texture, angularity, and shape indices, which Weibull are the scale and shape parameters of a distribution, showed a good agreement with the resilient model parameters and in the permanent deformation parameters. Additionally, it is noted that the new defined MBV parameter and *pfc* concept are significant parameters in these prediction models.
- The improved methylene blue test is an effective way of determining the amount of clay percentage in an aggregate mixture. The traditional MBT has been improved significantly in terms of the time spent, the amount of sample used, and the method of presenting results in a graph.
- The Grace methylene blue test method has been improved through increasing the measurement range to give the ability of detecting non-clay and clay particles at the same time. The proposed graphical presentation allows plastic and non-plastic soils to be represented in the same C-shaped plot. The non-plastic material has an MBV lower than 7.00 mg/g while the plastic material has an MBV greater than 7.00 mg/g.
- These improvements enable the new methylene blue test not only to be a laboratory test but also to become a test for field investigations. The methylene

blue test and MBV is a promising method to be utilized in both the field and laboratory in the future. Furthermore, the improvements give a capability of determining a direct relationship between the MBV and percent fines content in an aggregate mixture.

- A totally new soil dielectric constant curve (*SDCC*) concept was proposed, which is one of the most significant outcomes of this study. The dielectric constant of nine pits was determined by using a percometer device. These measurements are combined with the suction measurements to determine an S-shape curve. The matric suction that was measured by the filter paper test for the base course material is superimposed on the *SDCC* curve to generate the curve over the full range of suction. This good agreement between soil suction and dielectric constant is explained with the soil suction dielectric constant curve (*SDCC*).
- The *SDCC* model consists of the two fitting parameters α and γ, which control the shape of the curve. These parameters were correlated to the percent fines content and methylene blue value to predict the *SDCC* for any type of pits. The fitting parameters are entirely dependent on the *pfc* and MBV of the unbound base course aggregate mixture.
- The *SDCC* method uses a totally non-destructive measurement technique to determine soil suction not only in the laboratory condition but also the in-situ condition as well.
- An experimental investigation was described using the filter paper test and methylene blue test in an efficient method to generate the soil water

characteristic curve (*SWCC*) for the unbound base course aggregate material. This approach determined the equations for the four important fitting parameters in the *SWCC*. The proposed new methodology enables one to calculate the fitting parameters using the relationships developed with the methylene blue value (MBV).

- The improved methylene blue test is an efficient and practical test method to determine the percent fines content, and the MBV. These results of the methylene blue test can assess reliable values of the four parameters of the *SWCC*.
- The MBT is a practical test method. The soil suction can be predicted at any level of volumetric water content by using a *SWCC*. The suction value is one of the key parameters to be used in the resilient modulus and permanent deformation models. The expected performance of the as-built base course can be predicted in the field based on these resilient and permanent deformation properties.
- One of the major challenges, working with aggregate materials at the construction site, is significant variability in the in-place compaction or density of the aggregate materials. Therefore, a compaction curve model was developed to predict the full range of the dry unit weight versus water content curve of the base course aggregate. This model is capable of predicting the maximum dry unit weight and optimum moisture content, as well.

- The developed compaction model can also predict the optimum moisture content. Using the optimum moisture content in the compaction curve produces the maximum possible dry unit weight.
- The mechanics behind the proposed compaction curve includes the three fitting parameters a_d, b_d, and n_d, which can be predicted simply. An investigation was conducted on the fitting parameters, and it was found that these parameters can be predicted by using the MBV, *pfc*, and Gs.
- The variability in the fines should be controlled and be consistently monitored with a convenient method in the projects requiring compaction. The methylene blue test is a suitable test method to monitor the variation of the fines in the base course aggregate. Quality management engineers can monitor the in-place as compacted aggregate materials by using the methylene blue value.
- The diffusion rate value of unbound base course aggregates was determined for each pit by using a laboratory experiment in a three month period. A correlation showed that there is a trend between the base course diffusion rate and the percent fines content and the methylene blue value. The results were divided into two groups with the MBV is greater than 7.00 mg/g and smaller than 7.00 mg/g. This correlation enables pavement engineers to determine the rate of which moisture from the subgrade diffuses into the base course.
- The Atterberg limits are one of the most widely used engineering index properties but there was no significant correlation to link them a simple and

rapid test method. This study found a substantial correlation between the Atterberg limits and the methylene blue test.

- The specific gravity of soil is also a very well-known parameter. It is used in many soil mechanics equations. It can be determined by using a standard laboratory test. There are some places, such as construction sites, that requires a quick and accurate estimate of the specific gravity. In order to meet this need, a simple correlation was developed to express the Gs. This equation is simple and depends only on the Atterberg limits as predicted by the methylene blue test.
- Ground Penetrating Radar (GPR) is a nondestructive measurement device that surveys the pavement layer thicknesses while driving at highway speeds. The potential use of the GPR technology is to estimate pavement layer thickness on a network wide basis. A case study was conducted and the results were analyzed. It was found that the GPR is capable of estimating the base course characteristics that are directly related to its subsequent performance. The GPR dielectric constant is used to estimate the important the following base course characteristics: matric suction, dry unit weight, volumetric water content, and gravimetric water content along with the layer thickness.
- The advances in the GPR data analysis using the dielectric constant value are widen the amount of knowledge about the pavement system characteristics during the construction phase in the field. Its uses enables pavement engineers to have a better understanding of the as-built pavement and to verify its compliance with the pavement as it was designed.

- Falling Weight Deflectometer (FWD) is a nondestructive test device to determine the modulus of pavement layers including the base and subgrade. The deflection profile of each of the geophones is determined and analyzed by using backcalculation. The resilient modulus of base course is also determined using the GPR-MBV method that was developed in this study. In this latter analysis process, the calculated moduli for each layer from the FWD measurements and the estimated moduli based on the proposed approach are compared. The comparison showed that the proposed model is considerably successful in estimating the base course modulus.
- The LayerMAPP program is a new software program, which was developed and integrated into this study. It can be used for the measurement of the aggregate performance prediction by using methylene blue test, AIMS test, and the percometer test. It is capable of predicting the base course performance by utilizing the fundamental material properties of the base course. A user friendly manual was included describing the input process and illustrating the calculated results.

13. CONCLUSION

The transportation sector has always played a central role in economic development and prosperity of a community. The parallel growth of the economy with advancements in transportation is historically evident from the evolvement of cities and commercial interests around ports and navigable rivers to interstate highways and large airports. Furthermore, inadequate and stagnant transportation access leads to a shift of businesses, jobs and people resulting in rapid decline of a region's economy, for most businesses rely heavily on primarily road and also rail, air, port access for movement of freight and employees. For dispersed industries like the agriculture industry for instance, the productivity and yield virtually halts without the aid of the various modes of travel.

While it is established firmly that the economy thrives with advancements in the transportation industry, the quality of life experienced by the public is also influenced directly by the sector due to its impact on the cultural and environmental resources. Through the improved mobility that good roads and public transit offers to citizens several employment opportunities have opened up for individuals to make a living. Consequently however, the increased use of roads calls for frequent maintenance and reconstruction due to the problems such as traffic congestion and overloading. The funding required to tackle these maintenance projects and obstacles is mainly billed to the public and invariably results in a backlog every year.

The net result of this study is a quick, accurate and simple process for determining reliable values of the in-place as compacted base course modulus and permanent deformation properties. In addition, the measurements that are made should

also contribute to the assurance of the quality of the process of taking the base course from its quarry, transfer it to a stockpile and then haul it to a job site and compact it in place. From design to construction to quality control and assurance and ultimately to performance, the entire process depends principally upon the principles and properties of unsaturated soil mechanics.

This study evaluates the significance of using the fundamental material properties to develop important base course models. These new methods will make remarkable contributions to soil mechanics and highway design procedures. This research and the developed models depend upon fundamental aggregate properties. This work capitalizes upon fundamental properties to carry out extensively useable models for Quality Control and Quality Assurance, in predesign procedures, and construction processes. The most notable impact of the work is to replace and improve current methods, increase work efficiency, minimize time spent in the laboratory, find more convenient relationships, and reduce costs and sustainability. Additionally, the simply, quickly and accurately measured aggregate characteristics of base course properties will be used to determine the in-place and as-compacted modulus properties for QC and QA.

One of the major concerns on highways is the continuation of the traffic flow without delay due to construction works. This challenge can be overcome with only monitoring the highway infrastructure and to provide maintenance and rehabilitation to the pavement structure at the most cost-effective time. Nondestructive test devices can be used to overcome this challenge by providing the current condition of pavement

structures. Efficient maintenance and rehabilitation will decrease the fuel consumption, traffic delay costs and travel time.

14. FUTURE WORK

This part of the study presents expected future applications to the quality control and quality assurance programs by utilizing the nondestructive test methods together with the developments reported in this work.

The percometer is a nondestructive test device to measure the dielectric value of a base course material in a precise, accurate fashion. The SDCC model is generated by using the percometer device readings of dielectric constant values together with the measurement of the methylene blue value of the base course. There is considerable synergy in integrating the two analysis methods. The integration will use a model that is capable of providing a base course layer stiffness map along with the water content, density, and suction. This integrated model will present the as-built base course properties. This developed capability can be used in a quality assurance phase of construction.

The ultimate goal of a research study is to integrate the developed theories in a software program to be used by more people. The LayerMAPP program was created with this philosophy. It is a computer program capable of determining the base course moisture content, suction, and dry unit weight as well as the resilient modulus and permanent deformation properties of a base course.

The existing version of the LayerMAPP software database consists of the data on aggregates from nine different selected quarried and one generalized quarry for all of Texas. The properties of some quarries show similarities to others, and thus it is possible to select a quarry in the database that has similar characteristics to the new quarry.

However, this software is arranged to accept and store the characteristics of more quarries in order to have more accurate calculations.

The prediction of the base course properties can be accelerated by loading the GPR data file directly to the LayerMAPP program, which only requires an additional step in the LayerMAPP program. This program can determine the dry unit weight during the data collection phase by analyzing the measured GPR data instantly. This process can provide knowledge about the weak spots immediately during construction and even in the compaction stage. If a spot is outside the minimum and maximum limits of the state transportation standard, these deficient spots can be re-compacted before covering the base course layer with asphalt.

The methods developed in this study determine the base course layer properties and modulus. This advance approach allows the LayerMAPP program to predict the modulus while a radar survey is being conducted on a base course layer in the field. This approach only requires the determination of the MBV from a selected spot/location during the survey data collection. Conducting an FWD measurement of the base course modulus may not be required except as an independent spot check.

The application of the LayerMAPP program can be broadened from a base course aggregate layer to an asphalt layer. This will increase the current potential of the GPR to estimate the asphalt layer properties, such as the asphalt content and density, rather than merely determining the dielectric constant and thickness. This future application can provide a quality control and quality assurance protocol not only for a base course but also for an asphalt layer, as well. It is well known that designing a

pavement is intended to determine the quality of the pavement life; however, merely a quality design is not enough because the pavement service life depends on the implementation of the design parameters in each phase of the construction. Because of this, advanced and innovative quality control and quality assurance methods and software programs can play a significant role in quality maintenance. Furthermore, it was demonstrated that the LayerMAPP program has potential to assist pavement engineers in forensic investigations and pavement rehabilitation studies.

Apart from the modulus prediction, unbound aggregate characteristic properties can be predicted with the least amount of effort based on the radar data. This will decrease the number of tests conducted during the construction. In addition, the quality control process will become more accurate because the risk involved due to false measurement will dramatically decrease. Furthermore, a pavement management program can be established at the construction phase because the required life-cycle prediction parameters used to manage the maintenance plan can be determined.

This study proposes an accurate and efficient methodology to estimate the permanent deformation properties of unbound aggregates. The VESYS and Tseng-Lytton model parameters are defined, and the equations used to calculate the parameters were presented. The permanent prediction models are determined under only one stress state. When this is done in future studies, the influence of the stress ratio, stress path, moisture stress and shear strength on permanent deformation behavior of aggregate material might be investigated in a subsequent study. The permanent deformation behavior of unbound aggregates can be predicted in any given stress state.

REFERENCES

AAS T O T100 (2010). “Standard e thod of Test for Specific Gravity of Soils”. American Association of State Highway and Transportation Officials (AASHTO), Washington, D.C.

AAS T O T180 (2010). “Standard ethod of Test for ois ture-Density Relationship of Soils Using a 4.54 kg (10-lb) Rammer and a457-mm (18-in) Drop.” American Association of State Highway and Transportation Officials (AASHTO). Washington, D.C.

AAS T O T27 (2006) “Standard e thod of Test for Sieve Analysis of Fine and Coarse Aggregates.” American Association of State i ghway and Transportation Officials (AASHTO). Washington, D.C.

AAS T O T307 (2003). “Standard method of test for resilient modulus of subgrade soils and untreated base/subbase materials.” AAS T O T307-99, American Association of State Highway and Transportation Officials, Washington, D. C.

AAS T O T90 (2000). “Standard e thod of Test for Determining the Plastic Limit and Plasticity Index of Soils.” American Association of State ig hway and Transportation Officials (AASHTO). Washington, D.C.

Adu-Osei, A. (2000). “Characterization of Unbound Granular Layers in Flexible Pavements.” Ph.D. Dissertation, Department of Civil Engineering, Texas A&M University, College Station, Texas.

Al- ussa ini, . ., (1977). “Contribution to the ng ineering Soil Classifications of Cohesive Soils,” Final Report, is cellaneous Paper S-77-21, U.S. Army Engineer Waterways Experiment Station, Vicksburg, Mississippi, 61 pp.

Annan, A.P. (2003) "Ground Penetrating Radar: GPR Principles, Procedures & Applications," Sensors & Software Inc., Technical Paper, Mississauga, ON, Canada.

Ashtiani, R.S. (2009). "Anisotropic characterization and performance prediction of chemically and hydraulically bounded pavement foundations." Ph.D. Dissertation, Department of Civil Engineering, Texas A&M University, College Station, Texas.

AST (1980). “Natural Building Stones; Soil and Rock,” American Society for Testing and Materials (ASTM), Annual Book of ASTM Standards, Part 19, 634 pp. Volume 04, ASTM Committee D18 on Soil and Rock West Conshohocken, West Conshohocken, PA.

ASTM D698 (2012). Standard Test Methods for Laboratory Compaction Characteristics of Soil Using Standard f fort (12 400 ft-lbf/ft3 (600 kN-m/m3)). American Society for Testing and Materials (ASTM), ASTM International, West Conshohocken, PA.

AST D845 (2002). "Standard Test e thods for Specific Gravity of Soil Solids by Water Pycnometer," American Society for Testing and Materials (ASTM), ASTM International, West Conshohocken, PA.

Barksdale, R. D. (1991). "The Aggregate andbook." National Stone Association, Washington D.C., Mercury Publishing Services, MD.

Barksdale, R.D. and Itani, S.Y. (1989). "Influence of Aggregate Shape On Base Behavior." Transportation Research Records 1227, Transportation Research Board, Washington D.C., pp.173-182.

Birchak, J.R., C.G. Gardner, J.E. Hipp, and J.M. Victor (1974). High dielectric constant microwave probes for sensing soil moisture. Proceedings of the Institute of Electrical and Electronics Engineers. 62: pp. 93-98.

Bohl, H. and K. Roth (1994). Evaluation of dielectric mixing models to describe the θ(ε)-relation in Time Domain Reflectometry in environmental, infrastructure and mining applications. Evanston, Illinois: United States Department of Interior Bureau of Mines.

Bonaquist, R., and Witczak, M. W. (1996). Plasticity modeling applied to the permanent deformation response of granular materials in flexible pavement systems. Transportation Research Record: Journal of the Transportation Research Board, 1540(1), 7-14.

Boyce, J.R. (1976). "The Behavior of a Granular a terial under Repeated Load." Ph.D. Dissertation, Department of Civil Engineering, University of Nottingham, Nottingham, United Kingdom.

Boyce, J.R. (1980). "A Nonlinear ode l for the la stic Behavior of Granular a terials under Repeated Loading. "International Symposium on Soils under Cyclic and Transient Loading, Swansea.

Boussinesq, J., (1883). Application des Potentials à L'Edude de L 'Equilibre et du Mouvement des Solides Elastiques, Gauthier-Villars, Paris.

Brown, S.F. and Pappin, J.W. (1981)."Analysis of Pavements with Granular Bases." In Transportation Research Record (TRB) 810, National Research Council, Washington D.C. pp. 17-23

Carver, R. H. (2010). Practical Data Analysis with JMP. SAS Institute. pp. 61–. ISBN 978-1-60764-475-0. Retrieved 16 November 2012.

Chaudhry, M. H. (2008). Open-channel Flow, page 34-38, Springer, Columbia, South Carolina.

Craig, R. F. (2004). Soil Mechanics. Seventh Edition, Spon Press pp144-155, New York, NY, USA.

Cornell Local Roads Program. An Important Tool for Highway Management. Cornel University, Tuesday 18 February 2014.

Cokca, E., and Birand, A. (1993). "Determination of Cation Exchange Capacity of Clayey Soils by the Methylene Blue Test." ASTM Geotechnical Testing Journal, 16(4), 518-524.

Curtis, J.O., C.A. Weiss Jr., and J.B. Everett, (1995). Effect of Soil Composition on Complex Dielectric Properties. U.S. Army Corps of Engineers, Waterways Experiment Station: Vicksburg, MS. p. 59.

Das, B. M. (2012). Principles of Geotechnical Engineering. Cengage Learning, Stamford, CT, USA.

Dobson, M.C., F.T. Ulaby, M.T. Hallikainen, and M.A. El-Rayes (1985). Microwave dielectric behavior of wet soil -Part II: dielectric mixing models. IEEE Transactions on Geoscience and Remote Sensing. GE-23(1): p. 35-46.

Duncan, J. ., and Chang, C. Y. (1970). ‘‘Nonlinear analysis of stress and strain in soils.’’ J. Soil e ch. and Found. Div., ASC , 96(5), 1629–1653.

Evett, S. R. 2000. Nuclear Gauge Module I, Design, Theory,and Operation. pp. NGMI-1 to NGMI-23. In Nuclear Gauge Train-the-Trainer Course, USDA-Radiation Safety Staff, Beltsville, MA. Available at http://www.cprl.ars.usda.gov/programs/ (Posted 30 Oct. 2000; verified 12 Dec. 2000).

Epps, J., Sebesta, S., Hewes, B., Sahin, H., Luo, R., Button, J., Lytton R.L., Herrera, C.A., Hatcher, R., and Gu, F. (2013). Development of a Specification for Flexible Base Construction (No. FHWA/TX-13/0-6621).

Fairbairn, P. E. and Robertson, R. H. S. (1957). Liquid limit and dye adsorption: Clay Minerals Bull. 3,129-136.

Fernando, E. G., and Maser, K. R. (1992). Development of a Procedure for the Automated Collection of Flexible Pavement Layer Thicknesses and Materials:

Phase I: Demonstration of Existing Ground Penetrating Radar Technology. Florida DOT State Project, 99700-7550.

Francke, J. C., and Yelf, R. (2003) "Application of GPR for Surface Mining," the Second International Workshop on Advanced GPR, Delft, the Netherlands, May 2003.

Fredlund, D.G. and Rahardjo, H. (1993) Soil Mechanics for Unsaturated Soils, New York: John Willey &Sons, Inc.

Fredlund, D.G. and Xing, A. (1994), " qua tions for the soil-water characteristic curve", Canadian Geotechnical Journal, Vol.31, pp.521-532.

ic ks, R.G. and oni smith, C.L. (1971). "Factors Influencing the Resilient Properties of Granular a terials." Transportation Research Record 345, Transportation Research Board, National Research Council, Washington D.C., 15-31.

Holtz, Robert D., and William D. Kovacs. An introduction to geotechnical engineering. No. Monograph. 1981.

Horiba Manual (1995). Horiba LA-910 Laser Scattering Particle Size Distribution Analyzer Manual, Horiba Instruments Incorporated, 17671 Armstrong Irvine Industrial Complex, Irvine, California 92614.

Jones, B. and Sall, J. (2011). "JMP statistical discovery software". Wiley Interdisciplinary Reviews: Computational Statistics 3 (3): 188–194. doi:10.1002/wics.162.

Joslin, J.G. (1959). "Ohio's Typical ois ture-Density Curves", Symposium on Application of Soil Testing in Highway Design and Construction, STP 239, American Society for Testing and Materials, Philadelphia PA, 111-118.

Juárez-Badillo, E. (1981). General compressibility equation for soils. In Proceedings of the International Conference in Soil Mechanics and Foundation Engineering, Stockholm, Sweden (pp. 171-178).

Juarez-Badillo, E. (1983). General permeability change equation for soils. In Proceedings of the International Conference on Constitutive Laws for Engineering Materials, University of Arizona, Tucson, Arizona (pp. 205-209).

Juárez-Badillo, E. (1985). General time volume change equation for soils. In 11th International Conference on Soil Mechanics and Foundation Engineering, San Francisco (Vol. 2, pp. 519-530).

Kancherla, A. (2004). “Resilient modulus and permanent deformation testing of unbound granular materials.” a ster of Science Thesis, Texas A& University, College Station, Texas.

Kenis, W. J. (1978). “Predictive design procedure.” SYS user’s manual: An interim design method for flexible pavement using the VESYS structural subsystem.

Knoll, M.D. and R. Knight (1994). Relationships between dielectric and hydrogeologic properties of sand-clay mixtures. in 5th International Conference on Ground Penetrating Radar. Kitchener, Ontario, Canada: Waterloo Centre for Groundwater Research.

Lee, S. I., Zollinger, D. G., Lytton, R. L., & Jackson, N. C. (2009). Automation of pavement sublayer moisture content determination using long-term pavement performance time domain reflectometry data and micromechanics.Transportation Research Record: Journal of the Transportation Research Board, 2116(1), 16-25.

Lekarp, F., and Dawson, A. (1998). ‘‘ od elling permanent deformation behavior of unbound granular materials.’’ Constr. and Build. a t., 12(1), 9–18.

Lekarp, F., Isaacson, U., and Dawson, A. (2000). “State of the Art. II: Permanent Strain Response of Unbound Aggregates.” Journal of Transportation n gineering, ASC , Vol. 126, No.1, 76-83

Lentz, R. W., and Baladi, G. Y. (1981). Constitutive Equation for Permanent Strain of Sand Subjected to Cyclic Loading. Transportation research record, (810).

Letto, A. R. (1968). A Computer Program for Function Optimization Using Pattern Search and Gradient Summation Techniques. Report for Master of Emgineering, Texas A&M University, College Station, TX, USA.

Liu, W., and Scullion, T. (2006). PAVECHECK: Integrating Deflection and Ground Penetrating Radar Data for Pavement Evaluation (No. FHWA/TX-06/0-4495-1).

Lytton, R.L. (1995). “Foundations and Pavements on Unsaturated Soils.” First International Conference on Unsaturated Soils, Paris.

Lytton, R. L., Aubeny, C.P., and Bulut, R. 2004. “Design Procedure for Pavements on x pansive Soils,” olu me 1, Technical Report 0-4518-1, Texas Transportation Institute, Texas A&M University, College Station, Texas.

Lytton, R. L., Aubeny, C.P., and Bulut, R. 2004. “Design Procedure for Pavements on x pansive Soils,” olu me 2, Technical Report 0-4518-1, Texas Transportation Institute, Texas A&M University, College Station, Texas.

Majidzadeh, K.; Aly, M.; Bayomy, F.; and El-Laithy, A. (1980) Implementation of a Pavement Design System Volumes 1 and 2 of the Final Report. Research Project EES 579. Ohio State University. Columbus, OH.

Martinez, A. and A.P. Byrnes, (2001). Modeling dielectric-constant values of geologic materials: an aid to ground penetrating radar data collection and interpretation, in Current Research in Earth Sciences. Kansas Geological Survey. p. 16.

P DG (2004). "Guide for e chanical-Empirical Design of New and Rehabilitated Pavement Structures". Final Report, Part 2 Design Inputs, Chapter 3 n vironment Effects. Prepared for National Cooperative Highway Research Program Transportation Research Board National Council (NCHRP).

Mitchell, P.W. 1979. "The Structural Analysis of Footings on x pansive Soil," Kenneth W.G. Smith and Associates Research Report No.1, (1st Edition), Newton, South Australia.

Nazarian, S., and Gucunski, N. (2007). Geophysical Methods for Rapid Assessment of Urban Transportation Infrastructure. Geo-Strata—Geo Institute of ASCE, 8(2), 24-29.

Nazzal, M. D., and Mohammad, L.N. (2010). Estimation of resilient modulus of subgrade soils for design of pavement structures. J. Mater. Civ. Eng., Vol. 22, 726-734.

Neshvadian Bakhsh, K. and Zollinger, D., (2014). Faulting Prediction Model for Design of Concrete Pavement Structures. ASCE Proceedings, Geo-Shanghai 2014.

NC RP (2003). " a rmonized test methods for laboratory determination of resilient modulus for flexible pavement design." Final Report. No. 1-28A, National Cooperative Highway Research Program (NCHRP), Washington, D. C.

Nevins .J . and Weinritt D.J. (1967) "Determination of cation exchange capacity by methylene blue adsorption." American Ceramic Society Bulletin, ol. 46, pp. 587-592.

Nguyen, B., A.M. Geels, J. Bruining, and E.C. Slob. (1997) Calibration measurements of dielectric properties of porous media, in SPE Annual Technical Conference and Exhibition, A.C. Dubey, et al., Editors. Society of Petroleum Engineers: San Antonio, TX. p. 930-941.

Oh, J. H., Lytton, R. L., and Fernando, E. G. (2006). Modeling of pavement response using nonlinear cross-anisotropy approach. Journal of transportation engineering, 132(6), 458-468.

Online source: AdekTM brand percometer by www.roadscanners.com taken in September 2012.

Pan, T., Tutumluer, E., and Anochie-Boateng, J. (2006). "Aggregate orpholog y Affecting Resilient Behavior of Unbound Granular a terials." Transportation Research Record: Journal of the Transportation Research Board, No. 1952, 12-20.

Perera, Y. Y., Zapata, C. E., Houston, W. N., & Houston, S. L. (2005). Prediction of the soil-water characteristic curve based on grain-size-distribution and index properties. Proceedings, GeoFrontier 2005.

Phelps G.W. and Harris D.L. (1967) "Specific surface and dry strength by methylene blue adsorption." American Ceramic Society Bulletin, ol. 47, pp. 1146 -1150.

Puppala, A. J. (2008). Estimating stiffness of subgrade and unbound materials for pavement design (Vol. 382). Transportation Research Board.

Roth, K., R. Schulin, H. Flühler, and W. Attinger (1990) Calibration of time domain reflectometry for water content measurement using a composite dielectric approach. Water Resources Research. 26(10): p. 2267-2273.

Sahin, H. (2011). Characterization of expansive soil for retaining wall design. MS Thesis, Texas A&M University, College Station, Texas, USA.

Sahin, H., Gu, F., and Lytton, R.L., (2014). Development of Soil Water Characteristic Curve for Flexible Base Materials Using the Methylene Blue Test. American Society of Civil Engineers (ASCE) Journal of Materials in Civil Engineering.

Sahin, ., Gu, F., Tong, Y., Luo, R., and Lytton, R. L. (2013). "Unsaturated soil mechanics in the design and performance of pavements." Pan-Am Unsaturated Soils, pp. 87-100.

Sall J., Creighton L., and Lehman A. (2005). JMP start statistics. Wadsworth Publishing Co., Belmout, California.

Saue, T., Kadaja, J., and Plakk, T. (2008). Measurement of soil water content by percometer. In Workshop Program and Papers: 1st Global Workshop on High Resolution Digital Soil Sensing and Mapping (pp. 184-192).

Schofield, R. K. (1935). "The pF of the Water in Soil," Transactions, 3rd International Congress of Soil Science, Vol.2 pp.37-48.

Seed, H., Mitry, F., Monismith, C., and Chan, C. (1967). "Factor Influencing the Resilient Deformations of Untreated Aggregate Base in Two-Layer Pavements

Subjected to Repeated Loading." i ghway Research Record 190, RR , National Research Council, Washington D.C., 19-57.

Seyhan, U., Tutumluer, E., & Yesilyurt, H. (2005). Anisotropic aggregate base inputs for mechanistic pavement analysis considering effects of moving wheel loads. Journal of materials in civil engineering, 17(5), 505-512.

Tex-113-E (2010) "Laboratory Compaction Characteristics and Moisture-density Relationship of Base Materials". Texas Department of Transportation (TxDOT) Designation, Construction Division, Austin, TX

Thompson, . R., and Nauman, D. (1993). "Rutting rate analyses of the AAS O road test flexible pavements." Transportation Research Record (No. 1384), TRB. National Research Council, Washington D.C.

Tseng, K. ., and Lytton, R.L. (1989). "Prediction of permanent deformation in flexible pavements materials, implication of aggregates in the design, construction, and performance of flexible pavements." AST STP 1016, American Society for Testing and Materials (ASTM), pp. 154-172, West Conshohocken, Pennsylvania.

Tutumluer, . (1995)."Predicting Behavior of Flexible Pavements with Granular Bases." Ph.D. Thesis, Georgia Institute of Technology, Department of Civil Engineering GA.

U.S. Army n gineer Waterways x periment Station (1960). "The Unified Soil Classification System," Technical e morandum No.3-357. Appendix A, Characteristics of Soil Groups pertaining to Embankments and Foundations, 1953; Appendix B, Characteristics of Soil Groups Pertaining to Roads and Airfields, 1957.

U.S. Bureau of Reclamation (1974). Earth Manual, 2nd Ed., Denver, 840 pp.

USDA (1986). Soil Mechanics Training Series Basic Soil Properties. Modulus 4: Volume-Weight Relations. United States Department of Agriculture (USDA), Soil Conservation Service.

Uzan, J., Lytton, R. L., and Germann, F. P. (1989). General procedure for backcalculating layer moduli. Nondestructive testing of pavements and backcalculation of moduli, 1026, 217-28.

van Dam, R. L., Borchers, B., & e ndrickx, J. . (2005). " ethods for prediction of soil dielectric properties: a review." In Defense and Security, pp. 188-197. International Society for Optics and Photonics.

Von Quintus, H. L. (2009). NDT technology for quality assurance of HMA pavement construction, Transportation Research Board.

Von Quintus, H. L., and Simpson, A. L. (2002). Back-Calculation of Layer Parameters for LTPP Test Sections, Volume II: Layered Elastic Analysis for Flexible and Rigid Pavements (No. FHWA-RD-01-113).

Wang, ., (2010) "Ground Penetrating Radar with Data Access and Control" Ph.D. Thesis, Department of electrical & Computer Engineering, University of Houston, Texa, USA.

Wensink, W.A. (1993) Dielectric properties of wet soils in the frequency range 1-3000 MHz. Geophysical Prospecting. 41: p. 671-696.

Witczak, .W . and Uzan, J. (1988). "The Universal Airport Pavement Design System Report I to : Granular a terial Characterization." University of a ryland, Department of Civil Engineering, MD.

Woods, K.B. and Litehiser, R.R. (1938). Soil Mechanics Applied to Highway Engineering In Ohio, Bulletin 99, the Ohio State University Experiment Station, Columbus, OH, July.

Zapata, C. . (1999). "Uncertainty in Soil-Water-Characteristic Curve and Impacts on Unsaturated Shear Strength Predictions." Ph.D. Dissertation, Arizona State University, Tempe, AZ.

Zapata, C. . (2010). "A National Catalog of Subgrade Soil-Water Characteristic Curve (SWCC) Default Inputs for Use with the PDG," The National Cooperative Highway Research Program (NCHRP), NCHRP Report 9-23A, Arizona State University, Temple, AZ.

Zhou, F., and Scullion, T. (2002). " SYS5 Rutting ode l Calibrations with Local Accelerated Pavement Test Data and Associated Implementation." Research Report

APPENDIX A

IMPROVED METHYLENE BLUE TEST FOR UNBOUND BASE COURSE AGGREGATE MATERIALS

A 1. SCOPE

A 1.1. Test method describes the measurement of methylene blue adsorbed by clay size fines. This measurement is denoted as the Methylene Blue Value (MBV).

A 1.2. Test method determines the amount of the fines content in an aggregate mixture.

A 1.3. Test method differentiates the fines property as clayey and non-clayey fines.

A 2. DEFINITIONS

A 2.1. *Methylene Blue Value (*MBV*)* – a measured reading from a colorimeter device and the MBV is an indicator of the amount of fines in the mixture.

A 2.2. *Critical Methylene Blue Value (*MBV_C*)* - a measured methylene blue value, which is a threshold between clayey and non-clayey fines.

A 2.3. The unit of methylene blue value (MBV) is considered as milligrams of methylene blue per gram of dry soil sample (mg/g).

A 3. APPARATUS

A 3.1. *Hach DR Colorimeter device* measures the color change of solution consisting of soil sample and methylene blue solution.

A 3.2. *Portable Weight Balance* must measure weight with a sensitivity of 0.01 gram.

A 3.3. *Methylene blue solution* which is a concentration of 1.00 percent aqueous solution. It is an anhydrous form of methylene blue ($C_{16}H_{18}N_3SCl$). The methylene blue concentration is diluted to 0.50 percent by weight.

A 3.4. *Micropipette which* is used to measure and transfer a 130 μL volume of methylene blue solutions.

A 3.5. *Pipet Tip* which is capable of holding a volume from 50 to 1000 microliter.

A 3.6. *Glass Tube Culture* which is a clear color, rounded cylindrical round shape and includes a screw cap. The size is O.D. x L. 16 x 100 mm respectively.

A 3.7. *Syringe (without needles)* is a general purpose syringe which has a capacity of 3 mL with luer-lok adapter.

A 3.8. *Syringe Filter* has pore sizes of 0.20 micrometers and is capable of mounting a syringe.

A 3.9. *Plastic Tube* has a volume of 45 mL and a screw cap. It has visible gradations and is freestanding with conical a bottom.

A 3.10. *Plastic Storage Tubes* are capable of holding 1.4 mL volume, with a clear color, and screw cap.

A 3.11. *Weigh dish* is a pour boat to hold a minimum of 20.00 grams of sample.

A 3.12. *Eyedropper* is able of being squeezed and has a capacity of 7.50 mL.

A 3.13. *Distilled water* has to be processed one or two times to become the distilled form.

A 3.14. *Disposable Latex Gloves* which are strong enough to protect hands.

A 3.15. *Funnel* will be used to add the sample into the 45 mL plastic tube.

A 3.16. *Timer* will count minutes while shaking the sample.

A 3.17. *No. 4 Sieve* will be used to obtain the passing No. 4 sieve portion.

A 3.18. *Blow drier* will be used for field operation to dry soil sample.

A 3.19. *Ziploc bag,* to store and transport the soil samples.

A 3.20. *Beaker* will be used to store the distilled water during the test. For field operations, the top of the beaker must be covered to protect it from dirt or other contamination.

A 4. CALIBRATING SOLUTION

A 4.1. Methylene blue concentration must be calibrated due to different types of industrial methylene blue sources.

A 4.2. Correction factor must be determined for each new bottle of methylene blue concentration before testing.

A 4.3. Tare a new clean 45 mL plastic tube and transfer 130 μL methylene blue concentration solution into the this plastic storage tube by using the micropipette.

A 4.4. Add accurately 45.00 grams of distilled water into the plastic storage tube with the eyedropper.

A 4.5. Close the cap of the plastic tube and shake it gently.

A 4.6. Transfer the diluted solution into a glass tube and screw the cap.

A 4.7. Turn on the Hach DR Colorimeter and press the PRGM button. Type 106 then hit the ENTER key.

A 4.8. Insert a glass tube filled with water into the colorimeter and press the ZERO. The colorimeter must display the value of 0.00 ppm.

A 4.9. Insert the glass tube filled with the solution into the colorimeter and press the READ key.

A 4.10. The colorimeter will display a reading. The reading of 14.44 ppm corresponds to the 0.50 percent concentration by weight.

A 4.11. Convert the reading (ppm) to actual Methylene Blue concentration by weight, using the calculations provided in sections A 8.2 to A 8.4.

A 4.12. Actual Methylene blue concentration must be between 0.480% and 0.502%

A 4.13. If the converted methylene blue is higher than 0.502%, dilute the methylene blue solution with distilled water.

A 4.14. If the converted methylene blue solution is lower than 0.48%, discard the methylene blue solution and prepare a new solution.

A 4.15. Repeat the process until an actual methylene blue concentration is obtained.

A 5. SAMPLE PREPARATIONS (LABORATORY)

A 5.1. A representative sample of passing No. 4 sieve size is placed in a ziploc bag until the test.

A 5.2. Store samples in the container prior to test at a room temperature between 28ºC and 30ºC.

A 5.3. Keep the ziploc bag open. Allow sample to lose moisture and reduce the moisture to the air dry state. The drying process normally takes two days.

A 6. SAMPLE PREPARATIONS (FIELD)

A 6.1. Take a representative sample from the surface of the aggregate mixture.

A 6.2. Sieve the aggregate mixture with No. 4 sieve, and take the passing aggregate portion. Sieve a minimum of 200 gram to permit replicate measurements.

A 6.3. Dry the sample by using an air drier. This process will require no more than 10 minutes.

A 6.4. Place the dried sample in a ziploc bag and keep the zipper open.

A 7. TEST PROCEDURE

A 7.1. Place a weigh dish on the balance and add a 20.00 gram sample from the ziploc bag.

Note 1- Always select a representative sample from the ziploc bag in all cases. Mix the sample thoroughly and do not allow segregation.

A 7.2. Add 30.00 mL of diluted methylene blue solution in a new clean 45 mL plastic tube.

A 7.3. Add the 20.00 gram sample into the 30.00 mL solution by using a funnel and close the cap of the plastic tube.

Note 2- Make sure all the sample is added into the plastic tube. Be careful not to pour any sample outside of the plastic tube.

A 7.4. Start off the timer, and at the same time begin shaking the plastic tube for 1 minute.

A 7.5. Allow the sample to rest for 3 minutes.

A 7.6. Shake the plastic tube after for additional 1 more minute.

A 7.7. Remove the plunger from the 3 mL- syringe and place a filter syringe on the luer-lok fitting.

A 7.8. Add nearly 2 mL solution (sample and methylene blue) to the syringe and place the plunger back.

A 7.9. Slowly push the plunger in and filter the solution into a plastic storage tube.

Note 3- Initially there will be some resistance because of the very fine syringe filter pore size. The plunger has to be pushed but not hard. If the plunger is pushed harder than necessary, the syringe filter will explode.

A 7.10. Tare a new clean 45.00 mL plastic tube on the balance.

A 7.11. Take 130 μL filtered solution from the plastic storage tube, and then transfer it into the 45 mL plastic tube through the adjustable micropipette.

Note 4- Be careful to have accurate filtered solution. To do that, immerse nearly half of the pipet tip into plastic storage tube before aspirating the filtered solution.

Note 5- Make sure there is no solution stain on the pipet tip after dispersing the solution into the plastic tube.

A 7.12. Fill the plastic tube with distilled water accurately total to a 45.00 gram using the balance.

A 7.13. Fill the glass tube almost full with the newly diluted solution and close the cap. The solution is read to measure the methylene blue value.

A 7.14. Turn on the colorimeter. Press the PRGM button and type 107 then press the ENTER key.

A 7.15. Remove the colorimeter cover and place the glass tube filled with distilled water into the hole on the colorimeter. Next cover the glass tube and press the ZERO key.

A 7.16. The colorimeter will display a value of 7.50 mg/g which indicates there is no color change.

A 7.17. Place the glass tube filled with the solution after removing the tube filled with distilled water in the colorimeter. Then cover the tube and press the READ key.

A 7.18. The instrument will display a value that is the *Methylene Blue Value (MBV)*. The Methylene Blue Value expresses in *mg* methylene blue per g of dry sample.

A 7.19. If the methylene blue value is lower than 7.00 mg/g, it is a valid number.

A 7.20. This process will be closely repeated at least two times for each sample.

A 7.21. If the methylene blue value is higher than 7.00 mg/g then the sample size must be cut into half to 10.00 grams and this procedure will be repeated.

A 7.22. If sample size is10.00 grams and the methylene blue value remains higher than 7.00 mg/g, cut the sample size to 5.00 grams.

Note 6- The amount of methylene blue solution used will remain the same even though the sample size is reduced.

A 8. CALCULATION

A 8.1. Methylene blue value calculation is given in following equation:

$$MBV_{real} = S_{correction} x (MBV_{reading} + C_{factor})$$

where $MBV_{reading}$ is the methylene blue value reading from the colorimeter device, (mg/g), MBV_{real} is the real methylene blue value after applying two correction factors (mg/g), C_{factor} is the correction factor of concentration due to dilution (mg/g), $S_{correction}$ is the sample correction factor due to size of sample used. $S_{correction}$ is the factor are shown in Table 1.

Table A- 2 Tabulated Sample Correction Factor along with Corresponding Sample Sizes

Sample Size (gram)	20.00	10.00	5.00
$S_{correction}$	1.0	2.0	4.0

A 8.2. Actual concentration of the methylene blue solution and determination of the correction factor is given in following equation:

$$C_{initial\_actual} = (C_{PRGM106,ppm})\frac{45mL}{(130\mu L)(1000)}$$

A 8.3. If the methylene blue concentration used is not 0.5 % then the corrected methylene blue value ($MBV_{corrected}$) is determined by following equation:

$$MBV_{corrected} = \left[\frac{\left(C_{initial\_actual} - C_{initial\_theoretical} + \frac{MBV_{measured}(20g)}{(30mL)(1000)}\right)(30ml)}{20g}\right] x(1000)$$

A 8.4. A correction factor (C_{factor}) value is determined for each new bottle of the methylene blue concentration and is calculated by following equation:

$$C_{factor} = MBV_{corrected} - MBV_{measured}$$

where $C_{PRGM106,ppm}$ is the initial concentration of the methylene blue solution (ppm), $C_{initial\_actual}$ is the actual methylene blue concentration in the solution by weight, $MBV_{corrected}$ is the corrected methylene blue value (mg/g), $C_{initial\_theoretical}$ is theoretical concentration at 0.5 percent by weight, and $MBV_{measured}$ is the measured methylene blue value (mg/g).

A 9. REPORT

A 9.1. Report shall include the following.

A 9.2. Material source or quarry, and material type.

A 9.3. Amount of material used to run the test in grams.

A 9.4. All the methylene blue value reading to nearest 0.01 mg/g

A 9.5. Plot the data and check the value of the methylene blue value whether it is higher than the critical methylene blue value *(MBV_C)* of 7.00 mg/g.